Department of Organic and Macromolecular Chemistry

Polymer Chemistry Research Group

Functional and amphiphilic copolymers by means of copper-mediated polymerization

Frank Driessen

Promotor: Prof. Dr. Filip Du Prez

Ghent, 2017

Thesis submitted to obtain the degree of Doctor in Sciences: Chemistry

Exam commission

Prof. Dr. Peter Dubruel (Chair, Ghent University)

Prof. Dr. Ir. Dagmar D'Hooghe (Ghent University)

Prof. Dr. Richard Hoogenboom (Ghent University)

Dr. Nezha Badi (Ghent University)

Prof. Dr. Thomas Junkers (Hasselt University)

Dr. Remzi Becer (Queen Mary University of London)

Prof. Dr. Filip Du Prez (Promotor, Ghent University)

Research funded by the Agency for Innovation by Science and Technology in Flanders

Onderzoek gefinancieerd door het Agentschap voor Innovatie door Wetenschap en Technologie

Dankwoord

Met aan het einde te komen van dit doctoraat zou ik van de gelegenheid willen gebruik maken om verschillende mensen te bedanken. Zoals gekend is een doctoraat nooit een ‘one-man-show’ en zou dus ook in dit geval het beëindigen van dit doctoraat nooit mogelijk geweest zijn zonder de hulp van velen.

Allereerst zou ik mijn promotor, Prof. dr. Filip Du Prez willen bedanken voor de kans die hij mij gegeven heeft om zowel mijn masterthesis als doctoraat in zijn sterk uitgebouwde groep te kunnen uitvoeren. Daarnaast zou ik hem ook willen bedanken voor de verschillende mogelijkheden om mijn werk op (inter)nationale congressen te kunnen voorstellen.

Een paragraaf is veel te kort om de bijdrage van dr. Pieter Espeel aan dit doctoraat te beschrijven. Dank je wel Pieter voor de verschillende samenwerkingen en je fantastische begeleiding. Daarnaast zullen momenten zoals het zwembad op Summerschool in Spanje, teambuildings, resto-uitstapjes altijd in mijn geheugen gegrift staan.

I would like to thank the members of the exam commission: Prof. Dr. Peter Dubruel, Prof. Dr. ir. Dagmar D’Hooghe, Prof. Dr. Richard Hoogenboom, Dr. Nezha Badi, Prof. Dr. Thomas Junkers and Dr. Remzi Becer for thoroughly reviewing my thesis and their constructive feedback.

Daarnaast zou ik al de rest van het PCR-labo willen bedanken om mijn gezaag, geslof, lawaai, … tijdens de afgelopen 4 jaar te verdragen, dank je wel Bernhard, Bastiaan, Otto, Seda, Pieter, Angel, Guadalupe, Oguz, Roberto, Stefan, Thu, Samira, Peter (Pan), Maryia, Fabienne, Sofie, Xander, Sanne, Stijn, Jonas, Wim, Rémi, Benji, Sophie, Steven, Kevin, Daniel, Cristina, Laetitia, Stef, Niels, Hannes, Josh, Maarten, Martijn, Yann, Ismail, Tolga. Graag zou ik wel nog enkele mensen wat meer in het bijzonder willen bedanken:

- Steven, de ‘buddy’ van het labo, voor alle steun, discussies en onnozele momenten.
- Roald, dank je wel voor al je harde werk tijdens je masterthesis. Onze Limburgse alliantie, was een fantastisch jaar.
- Bernhard, elke keer als ik je labo binnenstapte dacht je waarschijnlijk “oh nee”. Merci voor al je technische ondersteuning.

- Jan Goeman, dank je wel voor je vele werk met het onderhoud van de MALDI. Daarnaast ook merci aan Bart Dervaux om mij in het begin van mijn doctoraat de “tips and tricks” van de MALDI te leren.
- Stef en Martijn, merci voor de samenwerkingen binnen team ‘CRP’.
- Kevin, dank je wel voor al je hulp bij computerproblemen. Ik denk dat het moeilijk te beseffen is hoe groot soms je bijdragen aan de groep zijn.

During my PhD, I spent several days in Eindhoven. I would like to thank Prof. dr. Bert Meijer and dr. Anja Palmans for the constructive feedback and dr. Yiliu Liu for the help in the lab.

Tijdens mijn doctoraat was ik ook bestuurslid binnen de jongerensectie van de Koninklijke Vlaamse Chemische Vereniging (KVCV), wat een grote leerschool voor mij was. Daarbij ook dank aan alle werkgroepleden en specifiek aan ‘Team Gent’ met Bart en Geert-Jan. Niels en Jonas, merci dan ook om ‘Team Gent’ verder te zetten de komende jaren.

Bart, de 4 jaar samen op kot in Gent waren soms afzien (waarschijnlijk wel meer voor jou dan voor mij), samen met de vele uren die we op de trein gespendeerd hebben. Maar het zijn wel mooie jaren geweest waar ik soms met weemoed aan ga terugdenken. Geert-Jan, de 2 jaar dat je erbij zat op kot hebben het uiteraard des te plezanter gemaakt, dank je wel beiden. Uiteraard zou ik ook de studiegenoten uit Hasselt willen bedanken, Bart, Geert-Jan, Dennis, Linde, Stefanie. Nogmaals merci voor de hulp met de overstap uit Eindhoven.

De kameraden uit Limburg mag ik ook zeker hier niet vergeten. Zij waren vaak een steun en toeverlaat in de weekends. Dank je wel Nicky, Dimi, Brecht, Elisabeth, Ederick, Darline, Manuel, Ben. Ook de mensen binnen Kazou zou ik willen bedanken, op kamp gaan was vaak een moment waar ik naar uitkeek doorheen het jaar.

Ten slotte zou ik nog mijn ouders, zussen en grootouders, tantes en nonkels willen bedanken voor hun interesse, (financiële) steun en vertrouwen. Ondanks dat ik het vroeger vaak niet wou inzien hebben ze mij toch getoond dat doorzetten en hard werk belangrijk zijn.

ADMET	Acyclic Diene Metathesis
AGET	Activators Generated by Electron Transfer
ARGET	Atoms ReGenerated by Electron Transfer
AIBN	α,α'-AzoIsoButyroNitrile
ATRA	Atom Transfer Radical Addition
ATRP	Atom Transfer Radical Polymerization
Bpy	Bipyridine
BTA	Benzene-1,3,5-TricarboxAmides
BuTAD	4-Butyl-1,2,4-TriAzoline-3,5-Dione
CA	Citronellyl Acrylate
CD	Circular Dichroism
$CHCl_3$	Chloroform
Cp	Cyclopentadiene
CROP	Cationic Ring-Opening Polymerization
CuAAc	Copper Assisted Azide-alkyne cycloaddition reaction
CuPc	Copper Phtalocyanine
DBTL	DiButylTindiLaurate
DBU	1,8-DiazaBicyclo[5.4.0]Undec-7-ene
DCE	1,2-DiChloro-Ethane
DCM	DiChloroMethane
DLS	Dynamic Light Scattering
DIPEA	*N,N*-DiIsoPropylEthylAmine
DMF	*N,N*-DiMethylFormamide
DMPA	2,2-DiMethoxy-2-PhenylAcetophenone
DMSO	DiMethyl SulfOxide
DOSY	Diffusion Ordered SpectroscopY
DP_n	Degree of Polymerization
DSC	Differential Scanning Calorimetry
DTNB	5,5'DiThiobis(2-NitroBenzoic acid)
EEA	2-Ethoxy EthylAcrylate

FRP	Free Radical Polymerization
GC	Gas Chromatography
HDEO	*Trans,trans*-2,4-HexaDiEn-1-Ol
HMTETA	1,1,4,7,10-HexaMethylTriEthyleneTetrAmine
ICAR	Initiators for Continuous Activator Regeneration
ISET	Inner Sphere Electron Transfer
LC	Liquid Chromatography
LCxSEC	Liquid Chromatography x Size Exclusion Chromatography
MADIX	MAcromolecular Design *via* the Interchange of Xanthates
MALDI-TOF	Matrix Assisted Laser Desorption Ionization – Time Of Flight
MCH	MethylCycloHexane
Me_6TREN	*N,N,N',N',N'',N''*-hexamethyltris(aminoethyl)amine)
NMP	Nitroxide Mediated Polymerization
OSET	Outer Sphere Electron Transfer
PBA	Poly(Butyl Acrylate)
PCL	PolyCaproLactone
PDMA	Poly(*N,N)*DiMethylAcrylamide
PE	PolyEthylene
PEO	Poly(EthyleneOxide)
PiBA	Poly(isoBornylAcrylate)
PMDETA	*N,N,N',N'',N''*-PentaMethylDiEthyleneTriAmine
PMMA	Poly(MethylMethAcrylate)
PMVE	Poly(Methyl Vinyl Ether)
PPM	Post-Polymerization Modification
PS	PolyStyrene
RAFT	Reversible Addition Fragmentation Chain Transfer
RDRP	Reversible Deactivation Radical Polymerization
SARA	Supplementary Activator and Reducing Agent
SCPN	Single Chain Polymeric Nanoparticles
sCT	Salmon Calcitonin

SEC	Size Exclusion Chromatography
SET-LRP	Single Electron Transfer Living Radical Polymerization
SG1	N-*tert*-butyl-N-(1-diethylphosphono-2,2-dimethylpropyl)nitroxide
SR&NI	Simultaneous Reverse and Normal Initiation
TAD	1,2,4-TriAzoline-3,5-Dione
*t*BA	*Tert*-Butyl Acrylate
TCEP	Tris(2-CarboxyEthyl)Phosphine
TEM	Transmission Electron Microscopy
TEMPO	2,2,6,6-TEtraMethylPiperidinyl-1-Oxy
T_g	Glass transition temperature
THF	TetraHydroFuran
TL	ThioLactone
TLA	Thiolactone-containing acrylate
Ur	Urazole

Chapter I.
Introduction, aim and outline

Introduction and aim

Nowadays, technology-driven advancements in science and technology are astonishing and sometimes difficult to keep up with. Important contributions to the inventions we currently take profit from, e.g. automotive, aviation industry, microelectronics, construction materials were provided by polymer chemists as a result of continuous development and implementation of novel methodologies for the synthesis of advanced polymeric structures.[1] Therefore, modern-day research in polymer chemistry is amongst others focusing on fine-tuning the properties of materials by combining different monomers in various copolymer topologies as random, block, star-shaped or graft copolymers.[2-5]

These complex copolymer structures can be applied in a broad range of different applications, such as dispersants, viscosity modifiers, adhesives, etc. The interest in synthesizing the above mentioned copolymer architectures in this PhD-research originally arose from a joint PhD-project between the own research group and Dow Chemicals. In this thesis, a broad range of different complex polymer structures were synthesized and screened for the stabilization of polymer blends (WO2012154393). It was observed that the best results were obtained with structures different than the usually block or graft copolymers, namely complex structures such as toothbrush copolymers.[6] Furthermore, within the own research group it was demonstrated in previous PhD-projects that amphiphilic graft copolymers can be successfully applied in the dispersion of hydrophobic pigment particles in water.[7, 8]

Significant progress in the synthesis of these complex structures would not have been made possible without the development of controlled (radical) polymerization techniques (according to IUPAC now denoted as Reversible Deactivation Radical Polymerization or RDRP), as these

methods allow for the preparation of polymeric structures with precise control over molar mass, end group functionality, chain architecture and dispersity.[9, 10] In general, radical-based systems such as Atom Transfer Radical Polymerization (ATRP), Reversible Addition Fragmentation Transfer (RAFT) polymerization and Nitroxide Mediated Polymerization (NMP) have significant advantages compared to their ionic counterparts such as a broader range of monomers which can be polymerized and less stringent reaction conditions.[11-13] Since the introduction of these RDRP methods in 1994, more than 40,000 publications and 1,400 patents were released and the investments in this field are still increasing every year.

However, the industrial applications in which these systems are implemented are still moderate in comparison to their academic popularity as a result of low conversions, long reaction times and insufficient end group functionality obtained *via* these methods.[14-16] Furthermore, each of these techniques face additional restrictions; NMP can only be performed at high reaction temperatures, is limited in monomer classes and requires expensive nitroxides. In the case of RAFT polymerizations, a broad range of monomers can be utilized but the RAFT agents required for the polymerization are expensive, not stable and can produce an unpleasant smell. The most important drawbacks of ATRP are the price and toxicity of the metal catalyst. To circumvent this problem, many different systems were developed during the last decades, eventually leading up to a Cu(0)-mediated polymerization, enabling high end group fidelities at high conversion and low catalyst loadings.[17-19]

Additional to the use of reversible deactivation radical polymerization, the synthesis of complex polymer architectures can be facilitated by implementing efficient reactions. Over the last 10 years, click chemistry has played an important aspect in the synthesis of these highly interesting structures by facilitating complicated procedures and tedious work-ups.[20] Kolb, Finn and Sharpless defined a precise set of criteria for a reaction to be considered as "click".[21] The reaction should be modular, wide in scope, high yielding, generate only inoffensive side-products, use only readily available starting materials and little amounts of benign solvents.[22] Recently, these aspects were reevaluated within the context of macromolecular science, taking into account the different needs and perspectives for polymers. Besides modularity, chemoselectivity, single reaction trajectory and wideness in scope, polymer "click" reactions

should proceed equimolar and enable large scale purification.[23] In the framework of this project, two *in-house* developed "click" chemistries were chosen for the synthesis of complex polymers; thiolactone and triazolinedione (TAD) chemistry.[24, 25] A thiolactone unit serves as a protected thiol which can be liberated upon reaction with an amine and react in a one-pot approach with an acrylate unit.[26] On the other hand, triazolinedione functionalities can be obtained by oxidation of the corresponding urazole unit and react rapidly with (di)enes *via* a Diels-Alder or Alder-ene reaction.[27] Both chemistries will be described in more detail in the next chapter.

The aim of this research project was the synthesis of advanced polymeric structures by the use of a Cu(0)-mediated polymerization system in combination with thiolactone and triazolinedione chemistry as efficient linking-methodologies to facilitate the design of these complex materials. More specifically, the synthesis of the complex structures will be directed towards the stabilization of pigment materials in water.

Outline

Chapter II provides a theoretical description on controlled radical polymerization methods with a major focus on copper mediated polymerization systems. An overview will be provided on the evolution of the different copper mediated polymerization systems leading to the development of a Cu(0)-mediated polymerization. Furthermore, a critical comparison will be provided between two resembling but argued to be different methods. Next, the different aspects of "click"-chemistry will be elaborated, focusing on thiolactone and triazolinedione chemistry as *in-house* developed methods. Finally, different methodologies in the synthesis of complex polymer architectures will be discussed and examples of their use as dispersants elaborated.

First, to gradually increase the complexity of the required synthesis, the double modification of polymer end groups *via* thiolactone chemistry will be evaluated in **chapter III**. Therefore, different polymers containing thiolactone end groups will be synthesized *via* Cu(0)-mediated polymerization of a thiolactone-containing initiator or end group modification reaction *via* a thiolactone-containing isocyanate. Next, a model study will be performed regarding the double modification reaction in a one-pot approach in which the amine opens the thiolactone ring,

releasing the thiol which on its turn will react with the acrylate moiety. Furthermore, a library of different chemical functionalities will be introduced by variation of the amine and acrylate structure. Finally amphiphilic block copolymers will be prepared by linking of a polymeric hydrophilic amine with a hydrophobic thiolactone end functionalized polymer.

In **chapter IV** the complexity of the polymer synthesis will be further increased by the synthesis of precision macromolecular line-ups, which are multisegmented block copolymers containing chemical functionalities between each segment connection well-located along the polymer backbone. Therefore, a hetero-telechelic polymer containing a thiolactone and acrylate functionality will be synthesized *via* Cu(0)-mediated polymerization and subsequent end group modification reactions. Next, the multisegmented macromolecular line-up will be obtained *via* the nucleophilic ring-opening of the thiolactone unit by a functionalized amine and consecutive thiol-Michael addition. By the choice of the amine, a library of macromolecular structures will be obtained with functionalities equally spaced across the polymer backbone. Furthermore, the library of functionalities will be extended by post-polymerization modification reactions. Finally by introduction of a hydrophilic polymer amine at precise positions as side-chains on the hydrophobic backbone, precision multisegmented graft copolymers will be obtained. Additionally, by introducing sugar- or hydrogen-bonding units, the synthesis of glycosylated polymers or single chain polymeric nanoparticles will be enabled.

Finally the combination of a Cu(0)-mediated polymerization system and thiolactone chemistry will be utilized in **chapter V** for the synthesis of two interesting complex architectures, amphiphilic graft and toothbrush copolymers. Regarding the synthesis of the graft copolymers, a series of hydrophobic copolymers containing a varying amount of a thiolactone-units will be synthesized. Next, the graft copolymer will be obtained by coupling of the functionalized backbone with the hydrophilic PEO-acrylate. For the synthesis of the toothbrush structures, a series of different block copolymers will be synthesized containing a protected hydrophilic segment and a copolymer with varying amounts of the thiolactone units in a one-pot procedure. The toothbrush structures will be obtained by coupling of the block copolymer with a hydrophobic polymer containing acrylate end groups, obtained *via* post-polymerization

modification and deprotection of the hydrophilic segment. Finally, dispersion tests will be performed to evaluate the material properties of these structures.

Chapter VI as last experimental chapter will utilize TAD-chemistry for the synthesis of block, graft and toothbrush structures. For the synthesis of the block copolymers, polymers containing TAD and ene end groups will be obtained by Cu(0)-mediated polymerization and subsequent end group modification reaction. Regarding the synthesis of the graft copolymers, a series of hydrophobic copolymers containing a varying amount of "ene"-units and hydrophilic polymers containing TAD end groups will be synthesized. Next, the graft copolymer will be obtained by coupling of the polymer units. For the synthesis of the toothbrush structures, a series of different block copolymers will be synthesized containing a protected hydrophilic segment and a copolymer with varying amounts of "ene" units in a one-pot procedure. The toothbrush structure will be obtained by coupling of the block copolymer with hydrophobic segments containing TAD end groups and deprotection of the hydrophilic segment. Again, dispersion tests will be performed to evaluate the material properties of these structures.

References

1. Plastics - the facts 2011. In *An analysis of European plastics production, demand and recovery for 2010*, PlasticsEurope, Ed. PlasticsEurope: 2011.
2. Lutz, J. F.; Lehn, J. M.; Meijer, E. W.; Matyjaszewski, K. *Nature Reviews Materials* **2016,** 1, (5).
3. Hadjichristidis, N.; Pitsikalis, M.; Pispas, S.; Iatrou, H. *Chemical Reviews* **2001,** 101, (12), 3747-3792.
4. Fournier, D.; Hoogenboom, R.; Schubert, U. S. *Chemical Society Reviews* **2007,** 36, (8), 1369-1380.
5. Sheiko, S. S.; Sumerlin, B. S.; Matyjaszewski, K. *Progress in Polymer Science* **2008,** 33, (7), 759-785.
6. Petton, L.; Mes, E. P. C.; Van Der Wal, H.; Claessens, S.; Van Damme, F.; Verbrugghe, S.; Du Prez, F. E. *Polymer Chemistry* **2013,** 4, (17), 4697-4709.
7. Verdonck, B.; Goethals, E. J.; Du Prez, F. E. *Macromolecular Chemistry and Physics* **2003,** 204, (17), 2090-2098.
8. Verbrugghe, S.; Bernaerts, K.; Du Prez, F. E. *Macromolecular Chemistry and Physics* **2003,** 204, (9), 1217-1225.
9. Matyjaszewski, K., *Controlled Radical Polymerization*. American Chemical Society: 1998; Vol. 685, p 500.
10. Grishin, D.; Grishin, I. *Russian Journal of Applied Chemistry* **2011,** 84, (12), 2021-2028.

11. Wang, J. S.; Matyjaszewski, K. *Journal of the American Chemical Society* **1995,** 117, (20), 5614-5615.
12. Hawker, C. J.; Bosman, A. W.; Harth, E. *Chemical Reviews* **2001,** 101, (12), 3661-3688.
13. Chiefari, J.; Chong, Y. K.; Ercole, F.; Krstina, J.; Jeffery, J.; Le, T. P. T.; Mayadunne, R. T. A.; Meijs, G. F.; Moad, C. L.; Moad, G.; Rizzardo, E.; Thang, S. H. *Macromolecules* **1998,** 31, (16), 5559-5562.
14. Matyjaszewski, K.; Spanswick, J. *Materials Today* **2005,** 8, (3), 26-33.
15. Braunecker, W. A.; Matyjaszewski, K. *Progress in Polymer Science* **2007,** 32, (1), 93-146.
16. Destarac, M. *Macromolecular Reaction Engineering* **2010,** 4, (3-4), 165-179.
17. Percec, V.; Guliashvili, T.; Ladislaw, J. S.; Wistrand, A.; Stjerndahl, A.; Sienkowska, M. J.; Monteiro, M. J.; Sahoo, S. *Journal of the American Chemical Society* **2006,** 128, (43), 14156-14165.
18. Rosen, B. M.; Percec, V. *Chemical Reviews* **2009,** 109, (11), 5069-5119.
19. Konkolewicz, D.; Wang, Y.; Krys, P.; Zhong, M.; Isse, A. A.; Gennaro, A.; Matyjaszewski, K. *Polymer Chemistry* **2014,** 5, (15), 4396-4417.
20. Espeel, P.; Du Prez, F. E. *Macromolecules* **2015,** 48, (1), 2-14.
21. Kolb, H. C.; Finn, M. G.; Sharpless, K. B. *Angewandte Chemie International Edition* **2001,** 40, (11), 2004-2021.
22. Hawker, C. J.; Fokin, V. V.; Finn, M. G.; Sharpless, K. B. *Australian Journal of Chemistry* **2007,** 60, (6), 381-383.
23. Barner-Kowollik, C.; Du Prez, F. E.; Espeel, P.; Hawker, C. J.; Junkers, T.; Schlaad, H.; Van Camp, W. *Angewandte Chemie International Edition* **2011,** 50, (1), 60-62.
24. Espeel, P.; Du Prez, F. E. *European Polymer Journal* **2015,** 62, (0), 247-272.
25. De Bruycker, K.; Billiet, S.; Houck, H. A.; Chattopadhyay, S.; Winne, J. M.; Du Prez, F. E. *Chemical Reviews* **2016,** 116, (6), 3919-3974.
26. Espeel, P.; Goethals, F.; Du Prez, F. E. *Journal of the American Chemical Society* **2011,** 133, (6), 1678-1681.
27. Billiet, S.; De Bruycker, K.; Driessen, F.; Goossens, H.; Van Speybroeck, V.; Winne, J. M.; Du Prez, F. E. *Nat. Chem.* **2014,** 6, (9), 815-821.

Abstract

Maintaining a high level of control over the polymer structure is an important issue in advanced macromolecular engineering. During the last decades, various complex copolymer architectures were explored for different (commercial) applications. The progress in controlled (radical) polymerization techniques accelerated the development of various synthetic strategies in order to obtain these materials. Combining these methods with the toolbox of different efficient chemistries or "click" reactions available, enables polymer chemists to elaborate chemical procedures in order to obtain the desired structures in a straightforward manner. Furthermore, by thorough investigations of the structure-property relations of the different polymeric compounds, the time required to fulfil commercial applications criteria can be shortened significantly. In this chapter, an overview will be given on different controlled radical polymerization techniques available, with a major focus of Cu(0)-mediated RDRP, an industrial relevant method. Furthermore, the concept of "click"-chemistry will be explained and followed by synthetic strategies to obtain complex polymeric structures which can be used *e.g.* as dispersing materials.

Chapter II.

Theoretical description on reversible deactivation radical polymerization, click chemistry and complex polymer structures

II.1 Reversible Deactivation Radical Polymerization methods

II.1.1 Introduction

For decades, the synthesis of bulk polymer materials as polyethylene (PE), polystyrene (PS), or poly(methyl methacrylate) (PMMA) was performed *via* conventional free radical polymerization methods (FRP).[1] Today, nearly half of all commercial synthetic polymers are prepared applying radical chemistry, providing a platform for daily life materials which can be retrieved in a broad range of markets.[2] However, the low control over key elements such as the reactivity of propagating radicals and chain deactivation, limits the synthesis of well-defined complex polymer structures by preventing control over molecular weight, chain composition, dispersity and end-group functionality.[3]

Due to the reactive nature of these radical species, the demand for more controlled systems raised. As a result of extensive research in both academia and industry during the last 50 years, several methodologies for the controlled synthesis of complex macromolecules were developed (depicted as 'living'/controlled polymerizations).[4-6] These techniques allowed polymer chemists to design well-defined polymer structures with a variety of architectures, chain or end-group compositions etc. leading to well-controlled structure-property relations and thus creating an unprecedented advancement in material design.[7]

II.1.2 Criteria for a 'living'/controlled polymerization

The definition of the term 'living' polymerization was presented by Szwarc *et al.*[8] for the first time in 1956 as a chain growth polymerization without the occurrence of irreversible termination or transfer reactions. Under these circumstances, polymer chains will grow after the event of initiation until all monomer is consumed. In this way, a well-defined polymeric structure is obtained with control over initiator-, polymer- and end-group composition, enabling the synthesis of well-defined (multi)block copolymers when adding a next aliquot of monomer after full conversion of the previous one.

Additional prerequisites for 'living' polymerizations include[9-11]:

- Full consumption of the initiator, with every initiating group inducing the formation of one polymer chain, enabling control over the degree of polymerization (DP_n) and corresponding molecular weight by the ratio of monomer to initiator concentration ($DP_n = [M]/[I]$). Furthermore, initiation should be fast compared to propagation.
- Narrow distribution of molecular weight ($1.0 < Đ < 1.5$) and close to Poisson distribution $Đ \approx 1 + 1/DP_n$
- High end-group fidelity

Although some systems fulfill all these criteria, transfer or termination events cannot always be fully excluded (especially in radical-based systems), therefore the term controlled polymerization can sometimes be more appropriate.

Practically, kinetic measurements are performed to evaluate the controlled nature of (new) polymerization systems. Measurements determining conversion, molecular weight and dispersity (Đ) over time are performed and represented in different graphical illustrations (Figure II.1). To define a controlled polymerization, a system should meet the following requirements:

- A first order polymerization rate, evidenced by a linear evolution of $Ln([M]_0/[M]_t)$ vs. time, indicating a constant concentration of active centers during the polymerization process. In the ideal case, a linear curve will be

obtained, however a slow initiation will induce an acceleration of the polymerization over time, while termination events will delay the reaction, except for Reversible Addition Fragmentation Transfer (RAFT) polymerizations. During the process, a pre-equilibrium occurs, leading to a growing concentration of radicals until chain equilibration is reached (paragraph II.1.5).[12]

- The evolution of molecular weight (or DP_n) as a function of conversion should be linear. A decrease in molecular weight will indicate transfer reactions, while an increase will imply slow initiation effects or termination by recombination.
- A decrease of dispersity as a function of conversion since a significant increase typically indicates termination or transfer reactions.

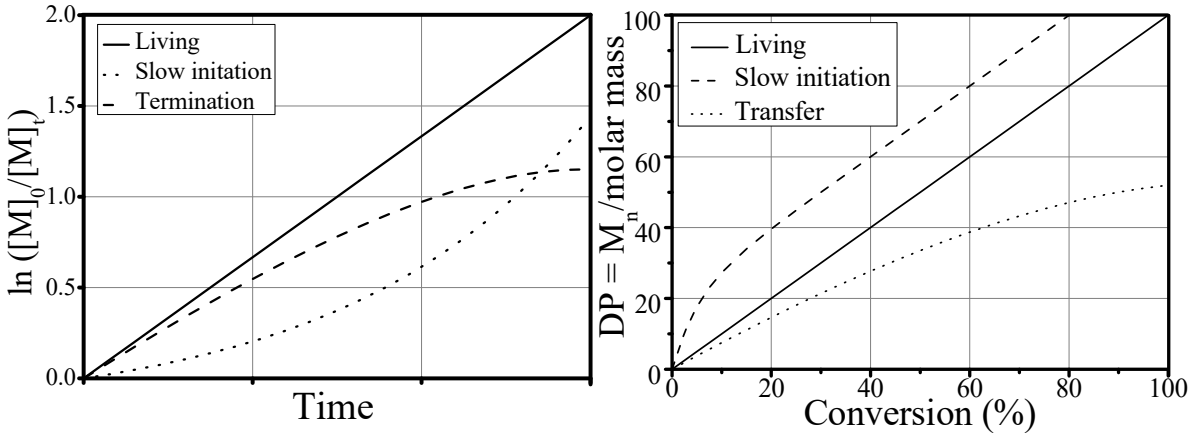

Figure II. 1: Evolution of Ln($[M]_0/[M]_t$) vs. time (left) and molecular weight or DP_n vs. conversion (right) for a controlled polymerization, including effects of slow initiation, termination and transfer.

Over time, different systems were developed and classified as controlled/'living' polymerization reactions. These methodologies can be divided in two major systems, ionic[13, 14] (cationic or anionic)-based polymerizations and radical-based reactions[15]. For a long time, only living ionic polymerization systems were available for the polymerization of vinyl monomers. However, the lack of tolerance of these polymerization systems towards protic species significantly reduced the library of monomers that can be polymerized *via* these methods due to the limited functional group tolerance. Additionally, the stringent purity obligations, mandatory for these reactions, limit the practical applicability of these methods.

These reasons mainly explain the popularity of radical based systems as controlled polymerization reactions. However, due to the inherent use of radicals, reversible deactivation

radical polymerization (RDRP) reactions should never be defined as truly living systems as radicals can easily terminate by recombination compared to ionic systems.

II.1.3 The development of a reversible deactivation radical polymerization

The limited control in FRP processes is mainly due to the high concentration of radicals during the polymerization ($[P_n^{\bullet}]$), inducing a significant amount of termination and transfer events, which makes it impossible to obtain well-defined structures. Minimizing the concentration of radicals during the polymerization has a significant benefit on the control of the reaction as termination reactions are second order in rate with respect to the growing radical chains ($R_t = 2k_t[P_n^{\bullet}]^2$) compared to propagation, which follows a first order kinetic ($R_p = k_p[P_n^{\bullet}][M]$). Thus, termination can be significantly reduced by preserving a low radical concentration during the polymerization (~ 10^{-7} – 10^{-8}M).[16, 17]

The creation of a quick and dynamic equilibrium between 'dormant' and 'active' species of the propagating chain is a possible way to lower the concentration of radicals (Figure II.2). With this strategy, the polymer will be unable to propagate or terminate in the 'dormant' state (P_n-X) compared to the 'active' situation ($P_n^{\bullet}$). In time, several RDRP methodologies were developed, based on this dynamic equilibrium: Copper-mediated polymerization systems[18], Nitroxide Mediated Polymerization (NMP)[19], Catalytic Chain Transfer Polymerization (CCTP)[20] etc.

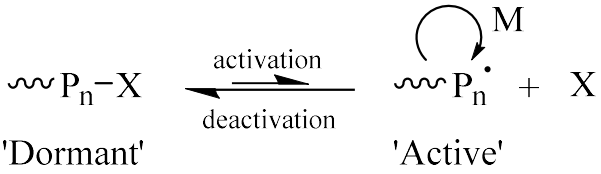

Figure II. 2: Dynamic equilibrium between the 'dormant' and 'active' state, preserving a low radical concentration.

Otherwise, the amount of termination events can be significantly reduced by applying a degenerative chain transfer mechanism (Figure II.3). In this case, the majority of chains are dormant species that take part in transfer/exchange reactions. This mechanism is mainly applicable to Reversible Addition Fragmentation Transfer (RAFT) polymerization.[21]

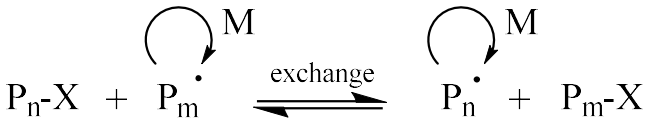

Figure II. 3: Degenerative chain transfer mechanism to retain a majority of 'dormant' species.

As NMP, RAFT and Copper-mediated polymerization systems are considered to be the most promising methods developed over the past 20 years, these techniques will be highlighted in the following paragraphs with a major focus on Copper-mediated systems since these approaches are the main subject of this dissertation.

II.1.4 Nitroxide Mediated Polymerization (NMP)

Nitroxide Mediated Polymerization (NMP) is probably considered as the most simple polymerization method from a mechanistically point of view. As reported for the first time in 1982 by Solomon *and coworkers*[19], nitroxides are capable of stable radical formation and trapping of carbon centered radicals. At low temperature, the introduced alkoxyamine is stable and considered as 'dormant' (Figure II.4). At elevated temperature, the carbon-oxide bond will cleave homolytically and proceed to the 'active' state with formation of the propagating radical and nitroxide. In brief, NMP is a controlled polymerization technique where a dynamic equilibrium between the 'dormant' alkoxyamine and the 'active' propagating radical and nitroxide is obtained at elevated temperature.[22-24]

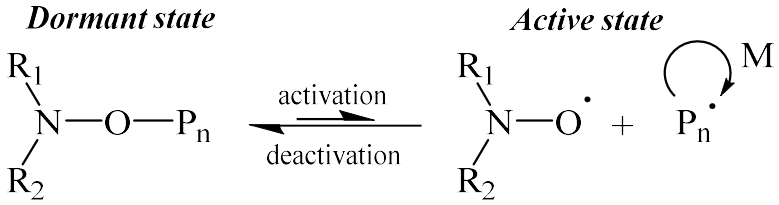

Figure II. 4: Dynamic equilibrium between the dormant and active state in NMP.

During the polymerization, the nitroxide should not react with itself in order to obtain a proper controlled system, therefore, typical NMP-agents are sterically hindered nitroxides such as 2,2,6,6-tetramethylpiperidinyl-1-oxy (TEMPO)[25] or N-*tert*-butyl-N-(1-diethylphosphono-2,2-dimethylpropyl)nitroxide (SG1)[26](Figure II.5). Initially, TEMPO was the most used NMP-agent and was applied for the controlled synthesis of complex styrenic architectures. However, TEMPO fails to mediate the polymerization of other monomer classes such as (meth)acrylates or acrylamides. In time, other NMP-agents such as SG1 were developed and they were capable of

properly mediating the polymerization of acrylate-based systems.[27] NMP can also be used for the polymerization of methacrylates, but due to termination events, e.g. disproportionation, copolymerization of methacrylates with acrylic or styrenic monomers should be performed. NMP is typically performed at temperatures above 100°C for TEMPO or 80-90°C for SG-1. A few years ago, new NMP agents were developed, enabling the polymerization of methacrylates at 40-50°C.[28] In general, NMP is a very interesting RDRP-methodology but mainly applicable to styrenic and acrylate derivatives.[29] Furthermore, commercial availability and high cost of these NMP-agents lowers the industrial relevance of this method.

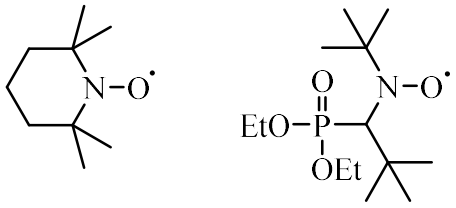

Figure II. 5: Chemical structures of TEMPO (left) and SG1 as stable free nitroxides.

II.1.5 Reversible Addition Fragmentation Transfer (RAFT) Polymerization

During RAFT polymerizations (Figure II.6), initiation occurs in the same manner as conventional free radical polymerization, by the use of a radical initiator e.g. α,α'-AzoIsoButyroNitrile (AIBN). During the start of the polymerization, propagating radicals ($P_n^\bullet$) will attack the thiocarbonylthio compound, a chain transfer agent (CTA) present in the reaction mixture. In this way, an intermediate radical adduct is created, which in turn will fragment to a polymeric thiocarbonylthio compound and a new radical species ($R^\bullet$). This new radical structure will subsequently reinitiate, producing a new propagating radical ($P_m^\bullet$). In the consecutive event of addition-fragmentation reactions, a rapid and dynamic equilibrium is established between the propagating radicals ($P_n^\bullet$ and $P_m^\bullet$) and dormant chains, allowing an equal probability of the polymeric chains to grow and ensuring a low dispersity at the end of the polymerization. Furthermore, as a result of constant fragmentation and transfer reactions during chain equilibration, radicals are neither created nor destroyed, but the majority of chains will be end-capped with thiocarbonylthio functionalities during the polymerization. During this process termination events are minimized.

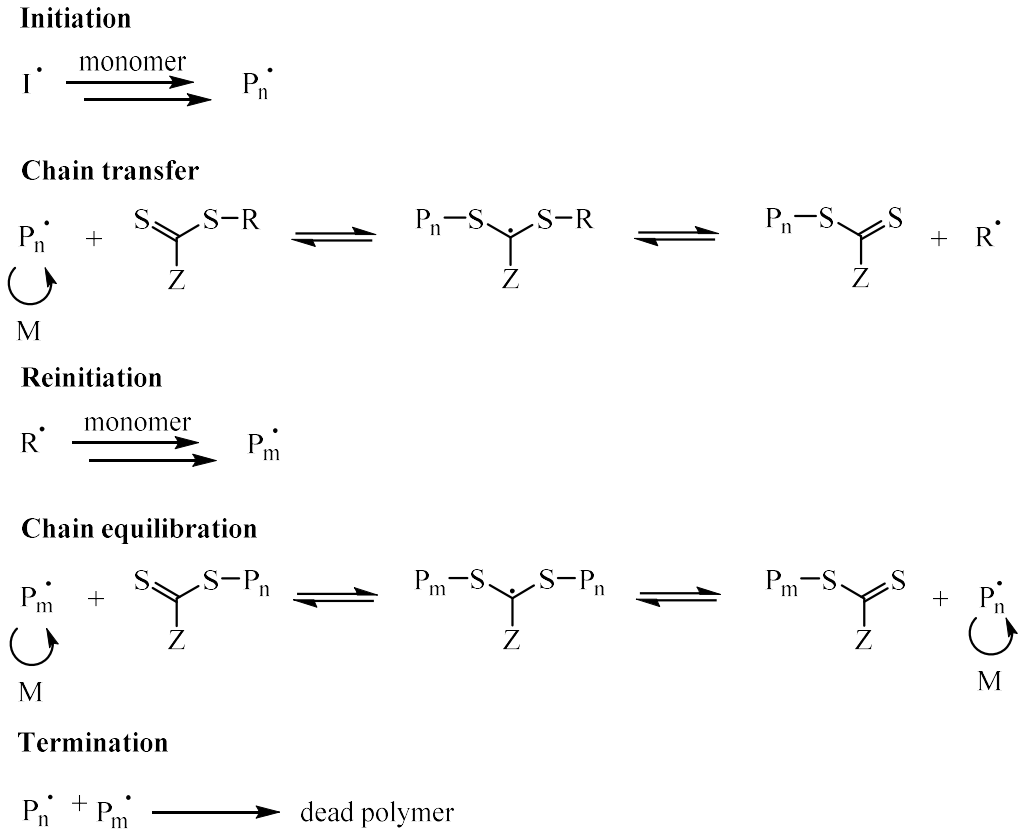

Figure II. 6: Mechanism of Reversible Addition Fragmentation Transfer (RAFT) polymerization.

In general, RAFT-agents are thiocarbonylthio compounds[30, 31], in which the Z-functionality (typically aryl, alkyl, …) is used to control the reactivity of the RAFT-agent with respect to the monomer, while the R moiety is the radical leaving group (-$C(CH_3)_2CN$, -$C(CH_3)_2Ar$, …) and needs to be capable of sufficient reinitiation of the monomer. In time, four different classes of RAFT-agents were developed to properly mediate the polymerization of a broad range of monomers: dithioesters, trithiocarbonates, dithiocarbamates and xanthates (Figure II.7). Trithiocarbamates are mainly used in the polymerization of styrenics, acrylates or acrylamides, while dithiocarbamates are selected when opting for methacrylates or methacrylamides. In case the polymerization of less activated monomers as vinyl esters or vinyl amides is desired, typically dithiocarbamates or xanthates are chosen. The use of the latter is also known as MAcromolecular Design *via* the Interchange of Xanthates (MADIX)[32].

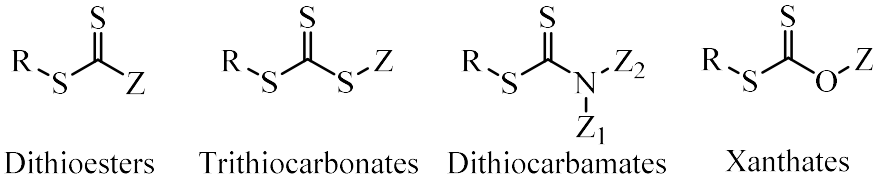

Figure II. 7: Representation of the four different classes of RAFT-agents.

In conclusion, RAFT-polymerization is a very versatile technique, applicable to a broad range of monomers with a high tolerance towards different functionalities (alcohols, acids, amides …). However, the instability and cost of RAFT-agents in combination with the synthetic struggle to obtain these compounds is still a hurdle for RAFT-involved projects to advance to industrial applications.

II.1.6 Copper-mediated polymerization

II.1.6.1 Introduction

The development of copper-mediated polymerization reactions initially originate from Atom Transfer Radical Addition (ATRA)[33] or the Kharasch reaction[34], in which an organic halide reacts with a double bound, catalyzed by a metallic species (Figure II.8). During this reaction, a transition metal catalyst ($M_t^nX_n$) donates one electron to an organic substrate with simultaneous abstraction of a halogen atom from the same substrate (R-X). In this way, a radical is generated ($R^\bullet$), together with the transition metal in a higher oxidation state ($M_t^{n+1}X_{n+1}$). After the addition of the radical to the alkene, the reverse reaction from the transition metal to the substrate will occur with consequent transfer of an electron from the substrate to the transition metal and donation of the halogen atom to the substrate, generating the desired compound.

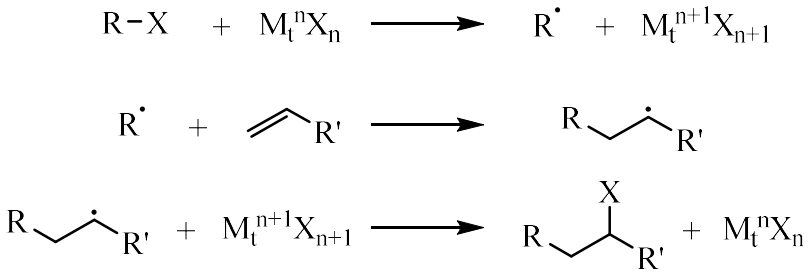

Figure II. 8: Reaction mechanism of Atom Transfer Radical Addition (ATRA).

During ATRA, only one single addition of the organic halide to the substrate is possible, since the radical intermediate is less stabilized compared to the radical starting compound, leading to an irreversible reaction with the transition metal, yielding the halide-bound end-structure. In 1995, the concept of ATRA was broadened to a polymer level by adjusting the reactivity of the initial and intermediate radical adduct. In this way, the persistent radical will propagate to more than one alkene unit. Matyjaszewski *and coworkers* demonstrated this concept by polymerizing styrene using a copper(I) catalyst.[35] Around the same time, Sawamoto *and coworkers* developed a similar system in which the controlled polymerization of methyl methacrylate was described applying a ruthenium(II) catalyst.[36]

II.1.6.2 Atom Transfer Radical Polymerization (ATRP)

In classical ATRP, a cuprous halide species ($Cu^{I}X$, with X = Br, Cl) is combined with a nitrogen based ligand (L) to obtain the transition metal complex ($[M_t^m(L)X]$ (Figure II.9). These ligands can be differentiated between σ-donors (*e.g. N,N,N',N'',N''*-pentamethyldiethylenetriamine (PMDETA), *N,N,N',N',N'',N''*-hexamethyltris(aminoethyl)amine) (Me_6TREN), 1,1,4,7,10,10-hexamethyltriethylenetetramine (HMTETA) …) or π-acceptors (bipyridine (Bpy), pyridine-imines).[37]

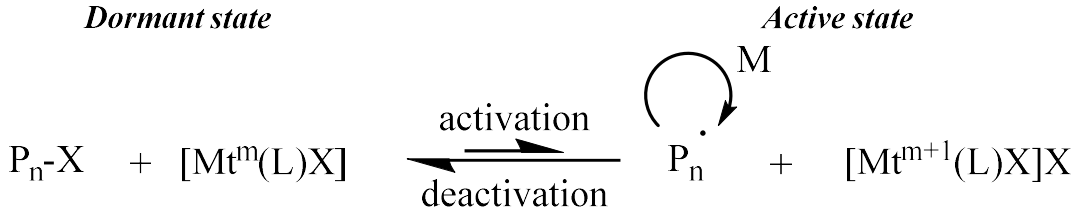

Figure II. 9: Reaction mechanism of Atom Transfer Radical Polymerization.

The organic halide or dormant polymer chain (P_n-X) can react with the transition-metal catalyst ($[M_t^m(L)X]$) *via* an inner-sphere electron transfer, yielding the active propagating radical ($P_n^{\bullet}$) and a deactivating complex ($[M_t^{m+1}(L)X]X$) with the metal in a higher oxidation state (persistent species). As usual, the dormant state is more favored compared to the active state at equilibrium to enhance control over molecular weight and chain-end fidelity. In the active state, the polymer will grow by monomer addition to the propagating radical. Termination can occur by bimolecular coupling or disproportionation. However, due to the dynamic equilibrium between

the active and dormant state, the concentration of radicals remains low during the polymerization and therefore only a few percent of the polymer chains undergo termination or transfer reactions. In view of these side reactions, ATRP and copper-mediated polymerizations in general are typically described as controlled systems, rather than living processes.[38]

Although copper is the most widely used metal when performing typical ATRP experiments, other metals received a significant amount of attention during the last decades. There are numerous examples that are applying transition metals as molybdenum[39], rhenium[40], iron[41], nickel[42] and palladium[43]. In general, ATRP is applicable to a wide range of monomers as (meth)acrylates[44, 45], styrene[46], (meth)acrylamides[47, 48] and acrylonitrile[49]. Furthermore, different halogen-based initiator structures can be applied in ATRP as halogenated alkanes, benzylic halides, sulfonyl halides, haloesters, halonitriles and haloketones. Depending on the class of monomer, different initiator efficiencies are obtained, leading to various levels of control. Finally, a polymer will be obtained containing a halogen end group, which can be applied in a broad range of end group transformations. The halogen can be removed by reaction with trialkyltin hydrides and AIBN or be displaced by nucleophilic substitution reaction with e.g. thiols or azides.[38]

Despite the success of ATRP as one of the most used systems for controlled polymerizations, significant issues can emerge, depending on the specific combination applied (monomer, solvent, catalyst…), leading to a loss of control over the reaction (termination, transfer, …). During the last years, different adaptations of classical ATRP were developed to improve the level of control over the polymerization system and the quality of the products obtained.

II.1.6.3 Evolution of copper-mediated polymerization systems

In classical ATRP, a considerable amount of copper catalyst is required to enable a proper control of the polymerization, leading to colored and toxic end-products if no proper purification step is performed. An appropriate balancing of the amount and type of catalyst is indispensable, as it has a major influence on the polymerization kinetics and consequent control over molecular

weight and end-group fidelity. In time, several derivatives of classical ATRP were developed, mainly focusing on the redox equilibrium between the metal in a lower or higher oxidation state (Figure II.10). This equilibrium can be tuned by applying external stimuli, favoring one of the two oxidation states.

A major step to improve control over the polymerization and lower the amount of catalyst was the development of reverse ATRP. In this method, the metal is added in a higher oxidation state [M_t^{n+1}(L)X] and converted to the active species [M_t^n(L)X] by reaction with a radical initiator (*e.g.* AIBN), which also acts as an initiator of the polymerization. However, due to the absence of an organic halide as initiator, the concentration of [M_t^{n+1}(L)X] should equal and preferably exceed the amount of radical initiator to enable a proper control. Additionally, the requirement of a radical initiator hampers the synthesis of well-defined block copolymers. To overcome these problems, simultaneous normal and reverse initiation (SR&NI) ATRP was developed. This technique comprises a dual initiation system: a free radical initiator (*cfr.* reverse ATRP) and an organic halide as initiator. Radicals are generated by conventional initiation and deactivated by the metal complex in a higher oxidation state [M_t^{n+1}(L)X] (present in low concentrations), generating [M_t^n(L)X], which in turn will activate the organic halide and subsequently initiate the polymerization. This method allows for a proper control of the polymerization and synthesis of block copolymers. However, it should be noted that the use of a few percentages of radical initiator will lead to a partial loss of end-group fidelity. To overcome this drawback, activators generated by electron transfer (AGET) ATRP was introduced. In this method, a stoichiometric amount of reducing agent, which is not a radical initiator, is used to reduce the metal in a higher oxidation state [M_t^{n+1}(L)X] and generate the activator [M_t^n(L)X]. This activator will then subsequently start the polymerization in the same manner as conventional ATRP. Typical reducing agents include tin 2-ethylhexanoate, ascorbic acid, zero-valent metals or triethylamine. Furthermore, this method is generally less air-sensitive as small amounts of [M_t^n(L)X] oxidized by air can be reduced by the excess of reducing agent.

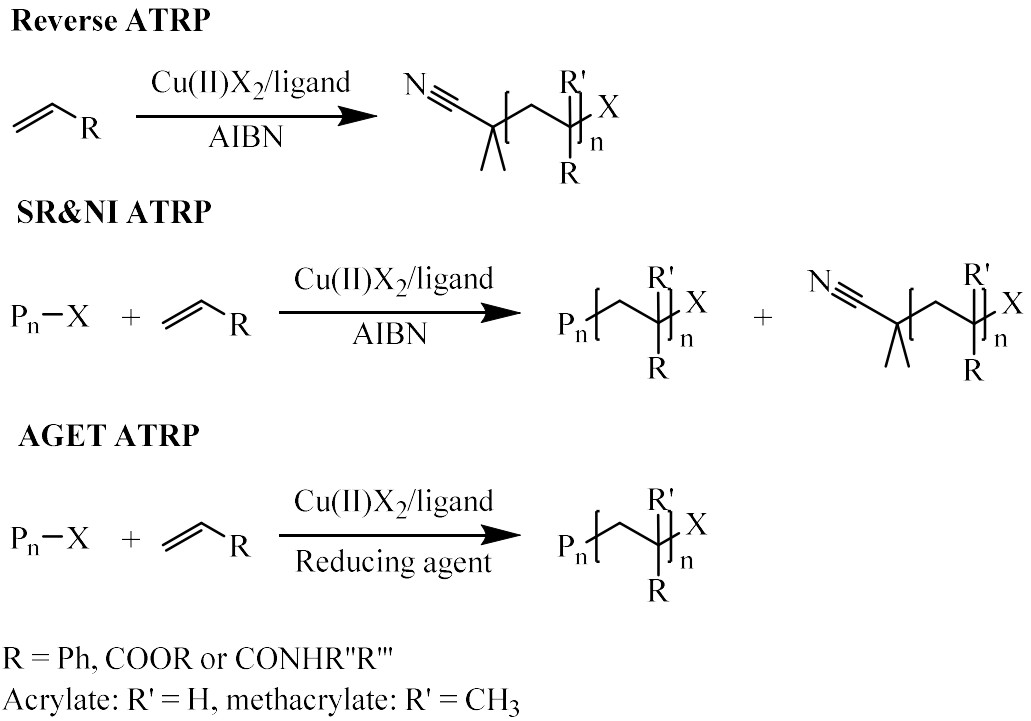

Figure II. 10: Schematic representation of reverse, SR&NI and AGET ATRP.

In order to further decrease the amount of catalyst to values in the order of 50 ppm, initiators for continuous activator regeneration (ICAR) ATRP was developed (Figure II.11). Again a radical initiator is used, which will slowly generate a small amount of propagating radicals and simultaneously reduce the metal in a higher oxidation state $[M_t^{n+1}(L)X]$ to generate the activator $[M_t^n(L)X]$ in small quantities. However, ICAR is significantly different from SR&NI ATRP by the fact that it requires a large excess of free radical initiator compared to the catalyst and radicals are slowly generated during the polymerization. Moreover, the use of a free radical initiator will still inevitably decrease the end-group fidelity.

Therefore atoms generated by electron transfer (ARGET) ATRP was developed, in which small quantities of reducing agent are used to introduce a low amount of active catalyst which will properly mediate the polymerization by keeping a low concentration of propagating radicals. The last years, zero-valent metals (Cu, Zn, Fe, Mg) became particularly popular as reducing agents, as these moieties can act both as supplementary activator and reducing agent (SARA-ATRP). This technique will be explained in more detail in paragraph II.1.6.5.

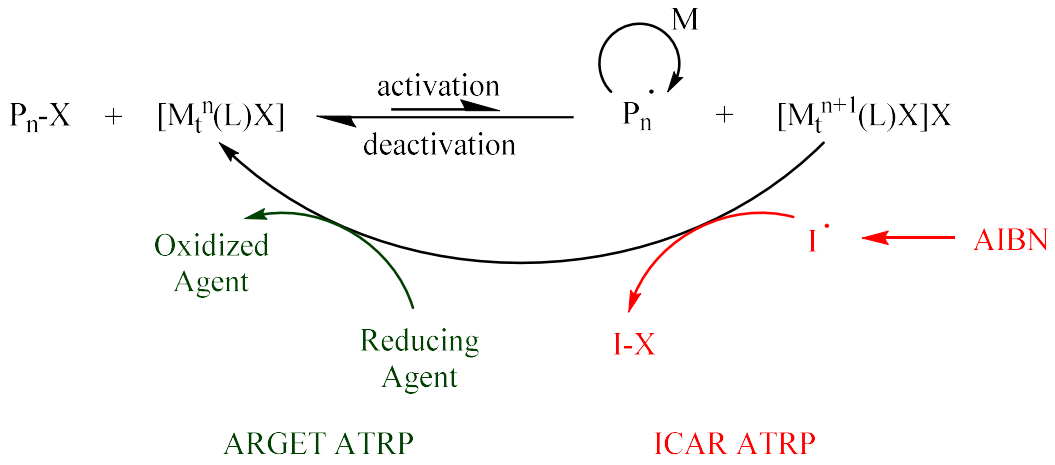

Figure II. 11: Schematic representation of ARGET and ICAR ATRP.

Besides the use of additives, ATRP and more specifically the activation/deactivation process can also be mediated by the use of external stimuli. Recently, Matyjaszewski *and coworkers* evidenced that an electric current (*e*-ATRP) can be applied to control the redox process between the metal in a lower and higher oxidation state, which in turn will control the concentration of propagating radicals. Furthermore, by the use of an electric current, the final concentration of copper in the polymer can be reduced by controlling the current and depositing the copper on the grid at the end of the polymerization. Additionally, the fact that this polymerization can be easily switched "on" and "off", still keeping a good control over the polymerization, introduces an extra dimension to ATRP.[50]

ATRP can be mediated not only with an electric current but also with light, which introduce a non-invasive temporal control over the process. For instance, different methods applying copper and iridium based complexes, or phenothiazines, as catalyst, to mediate the polymerization were developed by Yagci[51], Hawker[52], Haddleton[53, 54] and their *coworkers*. Furthermore, it was shown that the polymerizations could be performed at very low catalyst loadings by the use of this photo-mediated radical polymerization (~ 10 ppb), while maintaining a good control.[55]

II.1.6.4 Single Electron Transfer Living Radical Polymerization

The implementation of zero-valent metals in copper-mediated polymerizations became an effective tool for the synthesis of polymeric materials with a controlled structure and properties. However, a clear breakthrough of the power of this strategy only started after a report from Percec *et al.*[56] on the "ultrafast" synthesis of "ultrahigh" molecular weight polymers by the use of Single Electron Transfer Living Radical Polymerization (SET-LRP). Furthermore, straightforward reaction conditions, colorless end-products with low amounts of copper and high end group fidelities at high monomer conversion were obtained, enabling the polymerization of (meth)acrylates, (meth)acrylamides, styrene, acrylonitrile or vinyl chlorides [57-61].

Mechanistically, SET-LRP has some resemblances with ARGET-ATRP but is significantly different on certain aspects. The proposed reaction mechanism can be distinguished by four different processes (Figure II.12)[62-65]:

- Activation of the initiator/dormant chain by Cu(0) through a heterogeneous **single electron transfer** (SET) with *in situ* formation of Cu(I)X(L)
- **Disproportionation** of *in situ* Cu(I)X(L) to Cu(0) and Cu(II)X_2(L), providing a self-regulated regeneration of Cu(0) and Cu(II)
- **Propagation** of the growing polymer chain
- **Deactivation** of the propagating polymer radical chain by Cu(II)X_2(L), with *in situ* formation of Cu(I)X(L)

Each of these steps are influenced by parameters related to the choice of initiator, metal catalyst, ligand and solvent. These parameters will be explained in more detail in the next paragraph.

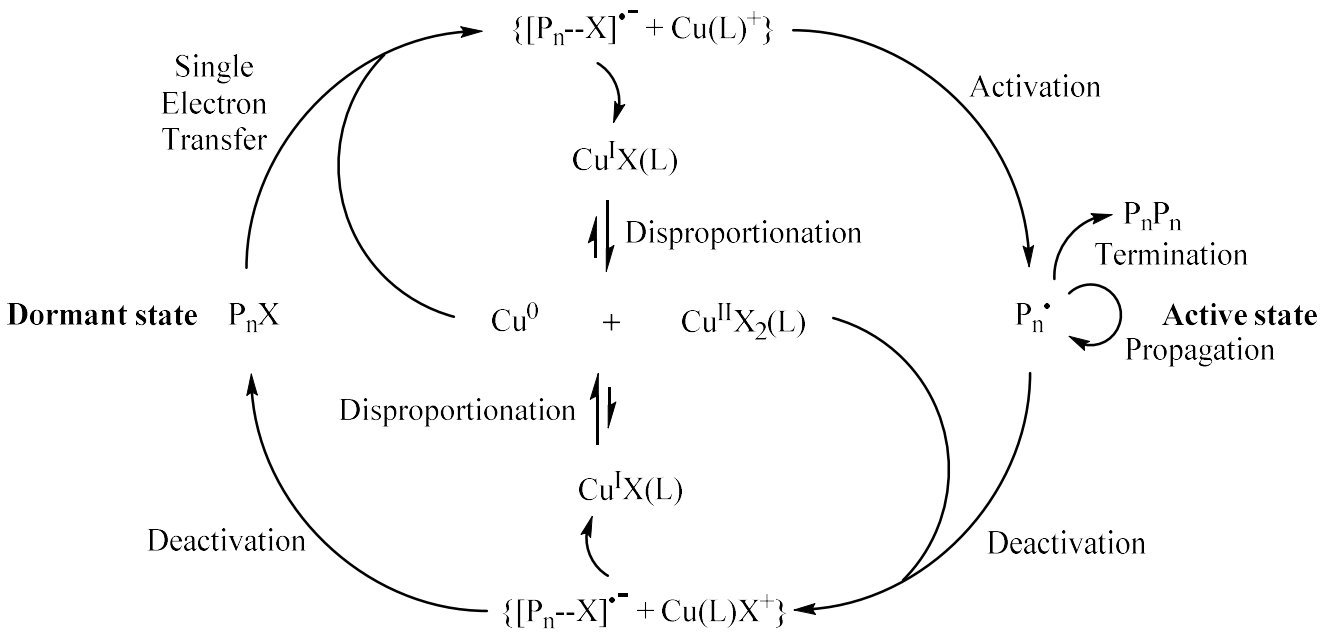

Figure II. 12: Proposed mechanism for SET-LRP reactions.

Alike ATRP, the choice of initiator for SET-LRP is crucial to obtain a well-controlled process. In general, bromo-initiators are applied except for methacrylates, in which case chloro-initiators are preferred. In most situations, the initiating organic halide is selected based on the structure/reactivity of the propagating monomer, and can be divided into different classes: haloforms ($CHCl_3$, $CHBr_3$), α-haloesters, sulfonyl halides (easily prone to side reactions) etc..[66-68] However, in this dissertation α-haloesters such as α-bromoisobutyrates and 2-bromopropionates were preferred due to their general applicability. As SET-LRP is frequently used in the synthesis of complex structures, the introduction of functional initiators enables further modification reactions, it. disulfide-containing initiators for nucleophilic thiol-ene "click"-chemistry[69, 70], substitution of the bromine *via* thio-bromo reaction[71, 72] or macro-initiators derived from poly(ethylene oxide) (PEO)[73].

The disproportionation step is essential to the polymerizations *via* SET-LRP, providing the formation of activated and deactivated species. Without this reaction, no control over the polymerization is obtained due to loss of persistent species and increase of the radical concentration. Depending on the applied ligand and polarity of the solvent, the equilibrium can be altered in favor of disproportionation or comproportionation.[74-78]

$$2\ Cu(I)X(L) \underset{\text{comproportionation}}{\overset{\text{disproportionation}}{\rightleftharpoons}} Cu(0) + Cu(II)X_2(L)$$

The addition of multidentate ligands, typically nitrogen based, is required to solubilize the metal catalyst. However, the polymerization properties can be strongly influenced by the ligand structure. Ligands such as Me_6TREN are able to adopt multiple geometries, an in-depth computational study indicated that Cu(II) with Me_6TREN will adopt a trigonal bipyramidal geometry as lowest energy conformation (Figure II.13 – left), while Cu(I) will be shaped into a trigonal pyramidal conformation (Figure II.13 – right). Furthermore, it was shown that under these circumstances, Cu(II) will be preferentially stabilized as a trigonal bipyramidal complex, which is lower in energy compared to a trigonal pyramidal conformation. Therefore, when Me_6TREN is applied, the equilibrium will be strongly shifted to the right.[79-82]

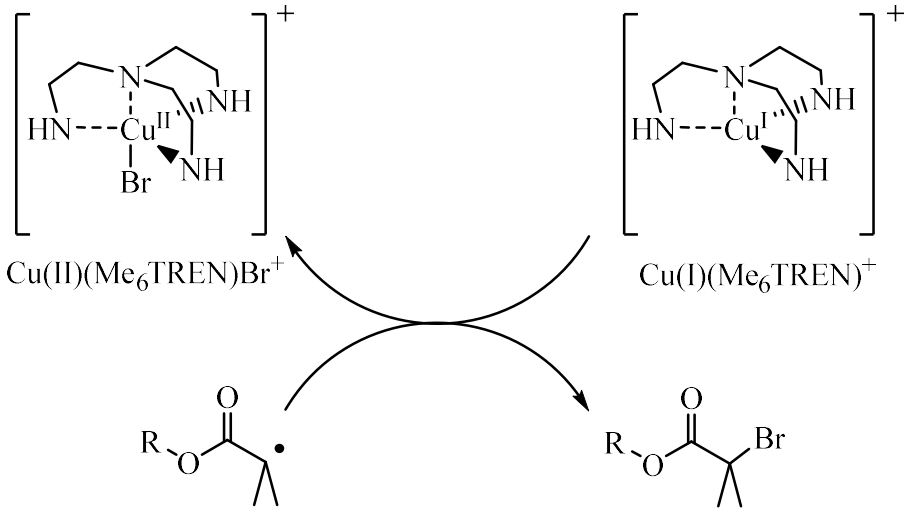

Figure II. 13: Trigonal pyramidal Cu(I) complex and trigonal bipyramidal Cu(II) complex.

As Cu(0) is crucial in these polymerizations, it can be utilized as powder or wire. It was shown that SET-LRP starts from a surface-mediated activation process, with an increased rate when smaller copper particles or wire with a smaller diameter were used (higher surface area). However, copper wire is typically preferred due to its recyclability and easy tuning of the reaction.[83-89]

Finally, the solvent plays also a major role in the polymerization. Highly polar solvents as water, *N,N*-dimethylformamide (DMF) or dimethyl sulfoxide (DMSO) will increase the solubility of the metal salts and favor the disproportionation over comproportionation, improving the control of

the reaction. However, monomers which are insoluble in these polar solvents cannot be polymerized. In these cases, isopropanol or mixtures of toluene/methanol or toluene/phenol can be preferred to mediate these polymerizations.[90-96]

II.1.6.5 SARA-ATRP vs. SET-LRP: A critical comparison

An intense debate started in 2006 between Matyjaszewski and Percec, from the moment the latter introduced the terminology of SET-LRP. Both research groups have published several articles, with a major focus on the reaction mechanism of Cu(0)-mediated polymerizations, each providing strong argumentations for two distinguished models: SARA-ATRP (Figure II.14, top) and SET-LRP (Figure II.14, bottom). The same species are involved in both methods, with a significant difference in equilibria and active concentrations of the different compounds.

In SARA-ATRP, Cu(I) is regarded as the major activator for alkyl halides, occurring *via* an Inner Sphere Electron Transfer (ISET) process. On the other hand, Cu(0) will act as supplemental activator and reducing agent of Cu(II) *via* comproportionation.[97-99] This in contradiction to SET-LRP, in which Cu(0) will function as activator *via* an Outer Sphere Electron Transfer (OSET) mechanism and Cu(I) will disproportionate almost instantly into Cu(0) and Cu(II) in a polar environment and in the presence of Me_6TREN.

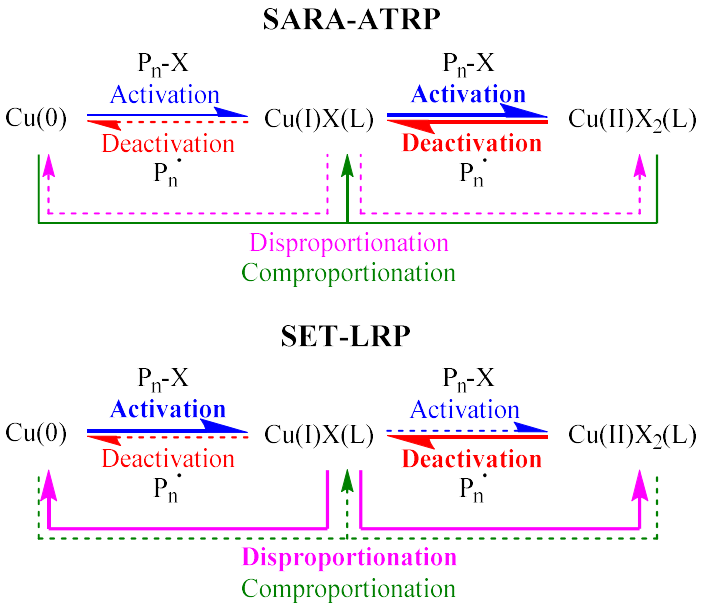

Figure II. 14: Proposed mechanisms of SARA-ATRP (top) and SET-LRP (bottom), with the most important reactions marked in bold.

A first aspect of comparison is the activation rate of Cu(I) compared to Cu(0). Matyjaszewski *and coworkers* have shown that in most systems, the activation rate of Cu(I) is 100 times higher than Cu(0) (both cases in the presence of Me_6TREN). It was also suggested that fast initiation from Cu(0) would cause large amounts of termination and significant decrease of end group fidelity due to an increased concentration of propagating radicals. However Percec *and coworkers*, evidenced the high reactivity of Cu(0) by predisproportionation of Cu(I) into Cu(II) and nascent Cu(0) with subsequent reaction by addition of an initiator. In-depth analysis by UV-Vis evidenced a fast consumption of Cu(0) by reaction with the organic halide.[87]

The second, and even most important aspect of comparison is the difference in rate between disproportionation and comproportionation during polymerization. According to Matyjaszewski *and coworkers* these reactions are slow compared to activation and propagation and are therefore not considered to evidence a SARA-ATRP or SET-LRP mechanism. However, Percec *and coworkers* demonstrated disproportionation reactions visually by monitoring the color shift from green to blue due to the formation of $CuBr_2$. Further proof was provided by UV-Vis analysis and examination of the obtained Cu(0)-nanoparticles by Transmission Electron Microscopy (TEM) and Dynamic Light Scattering (DLS).[75, 87]

A last point of discussion is the presence of an OSET or ISET mechanism. In SET-LRP, an OSET mechanism is suggested, involving the formation of radical anions during the polymerization, something which is not observed in SARA-ATRP, involving an ISET activation process. Calculations based on the Marcus theory by Matyjaszewski *and coworkers* suggested that the ISET process is favored due to a lower activation energy.[97]

Also other research groups participated to this vibrant discussion. Samanta *et al.* proposed a surface activation process by adsorption of the dormant chain onto the Cu(0) surface and consequent single electron transfer from Cu(0) to the organic halide.[83] It was stated that the propagating chains would remain adsorbed on the surface during propagation and deactivation, suppressing termination reactions. Furthermore, adsorption of the polymer chain to the surface would be improved due to the hydrophobic nature of both the copper surface and the polymer backbone.[83] However, re-evaluation of the data by Harrison *et al.* suggested that conclusions drawn are premature and further evidence is required to confirm the suggested mechanism.[99]

A paper from 2011 by Haddleton *and coworkers* describes the influence of Cu(0) and Cu(II) on the induction time of Cu(0)-mediated polymerizations. It was shown that polymerizations could be performed in the absence of Cu(II), demonstrating the high activity of Cu(0). However, an induction time was observed which could be avoided by addition of Cu(II). Another strategy for removing the inhibition period was by pretreatment of Cu(0) with acid to remove Cu_2O (present on the surface due to oxidation) or utilizing ultra-pure higly porous Cu(0).[58, 94]

A last paper by Haddleton *and coworkers* indicated a significant low rate of disproportionation in organic media, with even a further decrease after addition of a hydrophobic monomer. Furthermore, it was shown that Cu(0) particles, obtained by the *in situ* disproportionation of Cu(I), were slow activating species. However, the use of copper wire resulted in higher polymerization rates compared to Cu(I), which is contradictory to previous reports. Finally, it should be noted that the role of Cu(0) in these types of polymerizations is not yet fully understood, and further investigations are required.[96, 100]

However, within the framework of this thesis, the resulting polymers are more important independent whether a SARA-ATRP or SET-LRP mechanism is occurring. As will be more clear in the next chapters, the focus will be mainly set on the synthesis of polymers with high end group fidelities, an important prerequisite within this project when focusing on (hetero)telechelic structures or the synthesis of block copolymers yielding complex macromolecular architectures.

From a personal point of view, the definition of SARA-ATRP is more convenient. Depending on the solvent (organic or aqueous media), disproportionation and activation by Cu(0) or Cu(I) will always occur, each of them favored depending on the reaction conditions. As the term SARA (supplemental activator and reducing agent) suggests that both species are participating, this terminology might be more appropriate. Finally, as Cu(0) is or was the main source of copper applied in this thesis, only the term "Cu(0)-mediated RDRP" will be used in the next chapters.

II.1.7 RDRP in an industrial related context

While the fundamentals of RDRP methods originate from basic organic chemistry, developed in an academic context, the preparation of polymeric structures thereof leads to novel materials which in some cases can advance into new industrial applications. However, the final number of materials developed using RDRP methods is rather limited due to IP-related issues, costly experimental procedures, toxic byproducts or limited improvements compared to *e.g.* FRP-methods. However, in some cases RDRP methods are preferred due to their control over molecular weight, dispersity, chain architecture and site-specific functionalities introducing an added value to the final material properties. Many of these applications are situated within the field of surfactants, dispersants, coatings, adhesives, thermoplastic elastomers, personal care products, drug delivery systems, additives of which a short overview is provided below.[101]

DuPont Performance Coatings produces several commercial components of paints, coatings and inks using RDRP. IBM exploits the self-organizing ability of block copolymers to produce Si memory chips (WO211135046). Ciba, as part of BASF, prepares amphiphilic graft copolymers *via* copolymerization by ATRP and NMP, yielding well-defined comb-copolymers,

commercialized as EFKA (WO2000040630). Kaneka exploits a large pilot unit in Japan for the big-scale synthesis of telechelic materials *via* ATRP, with products including a range of moisture-curable polyacrylates for adhesive purposes (WO2007069600). Arkema developed a novel class of mediators for NMP (SG-1) for the polymerization of acrylates (US20050270751). Solvay produces the Rhodiblock RS as amphiphilic block copolymer *via* RAFT, which is used as stabilizer in water-in-oil emulsions (WO1998058974). Finally, Henkel produces telechelic polyacrylates *via* Cu(0)-mediated polymerization, exploiting the high end group fidelity. Most probably, many more applications involving RDRP exist but are difficult to find back in literature or patents due to IP-related issues.[102]

II.2 "Click" chemistry

II.2.1 Introduction

Besides the use of controlled radical polymerization techniques, chemical transformations of synthetic polymer materials is of great interest in both an academic and industrial environment. When focusing on precision polymer design, these reactions very often need to be high yielding and site-specific to obtain the fully reacted end-product and avoid tedious purification issues.[103, 104]

Within this framework, organic and polymer chemists have been continuously searching and collaborating to adjust advanced synthetic organic concepts into "click" reactions, a concept introduced in 2001 by Finn, Kolb and Sharpless.[105] Although "click" chemistry should be regarded as a philosophy rather than a method, it comprises a series of strict criteria whether a certain reaction should be defined as "click" or not.[106] Starting from the original definition these types of reactions should be modular, wide in scope, orthogonal, result in high yields and may generate only inoffensive side-products. Furthermore, reaction conditions should be simple, including readily available starting products and no or only small amounts of harmless solvents. However, when translating this concept to a macromolecular context, an alternative set of requirements should be taken into account due to the different needs and perspectives related to polymer synthesis.[107-109] Although original criteria as modularity, chemoselectivity,

orthogonality and wideness in scope still remain applicable, additional requirements include equimolarity and large scale applicability, the former mainly introduced within the concept of polymer-polymer conjugation. In classical organic synthesis, one can improve the conversion or reaction speed by utilizing an excess of reagent, however in polymer conjugation reactions, this would imply an excess of unreacted polymer after conjugation, difficult to remove from the final coupled product without the use of chromatographic methods. Furthermore, to be able to use these "click" reactions in an industrial polymer environment, they need to be applicable in large-scale synthetic procedures.[110] Therefore, reactions should be again high yielding, purification strategies should be minimized and chromatographic methods avoided.

The first and probably most common "click" reaction in polymer chemistry is the Huisgen 1,3-dipolar azide-alkyne cycloaddition. The popularity of this reaction lies in the ease of introducing alkyne- and azide-units on a polymer chain, the orthogonality of azides to other functional groups and the fulfillment of former mentioned criteria.[111] However, the uncatalyzed azide-alkyne cycloaddition typically proceeds slowly and requires high temperatures. By the addition of Cu(I) as a catalyst, regioselectivity can be obtained together with fast reactions at room temperature. Under these conditions the reaction is also known as the copper assisted azide-alkyne cycloaddition reaction (CuAAc).[112, 113]

Furthermore, the combination of controlled polymerization systems and "click" chemistry turned out to be a powerful combination for the design of tailored macromolecular structures, especially the combination of CuAAc with ATRP, as the alkyne and azide can be easily introduced through a functional initiator or nucleophilic substitution of the bromine respectively. Additionally, both methods utilize the same catalyst, Cu(I).[114] Tsarevsky *et al*. applied this method for the synthesis of multisegmented block copolymers (Figure II.15).[115] Polystyrene was synthesized, starting from an alkyne-containing ATRP-initiator. In a next step, the azide was introduced by nucleophilic substitution of the bromine. Finally, the multisegmented block copolymer was obtained by addition of Cu(I), yielding a polymer which increased in molecular weight and dispersity.

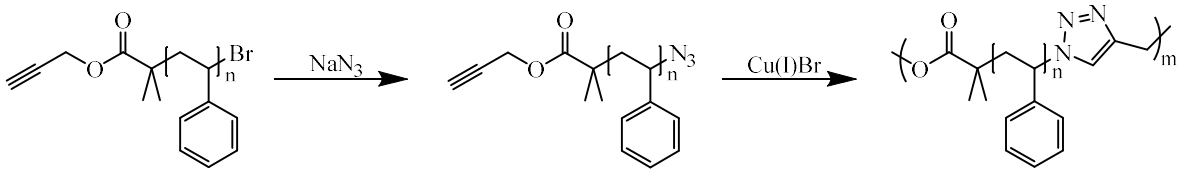

Figure II. 15: Combination of ATRP and CuAAc for the synthesis of multisegmented block copolymers.[115]

Despite the advantage of CuAAc and its broad applicability, the use of a toxic catalyst and safety issues related to working with explosive azides are major drawbacks which limits the use of this strategy. Although the strain-promoted azide-alkyne cycloaddition reaction[116] is a worth-mentioning alternative metal-free system, the synthetic difficulty and limited commercial availability of cyclooctynes significantly hinders the use of this method.[117]

Therefore, different alternative methods were developed, *e.g.* Diels-Alder type of reactions[118] or thiol-X chemistries[119]. In general, the polymer community increasingly aims for additive-free systems to avoid the use of catalysts and to simplify reaction procedures.

In this thesis, the use of copper-mediated polymerization systems was combined with two different "click" chemistries developed within our research group, *i.e.* triazolinedione and thiolactone chemistries. Both methods were explored for the synthesis of complex macromolecular structures and will be discussed in more detail in the next paragraphs.

II.2.2 Triazolinedione Chemistry

II.2.2.1 Introduction

A Diels-Alder reaction[120] is an important metal-free, and in some cases additive-free type of chemistry, which can be considered as "click" reaction under certain conditions[121]. It is a straightforward [4+2] cycloaddition reaction between an electron-rich diene and an electron-poor dienophile to form new carbon-carbon bonds, or heteroatom-heteroatom bonds in the case of a hetero-Diels-Alder reaction[122].

One of the most reactive dienophiles are triazolinedione (TAD) compounds.[123-125] These azodicarbonyl derivatives with distinct red color, display an enhanced reactivity towards dienes in Diels-Alder reactions.[126-128] This red color gives the user a visual feedback system as a distinct color switch from red to colorless can be observed during the reaction. TAD reagents are similar in chemical structure compared to maleimides, which are typically used in furan-maleimide type of Diels-Alder reactions.[129-131] However, the thermodynamic driving force related to reactions involving TAD is typically much higher, enabling their reaction at room temperature. The high reactivity of TAD-compounds can be explained by comparing this structure with singlet oxygen.[132, 133] Both reagents are known to easily react in a Diels-Alder type of reaction in which the energies of the frontier π-orbitals (HOMO and LUMO) are very similar.[134] Besides Diels-Alder reactions, these compounds can also serve as highly reactive enophiles in Alder-ene conjugations.[135, 136] In this method, an alkene bearing an allylic hydrogen (ene) will react with the TAD (enophile) and induce the migration of a σ-bonded hydrogen atom with formation of a new C-N σ-bond by displacement of the initial C-C π-bond (Figure II.16).[137]

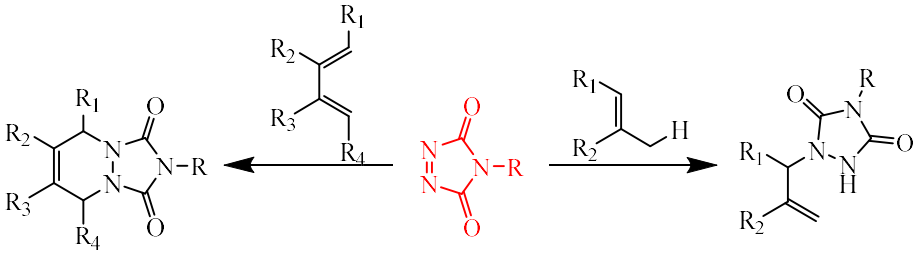

Figure II. 16: Reaction of a triazolinedione (TAD) with a diene (left) in a Diels-Alder reaction and an ene (right) in an Alder-ene reaction.

Due to its high reactivity, an important issue related to this chemistry is the shelf life of triazolinediones, as it readily reacts with water, air, amines or can be degraded by light. To circumvent this problem, TAD reagents are typically stored in their reduced form, urazoles, and generated when desired by simple oxidation methods (Figure II. 17).[138]

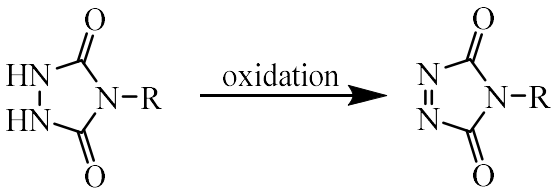

Figure II. 17: Oxidation of the urazole (left) to the corresponding triazolinedione (TAD) moiety.

II.2.2.2 TAD-chemistry in polymer science

Due to its unique reactivity, TAD-chemistry was picked up quite rapidly by the polymer community, including the PCR-group. First examples by Pirkle and Stickler in 1970 described the direct polymerization of TAD-based compounds, creating a polymer consisting of a nitrogen-based backbone.[139] The polymer itself was obtained by irradiation of 4-butyl-1,2,4-triazoline-3,5-dione (BuTAD) with a halogen lamp obtaining a colorless polymer (Figure II.18). Furthermore, bifunctional TAD-compounds can be reacted with bis-dienes, yielding the corresponding polymer *via* step-wise polymerization (Figure II.18).[140]

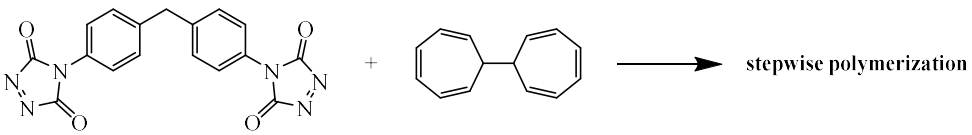

Figure II. 18: Stepwise polymerization starting from bifunctional TAD- and diene-compounds.

Besides the use of TAD-compounds as monomers for the synthesis of linear polymers, it can also be applied for the modification of existing polymers. TAD-chemistry can be used for post-polymerization functionalization of Acyclic Diene Metathesis (ADMET) derived polymers to improve the mechanical properties or to synthesize cross-linked structures[141]. Moreover, it can also be used as cross-linking method to obtain shape-memory materials[142] and for the modification and cross-linking of different polydienes (polybutadiene, polyisoprene, styrene-butadiene copolymer)[143].

A more recent example describes the use of TAD-chemistry for the synthesis of brush-type copolymers.[144] In this specific example by Xiao *et al*., a polymer backbone containing diene functionalities was prepared *via* a post-polymerization modification reaction. Next, linear polymer chains containing a TAD end group were synthesized *via* RAFT polymerization of a urazole-containing chain transfer agent. Afterwards, different graft copolymers, including amphiphilic structures, were prepared by grafting the TAD containing polymer onto the reactive backbone. Finally, these amphiphilic graft copolymers were used for their self-assembly properties and characterized in more detail.[144]

II.2.3 Thiol-ene and thiolactone chemistry

II.2.3.1 Introduction

Thiol-based chemistries have received a tremendous amount of attention, even more compared to Diels-Alder reactions, as valuable alternative to the copper-catalyzed azide-alkyne cycloaddition reaction, due to their versatility and the high reactivity of the thiol group. This high reactivity originates from the specific characteristics of the sulfur-atom, with a high electron density and available d-orbitals, enabling smooth formation of thiyl radicals or thiolate anions and facilitating further thiol-based reactions. Thiyl radicals will generally react rapidly with electron rich substrates such as alkenes or alkynes whereas thiolate anions will react quickly in thiol-Michael additions with electron-poor enes or with isocyanates, halogens or epoxides, creating a toolbox of efficient chemical reactions for macromolecular synthesis (Figure II.19).[119, 145]

However, it has to be noted that thiol-based chemistries are not a recent development and were already extensively studied over the last century with one of the first papers by Braun *et al.* dating back from 1926.[146] In the last years, thiols were used in the synthesis of polymer networks by implementation of the very popular thiol-ene reaction. Furthermore, thiols can be introduced as chain-transfer agents to enable an easy and cheap method to control molecular weight.

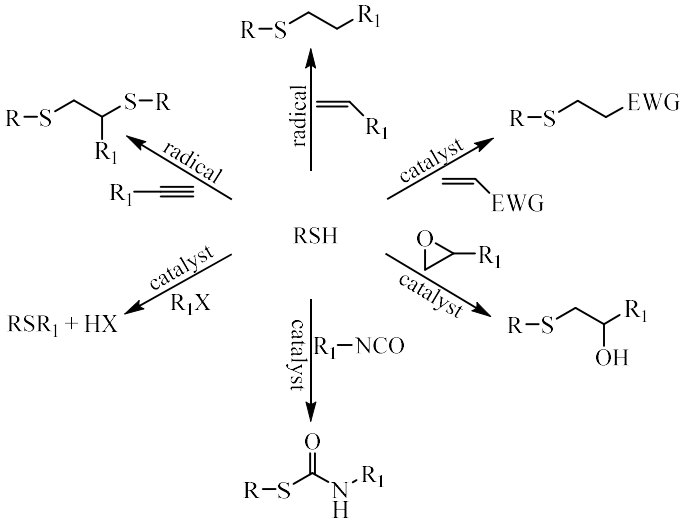

Figure II. 19: Toolbox of efficient thiol-X chemistries for the design of functional polymer materials. (with X: Br or F and EWG = electron withdrawing group).[119]

II.2.3.2 Radical thiol-ene chemistry

Thiol-ene reactions can proceed quite rapidly and are considered as useful tools for the synthesis of advanced polymeric structures.[147] These approaches typically advance *via* a chain process of initiation, propagation and termination (Figure II.20). Initiation can proceed thermally, photochemically or *via* a redox initiator depending on the reaction and the final use of the applied system. Generally, photoinitiators of type I (cleavable type), such as 2,2-DiMethoxy-2-PhenylAcetophenone (DMPA), provide the highest efficiencies compared to other well-known photoinitiators of type II (non-cleavable) such as benzophenone or camphorquinone.[148] In case thermal initiation is preferred, AIBN, which is also used in RAFT polymerizations to generate radicals, can be applied. After formation of the thiyl radicals, the chain growth process will start by reaction with the ene-substrate, yielding a carbon-centered radical. Finally, the end product is obtained by hydrogen abstraction of a thiol group by this radical, regenerating the thiyl radical. Furthermore, radical thiol-ene reactions significantly face issues regarding termination events as disulfide formation or recombination.[119]

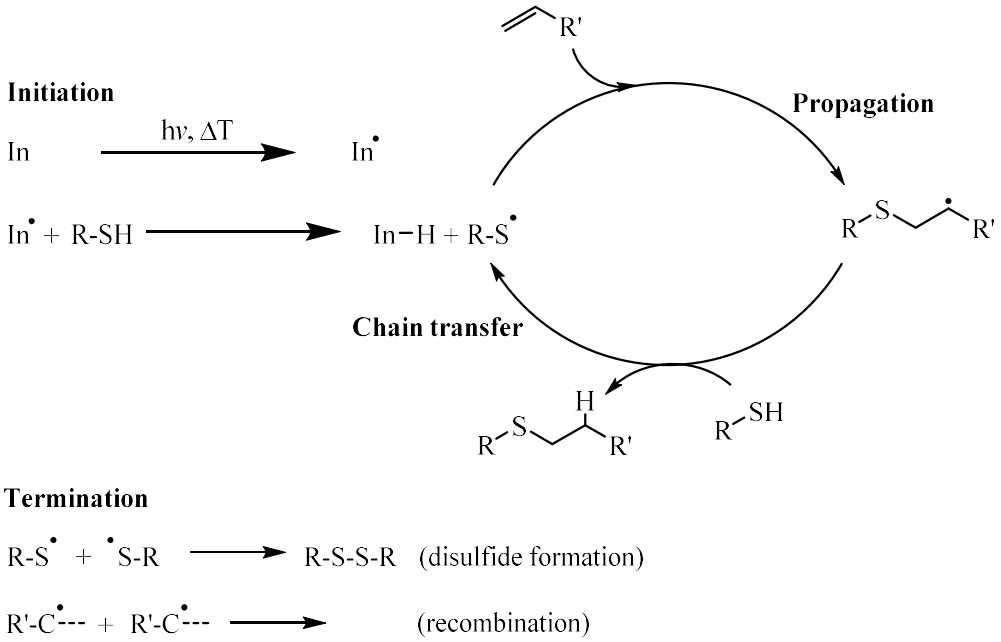

Figure II. 20: The radical thiol-ene reaction mechanism with initiation, propagation, chain transfer and termination events

Generally, the rate of radical thiol-ene reactions depends on the structure of the thiol and ene. Considering the structure of the ene, it was already mentioned that electron-dense enes react

more rapidly. Moreover, highly substituted enes are less reactive, due to sterical hindrance in the propagation sequence. Norbornene reacts exceptionally fast, due to the combined effect of ring strain relief and rapid hydrogen abstraction of the carbon-centered radical. At the opposite, in the case of methacrylates, styrenes or conjugated dienes, the radical is well stabilized, leading to a slow hydrogen abstraction rate. The influence of the thiol structure is mainly of importance when chain transfer is the rate-determining step. Finally, it should be noted that some side reactions can occur when performing radical thiol-ene reactions. For example, thiyl-thiyl radical coupling leads to disulfide formation and head to head coupling/recombination of the carbon centered radicals. These side reactions, in combination with the decreased efficiencies in polymer conjugation reactions makes the term "click" in combination with this chemistry somehow contradictory. Therefore, in some systems, nucleophilic thiol-X chemistries can be preferred.[149]

II.2.3.3 Nucleophilic thiol-X chemistry

In contrast to radical based thiol-X chemistries, nucleophilic thiol-ene reactions require electron-poor substrates as (meth)acrylates or maleimides.[150] Furthermore, thiolate anions are easily susceptible to react with other substrates such as isocyanates, epoxides or halogens. Within the framework of this thesis, only thiol-Michael additions will be discussed.

Thiol-Michael additions are one of the most important and efficient thiol reactions in polymer chemistry.[119, 151] These additions involve the reaction of thiolate anions with activated enes in the presence of a catalyst. The reaction starts by the abstraction of a proton by the base catalyst, generating the thiolate anion and the conjugated acid. Next, the thiolate anion will attack the β-carbon of the activated double bond, generating the carbon-centered anion as an intermediate species. In a final step, the carbon-centered anion will abstract the proton from the conjugated acid, yielding the thio-ether product and regenerating the base catalyst (Figure II.21). The efficiency of thiol-Michael additions is mainly influenced by solvent polarity, catalyst, pK_a of the thiol and nature of the activated double bond.[150]

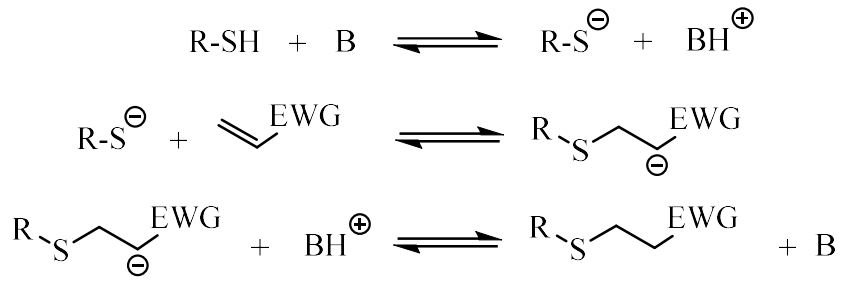

Figure II. 21: Base-catalyzed mechanism of the thiol-Michael addition between a thiol and an activated double bond.

Besides a base-catalyzed mechanism, thiol-Michael additions can also be catalyzed by nucleophiles, such as phosphines.[152-154] However, the nucleophile will not catalyze the reaction itself, but react with the activated double bond to generate a strong base. Therefore, the reaction mechanism alters and the reactivity will depend on the structure of the catalyst (Figure II.22).

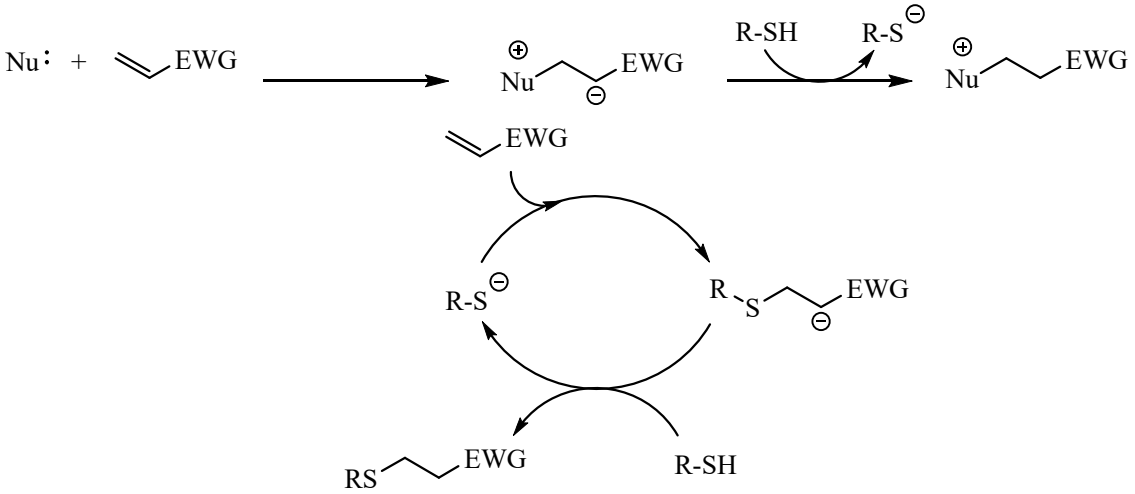

Figure II. 22: Proposed mechanism for the nucleophilic initiated thiol-Michael addition.

II.2.3.4 Thiolactone chemistry

II.2.3.4.1 Introduction

Despite the popularity of thiol-X related chemistries, their implementation is hampered due to different issues related to working with thiols. An important practical disadvantage is the unpleasant smell observed when using low-molecular weight thiols. Furthermore, from a synthetic point of view, the reduced stability of thiols is an important issue as thiols can easily oxidize, leading to disulfide formation. A final issue is the limited commercial availability of

functional thiols, limiting the introduction of a variety of functional groups. Therefore, different synthetic strategies were developed to protect the thiol functionality and solve odor and stability related issues when working with thiols.

Although known as a disadvantage, the formation of disulfides (when controlled) can be used as a protecting group strategy for thiols. This approach is applied in (bio-)polymer chemistry, for instance. Afterwards, oxidation can be performed by using air, peroxides, sulfoxides or certain metals. Haddleton *and coworkers* implemented the advantage of a disulfide linkage to synthesize polymer-peptide conjugates, which can be utilized in the area of polymer therapeutics. The disulfide linkage present in Salmon calcitonin (sCT), a therapeutic peptide, was reduced by tris(2-carboxyethyl)phosphine (TCEP), yielding the thiol functionalities which were then reacted with a linear α-methoxy ω-dibromomaleimide PEG (Figure II.23).[155, 156]

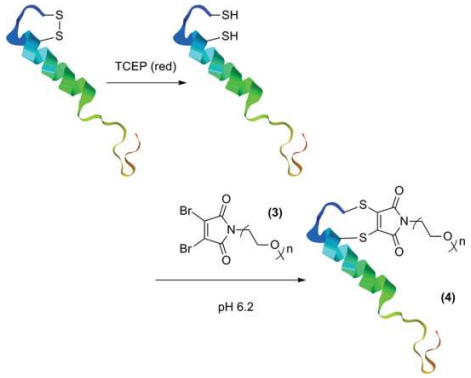

Figure II. 23: Use of disulfides in peptides for the synthesis of polymer-peptide conjugates.[150]

Besides its use as a RDRP method, RAFT can also be applied to introduce protected thiols on a macromolecular structure. After polymerization, the RAFT-group will be present on the chain-end of the polymer and can simply be transformed into the corresponding thiol by aminolysis. The generated thiol can be exploited for end-group modification or surface-grafting of gold nanoparticles.[157-160]

Another example amongst many is the implementation of methanethiosulfonates in polymeric structures. This class of reagents can be applied to introduce a protected thiol, which is liberated upon addition of a strong base. Boyer *et al.* implemented this chemistry for the end group

modification of methyl-, isobornyl- and *tert*-butyl acrylate, synthesized *via* ATRP.[161] After polymerization, the bromine was replaced by methanethiosulfonate through nucleophilic substitution with the corresponding sodium salt. Next, the asymmetric disulfide linkage could be used in disulfide exchange reactions or a one-pot thiol-Michael addition with simultaneous hydrolysis and thiol-acrylate reaction.

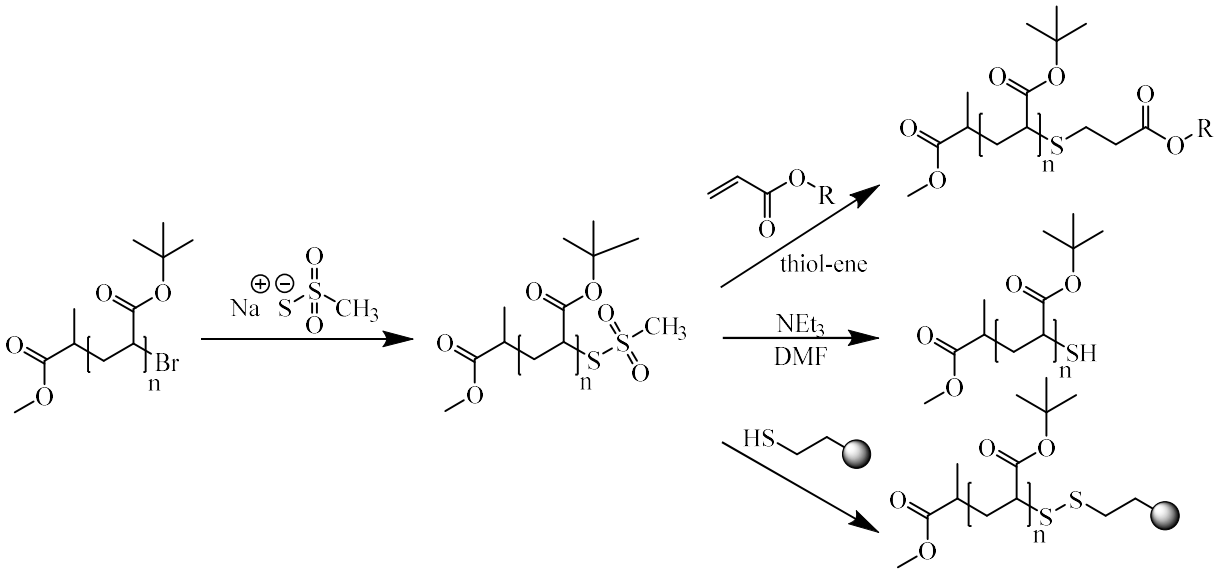

Figure II. 24: End group functionalization by the use of sodium methanesulfonate, which can be used in thiol-ene or disulfide exchange reactions.[161]

A straightforward strategy to introduce thiols in polymeric structures is the deprotection of thioesters.[162] These thioesters are generally introduced in macromolecular structures through nucleophilic substitution of the potassium salt of the corresponding thioacid (*e.g.* thioacetate or thiobenzoate). The thiol itself can then be liberated upon aminolysis, alcoholysis or hydrolysis. Liras *et al.* synthesized poly(methyl methacrylate) (PMMA) *via* ATRP followed by a nucleophilic substitution of the bromine with potassium thioacetate.[163] Next, the thiol was liberated by hydrolysis with sodium methoxide and functionalized *via* a radical thiol-ene modification.[163]

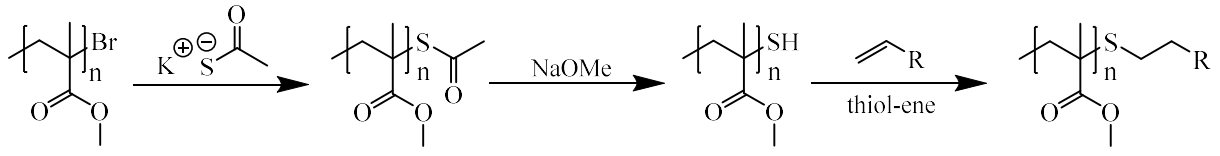

Figure II. 25 Introduction of a thioester *via* nucleophilic substitution, modification into a thiol through hydrolysis and tihol-ene reaction.

II.2.3.4.2 Thiolactones as atom-efficient latent thiol group

However, all of the above described methods suffer from a low atom efficiency, something important in an industrially related context. Atom-efficient approaches to introduce thiols imply the use of cyclic thiol-based structures such as thiolactones.[164, 165] Thiolactones are cyclic esters of mercapto-acids, from which the thiol can be liberated by reaction with an amine. Thiolactones can be obtained from direct lactonisation of the corresponding mercapto-acid in the presence of dehydrating agents as carbodiimides or phosphorus pentoxide. Depending on the structure of the mercapto-acid, one can obtain β-, δ- or γ-thiolactones (respectively four-, five- and six-membered rings) (Figure II.26).[166, 167]

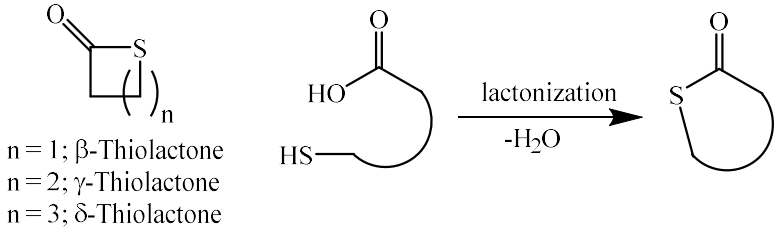

Figure II. 26: General structure of thiolactones and strategy for their synthesis.

The thiol can be liberated by reaction with nucleophiles, such as amines. However, thiolactones are more reactive towards ring-opening compared to lactones due to the decreased orbital overlap between the C-S bond, increasing the partial positive charge on the carbon atom. Furthermore, as a result of the ring strain, the susceptibility of thiolactones towards nucleophilic reaction decreases in the following order: β- > γ- > δ-thiolactones. When comparing the three represented structures in Figure II.26, γ-thiolactones are most popular due to the combination of their reactivity, stability and commercial availability as DL-homocysteine thiolactone is a natural occurring compound, which can be obtained from the ring-closure of methionine.[168]

Besides amines, many other nucleophiles can be considered for ring-opening of γ-thiolactones. However, it was observed that γ-thiolactones are not susceptible to reaction with alcohols, thiols, anilines and water without the presence of a strong base. Furthermore, it was shown that secondary or tertiary amines such as diethyl- or trimethylamine cannot react with thiolactones, with the exception of cyclic secondary amines, *e.g.* pyrrolidine or piperidine.

After aminolysis, the latent thiol is available for further modification reactions as thiol-X chemistries, introducing the possibility of performing a double modification of the polymer structure on each thiolactone handle.[169, 170] By careful selection of the functional groups present in the amine and acrylate unit, a toolbox of different structures can be easily obtained. Considering orthogonality issues, these reactions can be performed in a one-pot approach to facilitate synthetic efforts. In the last years, radical and nucleophilic thiol-ene reactions were implemented for the synthesis of functional polymers, *e.g.* starting from an AB'-monomer containing a thiolactone and a double bond. Depending on the structure of the double bond, a radical or nucleophilic pathway will proceed, however, the latter requires careful analysis of possible side-reactions between the amine and the acrylate (Aza-Michael addition) and disulfide formation. To evidence the absence of these side-reactions, a comprehensive model study was performed on the reaction between propylamine, butyl acrylate and γ-butyrothiolactone. In-depth *online* FT-IR analysis of the model reaction revealed an equal rate of consumption of γ-butyrothiolactone and butyl acrylate, in combination with an equal rate of formation of the amide bond (Figure II.27). These results evidenced that the amine almost solely reacts with the thiolactone unit, and the newly created thiol instantaneously reacts with the acrylate, present in the reaction mixture. Therefore, Aza-Michael addition and disulfide formation can be considered to be negligible.[171]

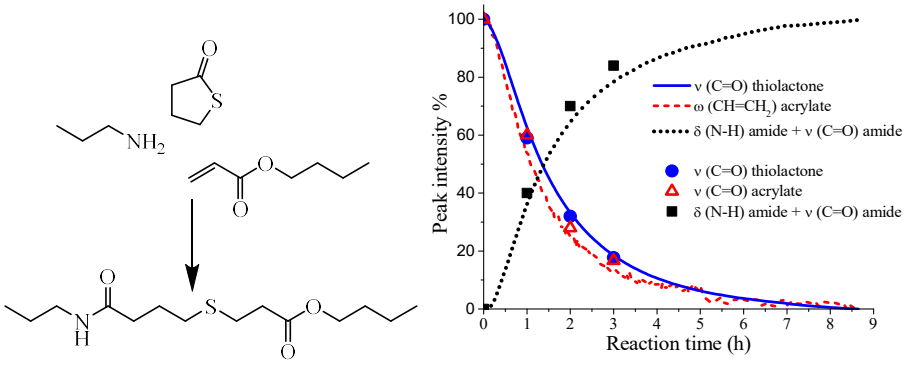

Figure II. 27 *Online* monitoring of the reaction between an amine, thiolactone and acrylate *via online* FT-IR.[171]

Over the last years, thiolactone chemistry has been used for the synthesis of complex polymer structures for a broad range of examples, e.g. the synthesis of cyclic or hyperbranched polymers *via* thiol-disulfide chemistry, the design of sequence-defined oligomers *via* thiolactones on a solid-support.[172-177]

II.3 Complex polymer structures

II.3.1 Introduction

A broad variety of new applications can be acquired by carefully transforming basic polymer structures as homo-, co- or block copolymers into more diverse geometries.[178, 179] In the last decade, the polymer community developed a broad spectrum of complex macromolecular architectures as cyclic-, graft- or star-copolymers of which synthetic efforts were facilitated by the use of RDRP techniques in combination with "click"-type reactions.[108, 180-182] The combination of these structures with a diverse set of monomers easily leads to materials for different applications such as dispersants, viscosity modifiers, adhesives etc. Part of this PhD research focused on the design and synthesis of complex macromolecular structures exhibiting amphiphilic properties. More specifically the synthesis of amphiphilic graft and toothbrush copolymers was envisaged. These categories can be classified as comb copolymers. Depending on variables such as dense or loose grafting, flexible or stiff chains and a homopolymer or copolymer backbone, the structure-property relation can be easily controlled.[183, 184]

Amphiphilic graft copolymers are typically composed of a hydrophobic backbone and hydrophilic segments present as side-chains, randomly distributed across the main chain. On the other hand, amphiphilic toothbrush copolymers, also denoted as comb-like, brush-block-linear or brush-coil semi-comb copolymers, are designed in a toothbrush shape with a hydrophilic linear tail as the first block and a graft copolymer with hydrophobic segments as the second block.[185, 186] These complex structures are typically obtained using three different synthetic strategies: *(i)* grafting through, involving the polymerization of macromonomers, *(ii)* grafting from, side chains are polymerized from a macroinitiator backbone and *(iii)* grafting onto, side chains are added to the polymer backbone by efficient conjugation strategies (Figure II.28).[183]

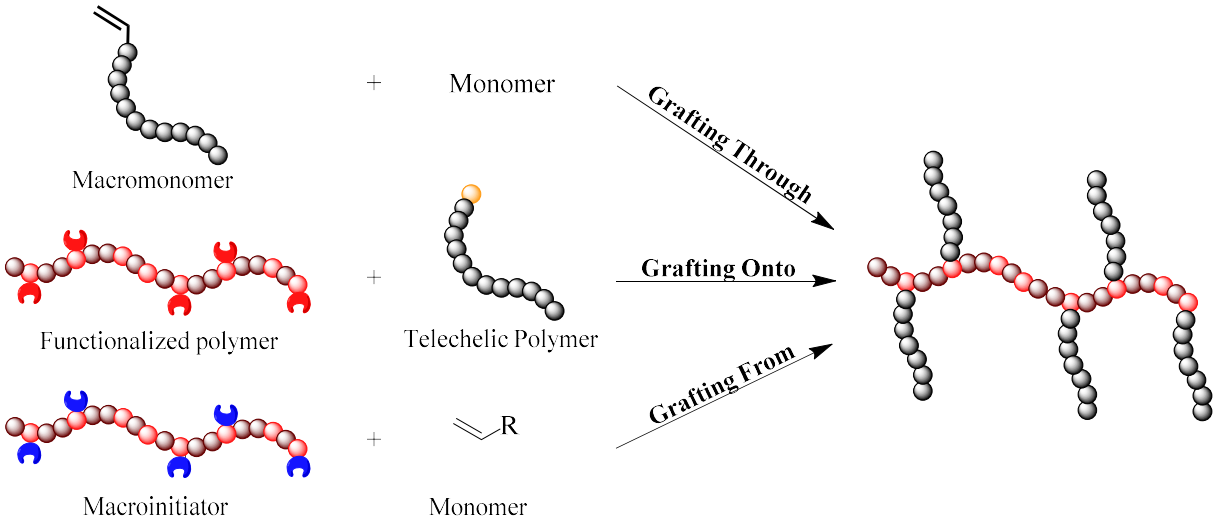

Figure II. 28: Different grafting methods for the synthesis of complex polymeric structures.

II.3.2 Grafting strategies

II.3.2.1 Grafting through

The grafting through method involves the copolymerization of macromonomers through their terminal functional group. The most attractive feature of this strategy is the direct access to the desired comb-copolymer by copolymerization of the macromonomer. Furthermore, characterization of the macromonomer prior to polymerization enables control over the length of the side-chains and grafting density. However, the most important drawback of this method is the low degree of polymerization obtained due to sterical hindrance from the grafted side-chains during the copolymerization. Furthermore, due to the low concentration of reactive groups when applying this strategy, reactions are typically slow and cannot proceed to high conversions, leading to unreacted macromonomer and tedious purification steps.

Petton *et al.* applied this method for the synthesis of toothbrush copolymers. The first block was obtained *via* homopolymerization of styrene by NMP.[187] In the second block, a copolymerization of styrene and a polyether end-capped with methylstyrene was performed, yielding the toothbrush copolymer (Figure II.29).

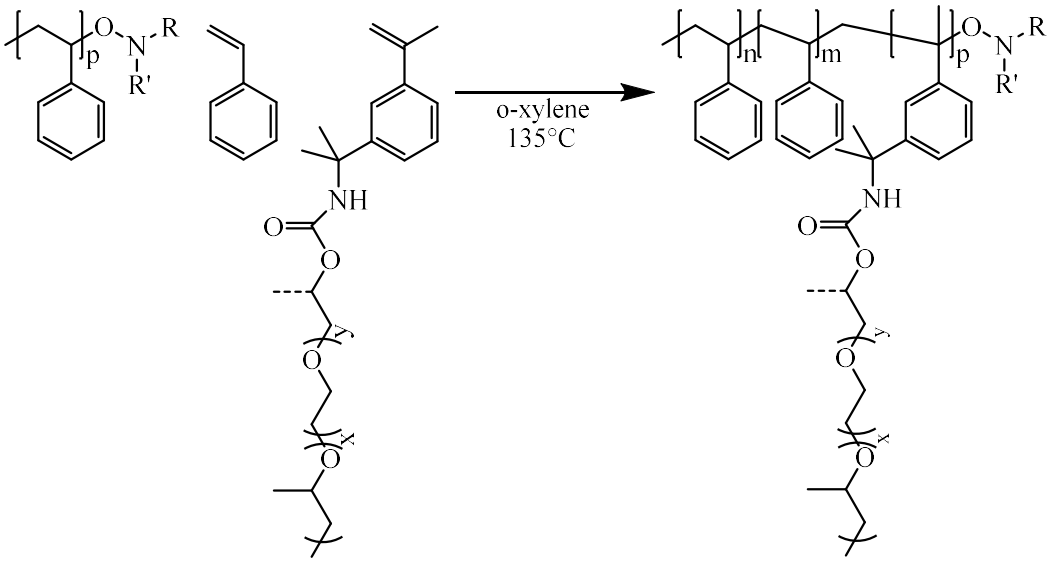

Figure II. 29: Synthesis of toothbrush copolymers *via* the grafting through method.[187]

II.3.2.2 Grafting from

In the grafting from strategy, a macro-initiator containing initiating functionalities on the polymer backbone is synthesized by direct polymerization of a reactive monomer or by introducing initiating functionalities in a post-polymerization modification (PPM) methodology. Next, the polymeric side-chains can be grown from the polymer backbone *via* controlled radical polymerization, ring-opening polymerization or other methods available. Although this approach leads to an easy purification of the final copolymer structure, the difficulty to characterize the individual segments can lead to less defined structure-property relationships of the comb-copolymers.

An example of the synthesis of toothbrush copolymers by the grafting from method was reported by Hadjichristidis *and coworkers* in 2005.[188] A block copolymer of polystyrene and poly(2-hydroxyethyl acrylate) was synthesized first by anionic polymerization. Next the hydroxyl-functionalities were transformed into initiating structures for ATRP by reaction with α-bromoisobutyryl bromide. Finally *tert*-butyl acrylate was polymerized and the toothbrush copolymer was obtained (Figure II.30).

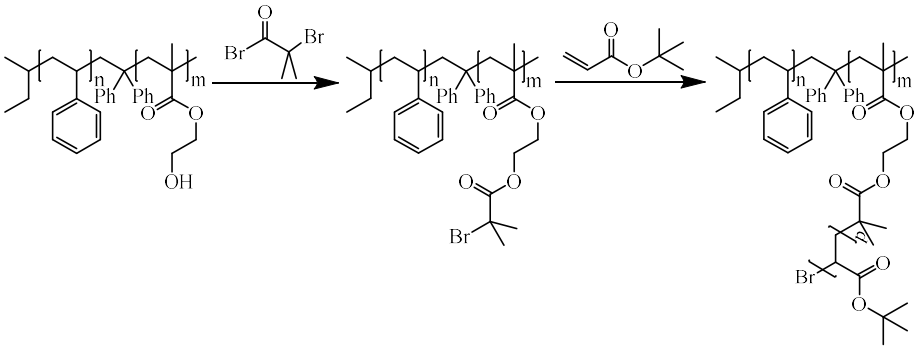

Figure II. 30: Synthesis of toothbrush copolymers *via* the grafting from method by Hadjichristidis *and coworkers*.[188]

II.3.2.3 Grafting onto

In the grafting onto method, the polymer backbone and side chains are prepared separately, enabling the use of polymerization mechanisms appropriate to the respective desired polymer structure and the precise characterization of the individual segments, providing a clear structure-property relationship of the final copolymer material. The different segments can be linked together by introducing the required functionalities on the end group and side chains. However, grafting efficiencies can be limited due to sterical hindrance between the bulky chains, yielding mixtures of the comb-copolymer and unreacted starting products and leading to problematic purification strategies. This issue can be partially avoided by the use of efficient conjugation strategies, typically "click"-type reactions, enabling high grafting densities.

For example, Matyjaszewski *and coworkers* utilized the combination of ATRP and CuAAc, sharing the same catalyst, in a grafting onto approach for the synthesis of graft copolymers.[189] 2-hydroxyethyl methacrylate was polymerized *via* ATRP and the hydroxyl-functionality was transformed into an alkyne by reaction with 4-pentynoic acid. Finally the graft-copolymer was obtained by reaction with a series of polymers containing an azide end-functionality (Figure II.31).

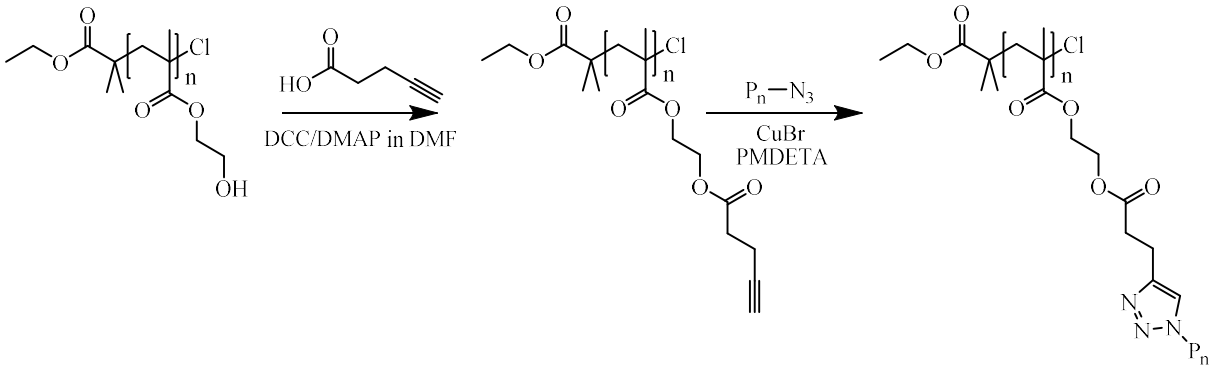

Figure II. 31: Synthesis of graft copolymers *via* the grafting onto method.[189]

II.3.3 Application as dispersants

Complex polymer architectures can be used for a broad set of applications such as surfactants, viscosity modifiers, adhesives, etc. An important application of these structures and more specifically complex amphiphilic structures is their use as dispersing agents for dyes and other types of particles.[190] Due to the Brownian motion[191], small particles will diffuse and collide. When these particles stick to each other, the particle size will increase leading to flocculation and sedimentation. By utilizing dispersing agents, flocculation and sedimentation of these particles is delayed. However, the dispersing quality will not only depend on the dispersing agent itself, but also on important parameters such as the type of particle (crystal structure, surface chemistry …), the medium (organic, aqueous …) and different stabilization mechanisms being present.

In general, low-molecular-weight molecules are used as dispersing agents due to cost issues and the limited features required for these compounds. However, polymeric dispersants are increasingly applied for high-end applications due to their advanced properties.[192, 193] They are generally more effective dispersing agents compared to their low-molecular weight counterparts as a result of an increased electrostatic and steric stabilization and stronger surface-interaction, increasing the potential energy barrier for particles to flocculate (E_a) (Figure II.32).

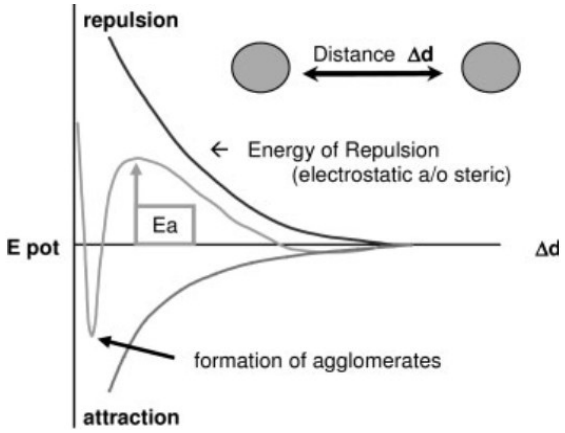

Figure II. 32: Schematic curve of the potential energy as a function of distance between particles in the coagulation process.

Stabilization by electrostatic charging of the surface can occur in aqueous medium due to dissociation of ionic groups present on the surface of the particle, adsorption of ions from the aqueous phase or adsorption of polymers with charged entities, *e.g.* poly(acrylic acid), poly(*N,N*-dimethylamino ethyl acrylate) etc. Because particles with a positively or negatively charged surface will attempt to re-establish electric neutrality, an electric layer consisting of negative or positive counterions will assemble around the particles, creating an electric double-layer. In this way, repulsive forces are build up when these particles come in close proximity.[194]

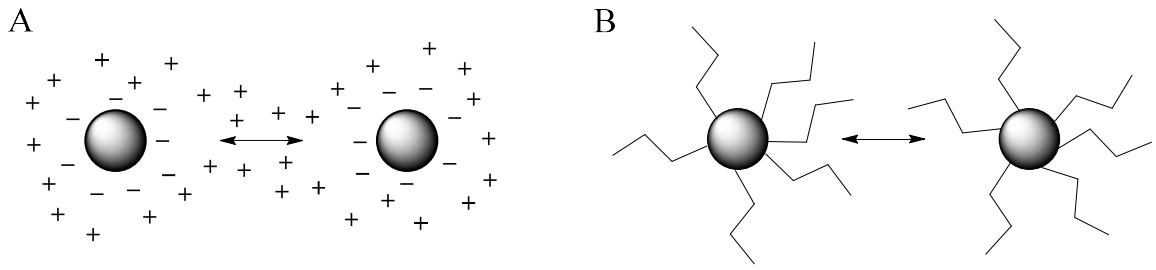

Figure II. 33: Electronic (a) and steric (b) stabilization mechanisms of particles in dispersion.

Generally, stabilization by polymeric dispersants depend on a steric repulsion mechanism. The macromolecular dispersant will adsorb on the particle, creating a polymeric shell surrounding the surface. Similar to electrostatic stabilization, repulsion forces between two approaching particles will prevent flocculation due to unfavorable sterical interactions. In contrast to low-molecular-weight dispersants, polymers will not cover the surface of the particle in a flat manner, but in a

train-loop fashion. When graft copolymers are applied, the hydrophobic backbone will typically adhere onto the hydrophobic particle surface, with the hydrophilic side-chains oriented towards the solvent.[195] In general, steric repulsion can be divided into entropic and osmotic stabilization mechanisms.

Entropic stabilization

When two particles, surrounded by a polymeric shell, will come in close proximity, the polymeric chains will interpenetrate. Due to the limited mobility of the polymeric chains in this situation, the number of available configurations is significantly reduced, lowering the entropy of the system. Therefore, the separation and repulsion of these polymeric shells will increase the freedom of movement and lower the total energy of the dispersing system.[196]

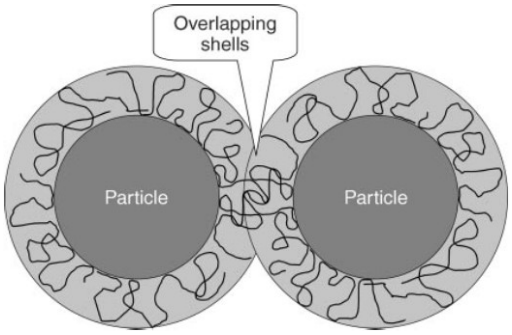

Figure II. 34: Entropic stabilization by avoiding overlapping polymeric shells.

Osmotic stabilization

As a consequence of overlapping shells when particles come in close proximity, solvent molecules are displaced from the region between the particles and the solvent concentration will significantly decrease. Due to a concentration difference of the solvent between the medium and the region between the particles, an osmotic pressure is build up, pulling back the solvent molecules to the region between the particles, increasing repulsion forces.[197]

Dispersing polymers applied for steric stabilization can have different architectures as linear, graft or block copolymers. In the ideal case, the polymer is chemically linked to the particle surface. However, in these cases it is difficult to create a platform of dispersants applicable to a broad variety of different particle systems. Therefore, the macromolecular structure is designed

in such a way that the polymer can adsorb onto the particle's surface through hydrogen bonding, dipole interactions … .[198] In parallel, the interaction between the polymer and the dispersing medium should be balanced to prevent desorption of the polymeric units, but still be sufficient enough to establish steric stabilization by proper stabilizer-polymer interaction. This can be outlined by the use of amphiphilic segmented structures, containing an insoluble part adhering to the particle surface and segments soluble in the dispersing medium, *e.g.* graft copolymers of which the backbone will adhere to the particle surface and the grafted segments will be directed towards the aqueous phase.

In general, it can be concluded that the use of complex polymer structures for the dispersion of pigments is an important aspect in an industrial context. To exhibit control over the polymer structure and improve the properties of the pigment dispersions, the use of controlled polymerization techniques and click reactions is of great importance. In the next chapters, thiolactone and triazolinedione chemistry will be explored for the synthesis of complex polymer structures.

References

1. Odian, G., *Principles of polymerization*. Fourth edition ed.; Wiley-Interscience: 2004.
2. Plastics - the facts 2011. In *An analysis of European plastics production, demand and recovery for 2010*, PlasticsEurope, Ed. PlasticsEurope: 2011.
3. Matyjaszewski, In *Handbook of Radical Polymerization*, John Wiley & Sons, Inc.: 2003.
4. Matyjaszewski, K., *Controlled Radical Polymerization*. American Chemical Society: 1998; Vol. 685, p 500.
5. Matyjaszewski, K.; Tsarevsky, N. V. *Nature Chemistry* **2009,** 1, (4), 276-288.
6. Matyjaszewski, K., *Advances in Controlled/Living Radical Polymerization*. American Chemical Society: 2003; Vol. 854, p 708.
7. Matyjaszewski, K. *Progress in Polymer Science* **2005,** 30, (8-9), 858-875.
8. Szwarc, M. *Nature* **1956,** 178, (4543), 1168-1169.
9. Quirk, R. P.; Lee, B. *Polymer International* **1992,** 27, (4), 359-367.
10. Matyjaszewski, K. *Journal of Physical Organic Chemistry* **1995,** 8, (4), 197-207.
11. Webster, O. W. *Science* **1991,** 251, (4996), 887-893.
12. Vana, P.; Davis, T. P.; Barner-Kowollik, C. *Macromolecular Theory and Simulations* **2002,** 11, (8), 823-835.
13. Sawamoto, M. *Progress in Polymer Science* **1991,** 16, (1), 111-172.
14. Baskaran, D.; Muller, A. H. E. *Progress in Polymer Science* **2007,** 32, (2), 173-219.
15. Matyjaszewski, K., *Controlled/Living Radical Polymerization*. American Chemical Society: 2000; Vol. 768, p 500.

16. di Lena, F.; Matyjaszewski, K. *Progress in Polymer Science* **2010,** 35, (8), 959-1021.
17. Braunecker, W. A.; Matyjaszewski, K. *Progress in Polymer Science* **2007,** 32, (1), 93-146.
18. Wang, J. S.; Matyjaszewski, K. *Journal of the American Chemical Society* **1995,** 117, (20), 5614-5615.
19. Moad, G.; Rizzardo, E.; Solomon, D. H. *Macromolecules* **1982,** 15, (3), 909-914.
20. Gridnev, A. A.; Ittel, S. D. *Chemical Reviews* **2001,** 101, (12), 3611-3660.
21. Chiefari, J.; Chong, Y. K.; Ercole, F.; Krstina, J.; Jeffery, J.; Le, T. P. T.; Mayadunne, R. T. A.; Meijs, G. F.; Moad, C. L.; Moad, G.; Rizzardo, E.; Thang, S. H. *Macromolecules* **1998,** 31, (16), 5559-5562.
22. Hawker, C. J.; Bosman, A. W.; Harth, E. *Chemical Reviews* **2001,** 101, (12), 3661-3688.
23. Moad, G.; Rizzardo, E. *Macromolecules* **1995,** 28, (26), 8722-8728.
24. Nicolas, J.; Guillaneuf, Y.; Lefay, C.; Bertin, D.; Gigmes, D.; Charleux, B. *Progress in Polymer Science* **2013,** 38, (1), 63-235.
25. Georges, M. K.; Veregin, R. P. N.; Kazmaier, P. M.; Hamer, G. K. *Macromolecules* **1993,** 26, (11), 2987-2988.
26. Benoit, D.; Grimaldi, S.; Robin, S.; Finet, J. P.; Tordo, P.; Gnanou, Y. *Journal of the American Chemical Society* **2000,** 122, (25), 5929-5939.
27. Grimaldi, S.; Finet, J. P.; Le Moigne, F.; Zeghdaoui, A.; Tordo, P.; Benoit, D.; Fontanille, M.; Gnanou, Y. *Macromolecules* **2000,** 33, (4), 1141-1147.
28. Detrembleur, C.; Jerome, C.; De Winter, J.; Gerbaux, P.; Clement, J.-L.; Guillaneuf, Y.; Gigmes, D. *Polymer Chemistry* **2014,** 5, (2), 335-340.
29. Guillaneuf, Y.; Gigmes, D.; Marque, S. R. A.; Astolfi, P.; Greci, L.; Tordo, P.; Bertin, D. *Macromolecules* **2007,** 40, (9), 3108-3114.
30. Moad, G.; Rizzardo, E.; Thang, S. H. *Polymer* **2008,** 49, (5), 1079-1131.
31. Moad, G.; Rizzardo, E.; Thang, S. H. *Australian Journal of Chemistry* **2006,** 59, (10), 669-692.
32. Destarac, M.; Bzducha, W.; Taton, D.; Gauthier-Gillaizeau, I.; Zard, S. Z. *Macromolecular Rapid Communications* **2002,** 23, (17), 1049-1054.
33. Pintauer, T.; Matyjaszewski, K. *Chemical Society Reviews* **2008,** 37, (6), 1087-1097.
34. Kharasch M., J. E. V., Urry W.H. *Science* **1945,** 102, (128).
35. Wang, J. S.; Matyjaszewski, K. *Macromolecules* **1995,** 28, (23), 7901-7910.
36. Kato, M.; Kamigaito, M.; Sawamoto, M.; Higashimura, T. *Macromolecules* **1995,** 28, (5), 1721-1723.
37. Pintauer, T.; Matyjaszewski, K. *Coordination Chemistry Reviews* **2005,** 249, (11-12), 1155-1184.
38. Matyjaszewski, K.; Xia, J. H. *Chemical Reviews* **2001,** 101, (9), 2921-2990.
39. Brandts, J. A. M.; van de Geijn, P.; van Faassen, E. E.; Boersma, J.; van Koten, G. *Journal of Organometallic Chemistry* **1999,** 584, (2), 246-253.
40. Kotani, Y.; Kamigaito, M.; Sawamoto, M. *Macromolecules* **1999,** 32, (8), 2420-2424.
41. Ando, T.; Kamigaito, M.; Sawamoto, M. *Macromolecules* **1997,** 30, (16), 4507-4510.
42. Granel, C.; Dubois, P.; Jerome, R.; Teyssie, P. *Macromolecules* **1996,** 29, (27), 8576-8582.
43. Lecomte, P.; Drapier, I.; Dubois, P.; Teyssie, P.; Jerome, R. *Macromolecules* **1997,** 30, (24), 7631-7633.
44. Grimaud, T.; Matyjaszewski, K. *Macromolecules* **1997,** 30, (7), 2216-2218.

45. Dervaux, B.; Van Camp, W.; Van Renterghem, L.; Du Prez, F. E. *Journal of Polymer Science Part a-Polymer Chemistry* **2008,** 46, (5), 1649-1661.
46. Matyjaszewski, K.; Patten, T. E.; Xia, J. H. *Journal of the American Chemical Society* **1997,** 119, (4), 674-680.
47. Teodorescu, M.; Matyjaszewski, K. *Macromolecules* **1999,** 32, (15), 4826-4831.
48. Teodorescu, M.; Matyjaszewski, K. *Macromolecular Rapid Communications* **2000,** 21, (4), 190-194.
49. Matyjaszewski, K.; Jo, S. M.; Paik, H. J.; Gaynor, S. G. *Macromolecules* **1997,** 30, (20), 6398-6400.
50. Magenau, A. J. D.; Bortolamei, N.; Frick, E.; Park, S.; Gennaro, A.; Matyjaszewski, K. *Macromolecules* **2013,** 46, (11), 4346-4353.
51. Tasdelen, M. A.; Uygun, M.; Yagci, Y. *Macromolecular Rapid Communications* **2011,** 32, (1), 58-62.
52. Treat, N. J.; Sprafke, H.; Kramer, J. W.; Clark, P. G.; Barton, B. E.; Read de Alaniz, J.; Fors, B. P.; Hawker, C. J. *Journal of the American Chemical Society* **2014,** 136, (45), 16096-16101.
53. Anastasaki, A.; Nikolaou, V.; Brandford-Adams, F.; Nurumbetov, G.; Zhang, Q.; Clarkson, G. J.; Fox, D. J.; Wilson, P.; Kempe, K.; Haddleton, D. M. *Chemical Communications* **2015,** 51, (26), 5626-5629.
54. Anastasaki, A.; Nikolaou, V.; McCaul, N. W.; Simula, A.; Godfrey, J.; Waldron, C.; Wilson, P.; Kempe, K.; Haddleton, D. M. *Macromolecules* **2015,** 48, (5), 1404-1411.
55. Laun, J.; Vorobii, M.; de los Santos Pereira, A.; Pop-Georgievski, O.; Trouillet, V.; Welle, A.; Barner-Kowollik, C.; Rodriguez-Emmenegger, C.; Junkers, T. *Macromolecular Rapid Communications* **2015,** 36, (18), 1681-1686.
56. Percec, V.; Guliashvili, T.; Ladislaw, J. S.; Wistrand, A.; Stjerndahl, A.; Sienkowska, M. J.; Monteiro, M. J.; Sahoo, S. *Journal of the American Chemical Society* **2006,** 128, (43), 14156-14165.
57. Nguyen, N. H.; Levere, M. E.; Percec, V. *Journal of Polymer Science Part a-Polymer Chemistry* **2012,** 50, (5), 860-873.
58. Jiang, X. A.; Rosen, B. M.; Percec, V. *Journal of Polymer Science Part a-Polymer Chemistry* **2010,** 48, (12), 2716-2721.
59. Nystroem, F.; Soeriyadi, A. H.; Boyer, C.; Zetterlund, P. B.; Whittaker, M. R. *Journal of Polymer Science Part a-Polymer Chemistry* **2011,** 49, (24), 5313-5321.
60. Anastasaki, A.; Nikolaou, V.; Nurumbetov, G.; Wilson, P.; Kempe, K.; Quinn, J. F.; Davis, T. P.; Whittaker, M. R.; Haddleton, D. M. *Chemical Reviews* **2015**.
61. Anastasaki, A.; Waldron, C.; Nikolaou, V.; Wilson, P.; McHale, R.; Smith, T.; Haddleton, D. M. *Polymer Chemistry* **2013,** 4, (15), 4113-4119.
62. Rosen, B. M.; Percec, V. *Chemical Reviews* **2009,** 109, (11), 5069-5119.
63. Zhang, N.; Samanta, S. R.; Rosen, B. M.; Percec, V. *Chemical Reviews* **2014,** 114, (11), 5848-5958.
64. Levere, M. E.; Willoughby, I.; O'Donohue, S.; de Cuendias, A.; Grice, A. J.; Fidge, C.; Becer, C. R.; Haddleton, D. M. *Polymer Chemistry* **2010,** 1, (7), 1086-1094.
65. Frick, E.; Anastasaki, A.; Haddleton, D. M.; Barner-Kowollik, C. *Journal of the American Chemical Society* **2015,** 137, (21), 6889-6896.
66. Rosen, B. M.; Percec, V. *Journal of Polymer Science Part a-Polymer Chemistry* **2008,** 46, (16), 5663-5697.

67. Fleischmann, S.; Percec, V. *Journal of Polymer Science Part a-Polymer Chemistry* **2010,** 48, (10), 2236-2242.
68. Hatano, T.; Rosen, B. M.; Percec, V. *Journal of Polymer Science Part a-Polymer Chemistry* **2010,** 48, (1), 164-172.
69. Jones, M. W.; Gibson, M. I.; Mantovani, G.; Haddleton, D. M. *Polymer Chemistry* **2011,** 2, (3), 572-574.
70. Syrett, J. A.; Jones, M. W.; Haddleton, D. M. *Chemical Communications* **2010,** 46, (38), 7181-7183.
71. Rosen, B. M.; Lligadas, G.; Hahn, C.; Percec, V. *Journal of Polymer Science Part a-Polymer Chemistry* **2009,** 47, (15), 3940-3948.
72. Zhang, Q.; Anastasaki, A.; Li, G. Z.; Haddleton, A. J.; Wilson, P.; Haddleton, D. M. *Polymer Chemistry* **2014,** 5, (12), 3876-3883.
73. Jing, R. K.; Wang, G. W.; Zhang, Y. N.; Huang, J. L. *Macromolecules* **2011,** 44, (4), 805-810.
74. Rosen, B. M.; Jiang, X.; Wilson, C. J.; Nguyen, N. H.; Monteiro, M. J.; Percec, V. *Journal of Polymer Science Part a-Polymer Chemistry* **2009,** 47, (21), 5606-5628.
75. Nguyen, N. H.; Percec, V. *Journal of Polymer Science Part a-Polymer Chemistry* **2011,** 49, (19), 4227-4240.
76. Levere, M. E.; Nguyen, N. H.; Leng, X. F.; Percec, V. *Polymer Chemistry* **2013,** 4, (5), 1635-1647.
77. Zhang, Q.; Wilson, P.; Li, Z.; McHale, R.; Godfrey, J.; Anastasaki, A.; Waldron, C.; Haddleton, D. M. *Journal of the American Chemical Society* **2013,** 135, (19), 7355-7363.
78. Nguyen, N. H.; Levere, M. E.; Kulis, J.; Monteiro, M. J.; Percec, V. *Macromolecules* **2012,** 45, (11), 4606-4622.
79. Nguyen, N. H.; Levere, M. E.; Percec, V. *Journal of Polymer Science Part a-Polymer Chemistry* **2012,** 50, (1), 35-46.
80. Nguyen, N. H.; Jiang, X.; Fleischmann, S.; Rosen, B. M.; Percec, V. *Journal of Polymer Science Part a-Polymer Chemistry* **2009,** 47, (21), 5629-5638.
81. Anastasaki, A.; Waldron, C.; Wilson, P.; McHale, R.; Haddleton, D. M. *Polymer Chemistry* **2013,** 4, (9), 2672-2675.
82. Simula, A.; Nikolaou, V.; Alsubaie, F.; Anastasaki, A.; Haddleton, D. M. *Polymer Chemistry* **2015,** 6, (32), 5940-5950.
83. Samanta, S. R.; Nikolaou, V.; Keller, S.; Monteiro, M. J.; Wilson, D. A.; Haddleton, D. M.; Percec, V. *Polymer Chemistry* **2015,** 6, (11), 2084-2097.
84. Levere, M. E.; Nguyen, N. H.; Sun, H. J.; Percec, V. *Polymer Chemistry* **2013,** 4, (3), 686-694.
85. Nguyen, N. H.; Sun, H. J.; Levere, M. E.; Fleischmann, S.; Percec, V. *Polymer Chemistry* **2013,** 4, (5), 1328-1332.
86. Nguyen, N. H.; Percec, V. *Journal of Polymer Science Part a-Polymer Chemistry* **2011,** 49, (19), 4241-4252.
87. Jiang, X.; Rosen, B. M.; Percec, V. *Journal of Polymer Science Part a-Polymer Chemistry* **2010,** 48, (2), 403-409.
88. Nguyen, N. H.; Percec, V. *Journal of Polymer Science Part a-Polymer Chemistry* **2010,** 48, (22), 5109-5119.
89. Nguyen, N. H.; Rosen, B. M.; Lligadas, G.; Percec, V. *Macromolecules* **2009,** 42, (7), 2379-2386.

90. Samanta, S. R.; Levere, M. E.; Percec, V. *Polymer Chemistry* **2013,** 4, (11), 3212-3224.
91. Nguyen, N. H.; Rosen, B. M.; Percec, V. *Journal of Polymer Science Part a-Polymer Chemistry* **2010,** 48, (8), 1752-1763.
92. Nguyen, N. H.; Rosen, B. M.; Jiang, X.; Fleischmann, S.; Percec, V. *Journal of Polymer Science Part a-Polymer Chemistry* **2009,** 47, (21), 5577-5590.
93. Wright, P. M.; Mantovani, G.; Haddleton, D. M. *Journal of Polymer Science Part a-Polymer Chemistry* **2008,** 46, (22), 7376-7385.
94. Levere, M. E.; Willoughby, I.; O'Donohue, S.; Wright, P. M.; Grice, A. J.; Fidge, C.; Becer, C. R.; Haddleton, D. M. *Journal of Polymer Science Part a-Polymer Chemistry* **2011,** 49, (8), 1753-1763.
95. Boyer, C.; Atme, A.; Waldron, C.; Anastasaki, A.; Wilson, P.; Zetterlund, P. B.; Haddleton, D.; Whittaker, M. R. *Polymer Chemistry* **2013,** 4, (1), 106-112.
96. Asubaie, F.; Anastasaki, A.; Nikolaou, V.; Simula, A.; Nurumbetov, G.; Wilson, P.; Kempe, K.; Haddleton, D. M. *Macromolecules* **2015,** 48, (18), 6421-6432.
97. Konkolewicz, D.; Wang, Y.; Zhong, M.; Krys, P.; Isse, A. A.; Gennaro, A.; Matyjaszewski, K. *Macromolecules* **2013,** 46, (22), 8749-8772.
98. Konkolewicz, D.; Wang, Y.; Krys, P.; Zhong, M.; Isse, A. A.; Gennaro, A.; Matyjaszewski, K. *Polymer Chemistry* **2014,** 5, (15), 4396-4417.
99. Harrisson, S.; Nicolas, J. *ACS Macro Letters* **2014,** 3, (7), 643-647.
100. Alsubaie, F.; Anastasaki, A.; Nikolaou, V.; Simula, A.; Nurumbetov, G.; Wilson, P.; Kempe, K.; Haddleton, D. M. *Macromolecules* **2015,** 48, (16), 5517-5525.
101. Destarac, M. *Macromolecular Reaction Engineering* **2010,** 4, (3-4), 165-179.
102. Matyjaszewski, K.; Spanswick, J. *Materials Today* **2005,** 8, (3), 26-33.
103. Barner-Kowollik, C.; Du Prez, F. E.; Espeel, P.; Hawker, C. J.; Junkers, T.; Schlaad, H.; Van Camp, W. *Angewandte Chemie International Edition* **2011,** 50, (1), 60-62.
104. Sumerlin, B. S.; Vogt, A. P. *Macromolecules* **2010,** 43, (1), 1-13.
105. Kolb, H. C.; Finn, M. G.; Sharpless, K. B. *Angewandte Chemie International Edition* **2001,** 40, (11), 2004-2021.
106. Hawker, C. J.; Fokin, V. V.; Finn, M. G.; Sharpless, K. B. *Australian Journal of Chemistry* **2007,** 60, (6), 381-383.
107. Espeel, P.; Du Prez, F. E. *Macromolecules* **2015,** 48, (1), 2-14.
108. Kempe, K.; Krieg, A.; Becer, C. R.; Schubert, U. S. *Chemical Society Reviews* **2012,** 41, (1), 176-191.
109. Golas, P. L.; Matyjaszewski, K. *Chemical Society Reviews* **2010,** 39, (4), 1338-1354.
110. Xi, W.; Scott, T. F.; Kloxin, C. J.; Bowman, C. N. *Advanced Functional Materials* **2014,** 24, (18), 2572-2590.
111. Lutz, J.-F. *Angewandte Chemie International Edition* **2007,** 46, (7), 1018-1025.
112. Rostovtsev, V. V.; Green, L. G.; Fokin, V. V.; Sharpless, K. B. *Angewandte Chemie-International Edition* **2002,** 41, (14), 2596-+.
113. Hein, J. E.; Fokin, V. V. *Chemical Society Reviews* **2010,** 39, (4), 1302-1315.
114. Golas, P. L.; Tsarevsky, N. V.; Sumerlin, B. S.; Walker, L. M.; Matyjaszewski, K. *Australian Journal of Chemistry* **2007,** 60, (6), 400-404.
115. Tsarevsky, N. V.; Sumerlin, B. S.; Matyjaszewski, K. *Macromolecules* **2005,** 38, (9), 3558-3561.
116. Agard, N. J.; Prescher, J. A.; Bertozzi, C. R. *Journal of the American Chemical Society* **2004,** 126, (46), 15046-15047.

117. Becer, C. R.; Hoogenboom, R.; Schubert, U. S. *Angewandte Chemie International Edition* **2009,** 48, (27), 4900-4908.
118. Tasdelen, M. A. *Polymer Chemistry* **2011,** 2, (10), 2133-2145.
119. Hoyle, C. E.; Lowe, A. B.; Bowman, C. N. *Chemical Society Reviews* **2010,** 39, (4), 1355-1387.
120. Diels, O.; Alder, K. *Justus Liebigs Annalen der Chemie* **1928,** 460, (1), 98-122.
121. Hansell, C. F.; Espeel, P.; Stamenovic, M. M.; Barker, I. A.; Dove, A. P.; Du Prez, F. E.; O'Reilly, R. K. *Journal of the American Chemical Society* **2011,** 133, (35), 13828-13831.
122. Tietze, L. F.; Kettschau, G. *Stereoselective Heterocyclic Synthesis I* **1997,** 189, 1-120.
123. Pirkle, W. H.; Stickler, J. C. *Chemical Communications* **1967**, (15), 760-&.
124. Sauer, J. *Angewandte Chemie-International Edition* **1967,** 6, (1), 16-+.
125. Butler, G. B. *Polymer Science U.S.S.R.* **1981,** 23, (11), 2587-2622.
126. Thiele, J.; Stange, O. *Justus Liebigs Annalen der Chemie* **1894,** 283, (1-2), 1-46.
127. Cookson, R. C.; Gilani, S. S. H.; Stevens, I. D. R. *Tetrahedron Letters* **1962**, (14), 615-618.
128. Cookson, R. C.; Gilani, S. S. H.; Stevens, I. D. R. *Journal of the Chemical Society C-Organic* **1967**, (19), 1905-&.
129. Pounder, R. J.; Stanford, M. J.; Brooks, P.; Richards, S. P.; Dove, A. P. *Chemical Communications* **2008**, (41), 5158-5160.
130. Northrop, B. H.; Frayne, S. H.; Choudhary, U. *Polymer Chemistry* **2015,** 6, (18), 3415-3430.
131. Fontaine, S. D.; Reid, R.; Robinson, L.; Ashley, G. W.; Santi, D. V. *Bioconjugate Chemistry* **2015,** 26, (1), 145-152.
132. Adam, W.; De Lucchi, O. *Tetrahedron Letters* **1981,** 22, (10), 929-932.
133. Singleton, D. A.; Hang, C. *Journal of the American Chemical Society* **1999,** 121, (50), 11885-11893.
134. Leach, A. G.; Houk, K. N. *Chemical Communications* **2002**, (12), 1243-1255.
135. Alder, K.; Pascher, F.; Schmitz, A. *Berichte der deutschen chemischen Gesellschaft (A and B Series)* **1943,** 76, (1-2), 27-53.
136. Mikami, K.; Shimizu, M. *Chemical Reviews* **1992,** 92, (5), 1021-1050.
137. Clarke, M. L.; France, M. B. *Tetrahedron* **2008,** 64, (38), 9003-9031.
138. De Bruycker, K.; Billiet, S.; Houck, H. A.; Chattopadhyay, S.; Winne, J. M.; Du Prez, F. E. *Chemical Reviews* **2016,** 10.1021/acs.chemrev.5b00599.
139. Pirkle, W. H.; Stickler, J. C. *Journal of the American Chemical Society* **1970,** 92, (25), 7497-7499.
140. Kuhrau, M.; Stadler, R. *Die Makromolekulare Chemie* **1992,** 193, (11), 2861-2874.
141. Vlaminck, L.; De Bruycker, K.; Turunc, O.; Du Prez, F. E. *Polymer Chemistry* **2016**.
142. Wang, Z.; Zhang, Y.; Yuan, L.; Hayat, J.; Trenor, N. M.; Lamm, M. E.; Vlaminck, L.; Billiet, S.; Du Prez, F. E.; Wang, Z.; Tang, C. *ACS Macro Letters* **2016,** 5, (5), 602-606.
143. Saville, B. *Journal of the Chemical Society D: Chemical Communications* **1971**, (12), 635-636.
144. Xiao, L.; Chen, Y.; Zhang, K. *Macromolecules* **2016,** 49, (12), 4452-4461.
145. Lowe, A. B. *Polymer Chemistry* **2010,** 1, (1), 17-36.
146. v. Braun, J.; Murjahn, R. *Berichte der deutschen chemischen Gesellschaft (A and B Series)* **1926,** 59, (6), 1202-1209.

147. Hoyle, C. E.; Lee, T. Y.; Roper, T. *Journal of Polymer Science Part A: Polymer Chemistry* **2004,** 42, (21), 5301-5338.
148. Uygun, M.; Tasdelen, M. A.; Yagci, Y. *Macromolecular Chemistry and Physics* **2010,** 211, (1), 103-110.
149. Koo, S. P. S.; Stamenović, M. M.; Prasath, R. A.; Inglis, A. J.; Du Prez, F. E.; Barner-Kowollik, C.; Van Camp, W.; Junkers, T. *Journal of Polymer Science Part A: Polymer Chemistry* **2010,** 48, (8), 1699-1713.
150. Chan, J. W.; Hoyle, C. E.; Lowe, A. B.; Bowman, M. *Macromolecules* **2010,** 43, (15), 6381-6388.
151. Nair, D. P.; Podgorski, M.; Chatani, S.; Gong, T.; Xi, W. X.; Fenoli, C. R.; Bowman, C. N. *Chemistry of Materials* **2014,** 26, (1), 724-744.
152. Liu, M. N.; Tan, B. H.; Burford, R. P.; Lowe, A. B. *Polymer Chemistry* **2013,** 4, (11), 3300-3311.
153. Chan, J. W.; Yu, B.; Hoyle, C. E.; Lowe, A. B. *Polymer* **2009,** 50, (14), 3158-3168.
154. Chan, J. W.; Wei, H. Y.; Zhou, H.; Hoyle, C. E. *European Polymer Journal* **2009,** 45, (9), 2717-2725.
155. Jones, M. W.; Strickland, R. A.; Schumacher, F. F.; Caddick, S.; Baker, J. R.; Gibson, M. I.; Haddleton, D. M. *Journal of the American Chemical Society* **2012,** 134, (3), 1847-1852.
156. Jones, M. W.; Strickland, R. A.; Schumacher, F. F.; Caddick, S.; Baker, J. R.; Gibson, M. I.; Haddleton, D. M. *Chemical Communications* **2012,** 48, (34), 4064-4066.
157. Boyer, C.; Granville, A.; Davis, T. P.; Bulmus, V. *Journal of Polymer Science Part a-Polymer Chemistry* **2009,** 47, (15), 3773-3794.
158. Boyer, C.; Bulmus, V.; Davis, T. P. *Macromolecular Rapid Communications* **2009,** 30, (7), 493-497.
159. Willcock, H.; O'Reilly, R. K. *Polymer Chemistry* **2010,** 1, (2), 149-157.
160. Li, M.; De, P.; Gondi, S. R.; Sumerlin, B. S. *Journal of Polymer Science Part A: Polymer Chemistry* **2008,** 46, (15), 5093-5100.
161. Boyer, C.; Soeriyadi, A. H.; Roth, P. J.; Whittaker, M. R.; Davis, T. P. *Chemical Communications* **2011,** 47, (4), 1318-1320.
162. van den Berg, O.; Dispinar, T.; Hommez, B.; Du Prez, F. E. *European Polymer Journal* **2013,** 49, (4), 804-812.
163. Liras, M.; Garcia, O.; Quijada-Garrido, I.; Paris, R. *Macromolecules* **2011,** 44, (6), 1335-1339.
164. Benesch, R.; Benesch, R. E. *Proceedings of the National Academy of Sciences of the United States of America* **1958,** 44, (9), 848-853.
165. Espeel, P.; Goethals, F.; Du Prez, F. E. *Journal of the American Chemical Society* **2011,** 133, (6), 1678-1681.
166. Linkova, M. G.; Kuleshova, N. D.; Knunyants, I. L. *Russian Chemical Reviews* **1964,** 33, (10), 493-507.
167. Paryzek, Z.; Skiera, W. *Organic Preparations and Procedures International* **2007,** 39, (3), 203-296.
168. Espeel, P.; Goethals, F.; Du Prez, F. E., CHAPTER 9 Thiolactones as Functional Handles for Polymer Synthesis and Modification. In *Thiol-X Chemistries in Polymer and Materials Science*, The Royal Society of Chemistry: 2013; pp 195-216.

169. Espeel, P.; Goethals, F.; Stamenovic, M. M.; Petton, L.; Du Prez, F. E. *Polymer Chemistry* **2012,** 3, (4), 1007-1015.
170. Reinicke, S.; Espeel, P.; Stamenović, M. M.; Du Prez, F. E. *ACS Macro Letters* **2013,** 2, (6), 539-543.
171. Espeel, P.; Goethals, F.; Driessen, F.; Nguyen, L. T. T.; Du Prez, F. E. *Polymer Chemistry* **2013,** 4, (8), 2449-2456.
172. Espeel, P.; Du Prez, F. E. *European Polymer Journal* **2015,** 62, (0), 247-272.
173. Stamenovic, M. M.; Espeel, P.; Baba, E.; Yamamoto, T.; Tezuka, Y.; Du Prez, F. E. *Polymer Chemistry* **2013,** 4, (1), 184-193.
174. Espeel, P.; Carrette, L. L. G.; Bury, K.; Capenberghs, S.; Martins, J. C.; Du Prez, F. E.; Madder, A. *Angewandte Chemie International Edition* **2013,** 52, (50), 13261-13264.
175. Martens, S.; Van den Begin, J.; Madder, A.; Du Prez, F. E.; Espeel, P. *Journal of the American Chemical Society* **2016,** 138, (43), 14182-14185.
176. Vandewalle, S.; Wallyn, S.; Chattopadhyay, S.; Becer, C. R.; Du Prez, F. *European Polymer Journal* **2015,** 69, 490-498.
177. Goethals, F.; Frank, D.; Du Prez, F. *Progress in Polymer Science* **2017,** 64, 76-113.
178. Hadjichristidis, N.; Pitsikalis, M.; Pispas, S.; Iatrou, H. *Chemical Reviews* **2001,** 101, (12), 3747-3792.
179. Lutz, J. F.; Lehn, J. M.; Meijer, E. W.; Matyjaszewski, K. *Nature Reviews Materials* **2016,** 1, (5).
180. Gregory, A.; Stenzel, M. H. *Progress in Polymer Science* **2012,** 37, (1), 38-105.
181. Johnson, J. A.; Finn, M. G.; Koberstein, J. T.; Turro, N. J. *Macromolecular Rapid Communications* **2008,** 29, (12-13), 1052-1072.
182. Fournier, D.; Hoogenboom, R.; Schubert, U. S. *Chemical Society Reviews* **2007,** 36, (8), 1369-1380.
183. Sheiko, S. S.; Sumerlin, B. S.; Matyjaszewski, K. *Progress in Polymer Science* **2008,** 33, (7), 759-785.
184. Pyun, J.; Kowalewski, T.; Matyjaszewski, K. *Macromolecular Rapid Communications* **2003,** 24, (18), 1043-1059.
185. Lessard, B.; Marić, M. *Macromolecules* **2008,** 41, (21), 7870-7880.
186. Zhang, W.; Li, Y.; Liu, L.; Sun, Q.; Shuai, X.; Zhu, W.; Chen, Y. *Biomacromolecules* **2010,** 11, (5), 1331-1338.
187. Petton, L.; Mes, E. P. C.; Van Der Wal, H.; Claessens, S.; Van Damme, F.; Verbrugghe, S.; Du Prez, F. E. *Polymer Chemistry* **2013,** 4, (17), 4697-4709.
188. Khelfallah, N.; Gunari, N.; Fischer, K.; Gkogkas, G.; Hadjichristidis, N.; Schmidt, M. *Macromolecular Rapid Communications* **2005,** 26, (21), 1693-1697.
189. Gao, H.; Matyjaszewski, K. *Journal of the American Chemical Society* **2007,** 129, (20), 6633-6639.
190. Kissa, E., *Dispersions: characterization, testing, and measurement*. CRC Press: 1999; Vol. 84.
191. Morrison, I., *Kirk-Othmer Encyclopedia of Chemical Technology*. 5 ed.; John Wiley & Sons, Inc., 2000: Vol. 8, p 697.
192. Pirrung, F.; Auschra, C., Polymeric Dispersants. In *Macromolecular Engineering*, Wiley-VCH Verlag GmbH & Co. KGaA: 2007; pp 2135-2180.
193. Holmberg, K.; Bo, J.; Kronberg, B., *Surfactants and Polymers in Aqueous Solution*. 2002.

194. Heusch, R.; Reizlein, K., Disperse Systems and Dispersants. In *Ullmann's Encyclopedia of Industrial Chemistry*, Wiley-VCH Verlag GmbH & Co. KGaA: 2000.
195. Napper, D. H. *Journal of Colloid and Interface Science* **1977,** 58, (2), 390-407.
196. van den Haak, H. J. W., *Kirk-Othmer Encyclopedia of Chemical Technology*. 5 ed.; John Wiley & Sons, Inc., 2000: Vol. 8, p 672.
197. Smitham, J. B.; Evans, R.; Napper, D. H. *Journal of the Chemical Society-Faraday Transactions I* **1975,** 71, (2), 285-297.
198. Ma, S. H. Polymeric pigment dispersants having multiple pigment anchoring groups.

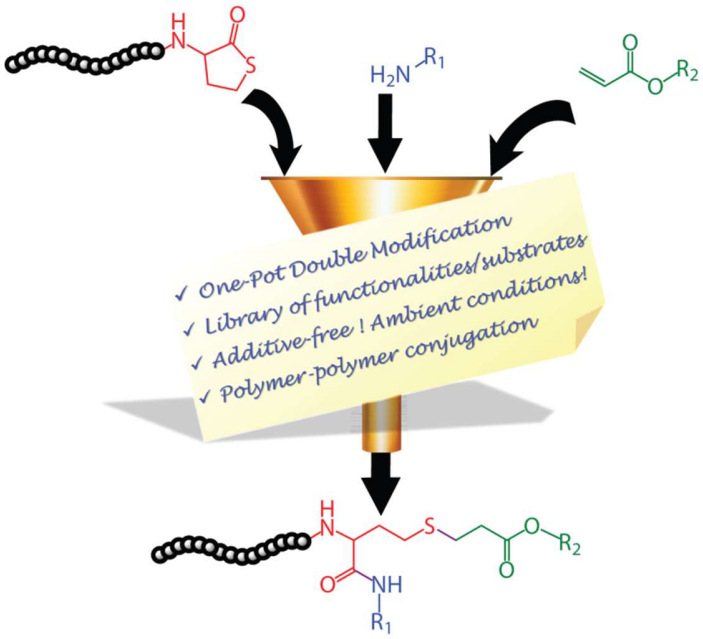

Abstract

This chapter describes a straightforward synthetic procedure for the double modification and polymer-polymer conjugation of telechelic polymers by the use of thiolactone chemistry. In a first part, thiolactone end functionalized polymers were prepared *via* two synthetically distinguished methods, through reversible deactivation radical polymerization of a thiolactone containing initiator or by modification of hydroxyl end functionalized polymers with a thiolactone containing isocyanate. Next, benzyl amine and benzyl acrylate were applied in a model study to acquire the reaction conditions for the amine-thiol-ene conjugation and the outcome was monitored *via* SEC, NMR and MALDI-TOF analysis. Furthermore, a library of different telechelic structures was obtained by selective variation of the amine and acrylate compounds. Finally, this methodology was applied for the synthesis of block copolymers through polymer-polymer conjugation and the final outcome was analyzed by the use of LCxSEC analysis.

Parts of this chapter were published as:

Driessen F., Martens S., De Meyer B., Du Prez F.E., Espeel P., *Macromolecular Rapid Communications*, **2016**, 37 (12), 947-951

Chapter III.

Double modification of polymer end groups through thiolactone chemistry

III.1 Introduction

This doctoral thesis implements the use of two efficient strategies (it. thiolactone- and triazolinedione chemistry) for the synthesis of functional and complex copolymer structures.[1-5] In a first part, thiolactone chemistry will be explored in the synthesis of tailor-made macromolecular architectures. To gradually increase the level of complexity of the targeted copolymers, this third section deals with the use of thiolactone chemistry through amine-thiol-ene conjugation for the synthesis of end functionalized polymers. As already described in more detail in chapter two, a thiolactone can react in a consecutive orthogonal manner with a functional amine and acrylate. The amine will open the five-membered ring first, releasing the thiol that reacts with the acrylate in a consecutive step. During this process, the side-reactions between the amine and acrylate and disulfide formation are significantly reduced as explained in chapter II. In this way, the introduction of two distinct functionalities at the same reactive site is enabled, performing the double modification of polymeric end groups.[6]

The introduction of more than one functional handle at the same site can be an interesting feature to further improve the design of tailor-made polymers and adjust its final properties for a broad range of applications. In literature, only few examples have been reported that provide the possibility of introducing more than one functionality at the same site, mainly from the groups of Tozzi, Theato, Sumerlin and our own research group. Tozzi *et al.* employed the nucleophilic ring-opening of pendant epoxides and subsequent modification of the released alcohol with an isocyanate to generate double functionalized polymers.[7] Several methods were described by Theato et al., it. the Cu-catalyzed three-component reaction between a terminal alkyne, sulfonyl azide and secondary amine; the Kabachnik-Fields reaction as alternative metal-free approach between poly(4-vinylbenzaldehyde), primary amines and phosphites and the coupling between a

pentafluorophenyl, primary amine and hydrazide or hydroxylamine.[8-10] The group of Sumerlin implemented triazines for the double modification of polymer side chains. Polymers containing pendant triazines were synthesized through RAFT polymerization of a triazine-based acrylate. Next, an amine or thiol was added to introduce the first functionality. After intermediate purification, double modification was accomplished by reaction of the side chains with another functional amine or thiol at elevated temperature.[11]

In literature, many examples can be retrieved on chemistries for end group modifications, it. transformation of the dithiocarbamate in RAFT or halogen in ATRP, functional terminators in Cationic Ring-Opening Polymerization (CROP), [2+2] cyclo-addition reactions, modification of azlactones and many others.[12-17] However, increasing the level of functionality at the end group can be an interesting approach for surface modification or oligomer synthesis for functional polyester, -amide, or –urethane design. One of the first examples on the double modification of polymer end groups was reported by Sumerlin *et al.*. PEO was modified with 2,4,6-trichloro-1,3,5-triazine, introducing a reactive handle as end group. As already mentioned for this triazine chemistry, amines and thiols can be applied for the double modification of the polymeric structure. However, this two-step modification procedure, with intermediate purification, use of different solvents and requirement of elevated temperatures could hinder the implementation of this synthetic platform for the double modification of tailored polymeric end groups. Furthermore, triazines can only be introduced by nucleophilic substitution, confining its implementation to the use of polymers end-capped with functional groups such as alcohols, amines or thiols.[18]

This chapter describes the one-pot double modification of a variety of different polymers containing a thiolactone as end group. The thiolactone handle was introduced *via* two different pathways, through RDRP of a thiolactone-containing initiator or by modification of hydroxyl-functionalized polymers with an isocyanate-containing thiolactone. Next, these polymeric structures were treated with a variety of different functional amines and acrylates, resulting in the double modification of the polymeric end groups in a one-pot approach without intermediate purification. In this way, a library of tailored end-functionalized polymers was created. Finally, this strategy was applied in the synthesis of amphiphilic block-copolymers *via* polymer-polymer

conjugation (Figure III.1). Simple mixing of thiolactone and amine end-functionalized polymers, opposite in polarity, yielded the corresponding block copolymer, as evidenced by LCxSEC analysis .[19-21]

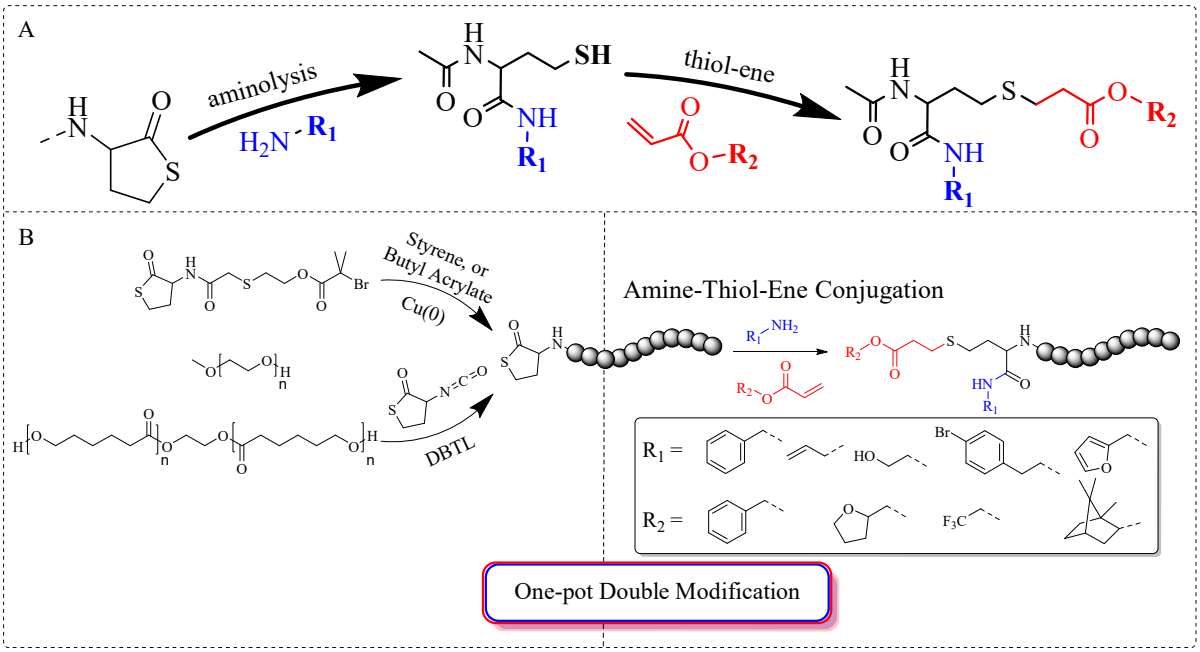

Figure III. 1: Synthetic strategy for the synthesis and one-pot double modification of polymers containing a thiolactone end group (B) *via* the amine-thiol-ene conjugation strategy (A).

III.2 Synthesis of thiolactone end functionalized polymers

III.2.1 Introduction of the thiolactone moiety *via* RDRP

Synthesis of a thiolactone functionalized initiator for Cu-mediated polymerizations

In this project, the first strategy to obtain thiolactone end-functionalized polymers was by the use of RDRP methods. A Cu(0)-mediated polymerization technique was chosen, as a result of the high end group fidelity which can be obtained and the straightforward approach in which the thiolactone moiety can be introduced by the use of a functionalized initiator. Therefore, a multigram synthesis of a thiolactone-containing initiator was performed. In a first step, *N*-(2-bromoacetyl)homocysteine-γ-thiolactone was obtained by reaction of the commercial DL-homocysteine thiolactone hydrochloride with bromoacetyl bromide and the product was isolated

by simple extraction. Next, *N*-(2-bromoacetyl)homocysteine-γ-thiolactone was treated with 2-mercaptoethanol. After full conversion of the *N*-(2-bromoacetyl)homocysteine-γ-thiolactone), α-bromoisobutyryl bromide was added to the crude reaction mixture (Figure III.2). Next, the final product was isolated by column chromatography and analyzed by NMR and LC-MS analysis (Figure III.3).

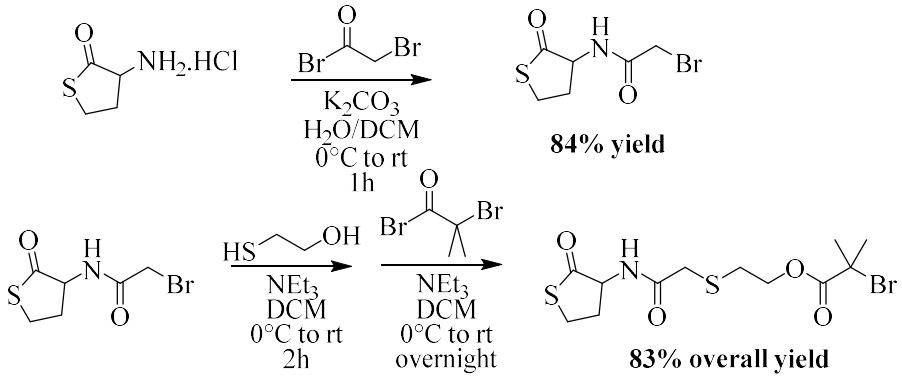

Figure III. 2: Synthesis of a thiolactone-containing intiator for Cu-mediated polymerization.

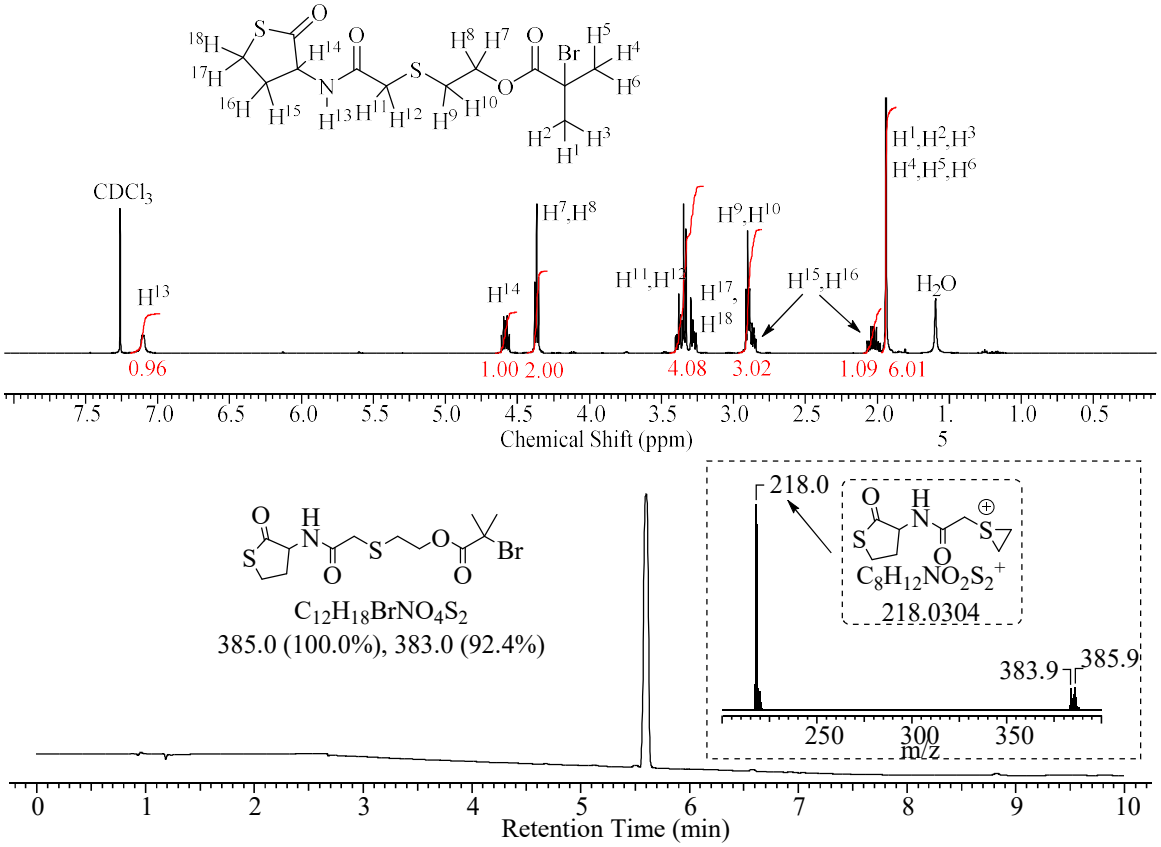

Figure III. 3: ^{1}H-NMR spectrum with peak assignment and integration (top) and HPLC trace with MS analysis (positive mode) of the dominant species (*bottom*) of the purified initiator.

Synthesis of thiolactone end-functionalized polymers

After the synthesis of the thiolactone containing initiator, two different monomers with distinct reactivity were polymerized to demonstrate the broad applicability of this method. First, styrene was polymerized *via* a Cu(0)-mediated polymerization system by the use of the thiolactone functionalized initiator (Figure III.4).

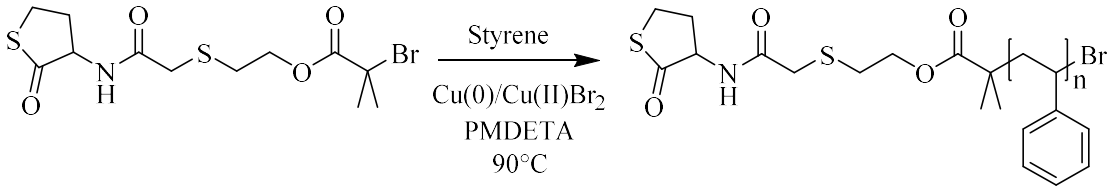

Figure III. 4: Cu(0)-mediated polymerization of styrene *via* a thiolactone containing initiator.

A kinetic study was performed to reveal the controlled nature of the polymerization. Samples were taken at regular time intervals and measured by SEC and Gas Chromatography (GC) to determine the molecular weight and conversion respectively (Figure III.5). The conversion was calculated *via* GC by integrating the signal of styrene and comparing it to the integration of 1,2-dichlorobenzene as internal standard as a function of time. NMR was not used to avoid long measuring times, due to the high number of samples. A linear relation between conversion and molecular weight can be observed. In combination with the dispersity decreasing with increasing conversion, this evidences the controlled nature of the polymerization.

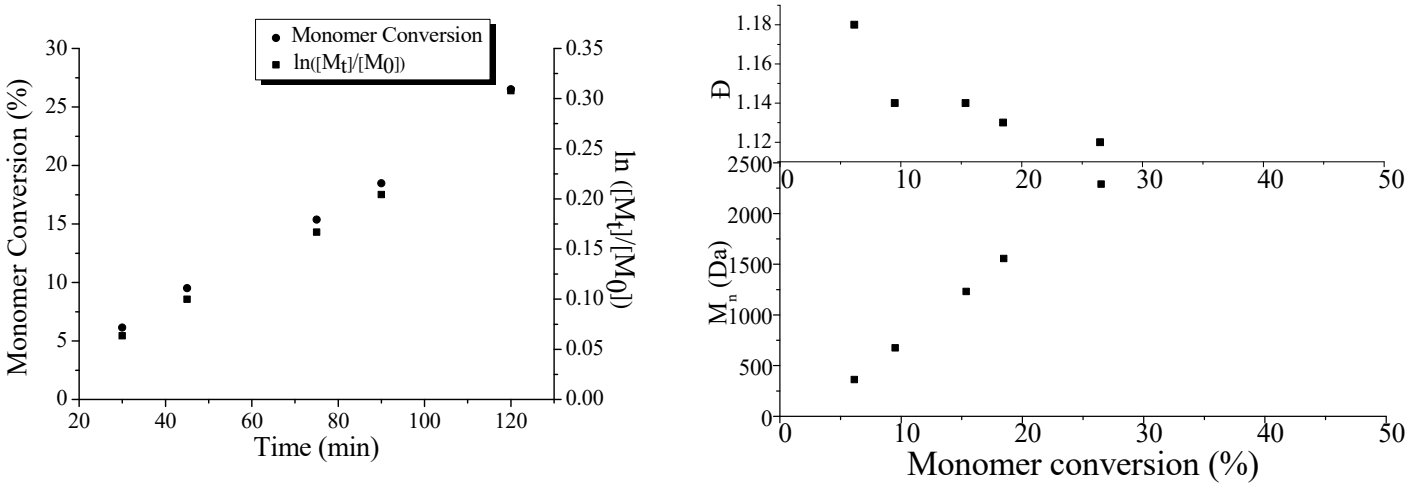

Figure III. 5: Kinetic data for the Cu(0)-mediated polymerization of styrene *via* a thiolactone initiator; (left) first order kinetic plot; (right) molecular weight and dispersity as a function of conversion.

To confirm the presence of the thiolactone moiety as end group on PS (TL-PS), the polymer was analyzed by ^{1}H-NMR and MALDI-TOF analysis (Figure III.6). In ^{1}H-NMR, the distinct signals of the thiolactone moiety at 2.8, 3.25 and 4.6 ppm can be observed. Furthermore, from MALDI-TOF analysis, the good agreement between theoretical and experimental molecular weight indicated the presence of the thiolactone end group. Furthermore, a mass difference of 104.06 Da between two successive analogous signals confirmed the presence of the styrenic unit. The presence of the second distribution coming from the sodium adduct is due to impurities, originating from the glassware.

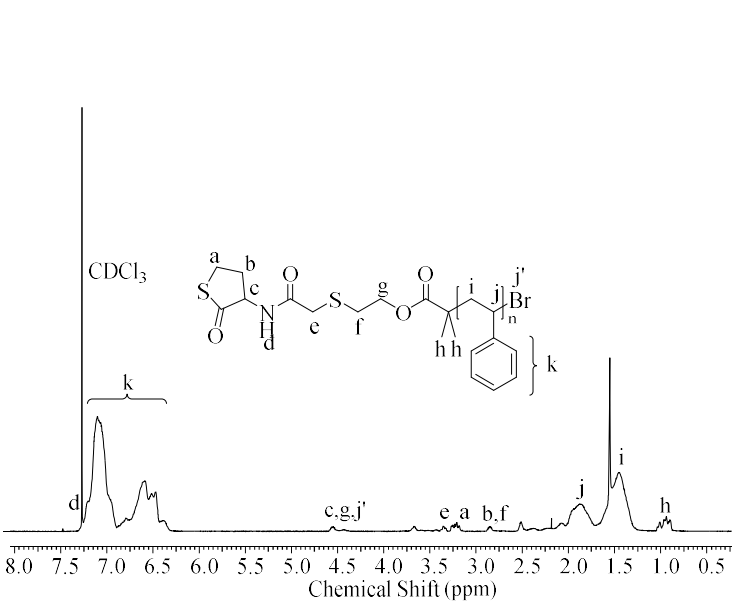

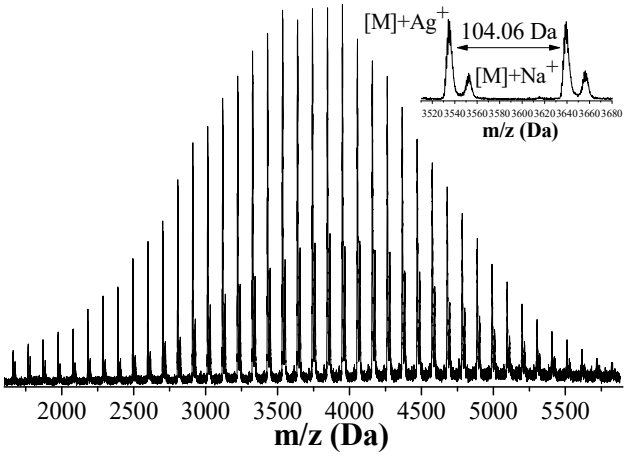

Theoretical m/z (Da)	Experimental m/z (Da)
3635.91	3635.31
3739.97	3739.36
3844.03	3843.41

Figure III. 6: ^{1}H-NMR (left) and MALDI-TOF analysis (right) of TL-PS.

Butyl acrylate as a second monomer was polymerized utilizing the thiolactone initiator. Again a Cu(0)-mediated polymerization was performed and kinetics were analyzed to evidence the controlled nature of the polymerization (Figures III.7-8).

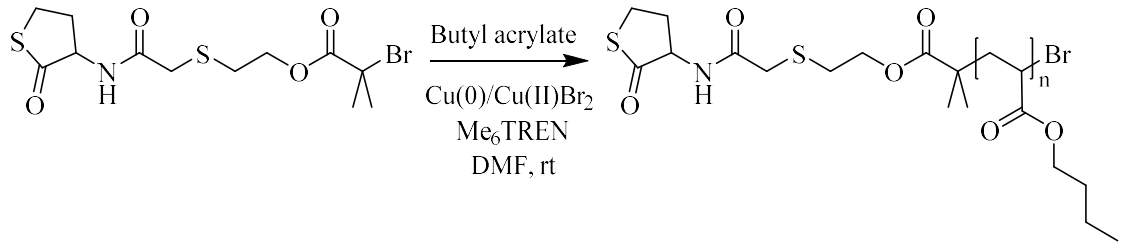

Figure III. 7: Cu(0)-mediated polymerization of butyl acrylate via a thiolactone containing initiator.

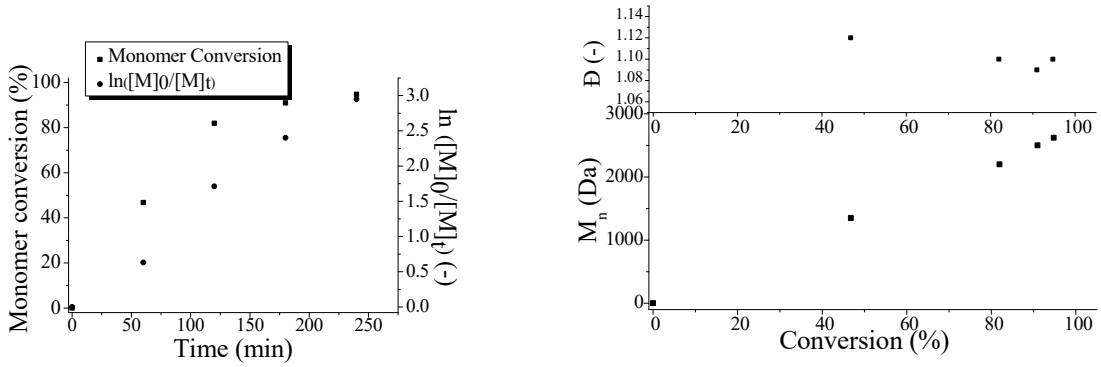

Figure III. 8: Kinetic data for the Cu(0)-mediated polymerization of butyl acrylate via a thiolactone initiator; (left) first order kinetic plot; (right) molecular weight and dispersity as a function of conversion.

To confirm the presence of the thiolactone containing poly(butylacrylate) (TL-PBA) moiety as end group, the polymer was analyzed by ^{1}H-NMR and MALDI-TOF analysis (Figure III.9). Again, the same signals from the thiolactone unit could be observed in the ^{1}H-NMR spectrum, confirming the structure of the polymer. From MALDI-TOF analysis, a good agreement between theoretical and experimental molecular weight and a mass difference of 128.08 Da were observed evidencing the TL-PBA structure (a slight increased difference compared to theoretical mass values was noted, possibly due to the broad signal as a result of the two different isotopes originating from the bromine end group). The extra distribution in MALDI-TOF can be explained by the β-elimination of the bromide (M_{theo} = 3143.90 Da).

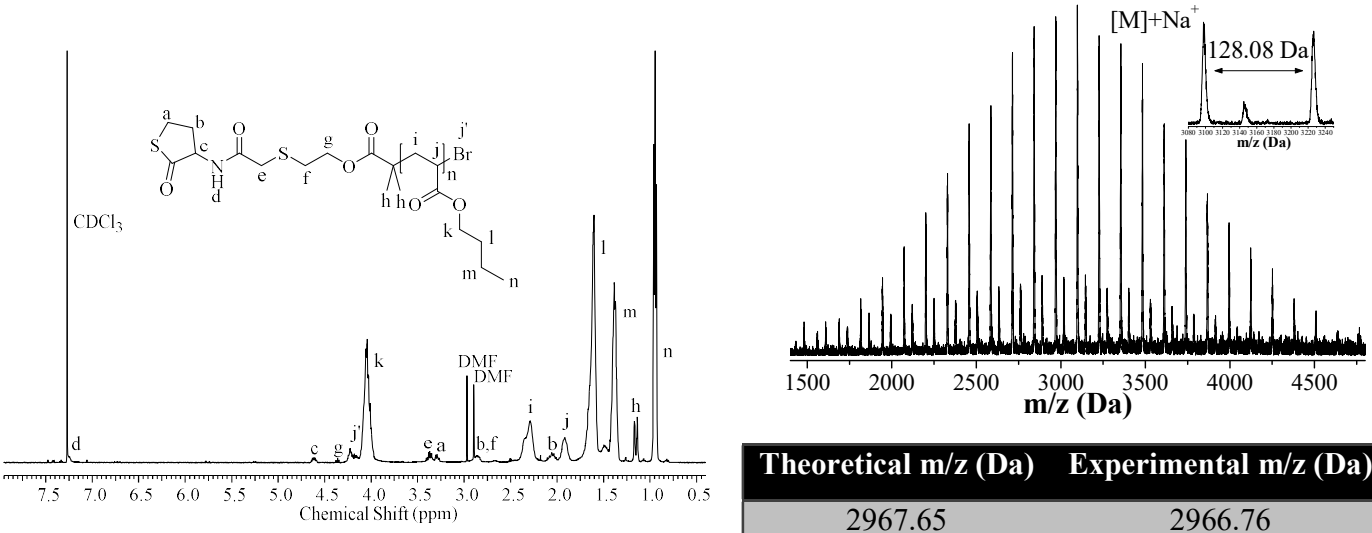

Theoretical m/z (Da)	Experimental m/z (Da)
2967.65	2966.76
3095.73	3094.84
3223.82	3222.93

Figure III. 9: ^{1}H-NMR (left) and MALDI-TOF (right) analysis of TL-PBA.

III.2.2 Introduction of thiolactone moiety through end group modification

A second method for the introduction of thiolactones as end group on a polymer chain is the use of end group modification reactions. In this case, the thiolactone was introduced by reaction of hydroxyl end-functionalized polymers with α-cyanato-γ-thiolactone, a thiolactone containing isocyanate. The isocyanate was prepared on multi-gram scale by reaction of DL-homocysteine thiolactone hydrochloride with triphosgene and isolated by distillation (Figure III.10).

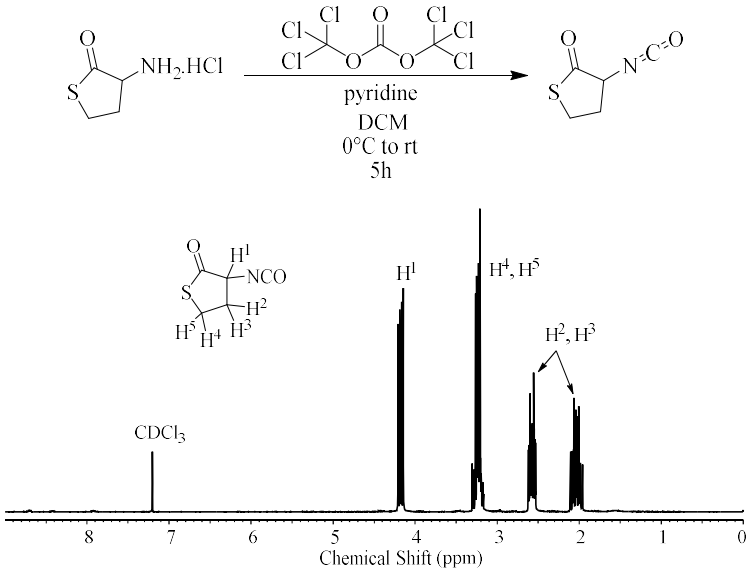

Figure III. 10: Synthetic scheme and ^{1}H-NMR of α-cyanato-γ-thiolactone by reaction of DL-homocysteine thiolactone hydrochloride with triphosgene.

Two different hydroxyl end-functionalized polymers were selected, the hydrophilic poly(ethylene oxide) methyl ether (PEO-OH, M_n ~ 2000 Da) and bifunctional polycaprolactone-diol (HO-PCL-OH, M_n ~ 6000 Da) as they can be easily precipitated in the appropriate non-solvent. Modification was performed by reaction with α-cyanato-γ-thiolactone in the presence of dibutyltin dilaurate (DBTL) as a catalyst to facilitate urethane formation. The successful outcome of both modification reactions was confirmed by ^{1}H-NMR and MALDI-TOF analysis (Figures III.11-12). In both cases, the presence of the thiolactone unit could be observed at 2.8, 3.25 and 4.25 ppm from ^{1}H-NMR analysis. From MALDI-TOF analysis, a good agreement between theoretical and experimental molecular weight could be observed in combination with the repeating mass unit of 44.03Da and 114.07 Da for PEO and PCL respectively, confirming the structures of TL-PEO and TL-PCL-TL.

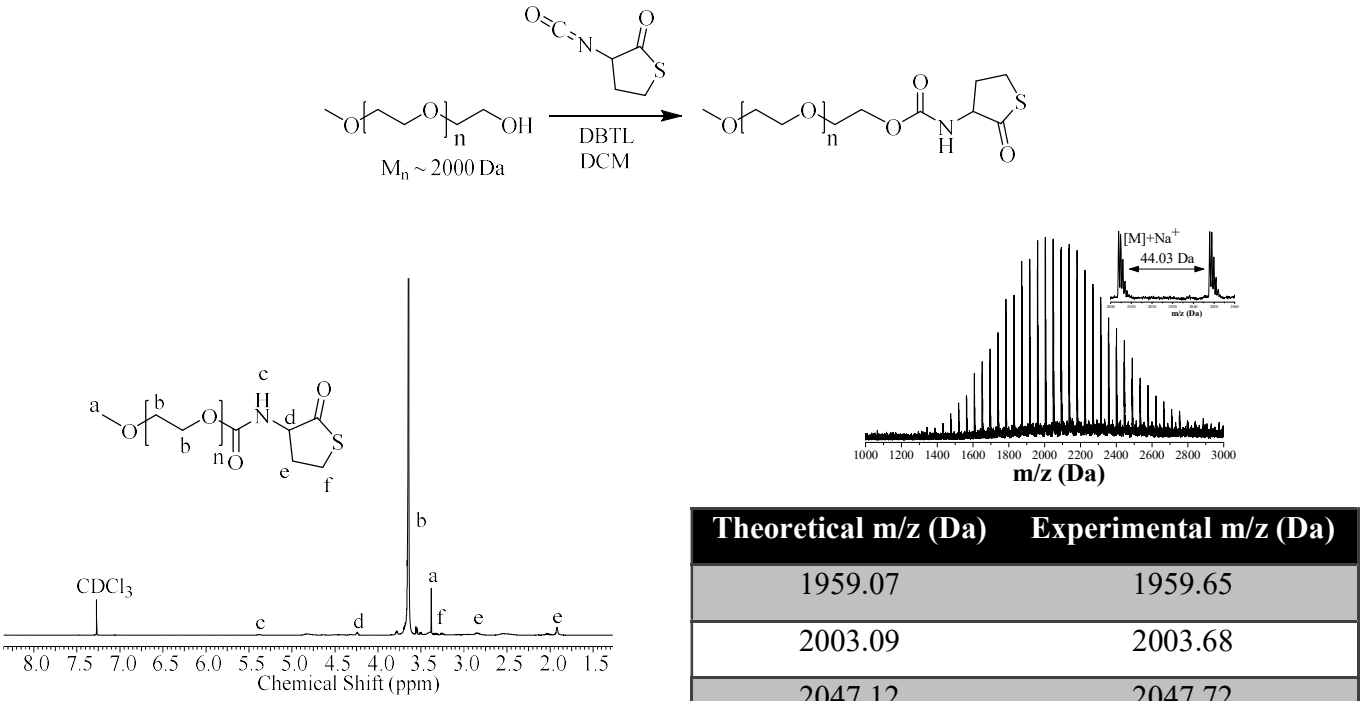

Theoretical m/z (Da)	Experimental m/z (Da)
1959.07	1959.65
2003.09	2003.68
2047.12	2047.72

Figure III. 11: End group modification of PEO-OH with a thiolactone-containing isocyanate with ^{1}H-NMR (left) and MALDI-TOF analysis (right).

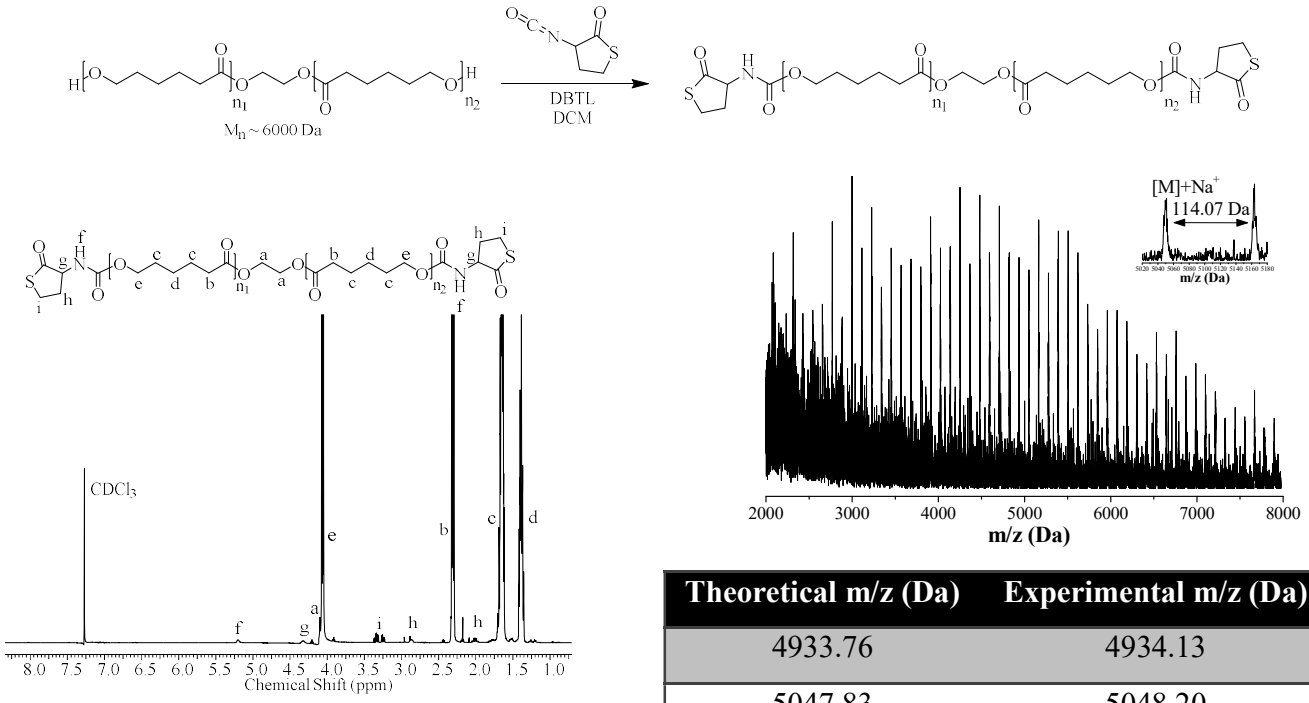

Theoretical m/z (Da)	Experimental m/z (Da)
4933.76	4934.13
5047.83	5048.20
5161.90	5162.27

Figure III. 12: End group modification of HO-PCL-OH with a thiolactone-containing isocyanate with ^{1}H-NMR (left) and MALDI-TOF analysis (right).

III.3 One-pot double modification reaction

III.3.1 Model studies

After the successful synthesis of four different thiolactone end-functionalized polymers (TL-PS, TL-PBA, TL-PEO and TL-PCL-TL), a series of different model studies were performed on each of the different polymers to determine the experimental conditions for the one-pot double modification reaction. As already described in the introductory part, when a primary amine, thiolactone and acrylate are present in the same reaction medium, a chemoselective discrimination, regarding the nucleophilic lysis of the amine to the thiolactone moiety and consecutive addition of the released thiol to the acrylate unit, is observed.

Benzylamine and benzyl acrylate were utilized as model compounds. A study was performed, reaction conditions of *in-house* results on the double modification of thiolactone-containing beads were used to develop a uniform straightforward protocol in which the acrylate and amine were added one after another. Taking into account aminolysis as rate determining step, in comparison to the nucleophilic thiol-ene reaction, side reactions (it. disulfide formation) were avoided by first evaluating different ratios of amine and acrylate for the double modification reaction.

In the case of polystyrene, a ratio of 10/15 equivalents of amine/acrylate in chloroform relative to the thiolactone unit, was sufficient for the effective post polymerization modification (PPM) reaction. Reaction times of 48 hours were used to assure a complete conversion. From SEC analysis, a clear unimodal shift in molecular weight can be observed from TL-PS to the corresponding PS reacted with benzylamine and benzyl acrylate, while the value of dispersity decreased. From ^{1}H-NMR analysis it can be observed that the original signal of the thiolactone at 3.25 ppm disappeared and the benzylic protons at 4.7 and 5.3 ppm appeared. Furthermore, MALDI-TOF analysis further evidenced the full conversion of the thiolactone to the double modified species. No remaining starting product could be observed, experimental and theoretical mass values were in good agreement and no side reaction between the amine or thiol with the bromine end group was observed as no extra distribution was detected after modification.

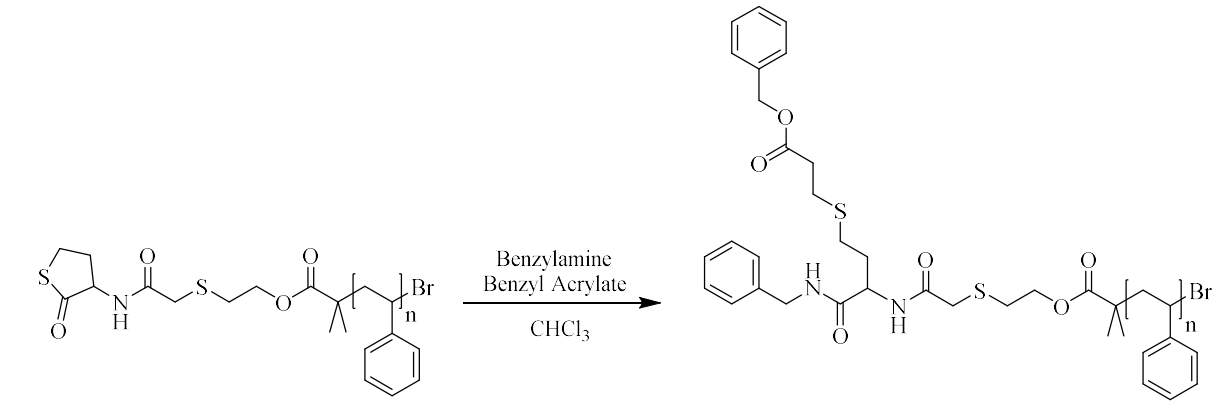

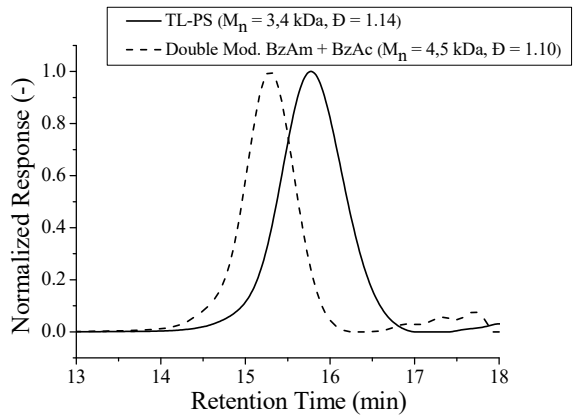

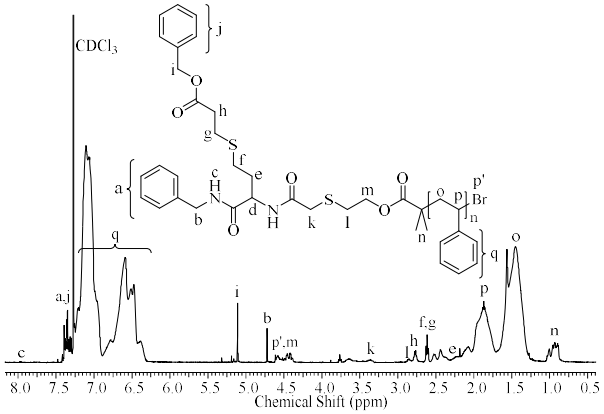

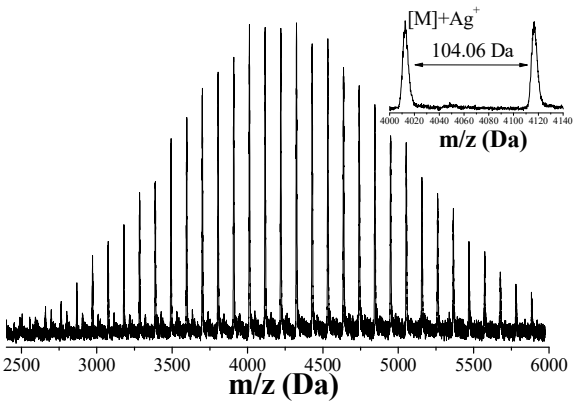

Theoretical m/z (Da)	Experimental m/z (Da)
4113.17	4112.23
4217.24	4216.29
4321.30	4320.34
4425.36	4424.40
4529.42	4528.47

Figure III. 13: One-pot double modification reaction of TL-PS with benzylamine/benzyl acrylate and SEC, ^{1}H-NMR, MALDI-TOF analysis.

For poly(butylacrylate), also a ratio of 10/15 equivalents of amine/acrylate was effective for the double modification reaction. A reaction time of 48 hours was applied to assure a complete conversion and a unimodal shift in molecular weight could be observed from SEC analysis while the value of dispersity decreased. From ^{1}H-NMR, the signal of the thiolactone at 3.25 ppm disappeared and aromatic signals at 7.3 ppm, benzylic signals at 4.7 and 5.3 ppm appeared.

MALDI-TOF analysis confirmed the complete modification reaction as no remaining starting product was observed, theoretical mass values matched with the experimental ones and no side reaction between the amine or thiol with the bromine end group was observed as no extra distribution was detected after modification

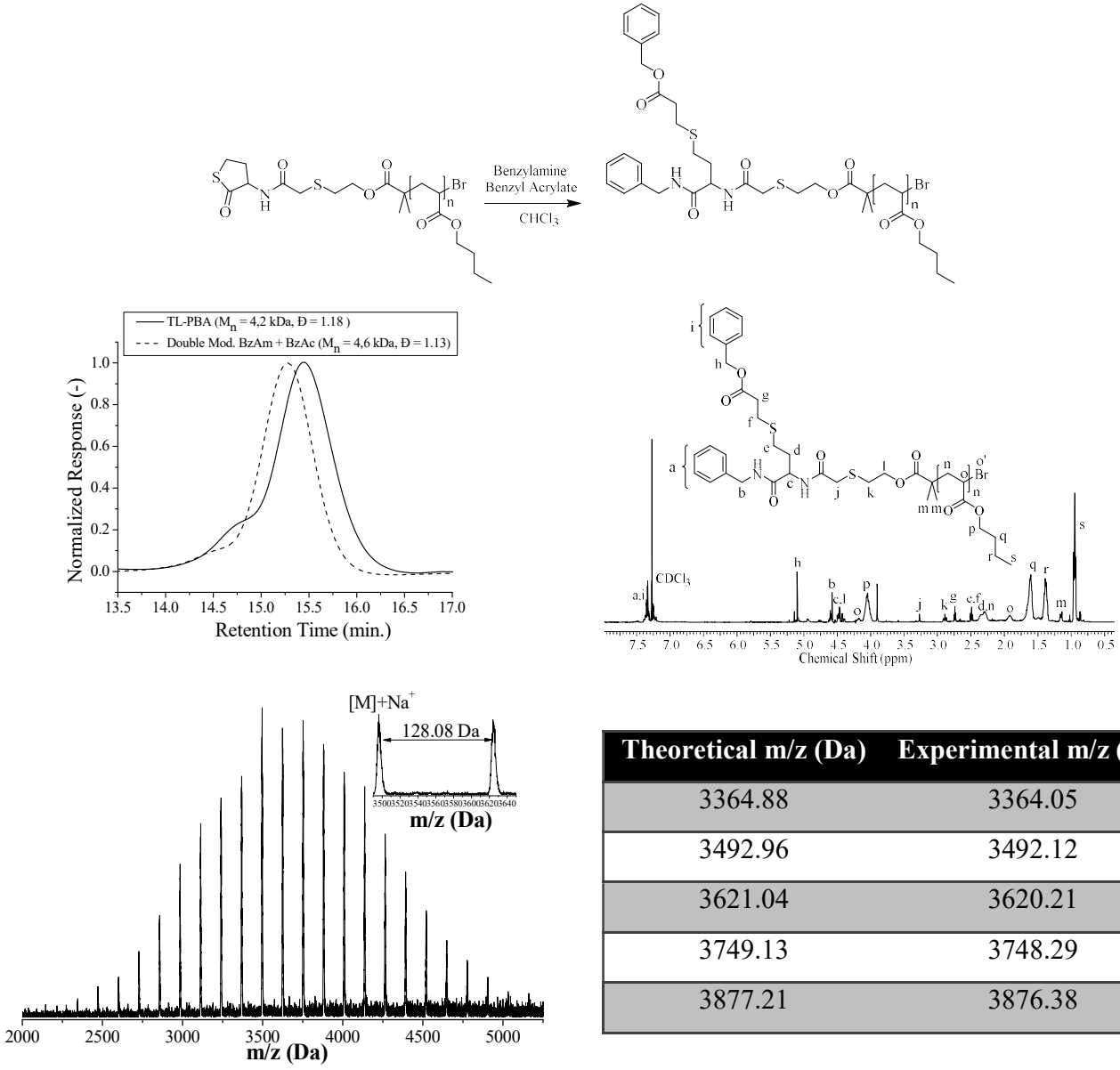

Theoretical m/z (Da)	Experimental m/z (Da)
3364.88	3364.05
3492.96	3492.12
3621.04	3620.21
3749.13	3748.29
3877.21	3876.38

Figure III. 14: One-pot double modification reaction of TL-PBA with benzylamine/benzyl acrylate and SEC, ^{1}H-NMR, MALDI-TOF analysis.

For the double modification of TL-PEO, a ratio of 15/30 equivalents of amine/acrylate was required for the double modification reaction and again a reaction time of 48 hours was applied to ensure complete end group transformation. From SEC analysis, a small uniform increase in

molecular weight was observed with no significant change in dispersity. ^{1}H-NMR analysis provided further proof for the double modification reaction as the signals of the thiolactone unit at 3.25 disappeared and signals of the benzylic protons at 4.4 and 5.3 ppm and the aromatic units at 7.3 ppm appeared. Final evidence for the double modification reaction was provided by MALDI-TOF analysis as experimental mass values of the double modified polymer matched with theoretical mass values (Figure III.15). However the small extra distribution, observed after the double modification reaction, could be ascribed to remaining PEO-OH starting material (2520.48 Da). This distribution is not present after the modification reaction with the thiolactone isocyanate, indicating a presence of only a few percentages. However, due to the significant increase in molecular weight after the double modification reaction, this signal will be overestimated as the masses of this polymer, which are lower, will arrive earlier at the detector. Finally, it has to be noted that TL-PEO as starting compound (2531.41 Da) is completely absent. These arguments in total provide full evidence of the double modification reaction.

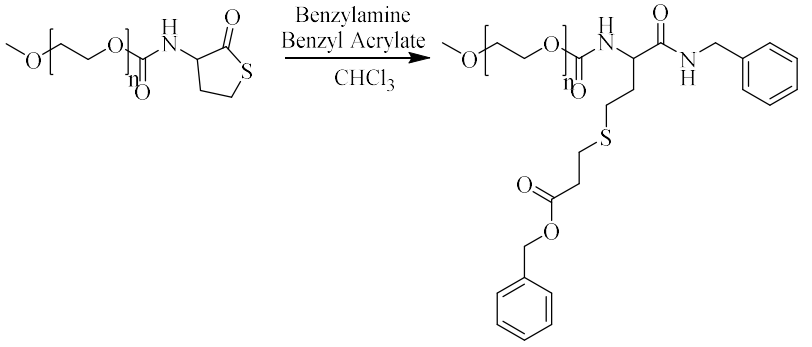

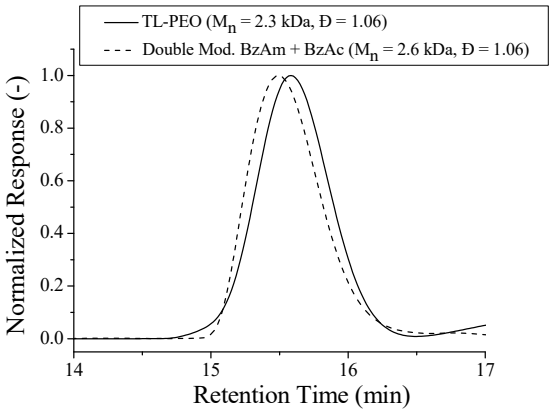

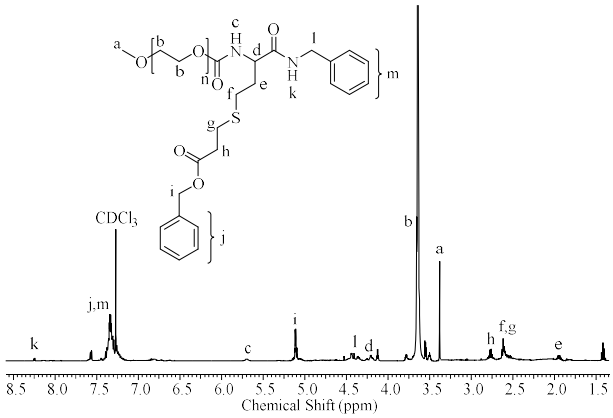

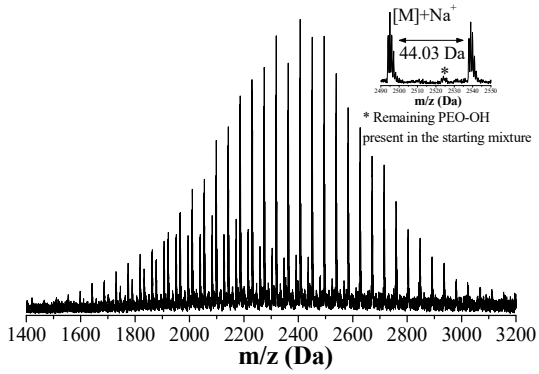

Theoretical m/z (Da)	Experimental m/z (Da)
2404.31	2405.05
2448.34	2449.09
2492.37	2493.12
2536.39	2537.12
2580.42	2581.18

Figure III. 15: One-pot double modification reaction of TL-PEO with benzylamine/benzyl acrylate and SEC, ^{1}H-NMR, MALDI-TOF analysis.

In case of the double modification of PCL, again a ratio of 15/30 equivalents of amine/acrylate was required for the double modification reaction and a reaction time of 48 hours was applied to ensure complete end group transformation. SEC analysis indicated a very small unimodal increase in molecular weight, with no significant change in dispersity. From ^{1}H-NMR analysis, it could be observed that the signals of the thiolactone unit at 3.25 ppm disappeared and signals from the benzylic units at 4.4 and 5.3 ppm appeared together with the signals of the aromatic units at 7.3 ppm. Furthermore, MALDI-TOF analysis indicated a complete conversion of the double modification reaction, theoretical and experimental mass values were in good agreement and no remaining starting product of TL-PCL-TL could be observed (Figure III.16).

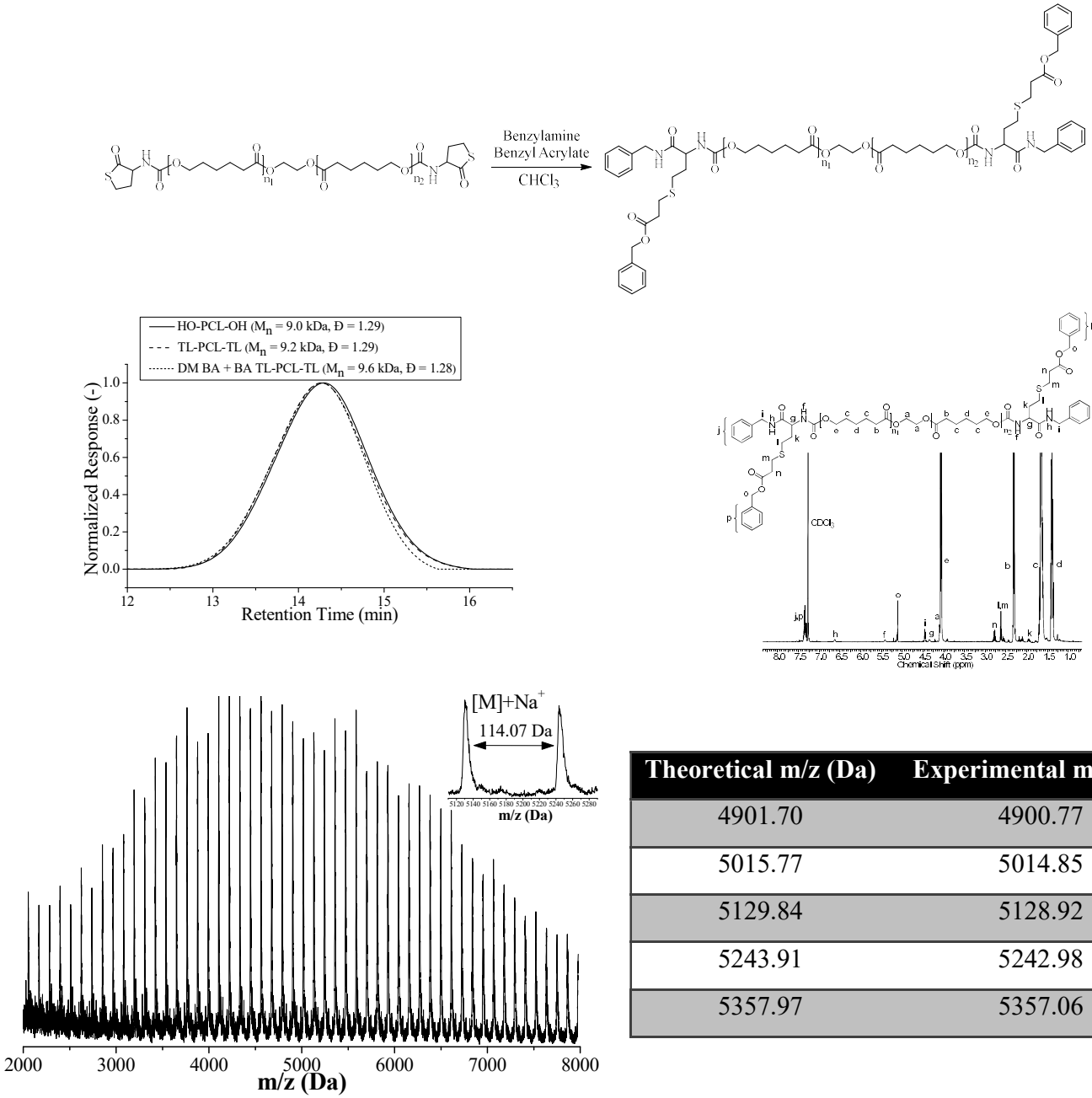

Theoretical m/z (Da)	Experimental m/z (Da)
4901.70	4900.77
5015.77	5014.85
5129.84	5128.92
5243.91	5242.98
5357.97	5357.06

Figure III. 16: One-pot double modification reaction of TL-PCL-TL with benzylamine/benzyl acrylate and SEC, ^{1}H-NMR, MALDI-TOF analysis.

III.3.2 Synthesis of a library of different end functionalized polymers

In the previous part, a model study was performed on four different thiolactone end-functionalized polymers. These structures were reacted with benzylamine and benzyl acrylate in a one-pot straightforward approach without the requirements of protection and deprotection strategies or intermediate purification steps. During this process, the amine will open the thiolactone ring, releasing the thiol, which on its turn will react with the acrylate in a one-pot approach.

To further strengthen this efficient methodology, a polymeric library of telechelic functionalized polymers was created by the double modification of PEO with a large variety of different amine and acrylate combinations and the outcome was analyzed *via* SEC and MALDI-TOF analysis. In this way, aromatic, furan, tetrahydrofurfuryl, double bond, halogen and hydroxyl functionalities could be easily introduced, demonstrating the functional group tolerance of the presented approach. From SEC analysis, a unimodal increase in molecular weight was observed in each case, while no change in the dispersity was observed (Table III.1).

Table III. 1: Summary of the double modification reactions of TL-PEO with different amine-acrylate combinations, including molecular weights and dispersities (Đ).

Entry	Polymer	Amine/Acrylate	Before Mod. [M_n (Da); Đ][a]	After Mod. [M_n (Da); Đ][a]
1	PEO	Benzylamine/Benzyl acrylate	2300; 1.06	2600; 1.06
2	PEO	Benzylamine/2,2,2-Trifluoroethyl acrylate	2300; 1.06	2700; 1.06
3	PEO	Ethanolamine/Tetrahydrofurfuryl acrylate	2300; 1.06	2400; 1.06
4	PEO	2-(4-Bromophenyl)ethylamine/ benzyl acrylate	2300; 1.06	2900; 1.06
5	PEO	Furfurylamine/Benzyl acrylate	2300; 1.06	2800; 1.06
6	PEO	Allylamine/Isobornyl acrylate	2300; 1.06	2400; 1.06

a) Molecular weights and dispersities determined by SEC in THF vs polystyrene standards.

On top of these modification reactions to introduce a broad range of different functionalities, an experiment altering the isotopic distribution of the polymeric unit was performed. Starting from TL-PEO as precursor polymer, 2-(4-bromophenyl)ethylamine, a bromine containing amine, and benzyl acrylate were added (Table III.1 – entry 4). Introducing the bromine unit induced a significant change in the isotopic pattern in MALDI-TOF analysis, due to the presence of the two abundant stable isotopes (^{79}Br and ^{81}Br). This effect was evidenced by comparing the theoretical and experimental isotopic distribution. Furthermore, the small distributions at 2036 and 2042 Da could be ascribed to remaining PEO-OH, as already explained, and an unknown fragmentation product in the MALDI-TOF respectively. TL-PEO (2047 Da) as starting compound was completely absent.

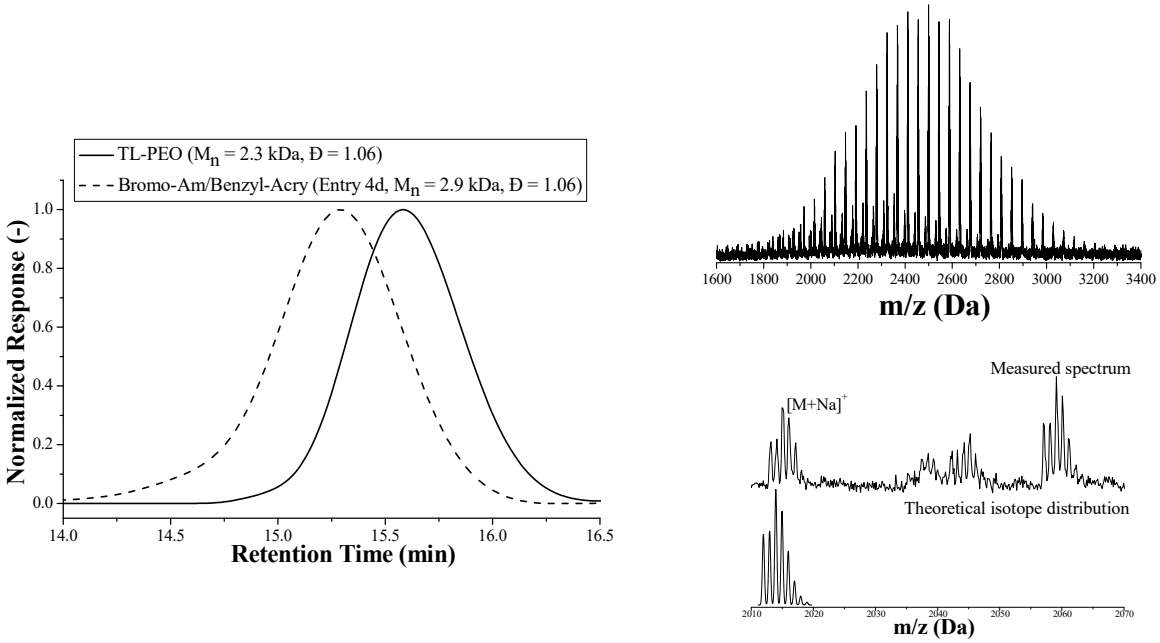

Figure III. 17: One-pot double modification reaction of TL-PEO with 2-(4-bromophenyl)ethylamine/benzyl acrylate and SEC and MALDI-TOF analysis.

III.4 Synthesis of midchain functionalized block copolymers

A library of tailored end-functionalized polymers was created by the double modification of polymer end groups through thiolactone chemistry. A diverse set of amines and acrylates were added to TL-PEO making use of the amine-thiol-ene reaction. In this way, different chemical functionalities such as aromatic, furan, tetrahydrofurfuryl, double bond, halogen and hydroxyl groups could be easily introduced in a one-pot approach without the requirement of protection and deprotection strategies.

To further extend the modification of the thiolactone group as chain-end functionality, this strategy was applied for the synthesis of midchain functionalized block copolymers *via* polymer-polymer conjugation. Therefore TL-PBA, used in the double modification reactions, was mixed with a 5-fold excess of PEO-NH_2 (800 Da) and methylacrylate in chloroform and reacted for 48 hours. Confirmation of the full modification reaction was evidenced by LCxSEC analysis of the crude reaction mixture (Figure III.18).

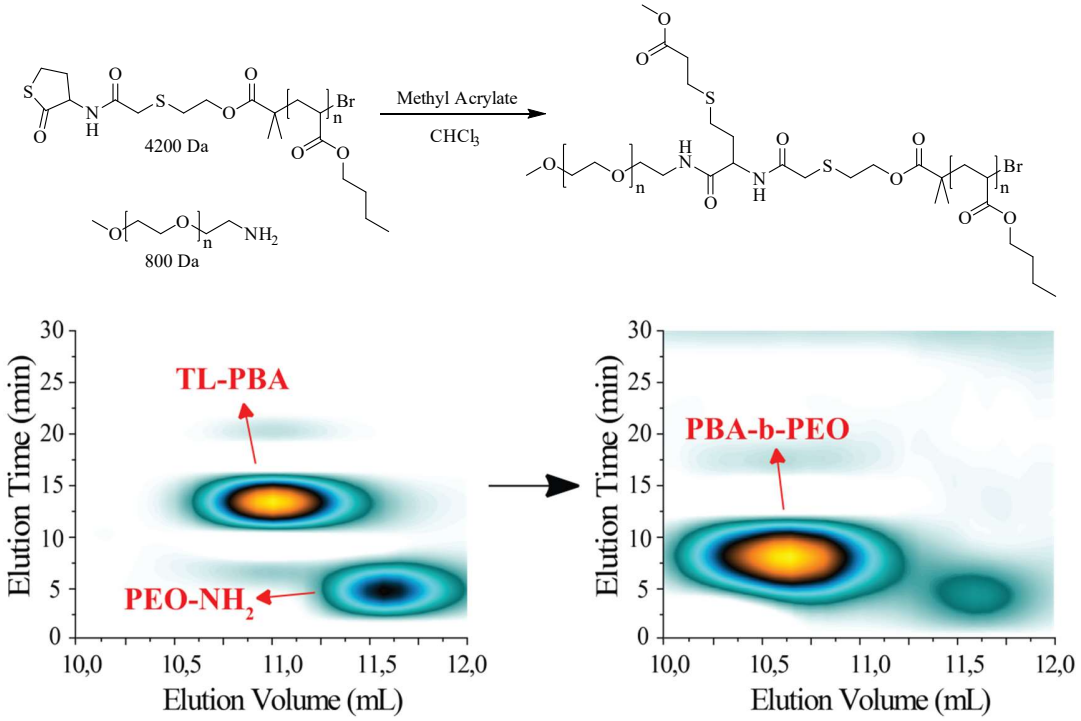

Figure III. 18: Coupling of TL-PS and PEO-NH_2 *via* the one-pot double modification of the thiolactone end group and LCxSEC analysis of a mixture of the starting polymers TL-PBA and PEO-NH_2 (left) and the coupled block copolymer PBA-b-PEO (right).

The chromatogram of a mixture of TL-PBA and PEO-NH_2 as starting materials (Figure III.18 – left) shows a clear separation in molecular weight (x-axis) and polarity (y-axis). After reaction, a new signal, originating from the coupled block copolymer, with a clear increase in molecular weight and shift in polarity can be observed (Figure III.18 – right). Furthermore, no starting material from TL-PBA remained, indicating a full conversion. PEO-NH_2 is still visible, since the crude reaction mixture was analyzed and a 5-fold excess was used in the modification reactions. In principle, a 4-fold excess of PEO-NH_2 should still be present in the crude reaction mixture. However, LCxSEC analysis indicated a lower amount. This can be explained by the decreased responsiveness of the signals at lower molecular weight. Different methods could be used afterwards (dialysis, selective precipitation or preparative SEC) to remove PEO-NH_2.

Furthermore, this strategy allows for the synthesis of midchain functionalized block copolymers containing a chemical functionality located at the junction between the two polymer chains. Therefore, evidence is required for the incorporation of the acrylate-unit after the reaction of TL-PBA with PEO-NH_2 and methyl acrylate. Therefore, the Ellman's reagent was used to detect the potential presence of free thiol units, which did not react with methyl acrylate.[22] The crude mixture of the block copolymer was therefore mixed with 5,5'dithiobis(2-nitrobenzoic acid) (DTNB) and *N,N*-diisopropylethylamine (DIPEA) in THF. In time, no change in color of the reaction mixture was observed, indicating the absence of free thiol-units and thus the full conversion of the double modification reaction. If free thiols were present, the reaction mixture would have become strongly yellow colored.

III.5 Conclusions

This chapter described the synthesis of tailored end-functionalized polymers *via* the double modification of the polymer end groups by the use of thiolactone end-functionalized polymers and amine-thiol-ene chemistry.

First, four different polymers containing a thiolactone end group were prepared *via* two significantly different strategies. TL-PS and TL-PBA were obtained *via* Cu(0)-mediated RDRP

starting from the corresponding thiolactone initiator, while TL-PEO and TL-PCL-TL were prepared by end group modification of the corresponding hydroxyl-functionalized polymer with a thiolactone containing isocyanate.

In a next step, a model study was performed regarding the double modification of the thiolactone unit. Benzylamine and benzyl acrylate were added in different ratios to a solution of the polymer mixture and the successful outcome of the modification reactions was evidenced by SEC, NMR and MALDI-TOF analysis. In case of TL-PS and TL-PBA, ratios of 10/15 equivalents of amine/acrylate relative to the thiolactone unit were sufficient for the double modification reaction, while for TL-PEO and TL-PCL-TL a ratio of 15/30 equivalents of amine/acrylate relative to the thiolactone unit was required for the double modification reaction.

To further strengthen this synthetic strategy, a library was created varying the amine and acrylate moieties, generating a series of double end-functionalized polymers. In this way, aromatic, furan, tetrahydrofurfuryl, double bond, halogen and hydroxyl-functionalities could be easily introduced.

Finally, the synthesis of block-copolymers *via* this strategy was envisaged. TL-PBA was mixed with a 5-fold excess of PEO-NH_2 and the full conversion was evidenced *via* LCxSEC analysis, a technique which separates polymers both on polarity and molecular weight.

From these results it can be concluded that this elegant versatile protocol is perfectly suitable for the one-pot double modification of polymeric end group functionalities, which is quite a unique protocol that has been picked up by different research groups. For example, Tao *et al.* applied this method for the fluorescent PEGylation in a one-pot approach. An amine end functionalized PEG was reacted with a fluorescent thiolactone, while afterwards the obtained polymer was utilized as fluorescent PEGylated protein as a model study for a sophisticated theranostic combination.[23]

III.6 Experimental part

III.6.1 Methods

^{1}H NMR

^{1}H- and ^{13}C-NMR (APT, HSQC, COSY) spectra were recorded in $CDCl_3$ on a Bruker AM500 spectrometer (500 MHz or 125 MHz for ^{1}H or ^{13}C respectively) or on a Bruker Avance 300 (300 MHz or 75 MHz for ^{1}H or ^{13}C respectively). Chemical shifts are presented in parts per million (δ) relative to $CDCl_3$ (7.26 ppm in ^{1}H- and 77.23 ppm in ^{13}C-NMR respectively) as internal standard. Coupling constants (*J*) in ^{1}H-NMR are given in Hz. The resonance multiplicities are described as *d* (doublet), *t* (triplet) or *m* (multiplet).

LC-MS

An Agilent technologies 1100 series LC/MSD system equipped with a diode array detector and single quad MS detector (G1946C) with an electrospray source (ESI-MS) was used for classic reversed phase LC-MS. Analytic reversed phase HPLC was performed with a Phenomenex Kinetex C_{18} column (5 µ, 150 x 4.6 mm) using a solvent gradient (0 → 100% acetonitrile in H_2O in 15 min) and the eluting compounds were detected *via* UV-detection (λ = 214 nm). High resolution mass spectra (HRMS) were collected using an Agilent 6220A time-of-flight (TOF) equipped with a multimode ionization (MMI) source.

SEC

Size Exclusion Chromatography (SEC) was performed using a Varian PLGPC50plus instrument, using a refractive index detector, equipped with two Plgel 5 µm MIXED-D columns 40 °C. Polystyrene standards were used for calibration and THF as eluent at a flow rate of 1 mL/min. Samples were injected using a PL AS RT autosampler.

LCxSEC

For two-dimensional liquid chromatography, sample fractions from the first dimension were transferred to the second-dimension column via an electronically controlled eight-port valve system (VICI Valco instruments, Houston, TX, USA), equipped with two 100 µL sample loops. The second dimension consisted of an Agilent Infinity 1260 isocratic pump and a PSS SDV LIN

M 5 µm column. Detection in the second dimension was accomplished by using an ELSD. Nitrogen was used as carrier gas in the ELSD at a flow rate of 2.5 L/min. Spray Chamber, Drift Tube and Optical Cell temperatures were set at 30 °C, 80 °C and 70 °C, respectively. The flow rates used in the first and second dimensions were 0.02 mL/min and 5 mL/min, respectively. Sample concentrations were between 0.25 and 2.0 mg/mL. an isocratic elution of methanol/hexane (70/30) was used as the solvent for the first dimension, THF was used as the solvent for the second dimension analysis. Data were recorded using PSS WinGPC Unichrom software.

MALDI-TOF

Matrix Assisted Laser Desorption Ionisation – Time of Flight (MALDI-TOF) was performed on an Applied Biosystems Voyager De STR MALDI-TOF spectrometer equipped with 2 m linear and 3 m reflector flight tubes, a nitrogen laser operating at 337 nm, pulsed ion extraction source and reflectron. All mass spectra were obtained with an accelerating potential of 20kV in positive ion mode and in reflector mode. Measurements of polybutyl acrylate were performed with dithranol (25 mg/mL in THF) as a matrix, sodium iodide (20 mg/mL in THF) as a cationizing agent, and polymer samples were dissolved in THF (5 mg/mL). Polymer solutions were prepared by mixing 5 µL of the polymer, 10 µL of the salt, and 10 µL of the matrix solution. Subsequently, 0.5 µL of this mixture was spotted on the sample plate, and the spots were dried in air at room temperature. Measurements of polystyrene were performed with dithranol (20 mg/mL in THF) as a matrix, silver trifluoro acetate (1 mg/mL in THF) as a cationizing agent, and polymer samples were dissolved in THF (10 mg/mL). Polymer solutions were prepared by mixing 5 µL of the polymer, 10 µL of the salt, and 10 µL of the matrix solution. Subsequently, 0.5 µL of this mixture was spotted on the sample plate, and the spots were dried in air at room temperature. Measurements of polyethylene oxide were performed with dithranol (10 mg/mL in THF) as a matrix, sodium trifluoro acetate (1 mg/mL in THF) as a cationizing agent, and polymer samples were dissolved in THF (10 mg/mL). Polymer solutions were prepared by mixing 2 µL of the polymer, 2 µL of the salt, and 16 µL of the matrix solution. Subsequently, 0.5 µL of this mixture was spotted on the sample plate, and the spots were dried in air at room temperature. Measurements of polycaprolactone were performed with *trans*-2-[3-(4-*tert*-Butylphenyl)-2-methyl-2-propenylidene]malonitrile (DCTB, 20 mg/mL in THF) as a matrix,

sodium iodide (1 mg/mL in THF) as a cationizing agent, and polymer samples were dissolved in THF (2 mg/mL). Polymer solutions were prepared by mixing 5 µL of the polymer, 5 µL of the salt, and 10 µL of the matrix solution. Subsequently, 0.5 µL of this mixture was spotted on the sample plate, and the spots were dried in air at room temperature. A poly(ethylene oxide) standard (M_n = 2000 g/mol) was used for calibration. All data were processed using the Data Explorer 4.0.0.0 (Applied Biosystems) software package.

GC

GC was performed on an Agilent 7890A system equipped with a VWR Carrier-160 hydrogen generator and an Agilent HP-5 column of 30 m length and 0.320 mm diameter. An FID detector was used and the inlet was set to 240 °C with a split injection ratio of 25 : 1. Hydrogen was used as the carrier gas at a flow rate of 2 mL/min . The oven temperature was increased at 20 °C/min from 50 °C to 120 °C, followed by a ramp of 50 °C/min to 150 °C.

III.6.2 Materials

Benzyl acrylate ([2495-35-4], 95%) was purchased from ABCR. 2-(4-Bromophenyl)ethylamine ([73918-56-6], 98%) was purchased from Alfa Aesar. Chloroform D ([865-49-6], ≥ 99.8 %) was purchased from Euriso-top. PEO-NH_2 (800 Da) was purchased from Iris Biotech GMBH. Polycaprolactone (average M_n ~ 6000 Da) was kindly donated by Solvay and was dried azeotropically over toluene prior to use. Dibutyltin dilaurate (DBTL, [77-58-7], > 95 %), 2,2,2-Tetrahydrofurfuryl acrylate ([2399-48-6], 98 %), Trifluoroethyl acrylate ([407-37-6], > 98 %) and Isobornyl Acrylate ([5888-33-5], > 90%) were purchased from TCI Chemicals. Allylamine ([107-11-9], ≥ 99 %), Aluminium oxide ([1344-28-1], basic), Benzylamine ([100-46-9], ≥ 99.5 %), Butyl acrylate ([141-32-2], ≥ 99 %), Cu(0)-pellets ([7440-50-8], ≥ 99.9 %), Cu(II)Br_2 ([7789-45-9], 99 %), 1,2-Dichlorobenzene ([95-50-1], 99 %) Dichloromethane ([75-09-2], ≥ 99.8 %) was dried in a solvent purification system (J.C. Meyer) before use as dry solvent, Diethylether ([60-29-7], ≥ 99.7 %), *N,N*-Dimethylformamide ([68-12-2], 99.8 %), 5,5'-Dithiobis(2-nitrobenzoic acid) ([69-78-3], ≥ 98 %), Ethanolamine ([141-43-5], ≥ 99 %), Furfurylamine ([617-89-0], ≥ 99 %), Methanol ([67-56-1], 99.8 %), *N,N,N',N'',N''*-Pentamethyldiethylenetriamine ([3030-47-5], 99%), Polyethylene oxide ([9004-74-4] was dried

azeotropically over toluene prior to use, average M_n ~ 2000 Da), Styrene ([100-42-5], ≥ 99 %), Tetrahydrofuran ([109-99-9], ≥ 99 %) were purchased from Sigma-Aldrich and used without purification. Me_6TREN[24] and *N*-(2-bromoacetyl)homocysteine-γ-thiolactone[25] were synthesized according to literature procedures.

III.6.3 Synthesis

Synthesis of thiolactone containing initiator for Cu(0)-mediated RDRP

An ice-cooled solution of *N*-(2-bromoacetyl) homocysteine-γ-thiolactone (11.9 g, 50 mmol) in anhydrous CH_2Cl_2 (70 mL) and anhydrous Et_3N (20.9 mL, 150 mmol) was treated with 2-mercaptoethanol (3.86 mL, 55 mmol) by dropwise addition. The reaction mixture was allowed to reach room temperature and stirred for 2 h. TLC analysis (*n*-Hexane/EtOAc = 1/2) indicated a clean conversion of the starting material. Next, α-bromoisobutyryl bromide (8.0 mL, 65 mmol) was added to the ice-cooled heterogeneous mixture, which was allowed to reach room temperature overnight. The crude residue was purified by column chromatography (silicagel, gradient elution: 100 % CH_2Cl_2 → CH_2Cl_2 / acetone: 95/5), yielding the thiolactone-containing initiator as an off-white white solid (16.1 g, 41.9 mmol, 83 %).

^{1}H-NMR (500 MHz, $CDCl_3$, ppm) δ 7.10 (*d*, 1 H, 6.0 Hz), 4.58 (*app dt*, 1 H, 13.0, 7.0 Hz), 4.36 (*app t*, 2 H, 6.5 Hz), 3.38 (app *dt*, 1 H, 11.5, 5.0 Hz), 3.36 (*d*, 1 H, 16.0 Hz), 3.31 (*d*, 1 H, 16.0 Hz), 3.27 (*ddd*, 1 H, 11.0, 7.0, 0.8 Hz), 2.88 (*m*, 3 H), 2.02 (*m*, 1 H), 1.94 (*s*, 6 H).
^{13}C-NMR (125 MHz, $CDCl_3$, ppm) δ 204.9 (C), 171.8 (C), 169.3 (C), 64.3 (CH_2), 59.7 (CH), 55.8 (C), 36.2 (CH_2), 31.7 (CH_2), 31.4 (CH_2), 30.9 (2 x CH_3), 27.7 (CH_2).
HR-ESI-MS: *calculated* m/z [M+H$^+$]: 383.9933, 385.9913; *experimental* m/z [M+H$^+$]: 383.9931, 385.9110

Cu(0)-mediated polymerization of styrene via a thiolactone-initiator

3 mL Styrene (26.10 mmol, 50 eq.), 200.59 mg thiolactone-initiator (0.52 mmol, 1 eq.) were weighed into a vial and degassed for 1 h with a continuous argon purge. In a separate flask, 3 mL styrene (26.10 mmol, 50 eq.), Cu(0) (20 pellets), 11.66 mg Cu(II)Br_2 (0.052 mmol, 0.1 eq.),

38.14 mg PMDETA (0.183 mmol, 0.35 eq.) were degassed separately via argon bubbling for 1 h. The reaction was started by the addition of the monomer and initiator solution to the ligand solution and the reaction was heated to 90°C for 2 h. Afterwards, the reaction mixture was cooled to room temperature and the remaining metal salts were removed by dilution with THF and filtration over a column of basic alumina. After evaporating the excess solvent, the polymer was precipitated in a 10-fold of cold methanol, and isolated by filtration. The polymer was then redissolved in 5 mL THF, precipitated again in 50 mL of cold methanol and obtained via filtration. Finally, the polymer was dried overnight in a vacuum oven at 40°C. In parallel, the same experiment was performed to determine the kinetics of the polymerization. Samples of the reaction mixture were taken for GC and SEC analysis, samples for GC analysis were dissolved in THF with phenothiazine as radical inhibitor (1,2-dichlorobenzene as internal standard), while samples for SEC analysis were diluted with THF, then passed over a basic alumina column to remove metal salts.

Cu(0)-mediated polymerization of butyl acrylate via a thiolactone initiator

1.5 mL butyl acrylate (10.46 mmol, 20 eq.), 2.73 mL DMF, Cu(0) (10 pellets), 201.04 mg thiolactone-initiator (0.52 mmol, 1 eq.) were weighed into a flask and degassed for 1 h with a continuous argon purge. In a separate vial, 5.84 mg Cu(II)Br_2 (0.03 mmol, 0.05 eq.), 14.46 mg Me_6TREN (0.06 mmol, 0.12 eq.) and 1 mL DMF were degassed separately via argon bubbling for 1 h. The reaction was started by the addition of the Cu(II)Br_2/ligand-solution to the reaction mixture at room temperature. Samples of the reaction mixture were taken for GC and SEC analysis, samples for GC analysis were dissolved in THF with phenothiazine as radical inhibitor (1,2-dichlorobenzene as internal standard), while samples for SEC analysis were diluted with THF, then passed over a basic alumina column to remove metal salts. After 6 h, the reaction mixture was diluted with THF and filtered over a column of basic Al_2O_3 to remove the copper catalyst. After evaporating the excess solvent, the polymer was poured in a petri dish and dried overnight in a vacuum oven at 40°C to strip solvents and remaining monomer.

Synthesis of α-cyanato-γ-thiolactone from DL-homocysteine thiolactone

Triphosgene (25 g, 84 mmol), to be handled with care, was dissolved in ice-cooled CH_2CL_2 (250 mL) and stirred for 15 minutes. Subsequently, an extra CH_2CL_2 (200 mL) and DL-homocysteine thiolactone hydrochloride (37 g, 241 mmol) were gently added. Next, pyridine (64.11 ml, 794 mmol) was added drop-wise to the reaction mixture. After one hour the reaction mixture was allowed to reach room temperature and was stopped after five hours. The work-up of this isocyanate must be done fast to prevent its degradation. The reaction mixture was directly filtered in a separation funnel to remove the salt that was formed during the reaction. The organic phase was washed with 2M HCl solution (250 mL), brine (250 mL) and ice water (250 mL). Subsequently, this phase was collected in a beaker with $MgSO_4$ to remove residual water. After filtration and evaporation of the CH_2Cl_2, a brown residue was obtained. Finally, this crude residue was purified by distillation (4 mm Hg, 65°C), yielding a yellow oil (30.33 g, 0.21 mol, 87%).

^{1}H-NMR (500 MHz, $CDCl_3$, ppm) δ 4.24 (*dd*, 2 H, 12.6, 6.8 Hz), 3.29 (*m*, 2 H), 2.64 (*m*, 1 H), 2.10 (*m*, 1 H).
^{13}C-NMR (125 MHz, $CDCl_3$, ppm) δ 203.1 (C), 127.6 (C), 62.6 (CH), 32.1 (CH_2), 27.0 (CH_2).
IR (cm^{-1}) 2944, 2869, 2227, 1691, 1440, 1336, 1280, 1172, 1142, 1057, 1033, 1000, 964, 884, 840, 744, 681, 643, 616

End group modification of PEO-OH with a thiolactone-containing isocyanate

1.5 g of dried PEO-OH (0.75 mmol, 1 eq.) was weighed into a flask and dissolved in 4 mL of dry dichloromethane. 429.6 mg of α-cyanato-γ-thiolactone (3 mmol, 4 equivalents) was weighed and transferred to the reaction mixture with 1 mL of dry dichloromethane. Afterwards, 0.02 mL DBTL (0.03 mmol, 0.04 equivalents) was added as a catalyst and the reaction proceeded for 48h. Afterwards the reaction mixture was precipitated twice in cold diethyl ether, filtrated, washed thoroughly with diethyl ether and dried in a vacuum oven overnight at 40°C.

End group modification of HO-PCL-OH with a thiolactone-containing isocyanate

1.5 g of dried HO-PCL-OH (0.25 mmol, 1 eq.) was weighed into a flask and dissolved in 4 mL of dry dichloromethane. 286.32 mg of α-cyanato-γ-thiolactone (2 mmol, 8 equivalents) was weighed and transferred to the reaction mixture with 1 mL of dry dichloromethane. Afterwards, 0.012 mL DBTL (0.02 mmol, 0.08 equivalents) was added as a catalyst and the reaction proceeded for 48h. Afterwards the reaction mixture was precipitated twice in cold methanol, filtrated, washed thoroughly with diethyl ether and dried in a vacuum oven overnight at 40°C.

One-pot double modification of TL-PS

50 mg of TL-PS (0.014 mmol, 1 eq.) was weighed into a flask and dissolved in 0.25 mL of chloroform. 70 mg of benzyl acrylate (0.43 mmol, 30 eq.) was weighed and transferred to the reaction mixture with 0.1 ml of chloroform. Next, 23 mg of benzylamine (0.21 mmol, 15 eq.) was weighed and transferred to the reaction mixture with 0.1 ml of chloroform. After 48 h of stirring, the reaction mixture was precipitated twice in cold methanol, filtered and obtained via filtration. Finally, the polymer was dried overnight in a vacuum oven at 40°C.

One-pot double modification of TL-PBA

50 mg of TL-PBA (0.02 mmol, 1 eq.) was weighed into a flask and dissolved in 0.25 mL of chloroform. 97 mg of benzyl acrylate (0.60 mmol, 30 eq.) was weighed and transferred to the reaction mixture with 0.1 ml of chloroform. Next, 32 mg of benzylamine (0.30 mmol, 15 eq.) was weighed and transferred to the reaction mixture with 0.1 ml of chloroform. After 48h of stirring, the polymer was dried overnight in a vacuum oven at 40°C.

One-pot double modification of TL-PEO

50 mg of TL-PEO (0.025 mmol, 1 eq.) was weighed into a flask and dissolved in 0.25 mL of chloroform. 122 mg of benzyl acrylate (0.75 mmol, 30 eq.) was weighed and transferred to the reaction mixture with 0.1 ml of chloroform. Next, 40 mg of benzylamine (0.375 mmol, 15 eq.) was weighed and transferred to the reaction mixture with 0.1 ml of chloroform. After 48 h of stirring, the reaction mixture was precipitated twice in cold diethylether, filtered and obtained via filtration. Finally, the polymer was dried overnight in a vacuum oven at 40°C. Same reaction

conditions were applied for other amine/acrylate combinations, 15 equivalents of amine and 30 equivalents of acrylate were used compared to the thiolactone functionality.

One-pot double modification of TL-PCL-TL

50 mg of TL-PCL-TL (0.008 mmol, 1 eq.) was weighed into a flask and dissolved in 0.25 mL of chloroform. 81 mg of benzylacrylate (0.50 mmol, 60 eq.) was weighed and transferred to the reaction mixture with 0.1 ml of chloroform. Next, 27 mg of benzylamine (0.25 mmol, 30 eq.) was weighed and transferred to the reaction mixture with 0.1 ml of chloroform. After 48h of stirring, the reaction mixture was precipitated twice in cold methanol, filtered and obtained via filtration. Finally, the polymer was dried overnight in a vacuum oven at 40°C.

Coupling of TL-PBA with PEO-NH_2

160 mg of TL-PBA (0.038 mmol, 1 eq.) was weighed into a flask and dissolved in 0.5 mL of chloroform. 16.4 mg of methyl acrylate (0.19 mmol, 5 eq.) was weighed and transferred to the reaction mixture with 0.1 ml of chloroform. Next, 152 mg of PEO-NH_2 (800 Da) (0.19 mmol, 5 eq.) was weighed and transferred to the reaction mixture with 0.1 ml of chloroform. After 48h of stirring, the solvent was evaporated and the crude mixture was analysed by LCxSEC analysis.

References

1. Hawker, C. J.; Bosman, A. W.; Harth, E. *Chemical Reviews* **2001,** 101, (12), 3661-3688.
2. Barner-Kowollik, C.; Du Prez, F. E.; Espeel, P.; Hawker, C. J.; Junkers, T.; Schlaad, H.; Van Camp, W. *Angewandte Chemie International Edition* **2011,** 50, (1), 60-62.
3. Espeel, P.; Du Prez, F. E. *European Polymer Journal* **2015,** 62, (0), 247-272.
4. De Bruycker, K.; Billiet, S.; Houck, H. A.; Chattopadhyay, S.; Winne, J. M.; Du Prez, F. E. *Chemical Reviews* **2016,** 116, (6), 3919-3974.
5. Espeel, P.; Goethals, F.; Du Prez, F. E. *Journal of the American Chemical Society* **2011,** 133, (6), 1678-1681.
6. Espeel, P.; Goethals, F.; Driessen, F.; Nguyen, L. T. T.; Du Prez, F. E. *Polymer Chemistry* **2013,** 4, (8), 2449-2456.
7. Benaglia, M.; Alberti, A.; Giorgini, L.; Magnoni, F.; Tozzi, S. *Polymer Chemistry* **2013,** 4, (1), 124-132.
8. Kakuchi, R.; Theato, P. *ACS Macro Letters* **2013,** 2, (5), 419-422.
9. Kakuchi, R.; Theato, P. *ACS Macro Letters* **2014,** 3, (4), 329-332.

10. Seuyep Ntoukam, D. H.; Luinstra, G. A.; Theato, P. *Journal of Polymer Science Part A: Polymer Chemistry* **2014,** 52, (19), 2841-2849.
11. Kubo, T.; Figg, C. A.; Swartz, J. L.; Brooks, W. L. A.; Sumerlin, B. S. *Macromolecules* **2016,** 49, (6), 2077-2084.
12. Willcock, H.; O'Reilly, R. K. *Polymer Chemistry* **2010,** 1, (2), 149-157.
13. Matyjaszewski, K.; Xia, J. H. *Chemical Reviews* **2001,** 101, (9), 2921-2990.
14. Aoshima, S.; Kanaoka, S. *Chemical Reviews* **2009,** 109, (11), 5245-5287.
15. Junkers, T. *European Polymer Journal* **2015,** 62, (0), 273-280.
16. Delplace, V.; Harrisson, S.; Ho, H. T.; Tardy, A.; Guillaneuf, Y.; Pascual, S.; Fontaine, L.; Nicolas, J. *Macromolecules* **2015,** 48, (7), 2087-2097.
17. Caroli, G.; Loos, K. *Macromolecular Chemistry and Physics* **2013,** 214, (22), 2602-2606.
18. Figg, C. A.; Kubo, T.; Sumerlin, B. S. *ACS Macro Letters* **2015,** 4, (10), 1114-1118.
19. Wong, E. H. H.; Boyer, C.; Stenzel, M. H.; Barner-Kowollik, C.; Junkers, T. *Chemical Communications* **2010,** 46, (11), 1959-1961.
20. Tonhauser, C.; Obermeier, B.; Mangold, C.; Lowe, H.; Frey, H. *Chemical Communications* **2011,** 47, (31), 8964-8966.
21. Driessen, F.; Martens, S.; Meyer, B. D.; Du Prez, F. E.; Espeel, P. *Macromolecular Rapid Communications* **2016,** 37, (12), 947-951.
22. Ellman, G. L. *Archives of Biochemistry and Biophysics* **1958,** 74, (2), 443-450.
23. Zhao, Y.; Yang, B.; Zhang, Y.; Wang, S.; Fu, C.; Wei, Y.; Tao, L. *Polymer Chemistry* **2014,** 5, (23), 6656-6661.
24. Ciampolini, M.; Nardi, N. *Inorganic Chemistry* **1966,** 5, (1), 41-44.
25. Espeel, P.; Carrette, L. L. G.; Bury, K.; Capenberghs, S.; Martins, J. C.; Du Prez, F. E.; Madder, A. *Angewandte Chemie International Edition* **2013,** 52, (50), 13261-13264.

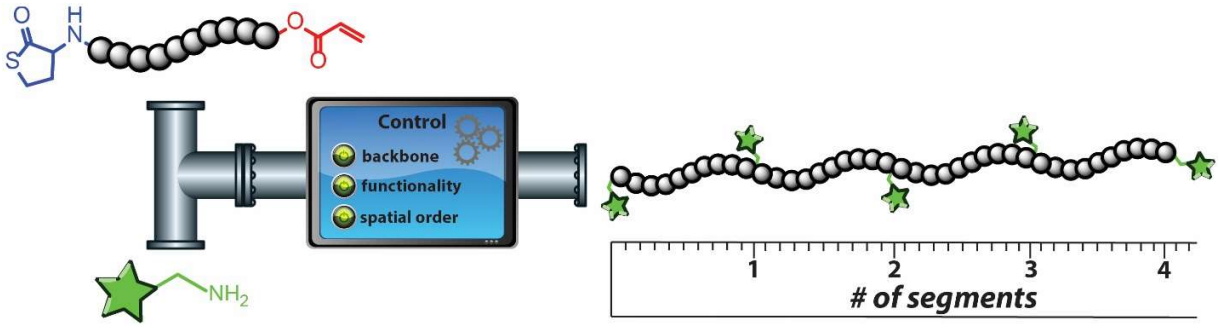

Abstract

This chapter illustrates the synthesis of unique, precisely decorated multi-segmented block copolymers *via* amine-thiol-ene conjugation. Therefore, a thiolactone-acrylate hetero-telechelic macromonomer was designed *via* a Cu(0)-mediated polymerization system and subsequent end group modification reactions. Through nucleophilic ring-opening of the thiolactone unit and consecutive thiol-Michael addition, the multisegmented block copolymer was isolated. By differentiating the amine, a library of functionalized scaffolds was obtained with functionalities positioned at each segment connection and thus equally spaced along the polymeric backbone. The toolbox of applicable functional handles was extended by post-polymerization modification reactions providing access to a plethora of tailor-made multisegmented line-ups. Furthermore, these materials were applied in the design of glyco- and amphiphilic polymers and analyzed by SEC, DOSY-NMR, LCxSEC and DLS, revealing the particular properties of these macromolecular structures. Finally, chiral benzene-1,3,5-tricarboxamides (BTAs) were introduced to investigate the supramolecular self-assembly of these structures.

Parts of this chapter were published as:
Driessen F., Du Prez F.E., Espeel P., *ACS Macro Letters*, **2015**, 4 (6), 616-619

Chapter IV.

Precision multisegmented macromolecular line-ups: A display of unique control over backbone structure and functionality

IV.1 Introduction

The previous chapter elaborated on the double modification of polymer end groups through thiolactone chemistry for the design of tailor-made macromolecular architectures. In this next part, this chemistry will be utilized to further increase the level of complexity of these copolymer structures.[1-4] Besides telechelic and block copolymer chains as well-known macromolecular structures, the polymer community developed a broad spectrum of complex architectures, it. cyclic or graft copolymers, for advanced material applications.[5, 6] Within this research area, multisegmented block copolymers received an increasing amount of attention, because of the possibility to regulate the polymer microstructure remains a challenging topic from a molecular perspective, intriguing synthetic chemists worldwide.[7, 8]

In general, two distinct synthetic strategies were developed to obtain well-controlled multi-segmented block copolymers. A first established procedure utilizes reversible deactivation radical polymerization techniques through sequential addition of (different) monomers in a one-pot approach.[9-11] Relying on the high end-group fidelity of these RDRP-strategies, structures ranging from deca- through icosa-blocks were obtained. However, as Sawamoto[12] and Meyer[13] expressed the requirement for the precision design of chemical functionalities throughout the polymer structure, it is practically impossible to incorporate strictly one functional handle between each segment, as exemplified by mid-chain functionalized block copolymers[14, 15] or styrene-maleimide co-polymerizations[16] and corresponding multi-segmented block copolymers[17].

Therefore, in this chapter the focus will be on a second methodology *via* efficient conjugation chemistries. Multi-segmented block copolymers can also be obtained through step-growth coupling *via* the end groups of a hetero-telechelic macromonomer. In spite of the synthetic simplicity this approach offers, already explored coupling reactions (it. CuAAc, ATRC) do not provide the possibility to incorporate any desired functionality in the macromolecular line-ups in a straightforward approach. In this regard, we targeted a strategy that enables the synthesis of polymeric chains, with a tailored backbone structure (segment length and composition) and readily diversified functionalities, positioned at each segment connection and thus equally spaced along the polymeric backbone (Figure IV.1).

This project started by the synthesis of a thiolactone-acrylate hetero-telechelic macromonomer through Cu(0)-mediated polymerization of a thiolactone-containing initiator and subsequent end group modification reactions to introduce the acrylate end group. Next, the multisegmented block copolymer was isolated by addition of an amine, which reacts in a chemoselective manner with the thiolactone, releasing the thiol, that reacts subsequently with the acrylate end group. In this way, multisegmented copolymers are obtained with functionalities equally spaced across the polymeric backbone. Furthermore, a polymeric library of functionalized structures was obtained by differentiating the amine with functionalities positioned at each segment connection, equally spaced along the polymeric backbone. Additionally, the toolbox of functional handles was extended by post-polymerization modification reactions, providing access to a plethora of tailor-made multisegmented line-ups. Finally, these materials were applied in the design of glyco- and amphiphilic polymers and analyzed by SEC, DOSY-NMR, LCxSEC and DLS.

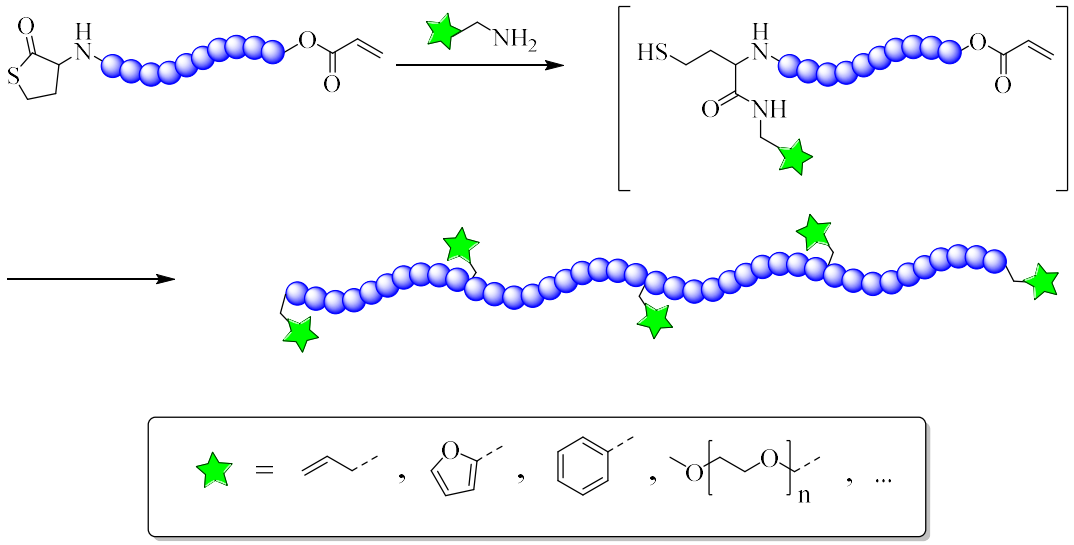

Figure IV.1: Synthetic concept for the synthesis of the functionalized multi-segmented macromolecular line-ups.

IV.2 Synthesis of a hetero-telechelic thiolactone-acrylate macromonomer

IV.2.1 Introduction

A first important aspect of this project is the efficient multi-gram synthesis of a narrow-disperse hetero-telechelic thiolactone-acrylate macromonomer featuring a high end-group fidelity. Therefore, a Cu(0)-mediated polymerization was utilized in response to the latter requirement.[18-20] Accordingly, the large-scale synthesis of a thiolactone-containing initiator was performed as described in full detail in the previous chapter. Next, isobornyl acrylate was selected to prepare the corresponding high-Tg polymer, facilitating purification issues. Subsequently, the bromine end group was transformed into an acrylate *via* a two-step approach through the intermediate alcohol, yielding the hetero-telechelic polymer with the required stringent purity as confirmed by NMR, SEC and MALDI-TOF analysis (Figure IV.2).

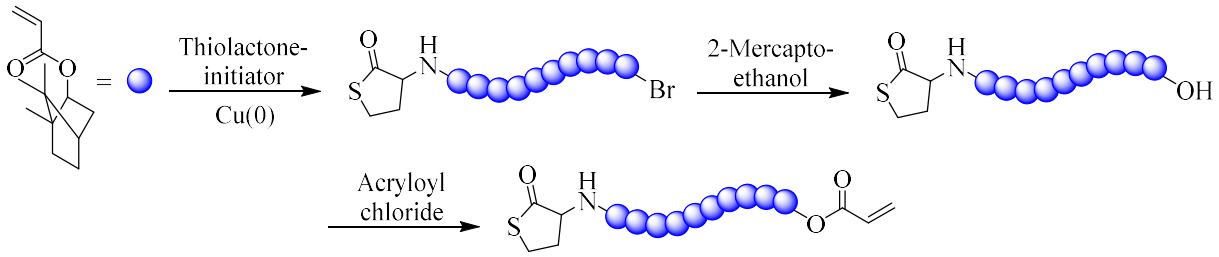

Figure IV.2: Synthetic strategy to obtain the hetero-telechelic thiolactone-acrylate macromonomer.

IV.2.2 Synthesis of TL-PiBA-Br

After the elaborated large-scale synthesis of a thiolactone-containing initiator applicable for Cu(0)-mediated RDRP, isobornyl acrylate was polymerized. This monomer was selected as a result of the high T_g of the corresponding polymer, facilitating purification *via* precipitation in methanol as non-solvent (Figure IV.3). Furthermore, a degree of polymerization (DP) of 10 was selected to control the distance between the different functionalities in the resulting multisegmented block copolymer.

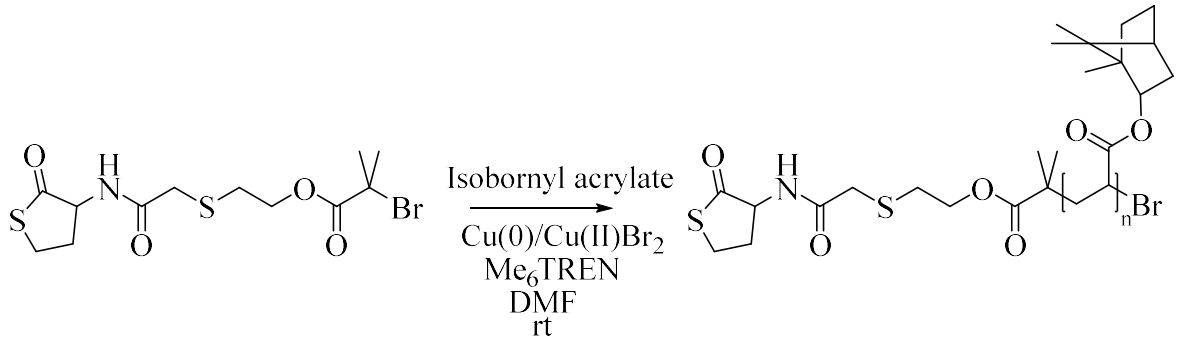

Figure IV.3: Cu(0)-mediated RDRP of isobornyl acrylate *via* a thiolactone-containing initiator.

A detailed kinetic analysis was performed to evidence the controlled nature of the polymerization. Samples were taken at regular time intervals and analyzed *via* SEC and GC analysis to determine the molecular weight and conversion respectively. The resulting kinetic plots illustrated the controlled nature of the polymerization (Figure IV.4).

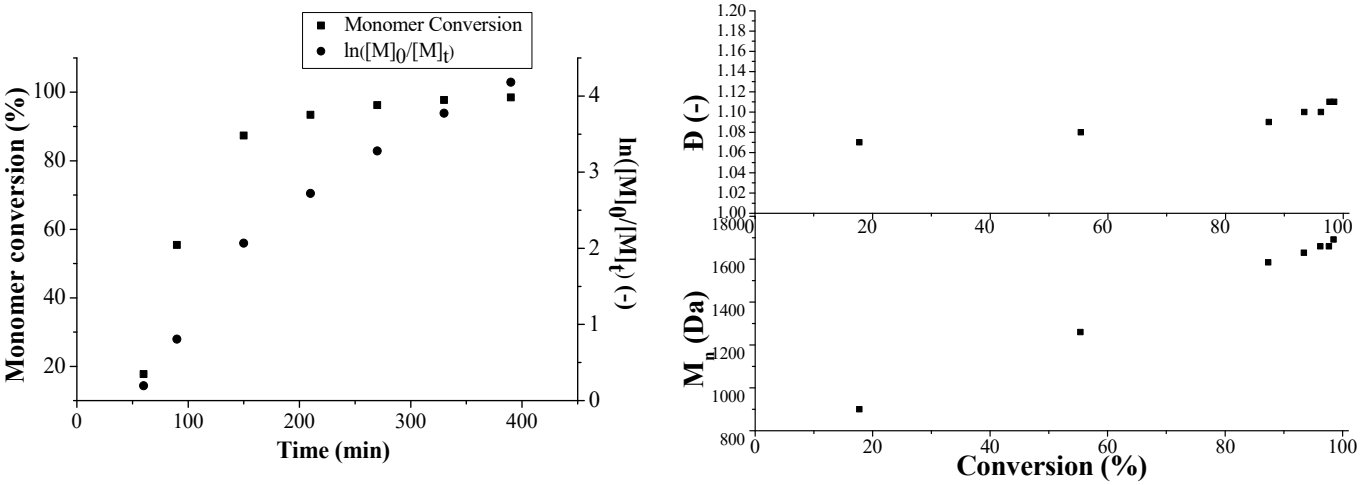

Figure IV.4: Kinetic data for the Cu(0)-mediated polymerization of isobornyl acrylate via a thiolactone initoator; (left) first order kinetic plot; (right) molecular weight and dispersity as a function of conversion.

To confirm the presence of the thiolactone moiety as end group on polyisobornylacrylate (TL-PiBA-Br), the polymer was analyzed by SEC, ^{1}H-NMR and MALDI-TOF analysis (Figure IV.5). SEC analysis evidenced the synthesis of TL-PiBA-Br with low dispersity and an average DP of 10 monomer units (near-quantitative conversion as indicated by GC analysis). From ^{1}H-NMR analysis, the signals of the thiolactone moiety can be observed at 2.8, 3.25 and 4.6 ppm (Figure IV.5), which was determined by 2D-NMR analysis

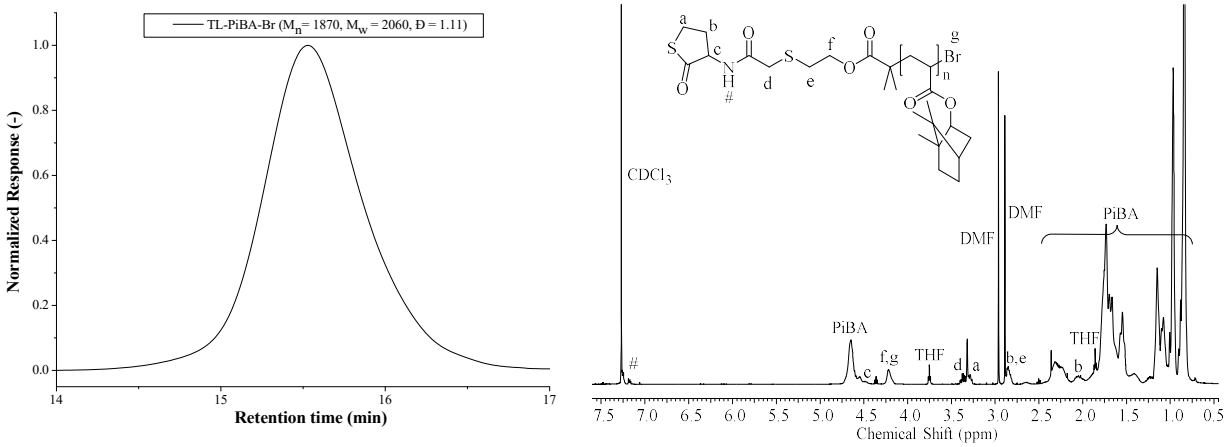

Figure IV.5: SEC and ^{1}H-NMR analysis of TL-PiBA-Br.

MALDI-TOF analysis further confirmed the structure of the TL-PiBA-Br homopolymer. A mass difference of 208.15 Da was observed between two successive analogous signals, confirming the presence of the isobornyl unit. Furthermore, a good agreement between the theoretical and experimental isotopic distribution was observed, providing the final evidence of the TL-PiBA-Br structure. However, some small extra mass distributions can be observed between the major series (Na^+-adduct), which can be attributed to the K^+-adduct, the exact assignment of the extra signals could not be provided but might be explained by fragmentation products during the MALDI-process and impurities in the starting monomer as already reported in literature (Figure IV.6).[21]

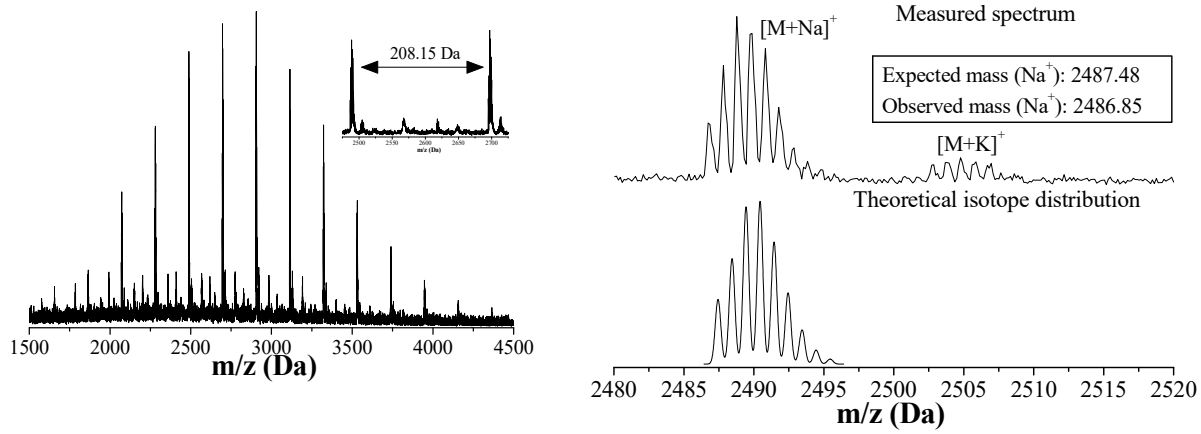

Figure IV.6: MALDI-TOF analysis of TL-PiBA-Br

IV.2.3 End-group modification to the acrylate moiety

In a next part, the bromine end group of TL-PiBA-Br was transformed into an acrylate moiety in a two-step modification procedure with intermediate purification. Synthetic efforts performing this modification step in a one-pot procedure by the use of acrylic acid and DBU as nucleophilic catalyst were thoroughly investigated but were however not compatible with the thiolactone moiety due an unknown side-reaction.[22] Therefore, the bromine was first transformed into an alcohol functionality (TL-PiBA-OH) *via* nucleophilic thio-bromo substitution by the use of 2-mercaptoethanol and triethylamine (NEt_3), purified by precipitation in methanol and analyzed *via* SEC, ^{1}H-NMR and MALDI-TOF analysis (Figure IV.7)

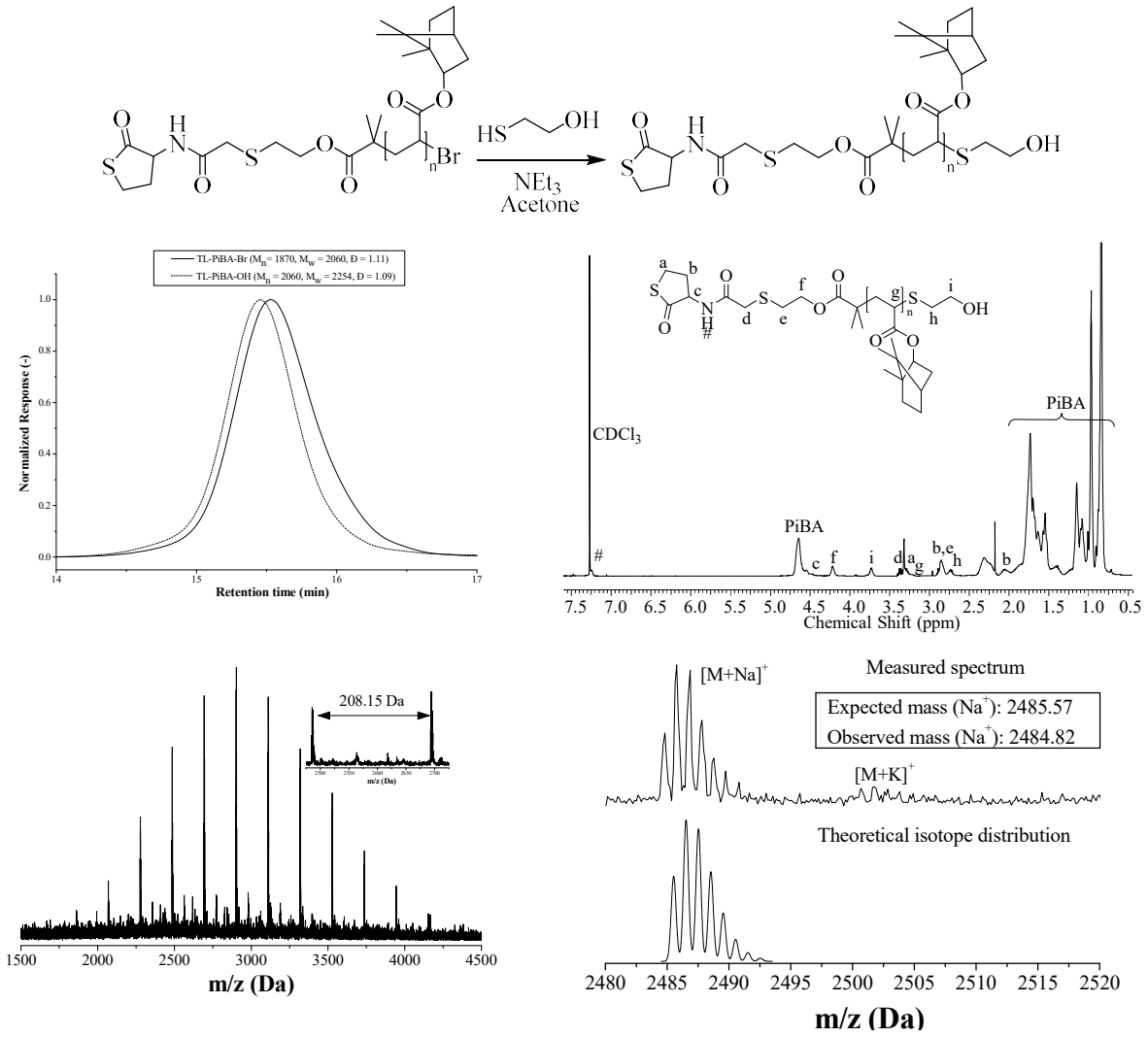

Figure IV.7: Nucleophilic thio-bromo substitution of TL-PiBA-Br with 2-mercaptoethanol to obtain the alcohol functionality (TL-PiBA-OH) and SEC, ^{1}H-NMR and MALDI-TOF analysis.

From SEC analysis, a unimodal increase in molecular weight can be observed, in combination with a very small decrease in dispersity. ^{1}H-NMR analysis (including 2D-NMR) provided further proof for the successful end group modification reaction as the signals from the CH_2's next to the alcohol appeared at 2.75 and 3.75 ppm. The disappearance of the signal from the CH_2 next to the bromine at 4.25 ppm could not be observed as it overlaps with a signal of the thiolactone initiator. Final indisputable proof was provided through MALDI-TOF analysis. A small shift of 2 Da to lower m/z value was observed for the main distribution, corresponding to the transformation of the bromine to the alcohol end group. Additionally, the removal of the bromine induced a significant change in the isotopic pattern in MALDI-TOF analysis, due to the presence

of the two abundant stable isotopes (^{79}Br and ^{81}Br). Furthermore, the small extra distributions between the major series can be attributed to unknown fragmentation products in the MALDI. As mentioned, these were already present in the starting TL-PiBA-Br polymer and also shifted in mass value after the modification reaction.

After this first successful modification reaction, the alcohol was transformed into an acrylate moiety in the subsequent step, yielding the thiolactone-acrylate heterotelechelic macromonomer (TL-PiBA-Acry). Acryloylchloride and triethylamine (NEt_3) were used to transform the alcohol into the acrylate moiety and the reaction was performed in dichloromethane (DCM). Finally, the macromonomer was isolated by precipitation in methanol and analyzed *via* SEC, ^{1}H-NMR and MALDI-TOF analysis (Figure IV.8).

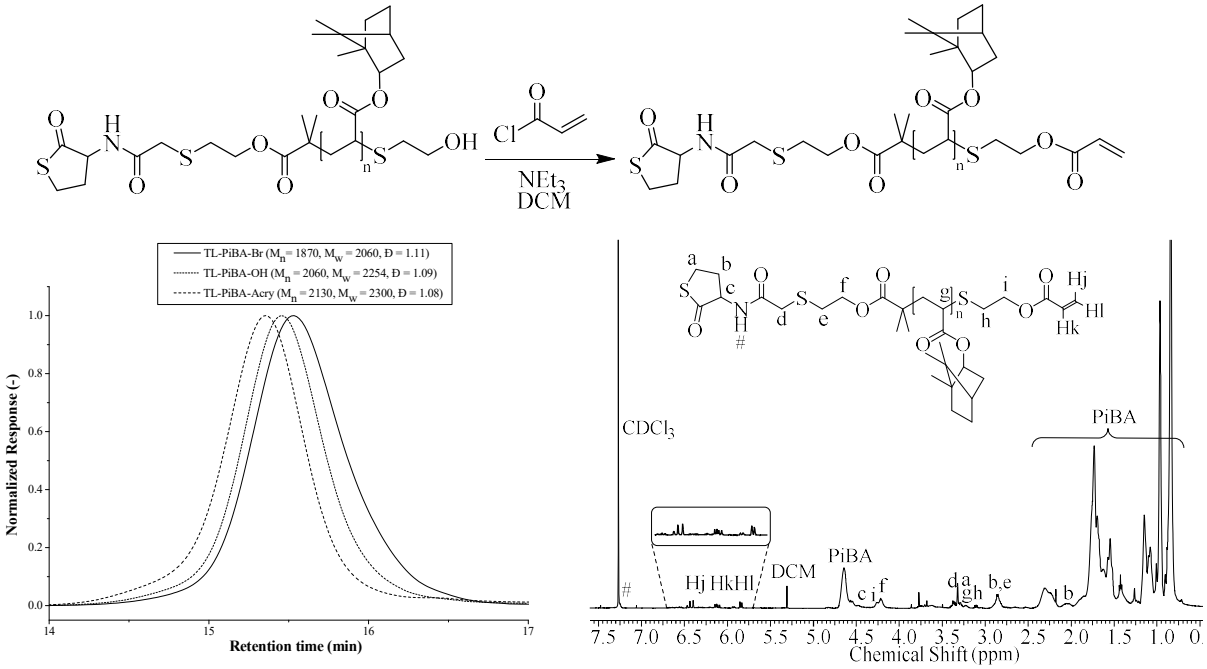

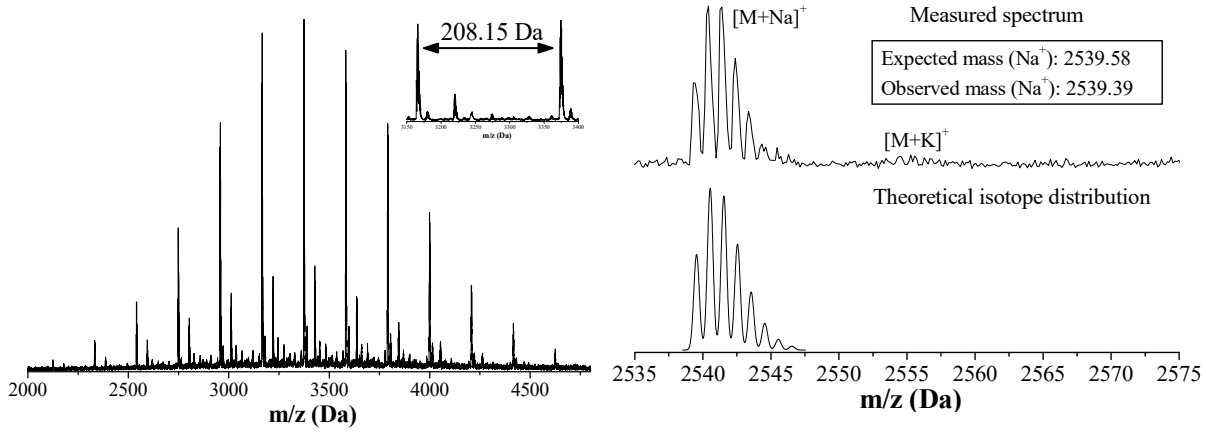

Figure IV.8: Acylation of TL-PiBA-OH with acryloylchloride to introduce the acrylate functionality (TL-PiBA-Acry) and SEC, ^{1}H-NMR and MALDI-TOF analysis.

From SEC analysis, again a unimodal increase in molecular weight can be observed, in combination with a small decrease in dispersity. From detailed ^{1}H-NMR analysis (including 2D-NMR), the disappearance of the signals from the CH_2's next to the alcohol at 2.75 and 3.75 ppm could be observed, as the appearance of the acrylate signals between 5.75 and 6.5 ppm (some small impurities are visible). Conclusive evidence for the successful modification reaction was provided by MALDI-TOF analysis. An increase in molar mass of 55 Da for the main distribution was observed, corresponding to the introduction of the acrylate moiety. The starting polymer TL-PiBA-OH could not be observed. Furthermore, theoretical and experimental mass values (and isotopic patterns) were in good agreement. Again, the small extra distributions between the major series can be attributed to unknown fragmentation products in the MALDI. As mentioned, these were already present in the starting TL-PiBA-Br and again shifted after this modification reaction.

IV.3 Synthesis of Macromolecular Line-ups

After the extensively elaborated synthesis of the TL-PiBA-Acry macromonomer, this compound was used as a platform for the synthesis of precision macromolecular line-ups with functionalities positioned at precise locations along the polymer backbone (Figure IV.9).

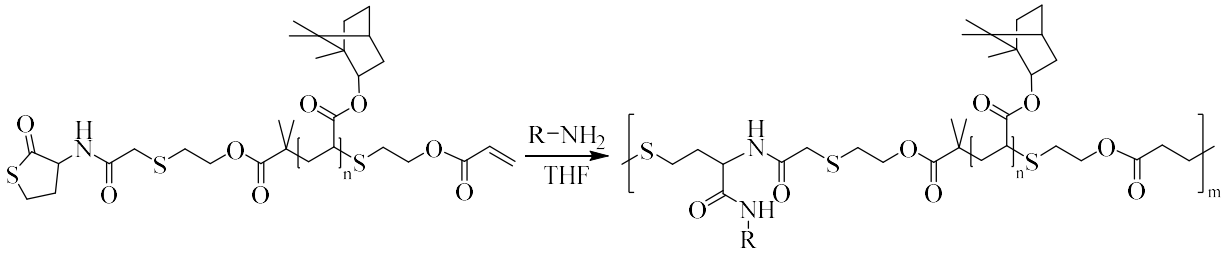

Figure IV.9: Synthesis of the multi-segmented block copolymer by the addition of an amine to TL-PiBA-Acry in THF.

First, a model experiment was performed. The TL-PiBA-Acry macromonomer was treated with octylamine in which the amine reacts with the thiolactone ring, releasing the thiol, which on its turn will react with the acrylate in an orthogonal manner. A series of different experiments were performed varying the ratio of amine/macromonomer and the concentration of the reaction mixture. It was observed that the best results were obtained when a near-equimolar amount of amine (1.1 equivalents) or small excess, in the case of more volatile amines (1.5 equivalents), was used in a minimal amount of THF or $CHCl_3$ (160 mg/0.1 mL). The resulting macromolecular line-up, with repeating octylamine-groups after every (in average) 10 monomer units, was isolated by precipitation in methanol. The success of this unassisted segment linking was evidenced by SEC analysis, in which an increase in molecular weight and broadening of dispersity was observed as a result of the step-wise addition after the reaction of the hetero-telechelic TL-PiBA-Acry macromonomer with octylamine (Figure IV.10). A small peak at low molecular weight can still be observed, which might be explained by cyclization during the segment linking or impurities in the starting macromonomer. Further investigation on the resulting conversion is discussed in section IV.5. Furthermore, the average number of segments in these periodically functionalized polymers was determined to support the success of this novel methodology. The multisegmented macromolecular line-up obtained by reaction of TL-PiBA-Acry with octylamine was purified by preparative SEC in THF to remove remaining unreacted macromonomer. The purified polymer was then analyzed by absolute molecular weight SEC in THF (universal calibration), evidencing a multi-segmented block copolymer with a number average molecular weight corresponding to about 10 linked precursor units. It has to be noted that the prepolymer, obtained by RDRP-methods, inherently will introduce a small distribution effect of side-chain functionalities.

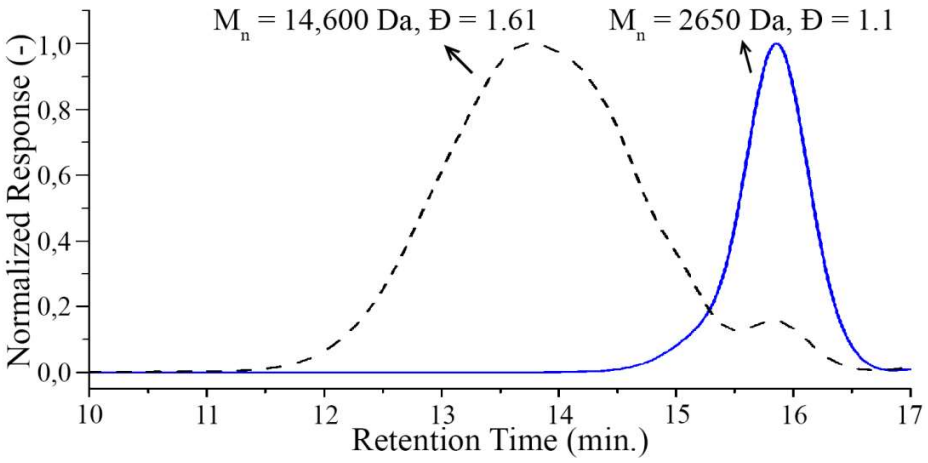

Figure IV.10: SEC-chromatogram of the heterotelechelic TL-PiBA-Acry macromonomer (blue) and the multisegmented macromolecular line-up after reaction with octylamine in THF (black).

Furthermore, both the heterotelechelic TL-PiBA-Acry macromonomer and the multisegmented macromolecular line-up were analyzed *via* Diffusion Ordered NMR-spectroscopy (DOSY-NMR), which is a technique that allows for the separation of the chemical shifts (x-axis) according to the diffusion coefficients (y-axis) of the compounds in solution. Two compounds, which differ in molecular weight will exhibit a different diffusion coefficient. Polymeric structures with higher molar masses will diffuse more slowly and their peaks are visible at the top of the DOSY spectrum, in contrast to polymeric structures with a lower molar mass resulting in signals at the bottom of the spectrum. When both the DOSY-NMR spectra of the heterotelechelic TL-PiBA-Acry macromonomer (Figure IV.11 – blue) and the multisegmented block copolymer (Figure IV.11 – black) are compared, it can be observed that the signals of the macromolecular line-up are visible at the top of the spectrum, while signals of the lower mass heterotelechelic macromonomer can be found in the middle of the spectrum in which the acrylate signals around 6-7 ppm can be clearly distinguished. Furthermore, also remaining solvent peaks, in this case THF and $CDCl_3$, can be observed at the bottom of the spectrum as these have the highest diffusion coefficients.

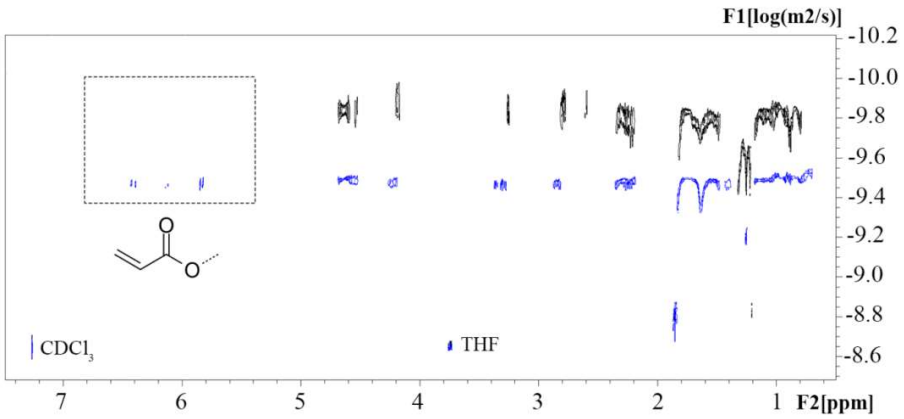

Figure IV.11: Overlay of the DOSY-NMR spectra of the heterotelechelic TL-PiBA-Acry macromonomer (blue) and the multisegmented macromolecular line-up after reaction with octylamine in THF (black).

Another proof of the successful synthesis of the macromolecular line-ups was provided by differential scanning calorimetry (DSC) analysis of the heterotelechelic TL-PiBA-Acry macromonomer and two different multisegmented macromolecular line-ups. In each case, a glass transition temperature (T_g) could be determined. It was observed that the T_g increased from 59°C for the heterotelechelic macromonomer to 69°C for the multisegmented macromolecular line-up after reaction with octylamine, as a result of the increase in molecular weight which can be explained by the Flory-Fox theory.[23] Furthermore, it could be noted that the glass transition temperature further increased to 74°C when benzylamine was used instead of octylamine, as a result of a decrease in flexibility of the side-chains, reducing the free-volume (Figure IV.12).

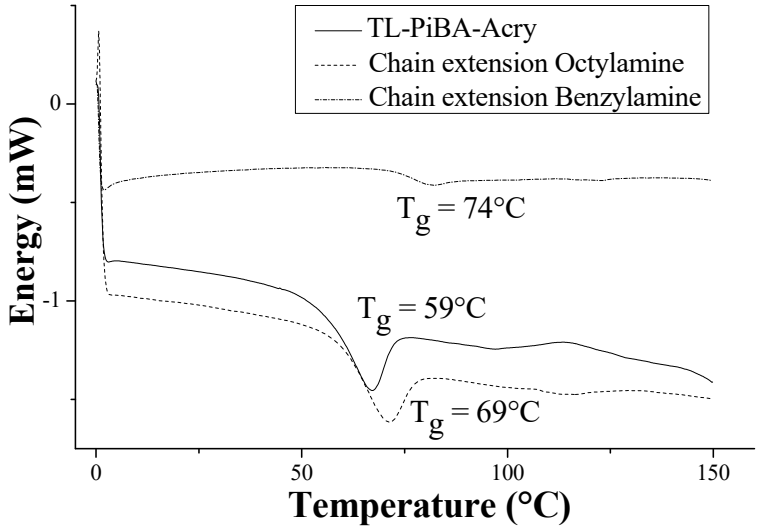

Figure IV.12: DSC-thermogram of TL-PiBA-Acry (solid), the octylamine- (dotted solid) and benzylamine multi-segmented block copolymer (dashed).

Finally, a polymeric library of precision multisegmented macromolecular line-ups was synthesized. The TL-PiBA-Acry macromonomer, serving as a polymeric platform was reacted with a series of different amines. In this way, a set of on-demand precisely decorated structures were obtained with functionalities accurately located across the polymer backbone. The variation of the amine structure enabled the synthesis of macromolecular line-ups with double bonds, furan, aromatic or PEGylated moieties at each segment connection, thus equally spaced across the polymer backbone without the need for protection and deprotection strategies (Table IV.1).

Table IV.1: Molecular weights and dispersities of functionalized multi-segmented block copolymers using different amines.

Entry	Amine	M_n (kDa)[a]	Đ[a]
1	*n*-Octylamine	14.6	1.61
2	Allylamine	11.1	1.62
3	2-(1-Cyclohexenyl)ethylamine	10.8	1.61
4	Furfurylamine	8.9	1.52
5	Benzylamine	10.6	1.58
6	PEG-amine (800 Da)	9.2	1.51
7	PEG-amine (2000 Da)	6.2	1.62

[a] Molecular weights and dispersities determined by SEC in THF vs. polystyrene standards

IV.4 Post-polymerization functionalization

By the use of the TL-PiBA-Acry macromonomer, functionalities can be directly introduced through the amine structure at precise locations across the polymer backbone. This platform of available distinct chemical handles can be extended by the use of post-polymerization modification (PPM) reactions to broaden the scope of this methodology and demonstrate its versatility. After the connection of the segments, the crude reaction mixture essentially consists of the targeted species and a minor amount of residual amine. By careful selection of the amine structure, specific PPM-reactions can be employed, installing a plethora of new functionalities at precise locations onto the macromolecular backbone. Two metal free PPM reactions were examined in this context. The first one being the radical thiol-ene reaction between *n*-octanethiol

and an alkene-containing multi-segmented block copolymer (Table IV.1 – entry 2). After reaction with 1.5 equivalents of allylamine, a solution of octanethiol in THF was added to the crude reaction mixture in combination with dimethoxy-2-phenylacetophenone (DMPA) as photo-initiator and the reaction mixture was stirred under UV irradiation (Figure IV.13).

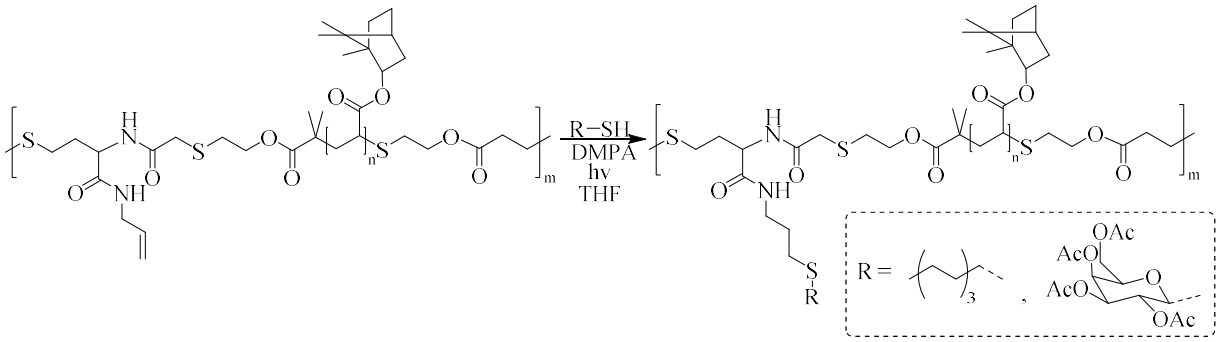

Figure IV.13: Post-modification of an allyl-containing multi-segmented block copolymer *via* the radical thiol-ene reaction.

After the reaction of the allyl-containing multi-segmented block copolymer with octylamine, the polymer was isolated by precipitation in methanol and analyzed by SEC and ^{1}H-NMR analysis (Figure IV.14). From SEC analysis, a unimodal increase in molecular weight can be observed after reaction of the allyl-containing macromolecular line-up with octylamine.

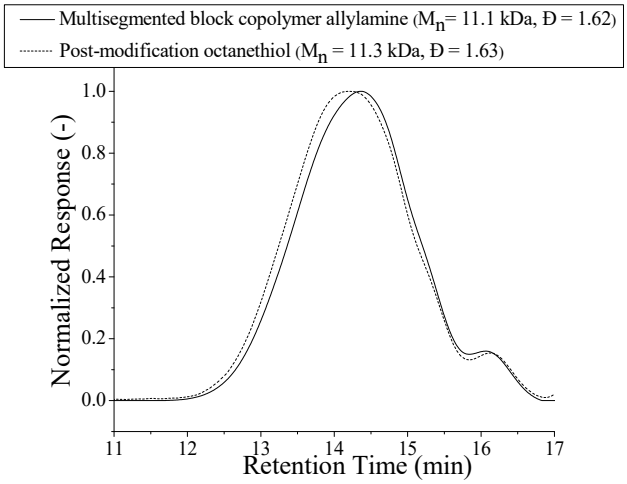

Figure IV.14: SEC-analysis of the allyl-containing multi-segmented block copolymer before and after the radical thiol-ene reaction with octanethiol and DMPA.

The NMR spectra of the allyl-containing multi-segmented block copolymer before and after the radical thiol-ene reaction were analyzed. Therefrom, it could be observed that the signals of the allyl-functionality between 5 and 6 ppm completely disappeared after reaction with octylamine (Figure IV.15).

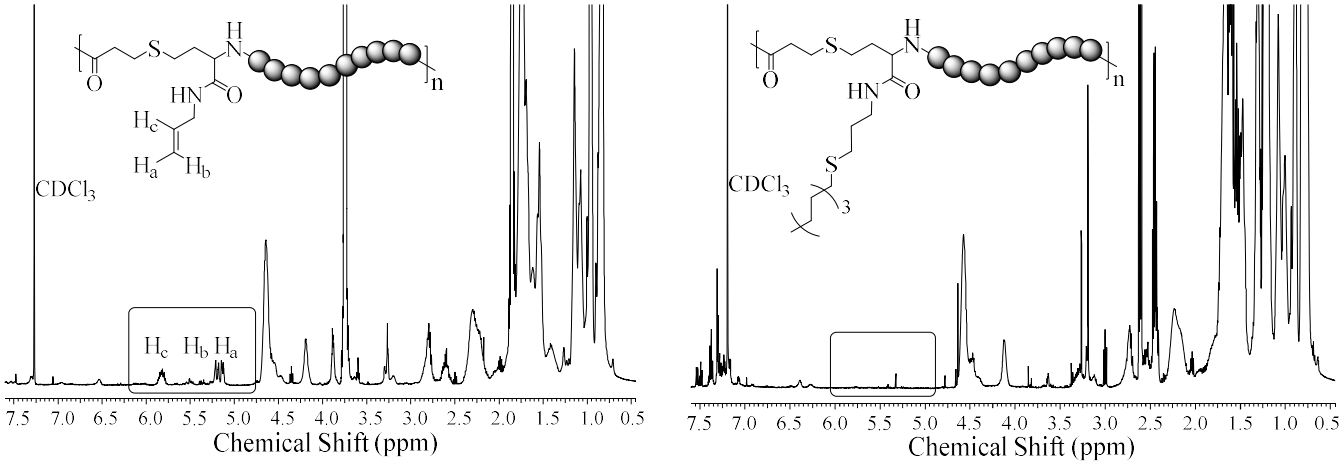

Figure IV.15: ^{1}H-NMR analysis of the allyl-containing multi-segmented block copolymer before and after the radical thiol-ene reaction with octanethiol and DMPA.

Furthermore, a sugar-containing thiol was used for the post-polymerization reaction of the allyl-containing multisegmented block copolymer. In this way, glycosylated macromolecular line-ups were obtained. These types of structures have acquired an intriguing interest in biomedical applications due to their ability to mimic biologic functions of natural carbohydrate-containing polymers.[24] It has to be noted that the applied galactopyranose-based sugar-moieties are not well soluble in the concentrated mixture, when introduced directly *via* the step-growth coupling through the amine-derivative. Therefore, sugar-moieties were introduced through radical thiol-ene reaction of the allyl-containing multi-segmented block copolymer with the corresponding sugar-thiol. The allyl-containing multi-segmented block copolymer was reacted with 2,3,4,6-tetra-O-acethyl-1-thio-b-D-galactopyranose, DMPA was used as radical source and the reaction mixture was stirred under UV-light. Finally, the polymer was isolated by precipitation in methanol and the obtained polymer was characterized by SEC and ^{1}H-NMR analysis (Figure IV.16).

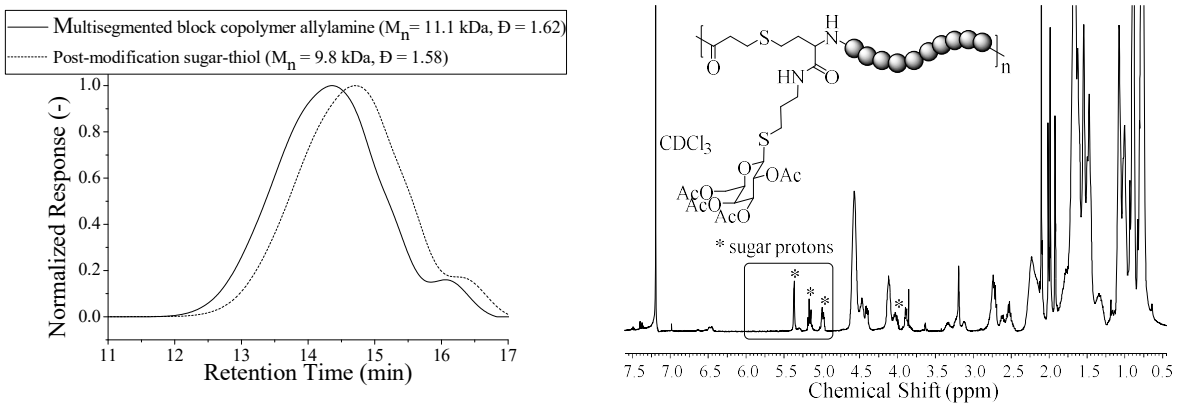

Figure IV.16: SEC and ^{1}H-NMR analysis before and after reaction with 2,3,4,6-tetra-O-acethyl-1-thio-b-D-galactopyranose to obtain the glycosylated multi-segmented block copolymer.

From SEC analysis, a unimodal decrease in molecular weight was observed, probably as a result of a significant change in the hydrodynamic volume due to the presence of the sugar-moieties, as observed by Becer *et al.*[25] Furthermore, the signals of the sugar moiety could be clearly distinguished from ^{1}H-NMR analysis as well as the disappearance of the signals of the allylic units between 5 and 6 ppm.

A second appealing metal-free post-polymerization modification reaction that was explored in this particular case is the Diels-Alder reaction between *N*-benzylmaleimide and the furan containing copolymer analogue (Table IV.1 – entry 4). After addition of furfuryl amine to the TL-PiBA-Acry macromonomer, the polymer was isolated by precipitation in methanol. Next, the furfuryl-containing macromolecular line-up was dissolved in ethyl acetate in combination with *N*-benzyl maleimide and the reaction mixture was stirred at 60 °C. The modified polymer was then purified by precipitation in methanol and analyzed by SEC and ^{1}H-NMR analysis (Figure IV.17).

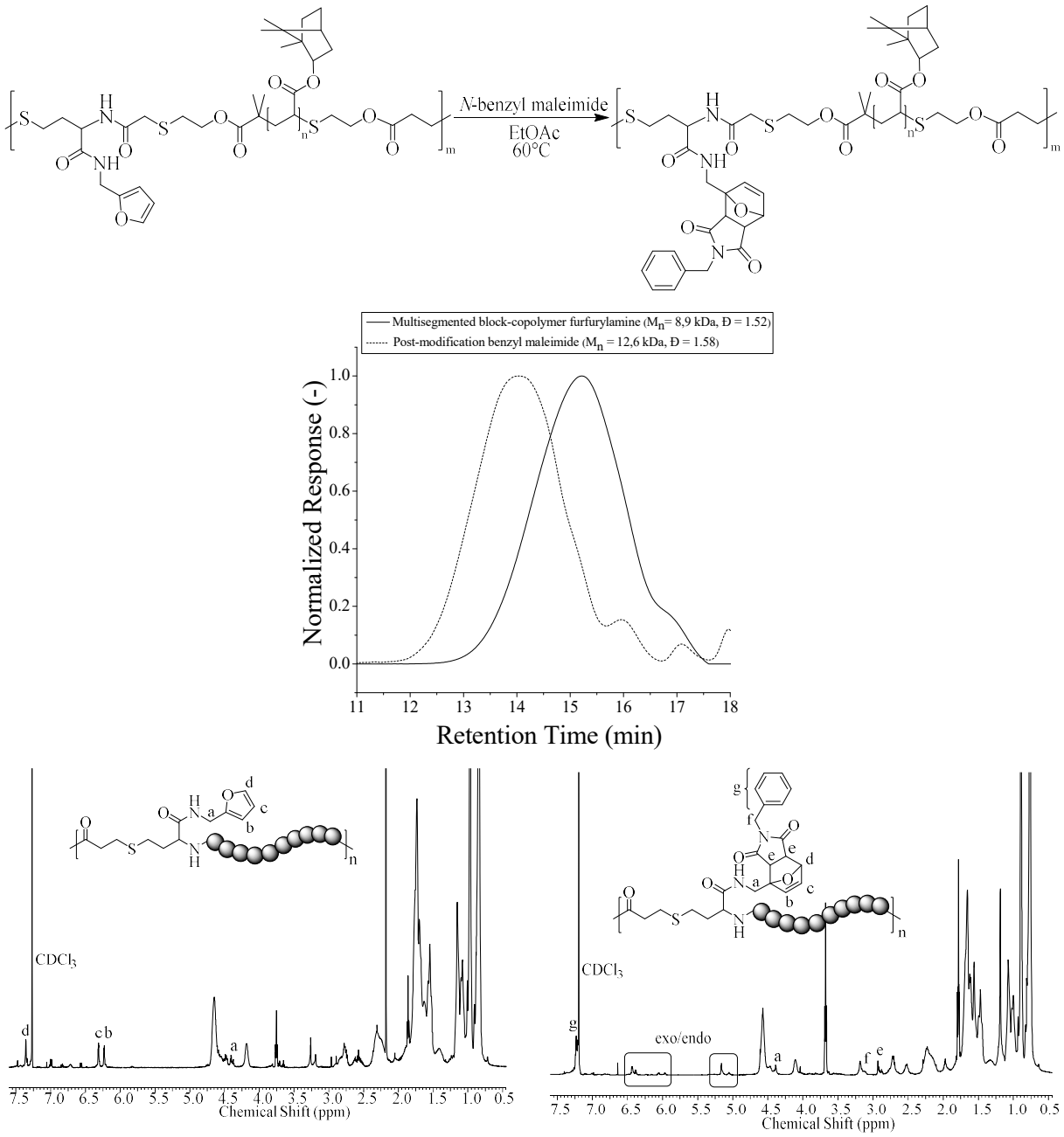

Figure IV.17: Post-modification of a furan-containing multi-segmented block copolymer *via* the furan-maleimide Diels-Alder reaction and SEC and ^{1}H-NMR analysis.

From SEC analysis, a unimodal increase in molecular weight can be observed after reaction of the furan-containing multisegmented block copolymer with *N*-benzyl maleimide. SEC-analysis further confirmed the success of the post-polymerization modification reaction as it can be

observed that the signals of the furan-moiety disappeared at 6.25 ppm and new signals from the Diels-Alder adduct appeared.

IV.5 Precision multisegmented graft-copolymers

When hydrophilic PEG-amines are used for the synthesis of these macromolecular line-ups (Table 1 – entries 6 and 7), multisegmented block copolymers are obtained with a hydrophobic backbone built up from polyisobornyl acrylate and hydrophilic side-chains containing PEG-moieties, located at precise positions across the polymer backbone. Furthermore, these structures will exhibit amphiphilic properties, as they are built up from hydrophilic and hydrophobic segments, and can be used for the stabilization of emulsions and dispersions.[26] Therefore, the hydrophobic TL-PiBA-Acry macromonomer was directly solubilized in THF and reacted with the amine-derived PEG-compound (800 or 2000 Da). Finally, LCxSEC measurements were performed to determine the success of the reaction (Figure IV.18).

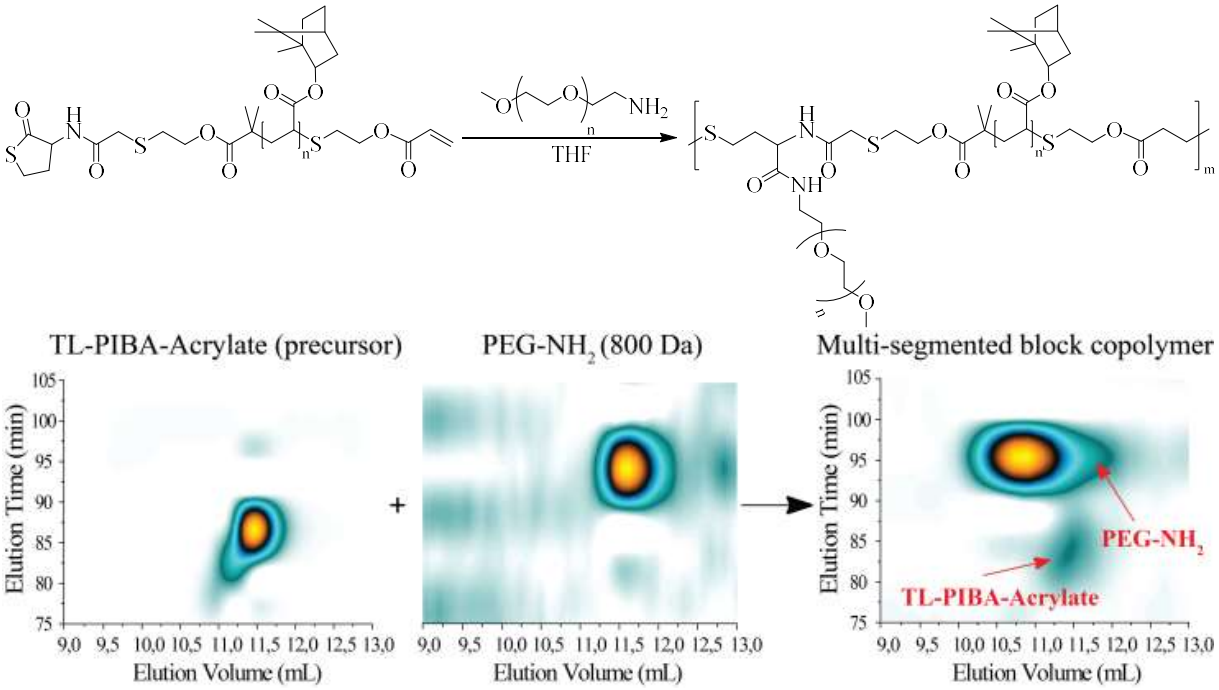

Figure IV.18: Synthesis of the precision multisegmented graft copolymer by reaction of TL-PiBA-Acry with PEG-amine and corresponding LCxSEC analysis.

From LCxSEC analysis, the difference in molecular weight (x-axis) and polarity (y-axis) of the two starting products can be monitored. After the reaction, it can be clearly observed that the

signal shifts to higher molecular weight compared to the starting precursor, along with an increase in polarity. It should be noted that in the corresponding amphiphilic multi-segmented block copolymer, only trace amounts of the residual starting material remain (< 1%), demonstrating the high yield and coupling efficiency.

In a next stage, the self-assembly behavior of the multisegmented block copolymer was investigated. A polymer solution of the macromolecular line-up in THF was prepared and slowly added to water (final concentration 1 mg/mL). Next, the aqueous aggregate solution was analyzed by dynamic light scattering (DLS), showing an average hydrodynamic volume of 130 nm (Figure IV.19).

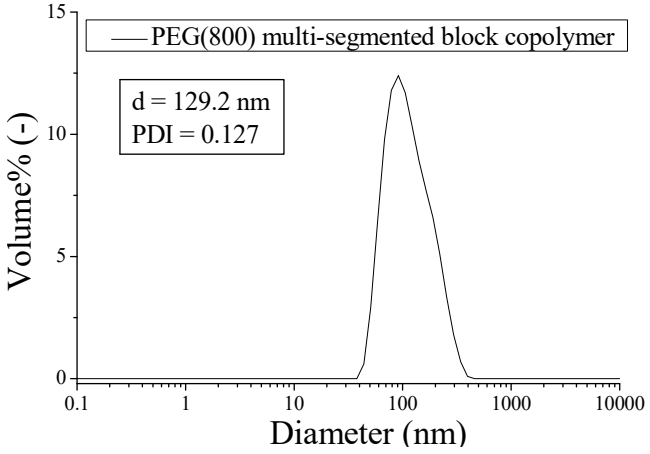

Figure IV.19: DLS-spectrum of the PEG(800) multi-segmented block copolymer.

IV.6 Single chain polymeric nanoparticles from precision multisegmented block copolymers

Another interesting aspect of these macromolecular line-ups, containing functionalities at precise positions on the polymer backbone is the introduction of chemical handles which can induce self-organization of the polymer chain to obtain the well-known single chain polymeric nanoparticles (SCPNs).[27, 28] These particles consist of a single polymer chain, functionalized with structural elements forcing the polymer to fold into well-defined objects by the use of covalent or noncovalent cross-links. One very well-known structural handle within the toolbox to

design SCPNs are chiral benzene-1,3,5-tricarboxamides (BTAs).[29, 30] In general, these BTAs are introduced onto polymer chains by the use of RDRP of the corresponding (meth)acrylate monomer or by PPM methodologies of pendant functional groups. However, in this way the BTA is introduced at random positions across the polymeric backbone. Therefore, in collaboration with Dr. Anja Palmans, Prof. Bert Meijer and Dr. Yiliu Liu at the Technical University of Eindhoven, the new developed strategy for the synthesis of macromolecular line-ups with functionalities located at precise positions onto the polymer backbone was utilized to investigate the effect of the precise positioning of the BTAs on the polymer backbone, and to investigate whether an influence could be observed on the folding behavior of the polymer into a SCPNs (Figure IV.20).

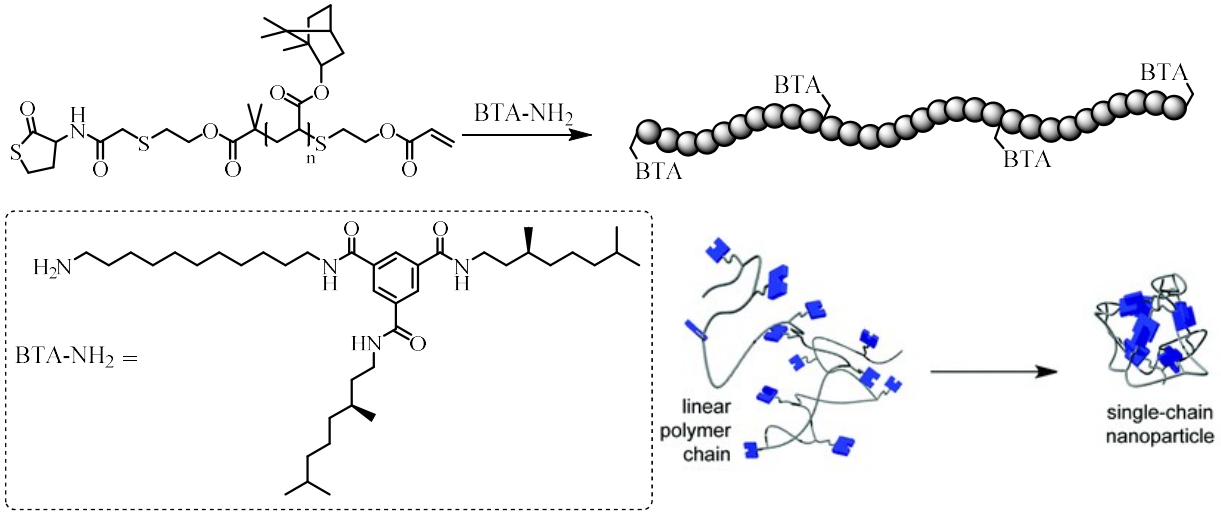

Figure IV.20: Synthesis of a macromolecular line-up containing BTA-functionalities and self-assembly to SCPNs.

In a first test, the BTA-amine was added to a solution of 160 mg of TL-PiBA-Acry in 0.1 mL of THF and the reaction mixture was stirred for 24 hours. Afterwards a sample of the crude reaction mixture was taken for SEC analysis. No significant increase in molecular weight was observed after 24 hours or even longer reaction times, probably due to the poor solubility of BTA-amine in the concentrated reaction mixture or the aggregation of the polymer units after coupling with the BTA-amine preventing further chain growth. Therefore, lithium bromide was added to break the hydrogen bonds between the BTA-units and increase its solubility in the concentrated reaction mixture. Different concentrations of LiBr were tested and it was observed that a saturated concentration of LiBr in THF was required for the segment linking. Therefore, the TL-PiBA-

Acry macromonomer was reacted with the BTA-amine in a solution of THF, saturated with LiBr, and a sample was taken for SEC analysis after 24 hours (Figure IV.21).

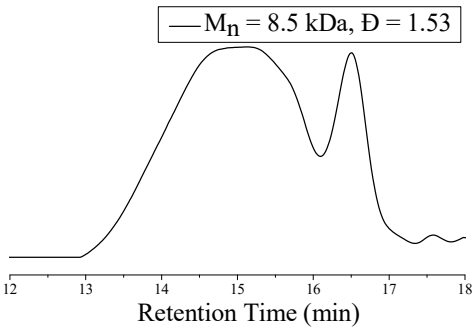

Figure IV.21: SEC chromatogram of the macromolecular line-up containing BTA-functionalities.

From SEC analysis, an increase in molecular weight was observed, evidencing the synthesis of the macromolecular line-up containing BTA-units between the different segments. However, it can also be noted that a significant amount of macromonomer is still present in the reaction mixture. Therefore, the macromolecular line-up was purified by the use of preparative SEC to remove unreacted macromonomer and remainings of LiBr.

In a next part, the self-assembly behavior of the BTA-containing macromolecular line-ups was investigated by the use of Circular Dichroism (CD), a technique that can provide structural identification of the assembled aggregates (α-helix, β-sheet, …) by measuring the interaction of the circular polarized light with the compounds in solution. In this specific case, the BTA-containing macromolecular line-up was dissolved in two different solutions: 1,2-dichloro-ethane and a 20/80 mixture of DCE/MCH and the CD-effect was measured (Figure IV.22) at a fixed BTA-concentration of 50 µM. The change of the CD-effect (y-axis) as a function of the wavelength (x-axis) is measured. The obtained shape of the plot will indicate the supramolecular aggregation (α-helix, β-sheet, …), while the intensity is a measure for the quality of the interactions.

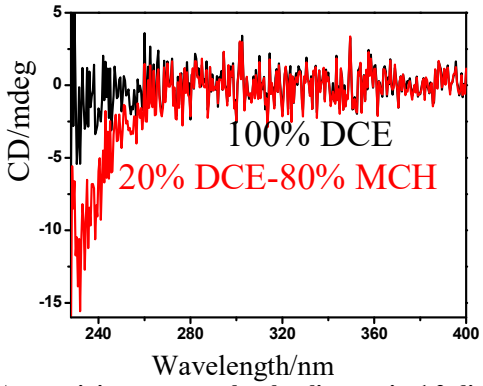

Figure IV.22: CD-spectrum of the BTA-containing macromolecular line-up in 1,2-dichloro-ethane (black) and a 20/80 mixture of 1,2-dichloro-ethane/methylcyclohexane.

1,2-Dichloro-ethane (DCE) serves as a good solvent for both the PiBA polymer and the BTA-units. However, the formation of SCPNs can be stimulated by the addition of methylcyclohexane, a non-solvent for the BTA units. From CD-analysis of the BTA-containing macromolecular line-ups, no CD-effect was observed when DCE was used as solvent. However, a small CD-effect was noted when measurements were performed in a mixture of 20% DCE and 80% MCH (typically values between -10 to -50 are observed).[28, 30] Furthermore, DLS measurements were performed to evidence that the CD-effect originates from the formation of SCPN's and is not due to the formation of large clusters. DLS-analysis indicated the formation of small particles with a diameter of 12 nm.

In a next stage, the influence of the molecular weight on the self-assembly behavior was investigated. Therefore, the obtained BTA-containing macromolecular line-up was fractionated by the use of preparative SEC in stabilized THF (to avoid the presence of peroxides) and the CD-effect of the different samples was analyzed in a 20/80 mixture of DCE/MCH (Figure IV.23).

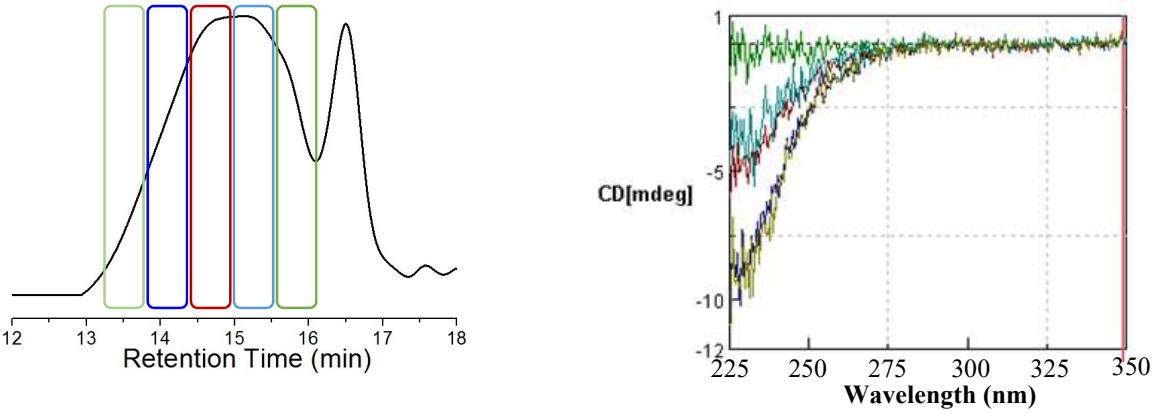

Figure IV. 23: Separation by preparative SEC (left) and corresponding CD-analysis of the different fractions with different molecular weight (right).

It was expected that the higher molecular weight fractions would exhibit the highest CD-effect due to an increasing driving force for self-assembly. However the opposite trend was observed, the CD-effect decreased with increasing molecular weight fractions. Due to this unexpected result, the different fractions obtained after preparative SEC were analyzed by ^{1}H-NMR. It was observed that the intensity of the BTA-signal was very low in all fractions. Furthermore, it could be noted that the isobornyl signals from the side chain slowly disappeared with increasing molecular weight fractions for an unknown reason. Therefore, the experiments were completely

repeated but the same results were obtained. No explanation could be provided for both the opposite expected trend in the CD-effect as for the decreasing intensity of the isobornyl signals from the side chains with increasing molecular weight. It could be argued that this might be explained by the presence of LiBr, which is the main difference (besides the BTA-amine) compared to the previous reactions in section IV.3. However no literature reports were found confirming this argument

IV.7 Conclusions

This chapter described the synthesis of precision functionalized multi-segmented block copolymers by the use of amine-thiol-ene chemistry with chemical handles located at precise positions on the polymer backbone.

First, a hetero-telechelic thiolactone-acrylate macromonomer was designed in an upscalable way. The Cu(0)-mediated polymerization of a thiolactone-based initiator was performed to ensure a high end group fidelity. Furthermore, isobornyl acrylate was chosen as monomer to facilitate purification issues of the corresponding high-T_g polymer. Next, the bromine end-group was transformed into an acrylate moiety *via* the intermediate alcohol in a two-step procedure with intermediate purification.

The multi-segmented macromolecular line-up was obtained *via* the nucleophilic ring-opening of the thiolactone unit by a functionalized amine and consecutive thiol-Michael addition. By the choice of the amine, a library of macromolecular structures was obtained with functionalities equally spaced across the polymer backbone ranging from PEG-chains and aromatic units to reactive functional handles.

Furthermore, PPM reactions provided access to a plethora of tailor-made, multi-segmented line-ups. The use of allyl- and furfuryl amine enabled the introduction of double bonds and furan moieties at exact locations on the polymer backbone, accessible for radical thiol-ene and furan-maleimide PPM reactions respectively. By the use of the corresponding thiol, sugar-moieties

were introduced onto the polymer backbone *via* the radical thiol-ene reaction, enabling the synthesis of glycosylated polymers.

Moreover, by introducing hydrophilic PEG-moieties at precise positions onto the hydrophobic PiBA-backbone, amphiphilic multisegmented block copolymers were obtained. The coupling of the hydrophobic TL-PiBA-Acry macromonomer with the hydrophilic PEG-amine was analyzed via 2D-SEC and an increase in molecular weight and shift in polarity was observed. Additionally, the amphiphilic properties were analyzed by dispersing these structures in water and measuring the size of the obtained amphiphilic structures by DLS.

Besides the synthesis of glycosylated and amphiphilic structures, this novel approach was also utilized to introduce hydrogen bonding units, which could induce self-assembly of the linear polymer chain to obtain single chain polymeric nanoparticles. In collaboration with the Technical University of Eindhoven, BTA-units were introduced at exact locations onto the polymer backbone to investigate the effect of the precise positioning of the BTA-units on the self-assembly behavior. CD-measurements were performed and a small CD-effect in a 20/80 mixture of DCE/MCH was observed. To investigate the influence of molecular weight on the formation of SCPNs, preparative SEC was used to separate the polymer into fractions of different molecular weights. In this case, it was noted that the CD-effect decreased with increasing molecular weight, opposite to what was expected. Furthermore after NMR-analysis, no isobornyl signals were observed of the high molecular weight fractions. However, no explanation could be provided for both observations after extensive analysis and discussions with all involved researchers.

Finally, from these results the presented methodology can be considered as a significant contribution within the field of precision polymer design and will hopefully be picked up by others in the area of sequence controlled polymer architectures.

IV.8 Experimental part

IV.8.1 Methods

^{1}H NMR

^{1}H- and ^{13}C-NMR (APT, HSQC, COSY) spectra were recorded in $CDCl_3$ on a Bruker AM500 spectrometer (500 MHz or 125 MHz for ^{1}H or ^{13}C respectively) or on a Bruker Avance 300 (300 MHz or 75 MHz for ^{1}H or ^{13}C respectively). Chemical shifts are presented in parts per million (δ) relative to $CDCl_3$ (7.26 ppm in ^{1}H- and 77.23 ppm in ^{13}C-NMR respectively) as internal standard. Coupling constants (*J*) in ^{1}H-NMR are given in Hz. The resonance multiplicities are described as *d* (doublet), *t* (triplet) or *m* (multiplet).

DOSY-NMR

DOSY measurements were performed using a convection compensated sequence, double stimulated echo with monopolar gradients with an extended phase cycle 15. All measurements were performed on a Bruker DRX spectrometer operating at a respective ^{1}H frequency of 500.13 MHz. A ^{1}H,^{13}C,^{15}N TXI-Z probe was used, with z-gradients calibrated to 56.1 G/cm. All measurements were performed at 298 K throughout. The diffusion encoding/decoding gradients were half sine bell shaped and were varied linearly between 2 % and 95 % of their maximum output over 32 increments. The duration of these gradients and the diffusion delay time were chosen in such a way that, at the highest gradient strength increment, the intensity of the signals of interest was decreased to less than 10 % of the lowest gradient strength increment.

LC-MS

An Agilent technologies 1100 series LC/MSD system equipped with a diode array detector and single quad MS detector (G1946C) with an electrospray source (ESI-MS) was used for classic reversed phase LC-MS. Analytic reversed phase HPLC was performed with a Phenomenex Kinetex C_{18} column (5 µ, 150 x 4.6 mm) using a solvent gradient (0 → 100% acetonitrile in H_2O in 15 min) and the eluting compounds were detected *via* UV-detection (λ = 214 nm). High resolution mass spectra (HRMS) were collected using an Agilent 6220A time-of-flight (TOF) equipped with a multimode ionization (MMI) source.

SEC

Size Exclusion Chromatography (SEC) was performed using a Varian PLGPC50plus instrument, using a refractive index detector, equipped with two Plgel 5 μm MIXED-D columns 40 °C. Polystyrene standards were used for calibration and THF as eluent at a flow rate of 1 mL/min. Samples were injected using a PL AS RT autosampler.

LCxSEC

For two-dimensional liquid chromatography, sample fractions from the first dimension were transferred to the second-dimension column via an electronically controlled eight-port valve system (VICI Valco instruments, Houston, TX, USA), equipped with two 100 μL sample loops. The second dimension consisted of an Agilent Infinity 1260 isocratic pump and a PSS SDV LIN M 5 μm column. Detection in the second dimension was accomplished by using an ELSD. Nitrogen was used as carrier gas in the ELSD at a flow rate of 2.5 L/min. Spray Chamber, Drift Tube and Optical Cell temperatures were set at 30 °C, 80 °C and 70 °C, respectively. The flow rates used in the first and second dimensions were 0.02 mL/min and 5 mL/min, respectively. Sample concentrations were between 0.25 and 2.0 mg/mL. an isocratic elution of methanol/hexane (70/30) was used as the solvent for the first dimension, THF was used as the solvent for the second dimension analysis. Data were recorded using PSS WinGPC Unichrom software.

MALDI-TOF

Matrix Assisted Laser Desorption Ionisation – Time of Flight (MALDI-TOF) was performed on an Applied Biosystems Voyager De STR MALDI-TOF spectrometer equipped with 2 m linear and 3 m reflector flight tubes, a nitrogen laser operating at 337 nm, pulsed ion extraction source and reflectron. All mass spectra were obtained with an accelerating potential of 20kV in positive ion mode and in reflector mode. *Trans*-2-[3-(4-*tert*-butylphenyl)-2-methyl-2-propenylidene]malonitrile (DCTB) (20 mg/mL in THF) was used as a matrix, sodium trifluoroacetate (1 mg/mL) was used as a cationizing agent, and polymer samples were dissolved in THF (2 mg/mL). Polymer solutions were prepared by mixing 10 μL of the matrix, 5 μL of the salt, and 5 μL of the polymer solution. Subsequently, 0.5 μL of this mixture was spotted on the sample plate, and the spots were dried in air at room temperature. A poly(ethylene oxide)

standard (M_n = 2000 g/mol) was used for calibration. All data were processed using the Data Explorer 4.0.0.0 (Applied Biosystems) software package.

GC

GC was performed on an Agilent 7890A system equipped with a VWR Carrier-160 hydrogen generator and an Agilent HP-5 column of 30 m length and 0.320 mm diameter. An FID detector was used and the inlet was set to 240 °C with a split injection ratio of 25 : 1. Hydrogen was used as the carrier gas at a flow rate of 2 mL/min . The oven temperature was increased at 20 °C/min from 50 °C to 120 °C, followed by a ramp of 50 °C/min to 150 °C.

DSC

Differential scanning calorimetry (DSC) was performed on a Mettler-Toledo DSC-1, equipped with an automatic sample robot, a liquid nitrogen-based cooling system and a FRS5 sensor based on a star-shaped arrangement of 56 thermocouples. DSC pans are standard Al pans of 40 µL and STARe Excellence Software was used to analyze the data.

DLS

Dynamic light scattering (DLS) was performed on a Zetasizer Nano-ZS Malvern apparatus (Malvern Instruments Ltd) using disposable cuvettes. The excitation light source was a He−Ne laser at 633 nm, and the intensity of the scattered light was measured at 173°. This method measures the rate of the intensity fluctuation and the size of the particles is determined through the Stokes−Einstein equation. 1 mg of PEO-NH_2 (800 Da) multi-segmented block copolymer was dissolved in 0.1 mL and precipitated in 1 mL H_2O, subsequently the polymer solution was heated at 40°C for 24h to evaporate THF, filtered through Millipore membranes with pore sized of 0.2 µm prior to measurement.

CD

UV/vis and circular dichroism measurements were performed on a Jasco J-815 spectro-polarimeter where the sensitivity, time constant and scan rate were chosen appropriately. The molar circular dichroism $\Delta\varepsilon$ was calculated as follows $\Delta\varepsilon = ((CDeffect)/(32890cl))$ wherein c is the concentration in $mol.L^{-1}$ and l is the optical path length in cm.

IV.8.2 Materials

Chloroform D ([865-49-6], ≥ 99.8 %) was purchased from Euriso-top. Triethylamine ([121-44-8], 99 %) was purchased from Acros Organics and dried in a solvent purification system (J.C. Meyer) before use as dry solvent. Isobornyl acrylate ([5888-33-5], technical grade) was distilled prior to use (70°C, 1 mbar). 2,3,4,6-Tetra-O-acetyl-1-thio-b-D-galactopyranose (> 99 %) was purchased from Glycon Biochemicals. Acryloyl chloride ([814-68-6]), 96%, stabilized with 400 ppm phenothiazine) was purchased from ABCR. PEO-NH_2 (800 and 2000 Da) was purchased from Iris Biotech GMBH. Acetone ([67-64-1], ≥ 99.9 %), allylamine ([107-11-9], ≥ 99 %), aluminium oxide ([1344-28-1], basic), benzylamine ([100-46-9], ≥ 99.5 %), *N*-benzylmaleimide ([1631-26-1], 99 %), α-bromoisobutyryl bromide, chloroform ([865-49-6], ≥ 99.8 %), Cu(0)-pellets ([7440-50-8], ≥ 99.9 %), Cu(II)Br_2 ([7789-45-9], 99 %), 2-(1-cyclohexenyl)ethylamine ([3399-73-3], 97 %), 1,2-dichlorobenzene ([95-50-1], 99 %), 1,2-dichloroethane ([107-06-2], 99.8 %), dichloromethane ([75-09-2], ≥ 99.8 %) was dried in a solvent purification system (J.C. Meyer) before use as dry solvent, 2,2-dimethoxy-2-phenylacetophenone ([24650-42-8]), 99 %), *N,N*-dimethylformamide ([68-12-2], 99.8 %), ethyl acetate ([141-78-6], 99,8 %), furfurylamine ([617-89-0], ≥ 99 %), 2-mercaptoethanol ([60-24-2], ≥ 99 %), methanol ([67-56-1], 99.8 %), methyl cyclohexane ([108-87-2], ≥ 99 %), 1-octanethiol ([111-88-6], ≥ 98.5 %), *n*-octylamine ([111-86-4], 99 %), phenothiazine ([92-84-2], ≥ 98 %), tetrahydrofuran ([109-99-9], ≥ 99 %) were purchased from Sigma-Aldrich and used without purification. Dichloromethane ([75-09-2], ≥ 99.8 %) was dried in a solvent purification system (J.C. Meyer) before use as dry solvent. Silicagel (ROCC, SI 1721, 60 Å, 40 – 63 µm) was used to perform preparative column chromatography, eluting with technical solvents. The collected fractions were analyzed by thin layer chromatography (TLC-plates, Macherey-Nagel, SIL G-25 UV_{254}). Me_6TREN[31], *N*-(2-bromoacetyl)homocysteine-γ-thiolactone[32], BTA-amine[33] were synthesized according to literature procedures.

IV.8.3 Synthesis

Cu(0)-mediated polymerization of isobornyl acrylate via a thiolactone-initiator

5 mL isobornyl acrylate (23.67 mmol, 10 eq.), 5 mL DMF, Cu(0) (50 pellets), 909.58 mg thiolactone-initiator (2.37 mmol, 1 eq.) were weighed into a flask and degassed for 1 hour with a continuous argon sparge. In a separate vial, 26.43 mg Cu(II)Br_2 (0.12 mmol, 0.05 eq.), 65.43 mg Me_6TREN (0.04 mmol, 0.12 eq.) and 1 mL DMF were degassed separately via argon bubbling for 1 hour. The reaction was started by the addition of the Cu(II)Br_2/ligand-solution to the reaction mixture at room temperature. Samples of the reaction mixture were taken for GC and SEC analysis, samples for GC analysis were dissolved in THF with phenothiazine as radical inhibitor (1,2-dichlorobenzene as internal standard), while samples for SEC analysis were diluted with THF, then passed over a basic alumina column to remove metal salts. After 6 hours, the reaction mixture was diluted with THF and filtered over a column of basic Al_2O_3 to remove the copper catalyst. After evaporating the excess solvent, the polymer was precipitated in a 10-fold excess of cold methanol, and isolated by filtration. The polymer was then redissolved in 5 mL THF, precipitated again in 50 mL of cold methanol and obtained via filtration. Finally, the polymer was dried overnight in a vacuum oven at 40°C.

End-group modification of TL-PiBA-Br to TL-PiBA-OH

5 g of TL-PiBA-Br (2.27 mmol, 1 eq.) was weighed into a flask and dissolved in 5 mL acetone. 1.28 mL of 2-mercaptoethanol (18.18 mmol, 8 eq.) and 2.53 mL of triethylamine (18.18 mmol, 8 eq.) were added. To obtain the alcohol functionalized polymer, after 48h, the reaction mixture was precipitated twice in cold methanol, filtrated, washed thoroughly with methanol and dried in a vacuum oven overnight at 40°C.

End-group modification of TL-PiBA-OH to TL-PiBA-Acry

5 g of TL-PiBA-OH (2.27 mmol, 1 eq.) was weighed into a flask and dissolved in 5 mL dry dichloromethane. 2.53 mL of dry triethylamine (18.18 mmol, 8 eq.) was added and the reaction mixture was cooled in an ice-bath for 30 min.. Then, 1.48 mL acryloylchloride (18.18 mmol, 8

eq.) was added dropwise. After full addition of the acryloyl chloride, the ice-bath was removed and the reaction mixture was stirred for 48h. To obtain the acrylate functionalized polymer, the reaction mixture was precipitated twice in cold methanol, filtrated, washed thoroughly with methanol and dried overnight on a vacuum pump.

Step-growth coupling reaction to obtain the multi-segmented block copolymer

In a small vial, the primary amine (1.1 eq.) was weighed, separately 160 mg (0.072 mmol, 1 eq.) of the precursor polymer was dissolved in 0.1 mL THF (of THF with a saturated amount of LiBr in case of BTA-NH_2). The viscous polymer solution was added to the amine at room temperature and the clear reaction mixture was stirred for 24h at ambient conditions. The multi-segmented block copolymer was isolated by precipitating the reaction mixture in cold methanol, the precipitate was filtered and washed thoroughly with methanol and dried overnight in a vacuum oven at 40°C.

Thiol-ene modification of allyl-containing multi-segmented block copolymer

In a small vial, 6.2 mg allylamine (0.108 mmol, 1.5 eq.) was weighed, separately 160 mg (0.072 mmol, 1 eq.) of the precursor polymer was dissolved in 0.1 mL THF. The viscous polymer solution was added to the amine at room temperature and the clear reaction mixture was stirred for 24h at ambient conditions. A sample was taken for ^{1}H-NMR and SEC-analysis. Consequently, thiol-ene modification was performed in the same pot by adding 15.8 mg 1-octanethiol (0.108 mmol, 1.5 eq.) and 5.54 mg DMPA (0.022 mmol, 0.2 eq.) as photo-initiator dissolved in 1 mL dry THF and shining UV-light (365 nm) for 24 h. The modified multi-segmented block copolymer was isolated by precipitating the reaction mixture in cold methanol, filtered and washed thoroughly with methanol and dried overnight in a vacuum oven at 40°C. Finally, a sample was taken from the clear reaction mixture for ^{1}H-NMR and SEC-analysis. In case of the thiol-containing sugar-derivative, 39.4 mg of 2,3,4,6-tetra-O-acetyl-1-thio-b-D-galactopyranose (0.108 mmol, 1.5 eq.) was added.

Furan-maleimide modification of furan-containing multi-segmented block copolymer

In a small vial, 7.7 mg furfurylamine (0.079 mmol, 1.1 eq.) was weighed, separately 160 mg (0.072 mmol, 1 eq.) of the precursor polymer was dissolved in 0.1 mL THF. The viscous polymer solution was added to the amine at room temperature and the clear reaction mixture was stirred for 24h at ambient conditions. The multi-segmented block copolymer was isolated by precipitating the reaction mixture in cold methanol, filtered and washed thoroughly with methanol and dried overnight in a vacuum oven at 40°C. Finally, the multi-segmented block copolymer was analysed via ^{1}H-NMR and SEC-analysis. In a next step, the multi-segmented block copolymer was dissolved in 1.5 mL EtOAc, 29.65 mg *N*-benzylmaleimide (0.158 mmol, 2 eq.), dissolved in 1 mL EtOAc was added and the reaction mixture was stirred at 60°C for 24h. Finally, the reaction mixture was precipitated in cold methanol, filtered, washed thoroughly with methanol and dried overnight on a vacuum pomp at 40°C. The purified sample was analyzed by ^{1}H-NMR and SEC-analysis.

References

1. Matyjaszewski, K.; Tsarevsky, N. V. *Nature Chemistry* **2009,** 1, (4), 276-288.
2. Kolb, H. C.; Finn, M. G.; Sharpless, K. B. *Angew. Chem., Int. Ed.* **2001,** 40, (11), 2004-+.
3. Espeel, P.; Du Prez, F. E. *Macromolecules* **2015,** 48, (1), 2-14.
4. Hawker, C. J.; Wooley, K. L. *Science* **2005,** 309, (5738), 1200-1205.
5. Bernaerts, K. V.; Du Prez, F. E. *Progress in Polymer Science* **2006,** 31, (8), 671-722.
6. Yamamoto, T.; Tezuka, Y. *Polymer Chemistry* **2011,** 2, (9), 1930-1941.
7. Badi, N.; Lutz, J.-F. *Chemical Society Reviews* **2009,** 38, (12), 3383-3390.
8. Lutz, J.-F.; Ouchi, M.; Liu, D. R.; Sawamoto, M. *Science* **2013,** 341, (6146).
9. Zhang, Q.; Wilson, P.; Li, Z.; McHale, R.; Godfrey, J.; Anastasaki, A.; Waldron, C.; Haddleton, D. M. *Journal of the American Chemical Society* **2013,** 135, (19), 7355-7363.
10. Gody, G.; Maschmeyer, T.; Zetterlund, P. B.; Perrier, S. *Nat. Commun.* **2013,** 4.
11. Soeriyadi, A. H.; Boyer, C.; Nystroem, F.; Zetterlund, P. B.; Whittaker, M. R. *J. Am. Chem. Soc.* **2011,** 133, (29), 11128-11131.
12. Hibi, Y.; Ouchi, M.; Sawamoto, M. *Angew. Chem., Int. Ed.* **2011,** 50, (32), 7434-7437.
13. Stayshich, R. M.; Weiss, R. M.; Li, J.; Meyer, T. Y. *Macromolecular Rapid Communications* **2011,** 32, (2), 220-225.
14. Tonhauser, C.; Obermeier, B.; Mangold, C.; Lowe, H.; Frey, H. *Chemical Communications* **2011,** 47, (31), 8964-8966.
15. Wong, E. H. H.; Boyer, C.; Stenzel, M. H.; Barner-Kowollik, C.; Junkers, T. *Chemical Communications* **2010,** 46, (11), 1959-1961.
16. Pfeifer, S.; Lutz, J.-F. *Journal of the American Chemical Society* **2007,** 129, (31), 9542-9543.

17. Berthet, M.-A.; Zarafshani, Z.; Pfeifer, S.; Lutz, J.-F. *Macromolecules* **2010,** 43, (1), 44-50.
18. Percec, V.; Guliashvili, T.; Ladislaw, J. S.; Wistrand, A.; Stjerndahl, A.; Sienkowska, M. J.; Monteiro, M. J.; Sahoo, S. *Journal of the American Chemical Society* **2006,** 128, (43), 14156-14165.
19. Konkolewicz, D.; Wang, Y.; Zhong, M.; Krys, P.; Isse, A. A.; Gennaro, A.; Matyjaszewski, K. *Macromolecules* **2013,** 46, (22), 8749-8772.
20. Simula, A.; Nurumbetov, G.; Anastasaki, A.; Wilson, P.; Haddleton, D. M. *Eur. Polym. J.* **2015,** 62, (0), 294-303.
21. Dervaux, B.; Van Camp, W.; Van Renterghem, L.; Du Prez, F. E. *Journal of Polymer Science Part a-Polymer Chemistry* **2008,** 46, (5), 1649-1661.
22. Van Renterghem, L. M.; Lammens, M.; Dervaux, B.; Viville, P.; Lazzaroni, R.; Du Prez, F. E. *Journal of the American Chemical Society* **2008,** 130, (32), 10802-10811.
23. Fox, T. G.; Loshaek, S. *Journal of Polymer Science* **1955,** 15, (80), 371-390.
24. Becer, C. R. *Macromolecular Rapid Communications* **2012,** 33, (9), 742-752.
25. Becer, C. R.; Babiuch, K.; Pilz, D.; Hornig, S.; Heinze, T.; Gottschaldt, M.; Schubert, U. S. *Macromolecules* **2009,** 42, (7), 2387-2394.
26. Sheiko, S. S.; Sumerlin, B. S.; Matyjaszewski, K. *Progress in Polymer Science* **2008,** 33, (7), 759-785.
27. Lyon, C. K.; Prasher, A.; Hanlon, A. M.; Tuten, B. T.; Tooley, C. A.; Frank, P. G.; Berda, E. B. *Polymer Chemistry* **2015,** 6, (2), 181-197.
28. Mes, T.; van der Weegen, R.; Palmans, A. R. A.; Meijer, E. W. *Angewandte Chemie International Edition* **2011,** 50, (22), 5085-5089.
29. Stals, P. J. M.; Gillissen, M. A. J.; Paffen, T. F. E.; de Greef, T. F. A.; Lindner, P.; Meijer, E. W.; Palmans, A. R. A.; Voets, I. K. *Macromolecules* **2014,** 47, (9), 2947-2954.
30. Hosono, N.; Palmans, A. R. A.; Meijer, E. W. *Chemical Communications* **2014,** 50, (59), 7990-7993.
31. Ciampolini, M.; Nardi, N. *Inorganic Chemistry* **1966,** 5, (1), 41-44.
32. Espeel, P.; Carrette, L. L. G.; Bury, K.; Capenberghs, S.; Martins, J. C.; Du Prez, F. E.; Madder, A. *Angewandte Chemie International Edition* **2013,** 52, (50), 13261-13264.
33. Liu, Y.; Pauloehrl, T.; Presolski, S. I.; Albertazzi, L.; Palmans, A. R. A.; Meijer, E. W. *Journal of the American Chemical Society* **2015,** 137, (40), 13096-13105.

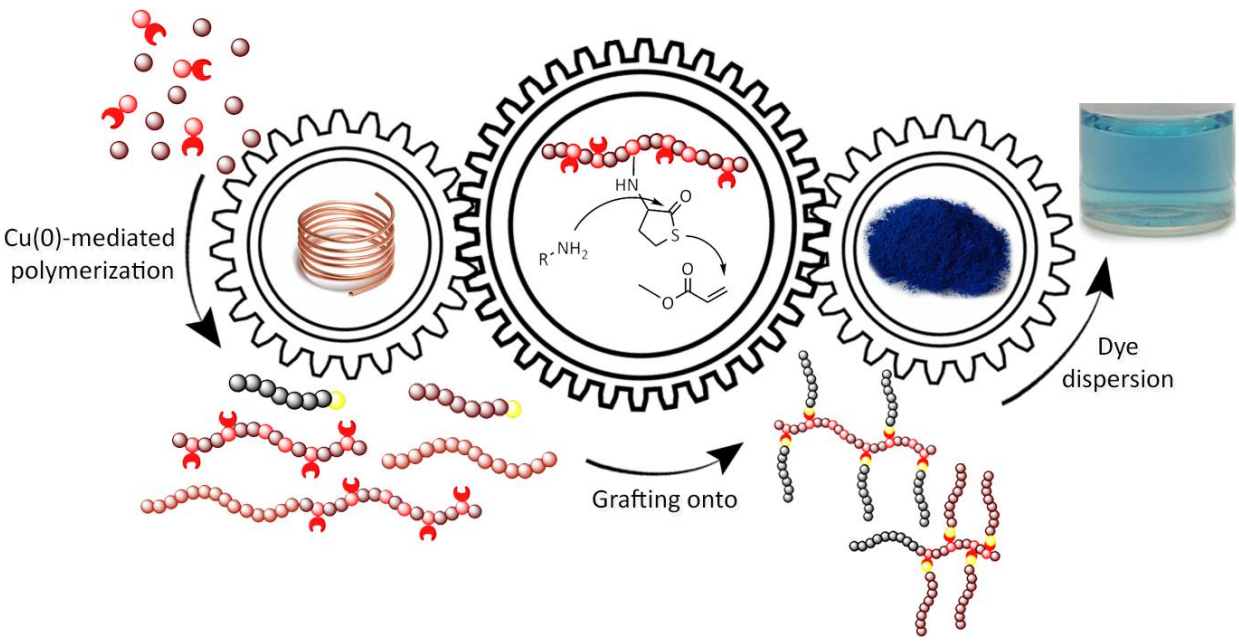

Abstract

This chapter describes a straightforward synthetic pathway for the synthesis of amphiphilic graft and toothbrush copolymers by combining copper-mediated controlled radical polymerization with the thiolactone-based amine-thiol-ene conjugation in a "grafting-onto approach". First, a series of well-defined, thiolactone containing macromolecular backbones were synthesized *via* copolymerization with a thiolactone-containing monomer. Next, acrylate end-functionalized polymers were obtained in a post-polymerization modification procedure and coupled to the backbones. Furthermore, in-depth characterization of the different structures was performed by the use of SEC, NMR, MALDI-TOF and LCxSEC analysis. In order to demonstrate the amphiphilic behaviour of these graft and toothbrush copolymers, micelle formation tests were carried out and measured with DLS, while the dispersing features of these comb-like copolymers were evaluated by pigment stabilization tests.

Parts of this chapter were published as:
Driessen F., Herckens R., Espeel P., Du Prez F.E., *Polymer Chemistry*, **2016**, 7 (8), 1632-1641

Chapter V.

Thiolactone chemistry and copper-mediated RDRP for the development of well-defined amphiphilic dispersing agents

V.1 Introduction

The preceding two chapters described the implementation of thiolactone chemistry for the synthesis of tailored telechelic structures and multisegmented macromolecular line-ups by the use of a Cu(0)-mediated polymerization system. One of the last parts of the previous chapter dealt with the synthesis of precision multisegmented amphiphilic graft copolymers, a very interesting complex polymer architecture that can be used for various applications as a result of its specific architecture. This next chapter will continue to combine thiolactone chemistry with a Cu(0)-mediated polymerization system for the synthesis of complex polymer architectures.

In general, tuning the properties of synthetic polymer materials to advanced levels by combining different monomers in various copolymer topologies as random, block, gradient, graft or star-shaped copolymers fits the current trends in macromolecular chemistry and increases the complexity of the final polymeric structure, regulating the structure-property relationship.[1-5] By careful monomer selection, these structures can be easily designed to exhibit amphiphilic properties and used for example as dispersants, emulsifiers, drug carriers, surfactants or nanoreactors.[6-12] Among these sophisticated materials, brush-type copolymers comprise an important platform in advanced macromolecular design. Their physical properties are controlled by composition, grafting density, chain stiffness and length of the side chains.[13, 14] One of the particularly interesting types of brush-type copolymers resemble toothbrush structures - also denoted as comb-like, brush-block-linear or brush-coil semi-comb copolymers - being block

copolymers containing polymer grafts in one of both segments.[15, 16] Due to their specific geometry (toothbrush shape), they are known to display increased stabilizing properties as dispersants or compatibilizers.[17]

In particular, the brush-type copolymers are build up in such a way that the different blocks are opposite in polarity. Anticipating the use of these materials as dispersants for hydrophobic pigments, the toothbrush copolymers will be designed with a hydrophilic linear chain and hydrophobic grafted segments. In this way, the grafted structures will interact with the hydrophobic surface of the pigment particles in a train-loop fashion while the hydrophilic tail will be directed towards the outside region of the tangled structure, providing steric stabilization.[18]

As already explained in the introductory part (chapter II), three established strategies can be applied to obtain toothbrush structures, the first one being the grafting through method[19, 20], which involves the polymerization of macromonomers as exemplified by Bernaerts *et al.*[21] For this, methyl vinyl ether was polymerized starting from an acrylate containing initiator, yielding the reactive macromonomer. Subsequently, the toothbrush copolymer was synthesized by polymerizing *tert*-butyl acrylate (*t*BA) as a macro-initiator *via* ATRP, followed by the polymerization of the poly(methyl vinyl ether) (PMVE) macromonomer in a consecutive step. However, this strategy typically results in low conversions due to the reduced reactivity of the macromonomer, leading to undefined toothbrush copolymers.

The grafting from strategy implies the synthesis of a macro-initiator *via* direct polymerization of a reactive monomer or by introducing initiating functionalities in a post-polymerization modification methodology. Thereby, initiating functionalities are obtained as side-chains in one of the two individual segments.[22, 23] In a next step, the polymeric side-chains can be grown from the polymer backbone *via* RDRP, ring-opening polymerization or other methods available[24-26]. Although this methodology leads to an easy purification of the final copolymer structures, the difficulty to characterize the individual segments can lead to less defined structure-property relationships of the comb-copolymers.

In the grafting onto strategy, the polymer backbone and side chains are prepared separately, enabling the use of polymerization mechanisms appropriate to the respective desired polymer structure. Furthermore, it enables the precise characterization of the individual segments,

providing a clear structure-property relationship of the final copolymer material, given the fact that efficient conjugation of macromolecular precursors is achieved.[27, 28] An example of Riyu and Hirao describes the preparation of a block copolymer of poly(*m*-bromomethylstyrene-*b*-styrene) and 1,1-diphenylethylene end-capped poly(styryllithium) as side-chain *via* anionic polymerization. In a next step, the two polymeric structures were coupled at -50°C for 72 h to obtain the comb copolymer.[29] As already explained in the introductory part, to increase the coupling efficiency between the different segments, often 'click'-type reactions are applied.[30-32] Numerous examples can be found in literature, illustrating the synthesis of graft copolymers by the use of copper(I)-catalyzed azide-alkyne cycloaddition (CuAAc).[33-35] However, the requirement of a metal catalyst and the use of azides typically pushes polymer chemists to apply metal-free alternatives such as thiol-ene or Diels-Alder type of reactions.[36, 37] A recent paper from the group of Keul describes the synthesis of a polyamide, containing free thiol-functionalities, followed by the nucleophilic thiol-ene reaction with a PEG-acrylate to introduce polymeric side-chains on the backbone, resulting in the graft copolymer structure.[38] As already explained in the introductory part, the use of thiols implies the occurrence of side reactions due to disulfide formation.[39, 40] Within our own research group, we introduced the use of thiolactones as an alternative strategy.[41, 42] The thiolactone group serves as a latent thiol functionality and through nucleophilic reaction with a functional amine in the presence of an acrylate. The generated thiol is consumed *in situ* in a conjugate (Michael-) addition.[43]

Because of the promising results reported for toothbrush copolymers as dispersants in a previous PhD-thesis[44], we investigated their synthesis making use of thiolactone chemistry in a grafting onto approach. In a similar way, the corresponding amphiphilic graft copolymers have been prepared to provide a direct comparison.[45] First, linear and block copolymers were synthesized containing thiolactone functionalities in the polymer backbone.[46, 47] For this purpose, Cu(0)-mediated RDRP was applied.[48, 49] To introduce the polymeric side-chains as grafts, polymers containing an acrylate end-group were synthesized *via* PPM reactions. In a next step, these structures were connected via amine-thiol-ene conjugation to obtain the amphiphilic graft and toothbrush copolymers. A range of different structures were synthesized, differing in molar mass and grafting density. Their properties were assessed by LCxSEC and by DLS measurements. Finally, their characteristics as dispersants were investigated through pigment stabilization tests.

V.2 Synthesis of amphiphilic graft copolymers

V.2.1 Introduction

The synthesis of the graft copolymers in this work was performed *via* the grafting onto strategy by the use of the amine-thiol-ene conjugation strategy. Segment lengths were selected based on the hydrophilic/hydrophobic balance of the backbone and polymer grafts or on the commercial availability of starting materials.[50] For the graft copolymers, a hydrophobic polymer backbone consisting of butyl acrylate (BA) and a thiolactone-containing acrylate (TLA) was prepared first via Cu(0)-mediated CRP. Next, the hydrophilic PEO-acrylate was synthesized by PPM reaction of the corresponding alcohol. Finally, side-chains were coupled via the amine-thiol-ene conjugation strategy to obtain the amphiphilic graft copolymers (Figure V.1).

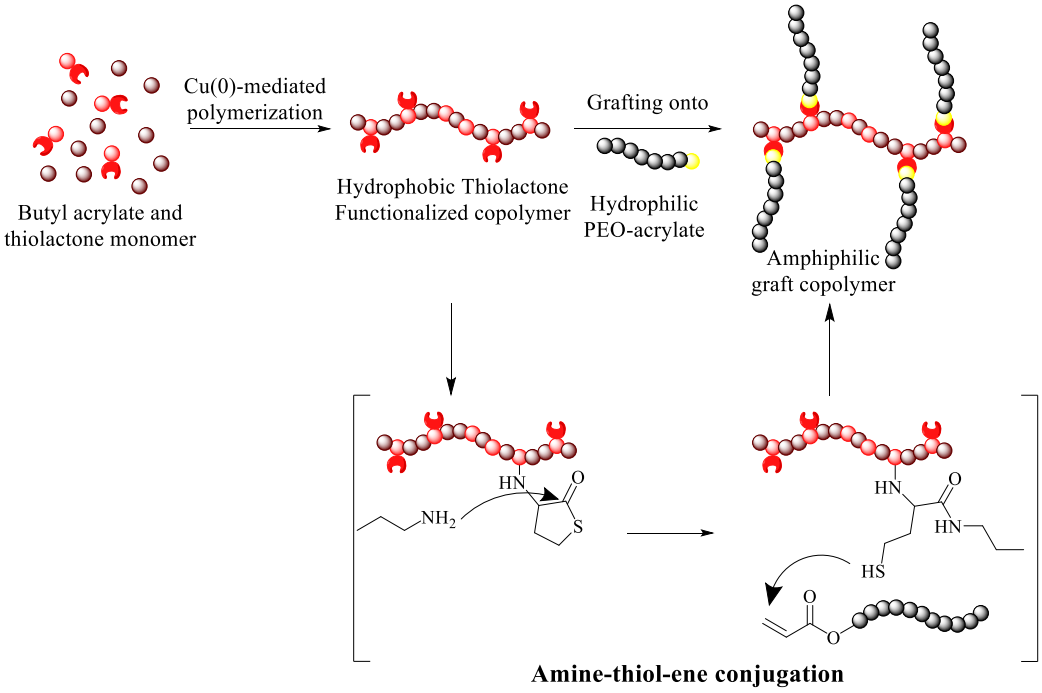

Figure V. 1: General synthetic strategy for the synthesis of amphiphilic graft copolymers *via* amine-thiol-ene conjugation.

V.2.2 Preparation of the hydrophobic TLA-functionalized copolymer

As mentioned, the first step in this project was the synthesis of a polymeric backbone containing thiolactone functionalities. Therefore, a thiolactone-based monomer was selected containing a reactive acrylate moiety available for Cu(0)-mediated polymerization. More specifically, 4-[methyl-N-(tetrahydro-2-oxo-3-thienyl)carbamate]cyclohexylmethyl acrylate (TLA) was selected due to its availability in the lab, as it was already used in previous projects, and stable as a powder in the freezer without the requirement of adding a radical inhibitor.[43] This monomer was synthesized by reaction of the α-cyanato-γ-thiolactone (synthesis described in chapter 3) with a commercial alcohol-containing acrylate in the presence of DBTL and purified by column chromatography.

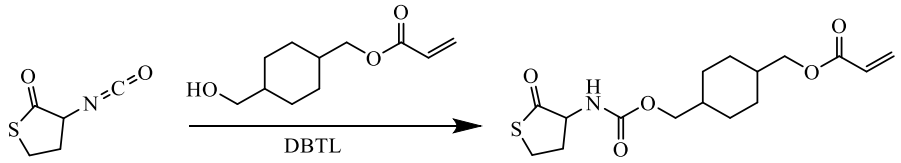

Figure V. 2: Synthesis of a thiolactone-containing acrylate monomer.

Next, the hydrophobic polymer backbone with thiolactone-containing functionalities was obtained by copolymerization of butyl acrylate (BA) with the thiolactone-containing acrylate (TLA) *via a* Cu(0)-mediated CRP (Figure V.3). A kinetic study of the copolymerization was performed to evidence a near-random distribution of the thiolactone units across the polymer chain. Samples were taken during the copolymerization at regular time intervals. The molecular weight and dispersity were determined *via* SEC analysis. Furthermore, a combination of GC and NMR analysis was used to calculate the conversion. The total acrylate conversion was measured *via* NMR, while the conversion of butyl acrylate was determined by GC. The conversion of the thiolactone-acrylate monomer was calculated out of these two results. From the kinetic results it can be observed that the copolymerization proceeded in a controlled manner and that both butyl acrylate and the thiolactone-acrylate based monomer were consumed in an almost equal rate evidencing a near-random distribution.

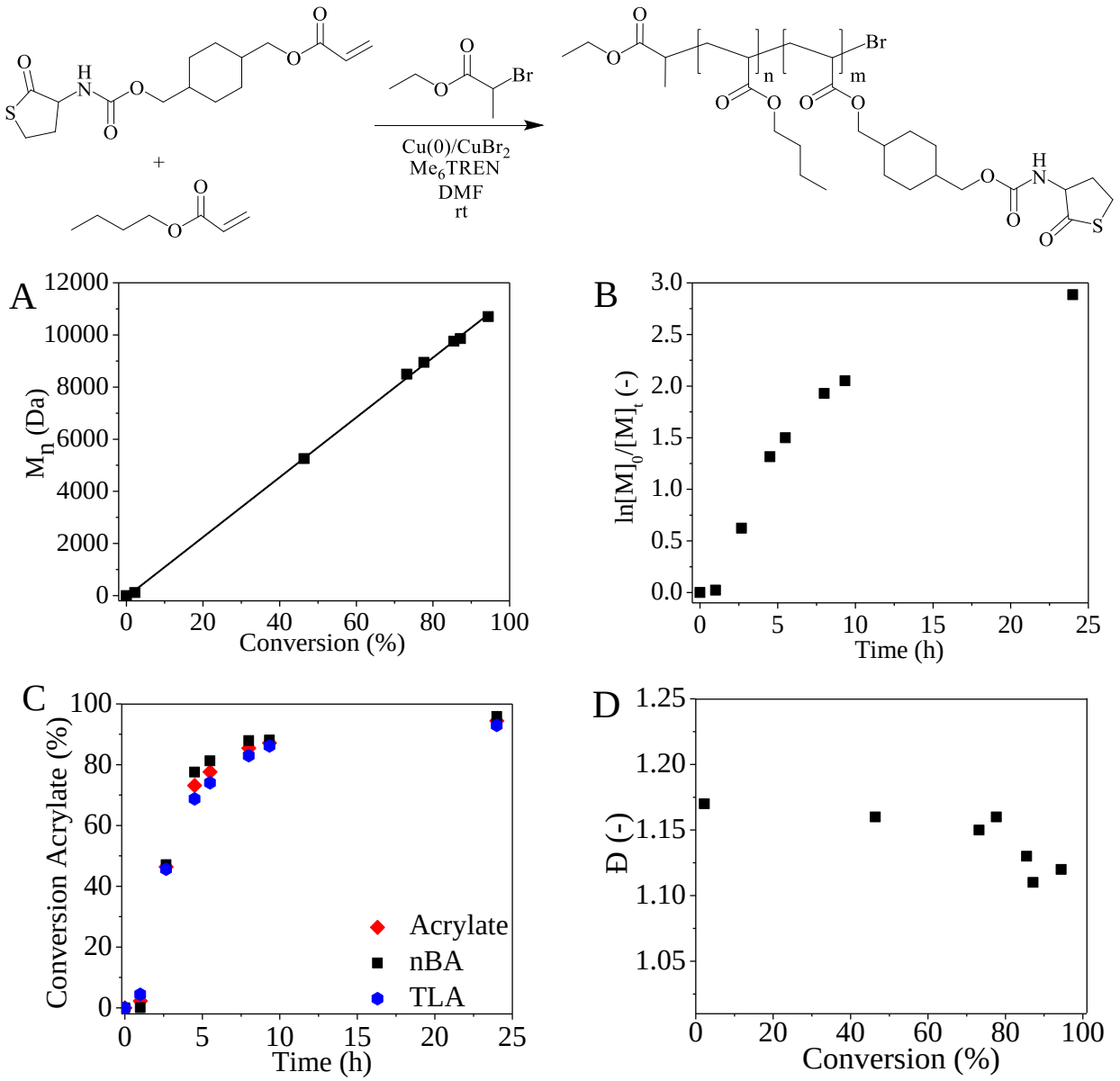

Figure V. 3: Kinetic data for the Cu(0)-mediated copolymerization of butyl acrylate and TLA; molecular weight as a function of conversion (A); first order kinetic plot (B); the conversion of the both nBA and TLA as function of time (C) and dispersity as a function of conversion (D).

Furthermore, different copolymers with varying DP's containing 5, 10 and 20 mol% of thiolactone units were prepared (Table V.1). The resulting concentration of thiolactone-units in the different copolymers was calculated from NMR by comparing the signal of the thiolactone unit at 3.25 ppm with the signal of butyl acrylate at 0.9 ppm (Figure V.4).

Table V. 1: Overview of the different copolymers synthesized *via* Cu(0)-mediated RDRP

Entry	Copolymer	M_n (kDa) (Đ[a])	Experimental % TLA[b]
1a	P(nBA-*co*-TLA$_{5\%}$)$_{100}$	11.7 (1.05)	6.0
2a	P(nBA-*co*-TLA$_{10\%}$)$_{100}$	12.5 (1.12)	10.5
3a	P(nBA-*co*-TLA$_{10\%}$)$_{200}$	21.2 (1.18)	15.5
4a	P(nBA-*co*-TLA$_{20\%}$)$_{100}$	10.8 (1.06)	24.5

[a]Molecular weights and dispersities determined by SEC in THF vs. polystyrene standards
[b]Experimental incorporation of thiolactone in copolymer calculated from NMR-analysis

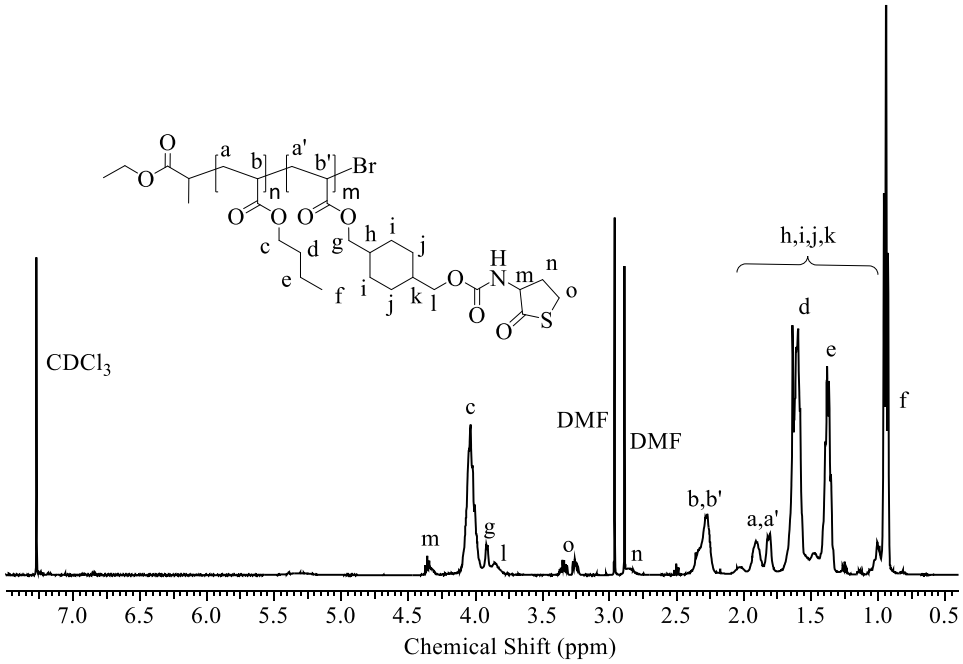

Figure V. 4: ^{1}H-NMR of the of the P(nBA-*co*-TLA$_{10\%}$)$_{100}$ copolymer.

V.2.3 Synthesis of PEO-acrylate

The hydrophilic PEO-acrylate, which will be linked to the thiolactone-containing copolymer as side-chain, was prepared by reaction of acryloyl chloride with PEO-OH in dry DCM in the presence of dry triethylamine and the reaction outcome was analyzed *via* SEC, ^{1}H-NMR and MALDI-TOF(Figure V.5).

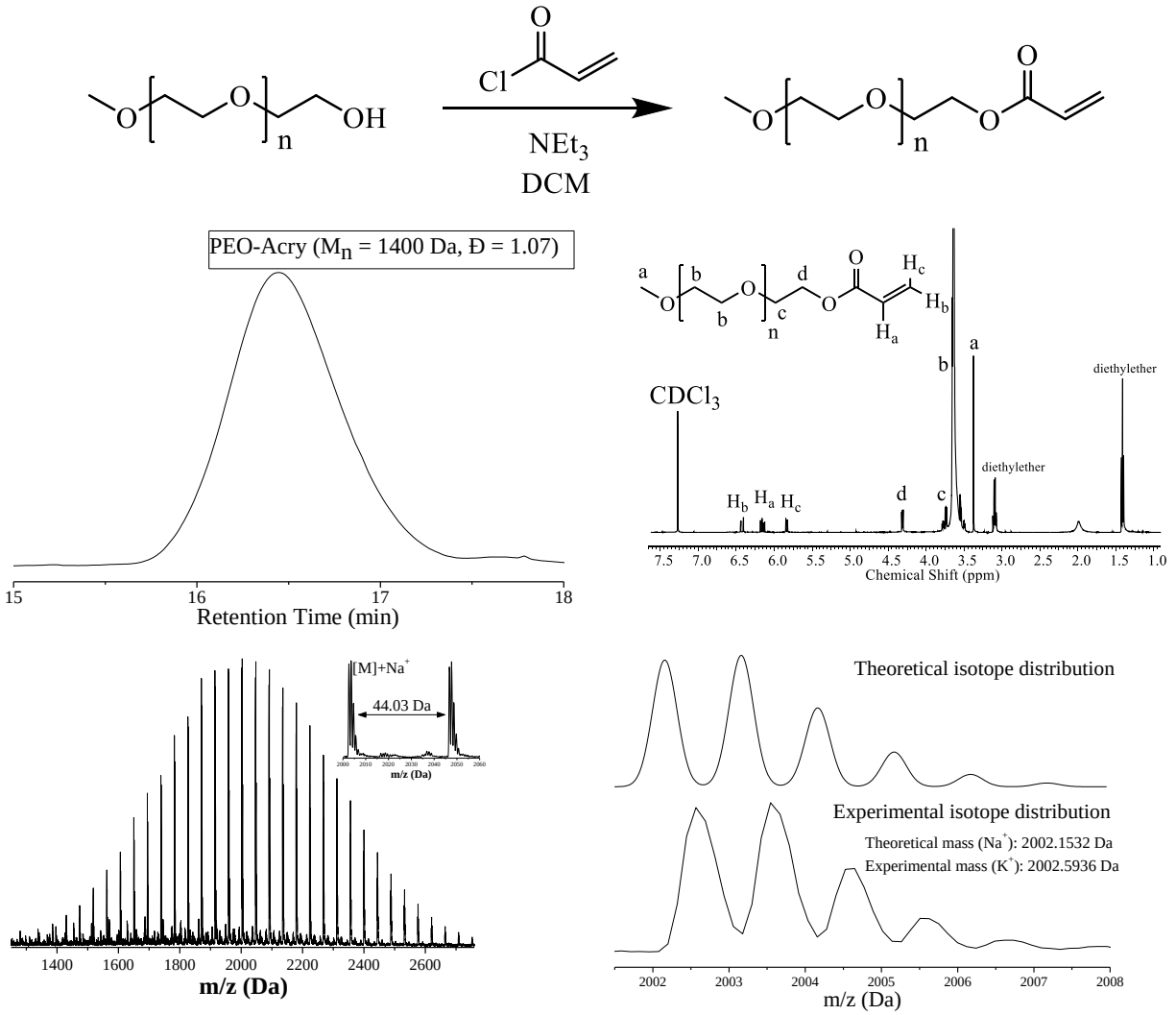

Figure V. 5: Synthesis of PEO-acrylate by reaction of PEO-OH with acryloylchloride and SEC, ^{1}H-NMR and MALDI-TOF analysis.

From SEC analysis, a unimodal distribution of the polymer can be observed. Furthermore, the acrylate signals can be clearly distinguished between 5.75 and 6.5 ppm. Indisputable proof was provided by MALDI-TOF analysis. The signals of the main distribution were in good agreement with the sodium adduct of PEO-acrylate as can be observed from a comparison between the theoretical an experimental isotope distributions. Furthermore, no signals of the starting product (PEO-OH) were observed. The additional distributions can be attributed to the potassium adduct (M_{theo} = 2018.29 Da) and an unknown impurity in the starting material.

V.2.4 Grafting onto

After the synthesis of the thiolactone-containing hydrophobic copolymer and hydrophilic PEO-acrylate side-chains, the amine-thiol-ene conjugation of the thiolactone units was investigated, surpassing drawbacks related to the instability of thiol compounds. First, a series of model experiments were performed in which P(nBA-co-TLA_{10}) was reacted with different amines in the presence of methyl acrylate, in which the amine will open the thiolactone ring, releasing the thiol *in-situ*, which on its turn will react with the methylacrylate *via* a thiol-Michael addition. After the model reactions, the outcome was analyzed *via* ^{1}H-NMR analysis by investigating the disappearance of the signals of the thiolactone moiety at 3.25 ppm. It was observed that only small amines, such as propyl- or allylamine, react quantitatively with the thiolactone ring, while more bulky amines did not, e.g. benzyl- or octylamine.

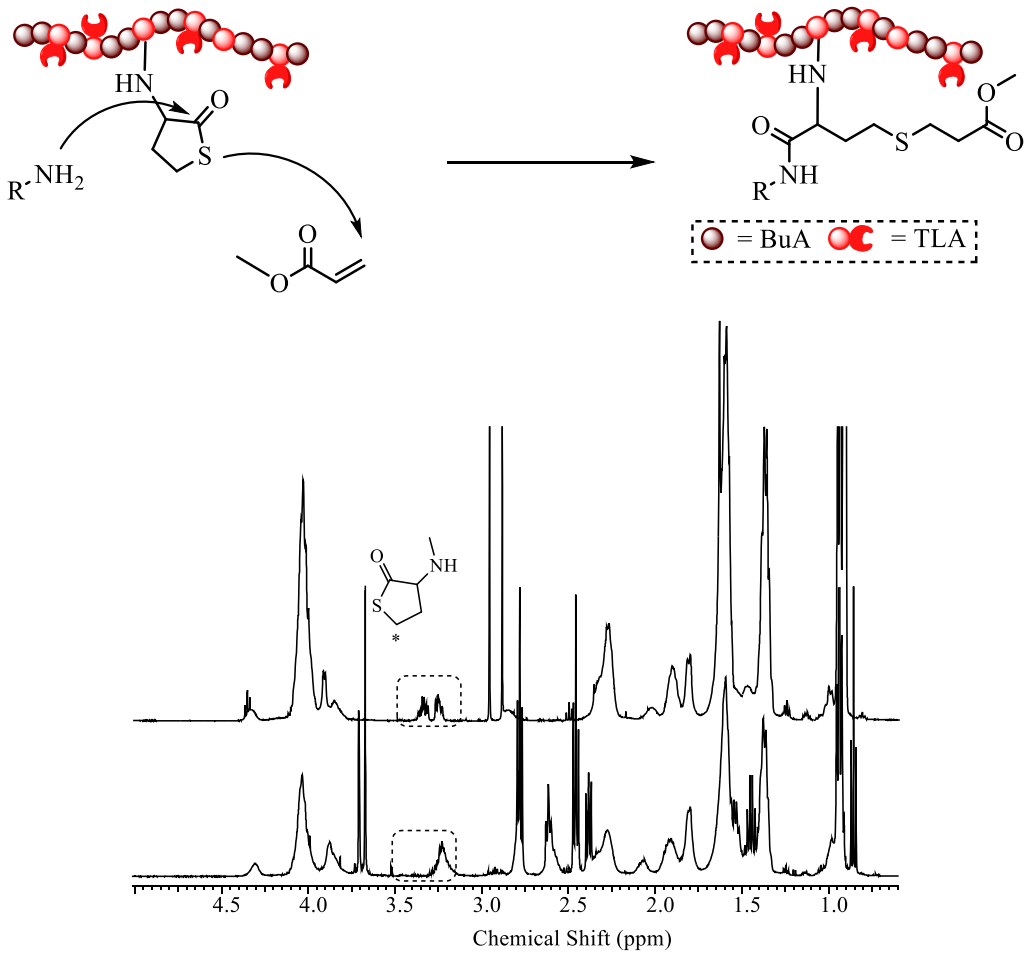

Figure V. 6: Aminolysis of the thiolactone-containing copolymer and analysis *via* ^{1}H-NMR in $CDCl_3$.

In a next stage, the information of the model study was used for the synthesis of the amphiphilic graft copolymers *via* the amine-thiol-ene conjugation strategy. Propylamine, as small amine, and PEO-acrylate were added in equimolar amounts to the copolymer solution and the reaction outcome was analyzed *via* SEC- and NMR (Figure V.7). From SEC analysis, a large extent of coupling was observed in combination with an amount of PEO-acrylate. No explanation could be provided for the presence of the thiolactone copolymer. A broad distribution of the graft copolymer was observed, attributed to the different degrees of coupling of the side-chains, similar to what Keul and coworkers. observed for the coupling of PEO-acrylate to a thiol-functionalized precursor-polymer.[38] The vertical dotted line indicates the separation by preparative SEC afterwards.

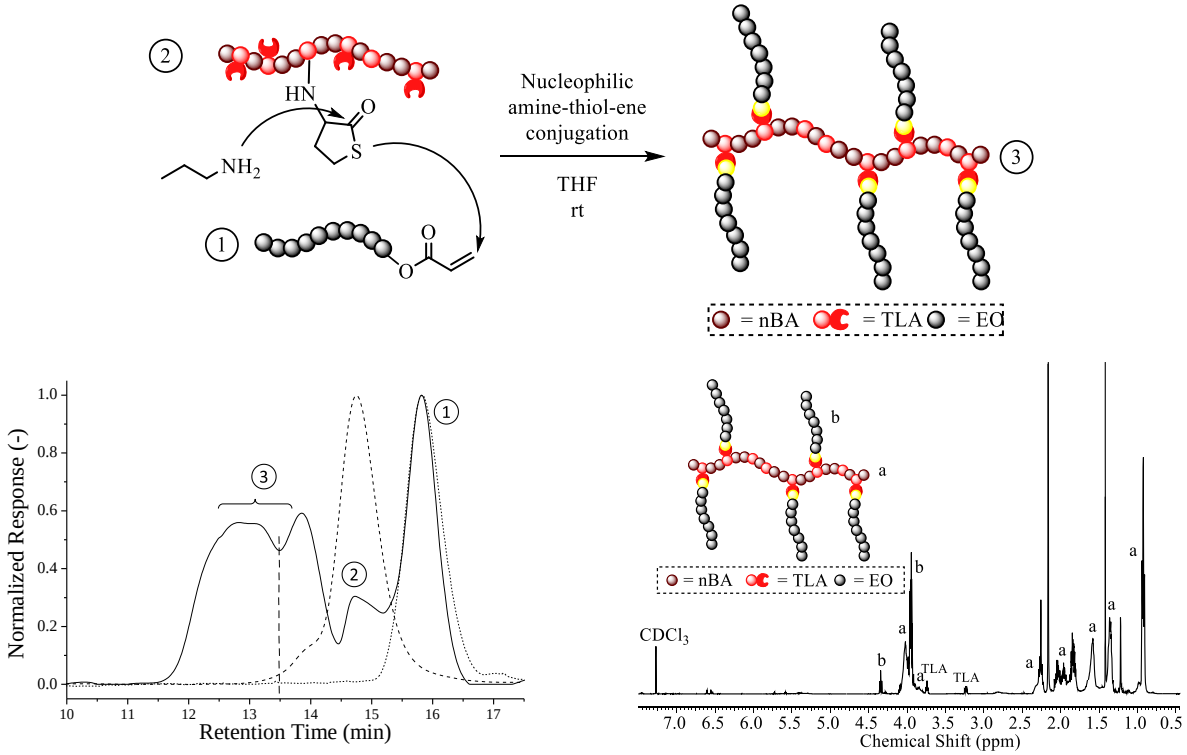

Figure V. 7: Synthetic strategy, SEC and ^{1}H-NMR analysis of the amphiphilic graft copolymer consisting of the hydrophobic TLA-containing backbone and the hydrophilic PEO side-arms.

Next, a variety of different graft copolymers with different molecular weight (backbone and PEO side-arm) and grafting density (TLA-content) were synthesized (Table V.2) and analyzed *via* SEC and ^{1}H-NMR analysis. The average number of grafts was calculated by comparing the signal of PEO at 4.3 ppm with the signal of butyl acrylate at 0.9 ppm.

Table V. 2: SEC-results of the graft copolymers *via* the amine-thiol-ene reaction between the hydrophobic P(nBA-co-TLA) copolymers and PEO-acrylate.

Entry	Graft copolymer	M_p (kDa)[a]	Aver. Grafts[b]	Theo. M_w (kDa)[c]
1a-g	P(nBA-*co*-TLA$_{5\%}$)-*g*-PEO$_{480}$	20.4	5.3	2.6
2a-g	P(nBA-*co*-TLA$_{5\%}$)-*g*-PEO$_{2000}$	32.6	4.4	8.8
3a-g	P(nBA-*co*-TLA$_{10\%}$)$_{100}$-*g*-PEO$_{480}$	21.5	9.3	4.5
4a-g	P(nBA-*co*-TLA$_{10\%}$)$_{100}$-*g*-PEO$_{2000}$	36.5	7.3	14.6
5a-g	P(nBA-*co*-TLA$_{10\%}$)$_{200}$-*g*-PEO$_{2000}$	49.2	20.5	20.4
6a-g	P(nBA-*co*-TLA$_{20\%}$)-*g*-PEO$_{480}$	25.3	20.6	9.9
7a-g	P(nBA-*co*-TLA$_{20\%}$)-*g*-PEO$_{2000}$	42.7	13.0	26.0

[a] Molecular weight determined by SEC (polystyrene standards)
[b] Number of side-arms calculated by NMR after separation *via* preparative SEC
[c] Theoretical M_w calculated by the sum of the molecular weight of the backbone and side-arms

Furthermore, the amphiphilic nature of the graft copolymer was evidenced by performing an LCxSEC analysis on an isolated species of the graft copolymer (Entry 4a – Figure V.8), separating the different polymers both on molecular weight and polarity. After the coupling of the hydrophilic PEO-acrylate side-arms to the hydrophobic P(nBA-co-TLA), a new signal can be observed with a clear shift in molecular weight. Additionally, an increase in dispersity can be observed (x-axis), as well as a shift in polarity from the hydrophobic P(nBA-co-TLA) backbone to the amphiphilic graft copolymer.

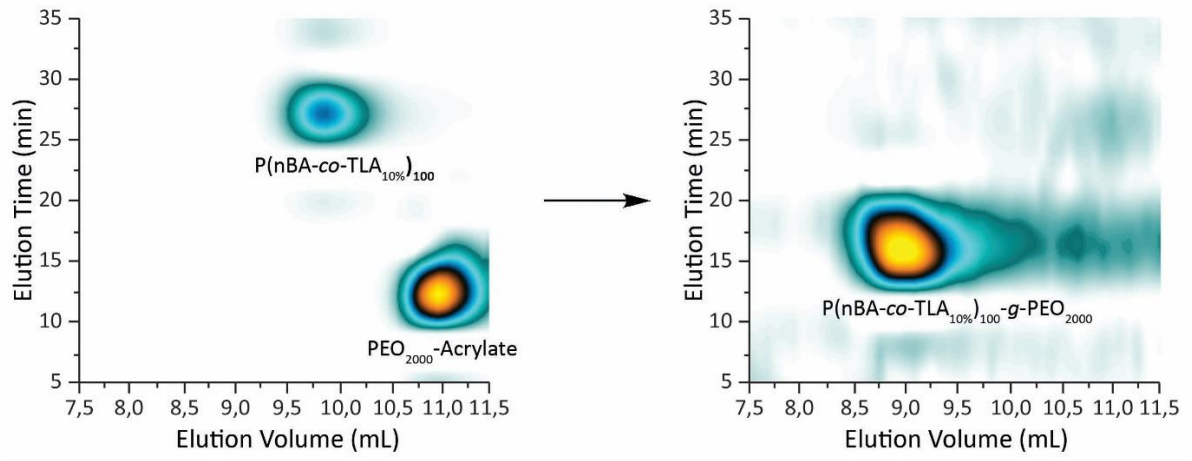

Figure V. 8: LCxSEC analysis of the isolated amphiphilic graft copolymer, evidencing the amphiphilic character of the structure *via* the shift in molecular weight and polarity.

V.3 Synthesis of amphiphilic toothbrush copolymers

V.3.1 Introduction

In a next stage, the synthesis of the amphiphilic toothbrush copolymers was carried out, materials which are known to exhibit improved stabilization behaviour as dispersing agents.[17] Again the grafting-onto strategy was used *via* the amine-thiol-ene conjugation reaction for the synthesis of the toothbrush copolymers. First, a block copolymer consisting of *tert*-butyl acrylate (*t*BA) as a protected hydrophilic first segment and a copolymer of nBA and TLA as a second segment was prepared in a one-pot procedure *via* Cu(0)-mediated RDRP, demonstrating the high end-group fidelity at high monomer conversion. Next, the hydrophobic side-chains, comprising of PnBA were synthesized separately. To enable the amine-thiol-ene conjugation, an acrylate functionality was introduced as an end-group onto the PnBA *via* a PPM reaction. The toothbrush copolymer was obtained by coupling the block copolymer and side-chains *via* the amine-thiol-ene conjugation strategy. Finally, the amphiphilic character of the complex macromolecular structure was introduced by the deprotection of the *t*BA with methyl sulphonic acid, yielding the poly(acrylic acid) segment (Figure V.9).

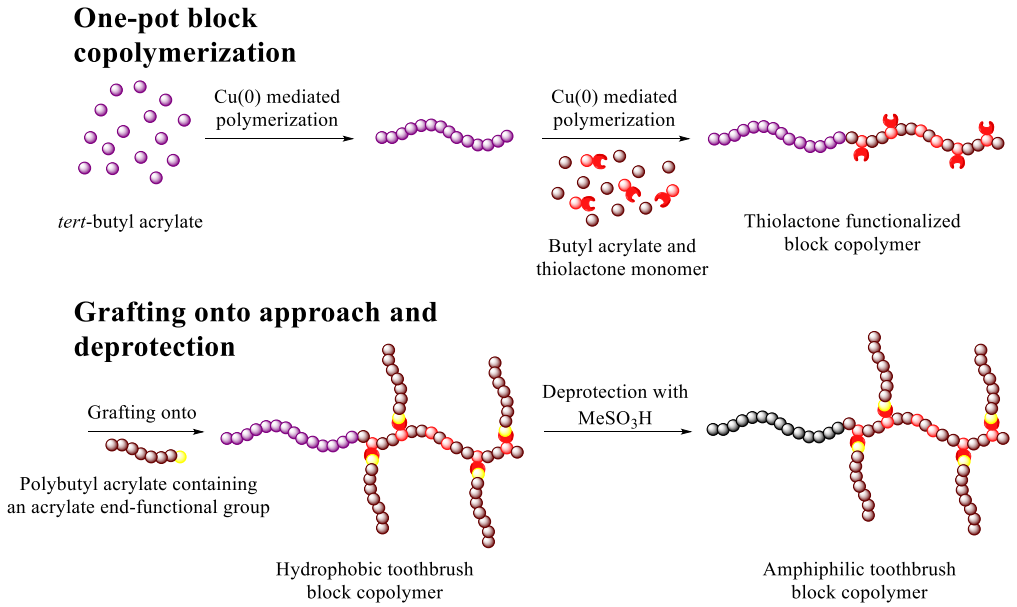

Figure V. 9: General synthetic strategy for the synthesis of amphiphilic toothbrush copolymers *via* amine-thiol-ene conjugation.

V.3.2 Synthesis of block copolymer

As mentioned, the first step in the design of the toothbrush copolymers is the synthesis of a block copolymer containing thiolactone functionalities in one of the two blocks. A Cu(0)-mediated polymerization system was again used due to the high end-group fidelities that can be obtained at high conversion, enabling a one-pot procedure of the synthesis of the block copolymer. For the hydrophilic block, *tert*-butyl acrylate was selected as a protected hydrophilic monomer, which can be easily hydrolyzed to acrylic acid using mild acidic conditions.

The synthesis was started by polymerizing *tert*-butyl acrylate for 8 hours to a near-quantitative conversion *via* a Cu(0)-mediated RDRP. Next, a mixture of butyl acrylate and the thiolactone-containing acrylate was added to the same reaction mixture in a one-pot procedure for the second block and the block copolymer was obtained after full monomer conversion (Figure V.10).

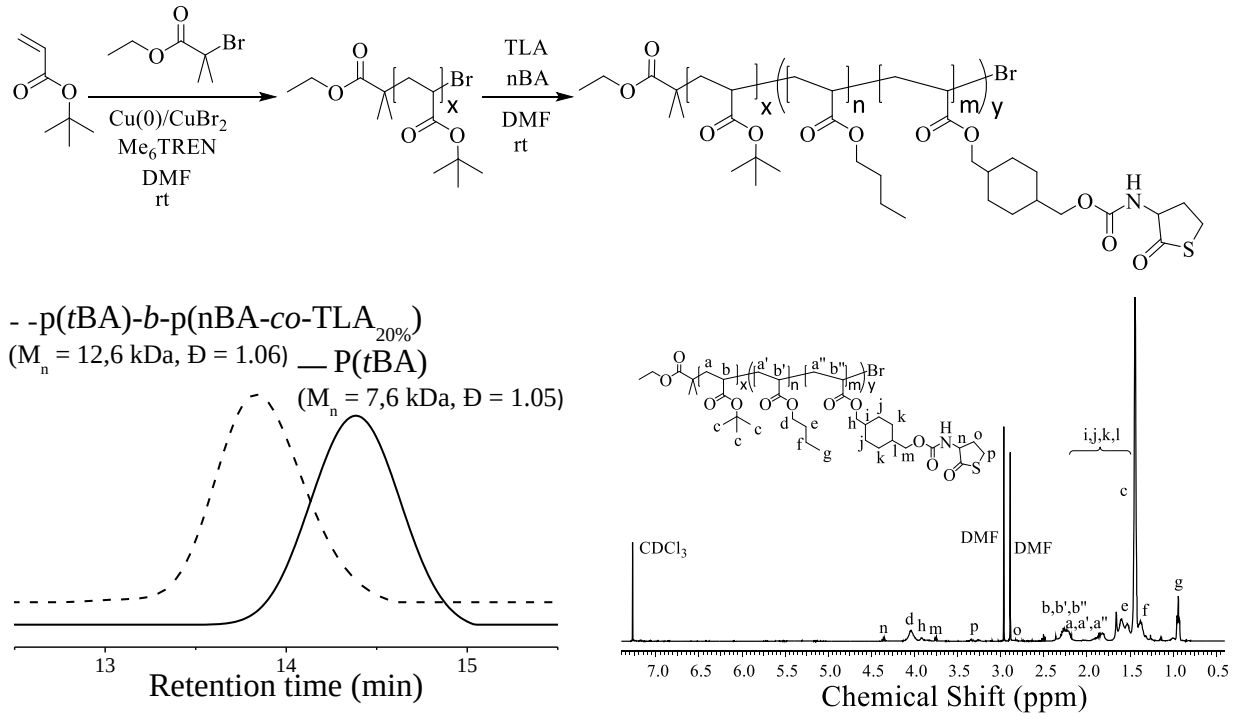

Figure V. 10: Synthesis of the hydrophobic TLA-functionalized block copolymer *via* one-pot block copolymerization and analysis *via* SEC and NMR.

From SEC analysis, a unimodal increase in molecular weight can be observed indicating the successful block copolymerization. As a model example, DP_s of 100 and 50 were targeted for P(*t*BA) and the copolymer respectively. Furthermore, two different block copolymers were synthesized containing 10 and 20 mol% of thiolactone units and the resulting concentration of thiolactone-units in the different block copolymers was calculated from NMR by comparing the signal of the thiolactone unit at 3.25 ppm with the signal of butyl acrylate at 0.9 ppm (Table V.3).

Table V. 3: Overview of the different block copolymers synthesized *via* Cu(0)-mediated CRP.

Entry	Block copolymer	M_n (kDa) (Đ[a])	Experimental % TLA[b]
1b	P(*t*BA)-*b*-P(nBA-*co*-$TLA_{10\%}$)	11.3 (1.07)	12.5
2b	P(*t*BA)-*b*-P(nBA-*co*-$TLA_{20\%}$)	12.6 (1.06)	22.6

[a] Molecular weights and dispersities determined by SEC (polystyrene standards).
[b] Experimental incorporation of thiolactone in copolymer calculated from NMR-analysis.

V.3.3 Synthesis of PnBA-Acry side-arms

Regarding the synthesis of the hydrophobic side-arms, polybutyl acrylate containing an acrylate end-group (PnBA-Acry) was synthesized. First PnBA was obtained *via* a Cu(0)-mediated polymerization, ensuring a high end-group fidelity of the bromine-functionality.[51] Next, to apply PnBA in the amine-thiol-ene conjugation, the bromine end-group was transformed into an acrylate functionality (Figure V.11).

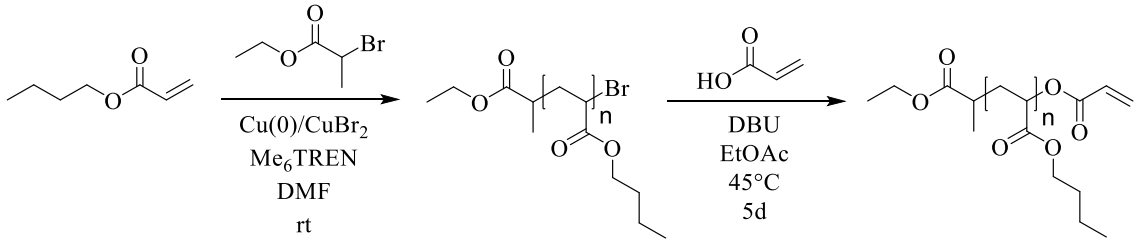

Figure V. 11: Synthetic strategy for the synthesis of the PnBA-Acry side-arms.

A kinetic study of the Cu(0)-mediated polymerization of butyl acrylate was performed to evidence the controlled nature of the polymerization by taking samples during the polymerization at regular time intervals. The molecular weight and dispersity were determined *via* SEC analysis. Furthermore, the conversion was calculated by GC measurements. A linear relation between conversion and molecular weight can be observed, this in combination with the dispersity decreasing with increasing conversion, evidences the controlled nature of the polymerization (Figure V.12). Furthermore, two different DP's of the PnBA were targeted (DP of 20 and 40) to investigate the influence of the length on the characteristics as toothbrush dispersant.

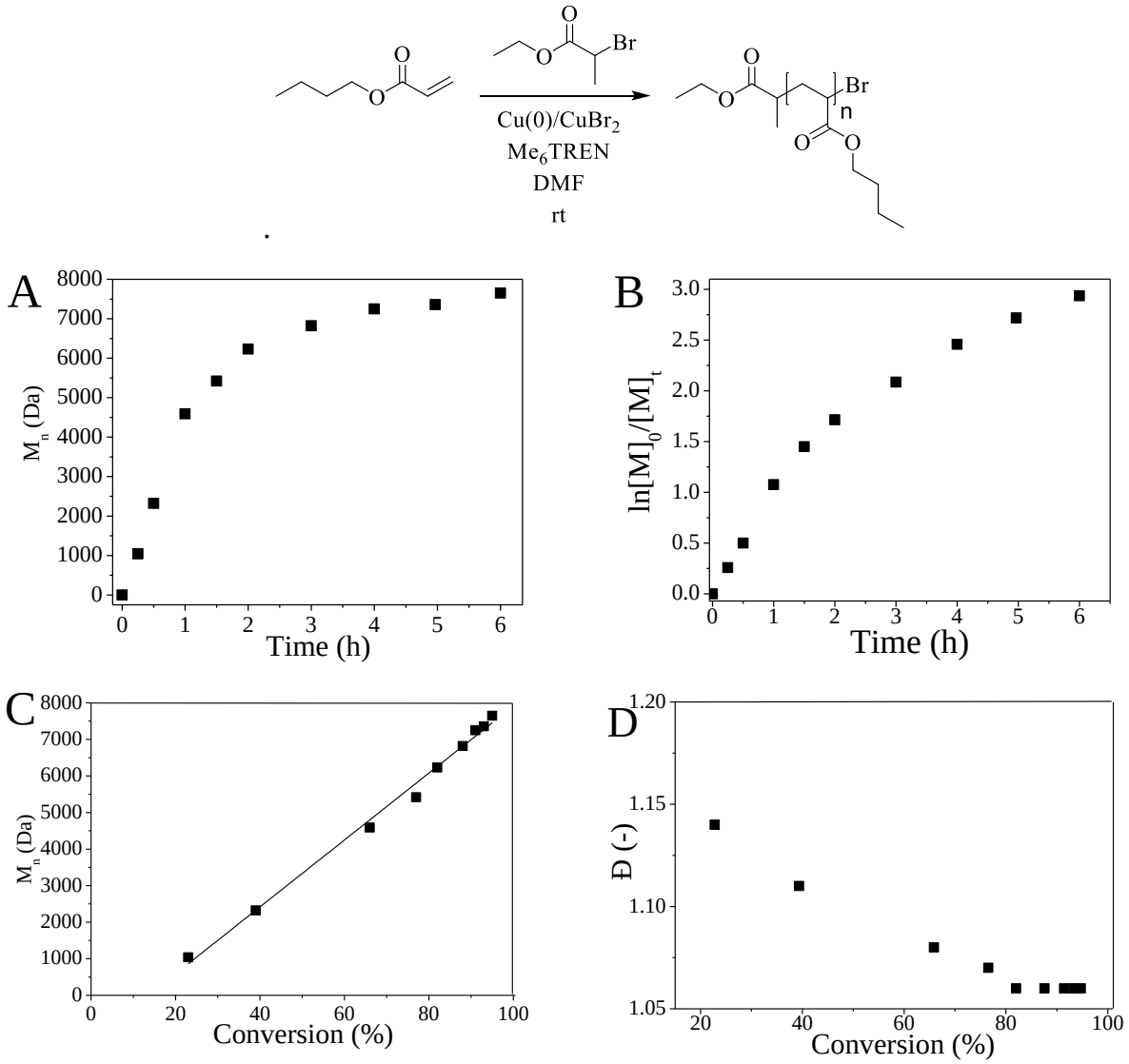

Figure V. 12: Synthesis and kinetic data for the Cu(0)-mediated polymerization of butyl acrylate: molecular weight as a function of time (A); first order kinetic plot (B); molecular weight as a function of conversion (C) and dispersity as a function of conversion (D).

Next, to apply the PnBA chains as side-arms in the amine-thiol-ene conjugation, the bromine end-group needs to be transformed into an acrylate moiety. Conditions for this modification reaction were obtained by adapting a literature procedure, using acrylic acid and 1,8 diazabicyclo[5.4.0]undec-7-ene (DBU) as base catalyst.[52] Finally, the outcome of the modification reaction was analyzed *via* SEC, ^{1}H-NMR and MALDI-TOF analysis (Figure V.13).

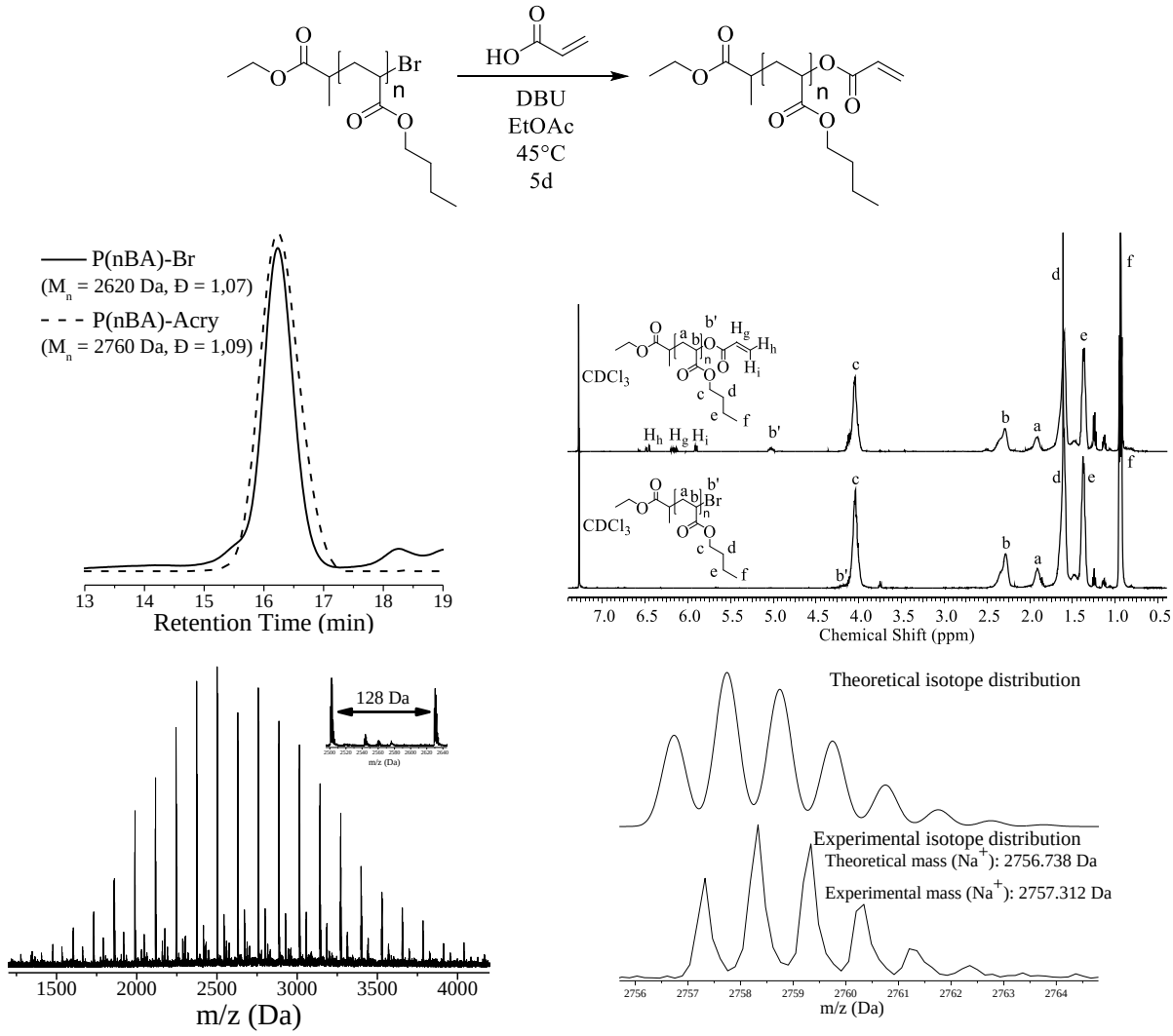

Figure V. 13: Synthesis of P(nBA) witn an acrylate end-functionality as hydrophobic side-chain and analysis of the modification reaction by SEC, ^{1}H-NMR and MALDI-TOF analysis.

From SEC-analysis, a small unimodal increase in molecular weight was observed after the modification reaction. Furthermore, from ^{1}H-NMR analysis, it was observed that the small signal of the bromine end-group at 4.25 ppm disappeared (signal b'). Additionally, the signals of the

acrylate moiety between 5.75 and 6.5 ppm appeared as well as the signal of proton next to the acrylate end group at 5 ppm. Final proof was provided by MALDI-TOF analysis as no remaining signals of the starting material were visible and the experimental mass values were in good agreement with the theoretical ones. The signal at 2556.57 Da can be explained by elimination of the end group, while no explanation could be provided for the other distributions. Finally, the experimental isotope distribution was in good agreement with the theoretical one, since the removal of the bromine will induce a significant change in the isotopic pattern in MALDI-TOF analysis, due to the presence of the two abundant stable isotopes (^{79}Br and ^{81}Br) as already described in chapter 4.

V.3.4 Grafting onto

To obtain the toothbrush copolymers, the amine-thiol-ene conjugation was applied in the same manner as for the synthesis of the graft copolymers. Propylamine, as small amine and the hydrophobic P(nBA) side-chains, containing the acrylate end group, were added in equimolar conditions to the thiolactone functionalized block copolymer P(*t*BA)-*b*-P(nBA-*co*-TLA) and the reaction outcome was analyzed *via* SEC- and NMR-analysis (Figure V.14). From SEC analysis, a large extent of coupling was observed in combination with an amount of unreacted P(nBA)-arms. No explanation could be provided for the presence of the block copolymer. Again, a broad distribution of the toothbrush copolymer was observed, attributed to the different degrees of coupling of the side-chains as observed by Keul and coworkers.[38] The vertical dotted line indicates the separation by preparative SEC afterwards.

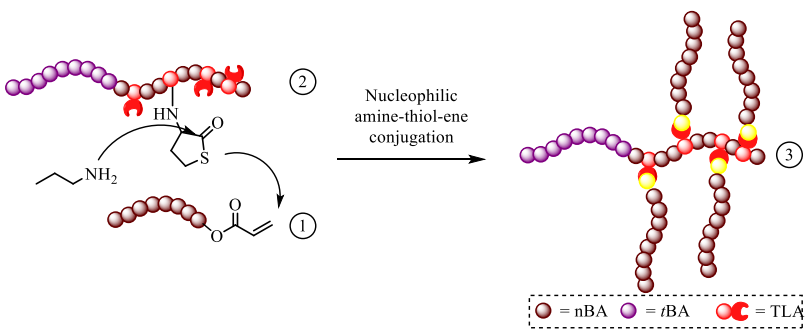

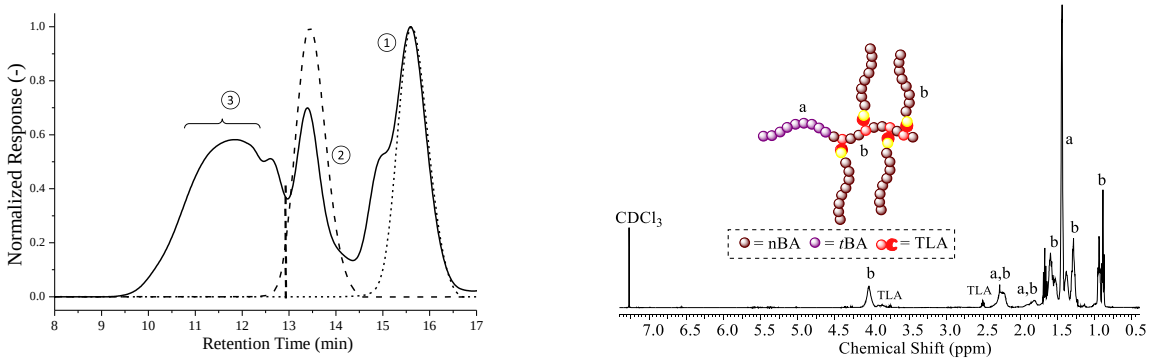

Figure V. 14: Synthetic strategy, SEC and ^{1}H-NMR analysis of the toothbrush copolymer consisting of the P(*t*BA)-*b*-P(nBA-*co*-TLA) block copolymer and the hydrophobic PnBA-acrylate.

Next, a variety of different toothbrush copolymers with different molecular weight (PnBA side-arm) and grafting density (TLA-content) were synthesized (Table V.4) and analyzed *via* SEC and ^{1}H-NMR analysis. The average number of grafts was calculated by determining the increase in ratio of the signal of butyl acrylate at 0.9 ppm compared to the signal of *tert*-butyl acrylate at 1.4 ppm.

Table V.4: SEC-results of the graft copolymers *via* the amine-thiol-ene reaction between the hydrophobic P(*t*BA)-*b*-P(nBA-*co*-TLA) block copolymers and PnBA-Acry.

Entry	Toothbrush copolymer	M_p (kDa)[a]	Aver. Grafts[b]	Theo. M_w (kDa)[c]
1b-tb	P(*t*BA)-*b*-(P(nBA-*co*-TLA$_{10\%}$)-*g*-P(nBA)$_{20}$)	129.7	5.1	14.1
2b-tb	P(*t*BA)-*b*-P(nBA-*co*-TLA$_{10\%}$)-*g*-P(nBA)$_{40}$)	145.4	4.7	23.9
3b-tb	P(*t*BA)-*b*-P(nBA-co-TLA$_{20\%}$)-*g*-P(nBA)$_{20}$)	136.2	7.9	21.8

[a] Molecular weight determined by SEC (polystyrene standards).
[b] Number of side-arms calculated by NMR after separation *via* preparative SEC.
[c] Theoretical M_w calculated by the sum of the molecular weight of the backbone and side-arms

V.3.5 Deprotection of the tBA

The final step in the synthetic strategy of the toothbrush copolymers is the deprotection of the *tert*-butyl ester in the side chain. Typical procedures for this reaction describe the use of HCl in dioxane.[53] Despite the success of this established method, it is not compatible with polymeric structures containing PnBA, which is also prone to hydrolysis under these circumstances. Therefore, an *in-house* developed procedure was applied, using methyl sulphonic acid ($MeSO_3H$) in DCM. The hydrolysis will occur *via* the same mechanism, but by the use of milder

reaction conditions. To facilitate analysis and to be able to adjust the correct amounts of acid added to the polymer solution, a purification step by preparative SEC was applied before the acid treatment. Finally, NMR analysis confirmed the full removal of the *tert*-butyl group, while the signals from the PnBA segments remained unaltered. Additionally, SEC analysis of the purified deprotected toothbrush copolymer displayed a small shift in hydrodynamic volume as a result of the transformation of the backbone structure (Figure V.15).

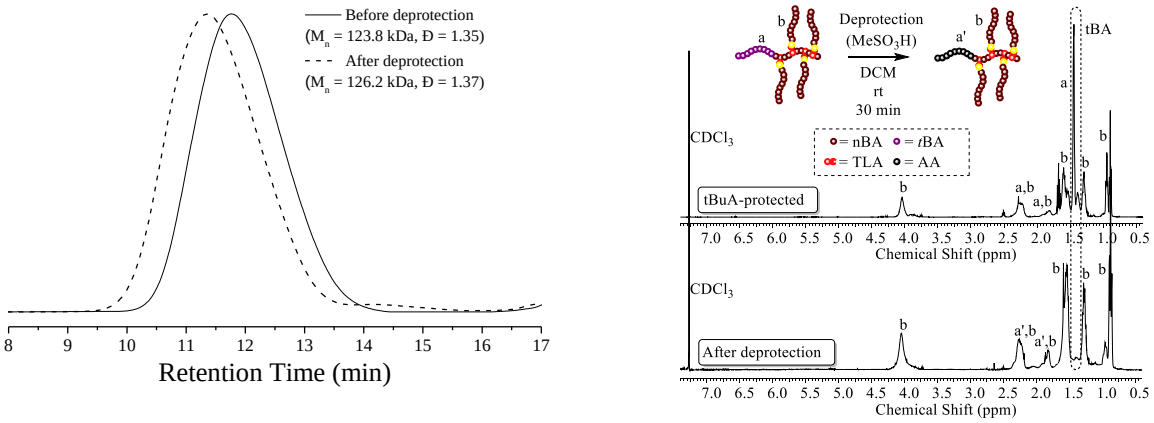

Figure V. 15: Deprotection of P(*t*BA)-*b*-(P(nBA-*co*-TLA$_{10\%}$)-*g*-P(nBA)$_{20}$) after preparative SEC in THF, yielding P(AA)-*b*-(P(nBA-*co*-TLA$_{10\%}$)-*g*-P(nBA)$_{20}$) and analysis by NMR and SEC.

V.4 Characterization of the amphiphilic graft and toothbrush copolymers

V.4.1 Introduction

One of the many important, industrially relevant applications of amphiphilic polymeric structures is their use as stabilizers in pigment dispersions. Their implementation enables the mixing of hydrophobic particles in water, creating aqueous dispersions which can be applied in paint industries. The application of these macromolecular architectures enables the long-term stabilization of these dispersed materials. The different graft- and toothbrush copolymers described in this paper were analyzed by dynamic light scattering (DLS) and pigment stabilization tests to determine and compare their structure-property relationships.

V.4.2 Dynamic Light Scattering

By measuring the rate at which the intensity of scattered light fluctuates, Dynamic Light Scattering (DLS) as a technique is able to determine the size of particles due to the particle movement. When the laser light of the DLS hits the small particles, the light will be scattered in all directions (Rayleigh scattering). Due to the constant change in distance between the particles in time, the constructive and destructive interference of the scattered light will vary. Therefore, indirectly, DLS is a technique that determines the Brownian motion of particles which is related to the size of these particles. The larger the particle, the slower the Brownian motion. It has to be noted that this technique incorporates the assumption of spherical particles which indirectly introduces an error when measuring more complex polymer structures. Still, interesting information can be obtained *via* this technique for the analysis of the obtained complex polymer structures (Table V.5).

Concerning the graft copolymers, it was observed that the hydrodynamic diameter increased from 60 to 240 nm when larger side-chains were applied (PEO_{480} vs. PEO_{2000}) and when the grafting density increased (5-10-20%) (Figure V.16 – A). Regarding the toothbrush copolymers, rather high hydrodynamic volumes and polydispersities (PDI) were measured, even after testing different sample preparation methods. This is most probably due to secondary aggregation as a second decay at higher correlation delay time can be observed corresponding to the presence of larger aggregates in each of the measurements, which was not visible in the analysis of the graft copolymers (Figure V.16 – B).[54, 55]

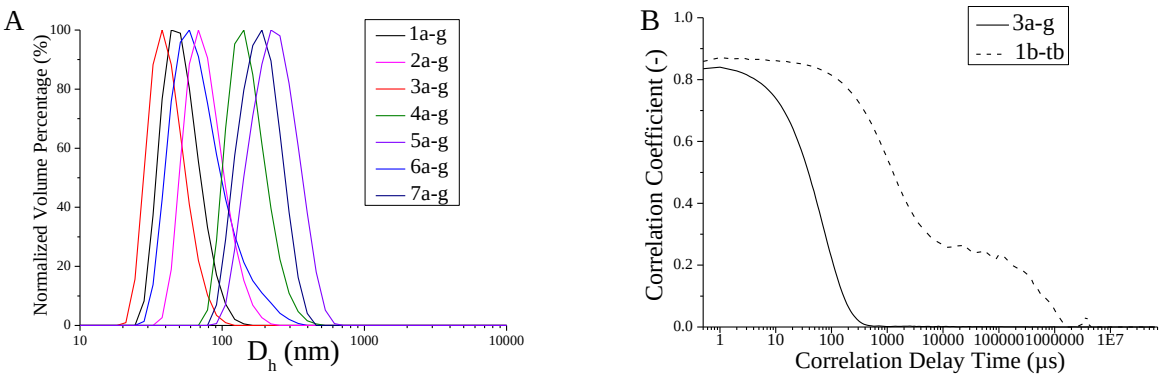

Figure V. 16: Hydrodynamic sizes of the different graft copolymers in water (A); correlation data of a graft- and toothbrush copolymer (B).

Table V. 5: DLS-results of the purified graft copolymers in water.

Entry	Polymer[a]	D_h (nm)	PDI
1a-g	P(nBA-*co*-TLA$_{5\%}$)-*g*-PEO$_{480}$	61 (± 5)	0.078
2a-g	P(nBA-*co*-TLA$_{5\%}$)-*g*-PEO$_{2000}$	79 (± 10)	0.097
3a-g	P(nBA-*co*-TLA$_{10\%}$)$_{100}$-*g*-PEO$_{480}$	49 (± 5)	0.073
4a-g	P(nBA-*co*-TLA$_{10\%}$)$_{100}$-*g*-PEO$_{2000}$	121 (± 10)	0.081
5a-g	P(nBA-*co*-TLA$_{10\%}$)$_{200}$-*g*-PEO$_{2000}$	238 (± 20)	0.105
6a-g	P(nBA-*co*-TLA$_{20\%}$)-*g*-PEO$_{480}$	93 (± 10)	0.184
7a-g	P(nBA-*co*-TLA$_{20\%}$)-*g*-PEO$_{2000}$	181 (± 15)	0.082

[a] Polymer structures were purified by prep-SEC, prior to analysis by DLS.

V.4.3 Dispersion tests

The amphiphilic graft and toothbrush copolymers have been applied to stabilize dispersions of copper phtalocyanine (CuPc) as a well-known hydrophobic pigment in water (Figure V.17 – top left). In both cases, the hydrophobic backbone of the copolymer structure will adhere onto the particle, while the hydrophilic side chains prevent the flocculation of the particles by steric and/or electronic repulsion. For the pigment stabilization tests, a literature procedure was applied in which copolymer solutions in water were prepared (5 wt.-%) and added to the hydrophobic pigment (1 wt.-%).[56] The solubilization of the pigment particles was induced by applying an ultrasonic treatment and stirring at a high sheer rate (700 rpm), obtaining a dark blue pigment solution as indicated by visual inspection and UV-Vis analysis (Figure V.16). The stability of the different dispersions was analyzed by determining the half-time of sedimentation, or the required period of time in which the dispersion boundary between the turbid and transparent zone reaches 50% of its initial height (Table V.6).

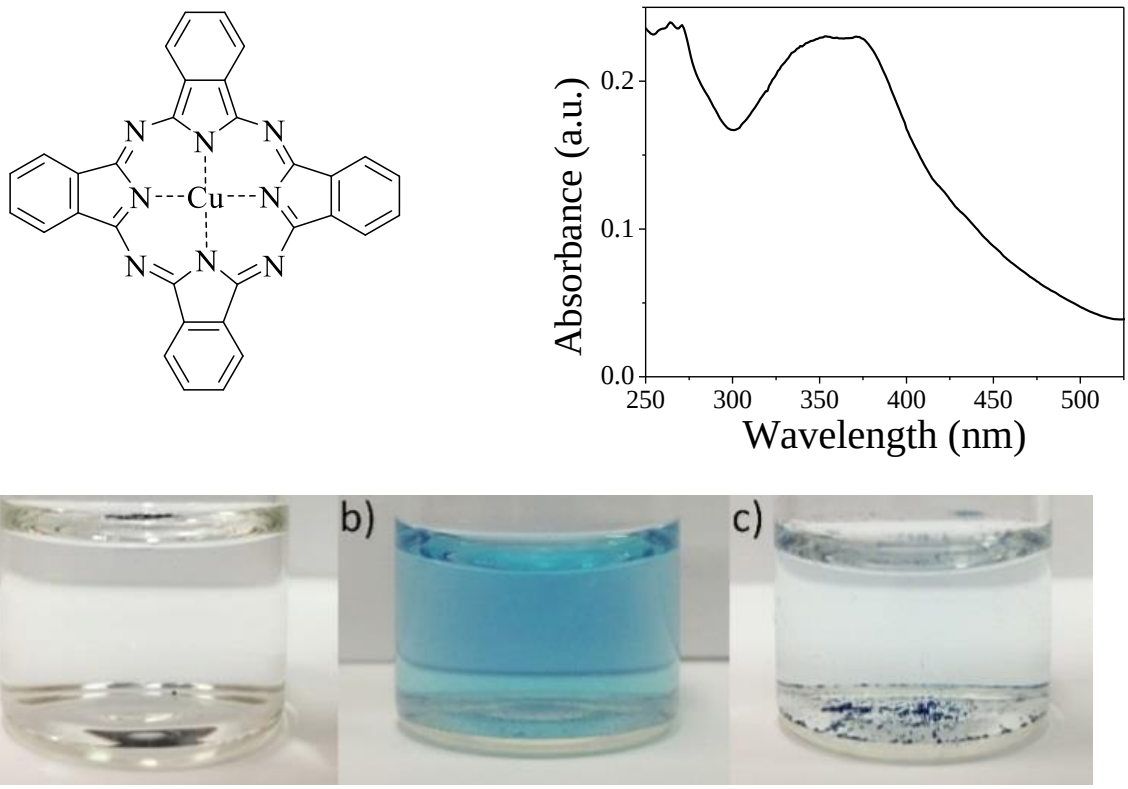

Figure V. 17: Copper phtalocyanine applied in the pigment stabilization tests (top - left), UV-Vis absorbance spectrum of CuPc stabilized by P(nBA-*co*-TLA$_{5\%}$)-*g*-PEO$_{2000}$ in water (top - right), visual confirmation of the formation of stable pigment dispersions (bottom): (a) the pigment floating in water without any copolymer added, (b) a stable pigment dispersion, (c) sedimentation of the pigment dispersion after 30 days.

In general, it was observed that the half-time of sedimentation ($\tau/2$) increased when toothbrush copolymers were applied (> 30 days) in comparison to the corresponding graft copolymers (3 to 30 days). Comparison of the graft copolymers demonstrated an improved stability when longer side-chains were introduced (PEO_{480} vs. PEO_{2000}), creating more steric stabilization or when higher grafting densities were applied (5% vs. 10%). Regarding the toothbrush copolymers, no significant change was observed between 10 and 20% of grafting density. However, when longer side-chains were applied (DP40 vs. DP20), a small decrease of $\tau/2$ was observed, probably due to steric hindrance between the brushes, which are in close proximity on the hydrophobic pigment particle. Additionally, it was observed that the deprotection of *t*BA to the corresponding acid was crucial for the stabilization of the pigment particles as the unprotected hydrophobic toothbrush-copolymer was unable to properly stabilize the pigment particles (entry 2b-tb). Finally, the stability of the pigment particles was confirmed by TEM-analysis, the solution was frozen directly after dissolving the polymer in water and defrosted right before TEM-analysis.

Average particle sizes of about 140 nm in case of the graft copolymers (entry 4a-g) and 170 nm for the toothbrush structures (entry 2b-tb) were measured of a solution.

Table V. 6: Sedimentation stability (τ/2) of the CuPc aqueous dispersions stabilized by the graft- and toothbrush copolymers.

Entry	Polymer[a]	τ/2 (days)
1a-g	P(nBA-*co*-TLA$_{5\%}$)-*g*-PEO$_{480}$	3
2a-g	P(nBA-*co*-TLA$_{5\%}$)-*g*-PEO$_{2000}$	15
3a-g	P(nBA-*co*-TLA$_{10\%}$)$_{100}$-*g*-PEO$_{480}$	6
4a-g	P(nBA-*co*-TLA$_{10\%}$)$_{100}$-*g*-PEO$_{2000}$	28
5a-g	P(nBA-*co*-TLA$_{10\%}$)$_{200}$-*g*-PEO$_{2000}$	25
6a-g	P(nBA-*co*-TLA$_{20\%}$)-*g*-PEO$_{480}$	7
7a-g	P(nBA-*co*-TLA$_{20\%}$)-*g*-PEO$_{2000}$	26
1b-tb	P(AA)-*b*-(P(nBA-*co*-TLA$_{10\%}$)-*g*-P(nBA)$_{20}$)	36
2b-tb	P(AA)-*b*-(P(nBA-*co*-TLA$_{10\%}$)-*g*-P(nBA)$_{40}$)	31
2b-tb*	P(*t*BA)-*b*-(P(nBA-*co*-TLA$_{10\%}$)-*g*-P(nBA)$_{40}$)	< 1
3b-tb	P(AA)-*b*-(P(nBA-*co*-TLA$_{20\%}$)-*g*-P(nBA)$_{20}$)	34

[a] Polymer structures were purified by prep-SEC, prior to the pigment stabilization test.

V.5 Conclusions

This chapter described the development of a new grafting-onto methodology for the synthesis of two different complex polymeric architectures, being graft and toothbrush structures. A combination of a Cu(0)-mediated RDRP and thiolactone chemistry turned out to be successful for the synthesis of these amphiphilic materials. Regarding the synthesis of the grafts, a series of copolymers containing butyl acrylate and a varying amount of a thiolactone-acrylate based monomer were synthesized. Next, the graft copolymer was obtained by coupling of the functionalized backbone with PEO-acrylate. For the synthesis of the toothbrush structures, a series of different block copolymerizations of *tert*-butyl acrylate as protected hydrophilic segment, a copolymer of butyl acrylate and varying amounts of the thiolactone acrylate as second segment were performed in a one-pot procedure. The hydrophobic side-arms, consisting

of poly(butyl acrylate), were synthesized separately, introducing the acrylate end-functionality through a PPM step. The final toothbrush structure was obtained by amine-thiol-ene conjugation and the amphiphilic character was introduced by the deprotection of the *tert*-butyl group to the corresponding acrylic acid with methyl sulphonic acid. Finally, the material properties were analysed by DLS and pigment stabilization tests. In DLS, it was observed that the hydrodynamic volume of the graft copolymers increased when larger side-chains were applied and with increasing grafting density. In case of the toothbrush structures, rather high hydrodynamic volumes and dispersities were measured, most probably due to secondary aggregation behaviour leading to undefined geometries. For the pigment stabilization tests, toothbrush structures turned out to exhibit increased stabilizing features compared to the corresponding graft copolymers, due to their specific stabilization mechanism.

In general, it can be concluded that the combination of Cu(0)-mediated RDRP and thiolactone chemistry turned out to be a powerful combination for the synthesis of sophisticated amphiphilic copolymers for dispersing applications.

V.6 Experimental part

V.6.1 Methods

^{1}H NMR

^{1}H- and ^{13}C-NMR (APT, HSQC, COSY) spectra were recorded in $CDCl_3$ on a Bruker AM500 spectrometer (500 MHz or 125 MHz for ^{1}H or ^{13}C respectively) or on a Bruker Avance 300 (300 MHz or 75 MHz for ^{1}H or ^{13}C respectively). Chemical shifts are presented in parts per million (δ) relative to $CDCl_3$ (7.26 ppm in ^{1}H- and 77.23 ppm in ^{13}C-NMR respectively) as internal standard. Coupling constants (*J*) in ^{1}H-NMR are given in Hz. The resonance multiplicities are described as *d* (doublet), *t* (triplet) or *m* (multiplet).

LC-MS

An Agilent technologies 1100 series LC/MSD system equipped with a diode array detector and single quad MS detector (G1946C) with an electrospray source (ESI-MS) was used for classic reversed phase LC-MS. Analytic reversed phase HPLC was performed with a Phenomenex Kinetex C_{18} column (5 µ, 150 x 4.6 mm) using a solvent gradient (0 → 100% acetonitrile in H_2O in 15 min) and the eluting compounds were detected *via* UV-detection (λ = 214 nm). High resolution mass spectra (HRMS) were collected using an Agilent 6220A time-of-flight (TOF) equipped with a multimode ionization (MMI) source.

SEC

Size Exclusion Chromatography (SEC) was performed using a Varian PLGPC50plus instrument, using a refractive index detector, equipped with two Plgel 5 µm MIXED-D columns 40 °C. Polystyrene standards were used for calibration and THF as eluent at a flow rate of 1 mL/min. Samples were injected using a PL AS RT autosampler. The preparative SEC system consists of a Shimadzu LC-2OAT pump, a Shimadzu SIL-IOAF autosampler, a RID-IOA Differential Refractive Index Detector, a FRC-1OA Fraction Collector, CBM-2OA PC Interface/System Controller. Software is LC solutions including LC solutions SEC software. Columns are originating from Shodex: a K-LG guard column and a KF-2004 prep column (elution 2.5 mL/min, THF, rt).

LCxSEC

For two-dimensional liquid chromatography, sample fractions from the first dimension were transferred to the second-dimension column via an electronically controlled eight-port valve system (VICI Valco instruments, Houston, TX, USA), equipped with two 100 µL sample loops. The second dimension consisted of an Agilent Infinity 1260 isocratic pump and a PSS SDV LIN M 5 µm column. Detection in the second dimension was accomplished by using an ELSD. Nitrogen was used as carrier gas in the ELSD at a flow rate of 2.5 L/min. Spray Chamber, Drift Tube and Optical Cell temperatures were set at 30 °C, 80 °C and 70 °C, respectively. The flow rates used in the first and second dimensions were 0.02 mL/min and 5 mL/min, respectively. Sample concentrations were between 0.25 and 2.0 mg/mL. an isocratic elution of methanol/hexane (70/30) was used as the solvent for the first dimension, THF was used as the solvent for the second dimension analysis. Data were recorded using PSS WinGPC Unichrom software.

MALDI-TOF

Matrix Assisted Laser Desorption Ionisation – Time of Flight (MALDI-TOF) was performed on an Applied Biosystems Voyager De STR MALDI-TOF spectrometer equipped with 2 m linear and 3 m reflector flight tubes, a nitrogen laser operating at 337 nm, pulsed ion extraction source and reflectron. All mass spectra were obtained with an accelerating potential of 20 kV in positive ion mode and in reflector mode. In case of the analysis of PEO, dithranol (10 mg/mL in THF) was used as matrix, sodium trifluoroacetate (1 mg/mL) was used as cationizing agent, and polymer samples were dissolved in THF (10 mg/mL). Polymer solutions were prepared by mixing 8 µL of the matrix, 1 µL of the salt and 1 µL of the polymer solution. Subsequently 0.5 µL of this mixture was spotted on the sample plate, and the spots were dried in air at room temperature. Regarding the analysis of poly(butyl acrylate), dithranol (25 mg/mL in THF), sodium iodide (20 mg/mL in THF), and polymer samples were dissolved in THF (5 mg/mL). Polymer solutions were prepared by mixing 10 µL of the matrix, 5 µL of the salt and 5 µL of the polymer solution. Subsequently, 0.5 µL of this mixture was spotted on the sample plate, and the spots were dried in air at room temperature. PEO 2000 was used for calibration. All data were processed using the Data Explorer 4.0.0.0 (Applied Biosystems) software package.

GC

GC was performed on an Agilent 7890A system equipped with a VWR Carrier-160 hydrogen generator and an Agilent HP-5 column of 30 m length and 0.320 mm diameter. An FID detector was used and the inlet was set to 240 °C with a split injection ratio of 25 : 1. Hydrogen was used as the carrier gas at a flow rate of 2 mL/min . The oven temperature was increased at 20 °C/min from 50 °C to 120 °C, followed by a ramp of 50 °C/min to 150 °C.

DLS

Dynamic light scattering (DLS) was performed on a Zetasizer Nano-ZS Malvern apparatus (Malvern Instruments Ltd) using disposable cuvettes. The excitation light source was a He−Ne laser at 633 nm, and the intensity of the scattered light was measured at 173°. This method measures the rate of the intensity fluctuation and the size of the particles is determined through the Stokes−Einstein equation. 1 mg of PEO-NH_2 (800 Da) multi-segmented block copolymer was dissolved in 0.1 mL and precipitated in 1 mL H_2O, subsequently the polymer solution was heated at 40°C for 24h to evaporate THF, filtered through Millipore membranes with pore sized of 0.2 µm prior to measurement.

UV-VIS

UV-Vis absorption was performed with a Specord 200 from Analityk Jena from 200 nm to 600 nm with a speed of 5 nm/s, a slit of 2nm and $\Delta\lambda = 0.1$ nm.

TEM

Transmission Electron Microscopy (TEM) analysis was performed using a JEM-2200FS FEG-TEM (Jeol), operatured at 200 keV and equipped with an in-column omega filter to reduce chromatic aberration.

V.6.2 Materials

Chloroform-D ([865-49-6], ≥ 99.8 %) was purchased from Euro-isotop. Triethylamine ([121-44-8], 99 %) was purchased from Acros Organics and dried in a solvent purification system (J.C.

Meyer). Acryloyl chloride ([814-68-6], 96%, stabilized with 400 ppm phenothiazine) was purchased from ABCR. Acrylic acid ([79-10-7], 99 %) was distilled prior to use, allylamine ([107-11-9], ≥ 99.9 %), aluminium oxide ([1344-28-1], basic), benzylamine ([100-46-9], ≥ 99.5 % chloroform ([865-49-6], ≥ 99.8 %), Cu(0)-pellets ([7440-50-8], ≥ 99.9%), Cu(II)Br_2 (([7789-45-9], 99 %), 1,8-diazabicyclo[5.4.0]undec-7-ene ([6674-22-2], 98 %), 1,2-dichlorobenzene ([95-50-1], 99%), dichloromethane ([75-09-2], ≥ 99.8 %) was dried in a solvent purification system (J.C. Meyer), *N*,*N*-dimethylformamide ([68-12-2], ≥ 99 %), ethyl acetate ([141-78-6], 99.8 %), ethyl α-bromoisobutyrate ([600-00-0], 98 %), ethyl 2-bromopropionate ([535-11-5, 99 %), methyl sulphonic acid ([75-75-2], ≥ 99.5 %), methyl acrylate ([96-33-3], 99 %), *n*-octylamine ([111-86-4], 99 %), phenothiazine ([92-84-2], ≥ 98 %), polyethyleneoxide-2000 (PEO) ([9004-74-4]), propylamine ([107-10-8], 99+ %), *tert*-butyl acrylate ([1663-39-4], 98 %), tetrahydrofuran (THF, [109-99-9], ≥ 99 %, stabilized with butylated hydroxytoluene) were purchased from Sigma Aldrich and used without purification. Me_6TREN and the thiolactone-containing acrylate (TLA) were synthesized according to literature procedures.[43, 57]

V.6.3 Synthesis

Synthesis of the P(nBA-co-TLA) copolymer

2 mL butyl acrylate (13.95 mmol, 90 eq.), 529.20 mg TLA (0.15 mol, 10 eq.), 3.75 mL DMF, Cu(0) (20 pellets), 28.06 mg ethyl 2-bromopropionate (0.16 mmol, 1 eq.) were weighed into a flask and degassed for 30 minutes with a continuous argon purge. In a separate vial, 1.73 mg Cu(II)Br_2 (7.75 µmol, 0.05 eq.), 4.29 mg Me_6TREN (0.02 mmol, 0.12 eq.) and 2 mL DMF were degassed separately via argon bubbling for 30 minutes. The reaction was started by the addition of the Cu(II)Br_2/ligand-solution to the reaction mixture at room temperature. Samples of the reaction mixture were taken for GC and SEC analysis, samples for GC analysis were dissolved in THF with phenothiazine as radical inhibitor (1,2-dichlorobenzene as internal standard), while samples for SEC analysis were diluted with THF, then passed over a basic alumina column to remove metal salts. After 6 hours, the reaction mixture was diluted with THF and filtered over a column of basic Al_2O_3 to remove the copper catalyst. After evaporating the excess solvent, the

product was poured into a beaker and placed into the vacuum oven overnight to remove traces of monomer and residual solvent. The final polymer was obtained as a yellowish oil. Polymers with 5 and 20 mol% TLA were synthesized accordingly as those with a DP of 200 with 10 mol% thiolactone content.

Synthesis of the P(tBA)-b-P(nBA-co-TLA) copolymer

2 mL tert-butyl acrylate (13.65 mmol, 100 eq.), 1.55 mL DMF, Cu(0) (20 pellets) and 26.63 mg ethyl 2-bromoisobutyrate (0.137 mmol, 1 eq.) were weighed into a flask and degassed for 30 minutes with a continuous argon purge In a separate vial, 1.53 mg Cu(II)Br_2 (6.83 µmmol, 0.05 eq.), 3.77 mg Me_6TREN (0.02 mmol, 0.12 eq.), and 1 mL DMF were degassed separately via argon bubbling for 30 minutes. The reaction was started by the addition of the Cu(II)Br_2/ligand solution to the reaction mixture at room temperature. After 8 hours at near-quantitative conversion, a mixture of 0.88 mL butyl acrylate (6.14 mmol, 45 eq.) and 233.08 mg TLA (0.68 mmol, 5 eq.) in 2.53 mL DMF was prepared, degassed for 30 minutes with a continuous argon purge and added to the reaction mixture and the reaction proceeded overnight. Finally, the reaction mixture was diluted with THF and filtered over a column of basic Al_2O_3 to remove the copper catalyst. After evaporating the excess solvent, the product was poured into a beaker and placed into the vacuum oven overnight to remove traces of monomer and residual solvent. The final polymer was obtained as a yellowish oil. A polymer with 20 mol% TLA was synthesized accordingly.

Synthesis of PEO-Acrylate

PEO (M_n = 2000 Da; 2,50 mmol; 5,00 g) was azeotropically dried over toluene. Dried PEO was dissolved in dry DCM (0,5 M; 5,00 ml), stirred under Ar and cooled for 30 minutes in an ice-bath. Dry Et_3N (5,00 mmol; 0,700 ml) was added to the reaction mixture. Next, acryloyl chloride (5,00 mmol; 0,410 ml) was added dropwise and the reaction proceeded overnight at room temperature. The reaction mixture was filtered over silica, the filtrate was collected and a radical inhibitor was added. Solvent was partially evaporated and the remaining solution was

precipitated in cold diethyl ether. The precipitated product was filtered over the residue was collected as a yellowish powder. ^{1}H-NMR, SEC and MALDI-TOF analysis was performed.

Synthesis and end-group modification of PnBA-acrylate

2 mL butyl acrylate (13.95 mmol, 20 eq.), 1.65 mL DMF, Cu(0) (20 pellets) and 126.36 mg ethyl 2-bromopropionate (0.698 mmol, 1 eq.) were weighed into a flask and degassed for 30 minutes with a continuous argon purge. In a separate vial, 7.79 mg Cu(II)Br_2 (0.035 mmol, 0.05 eq.), 19.35 mg Me_6TREN (0.035 mmol, 0.12 eq.) and 1 mL DMF were degassed separately via argon bubbling for 30 minutes. The reaction was started by the addition of the Cu(II)Br_2/ligand-solution to the reaction mixture at room temperature. Samples of the reaction mixture were taken for GC and SEC analysis. Samples for GC analysis were dissolved in THF with phenothiazine as radical inhibitor (1,2-dichlorobenzene as internal standard), while samples for SEC analysis were diluted with THF, then passed over a basic alumina column to remove metal salts. After 6 hours, the reaction mixture was diluted with THF and filtered over a column of basic Al_2O_3 to remove the copper catalyst. After evaporating the excess solvent, the product was poured into a beaker and placed into the vacuum oven overnight to remove traces of monomer and residual solvent. The final polymer was obtained as a clear oil.

For the end-group modification, 500 mg PnBA (0.23 mmol, 1 eq.) was dissolved in 4 mL of dry ethyl acetate and a spoon tip of phenothiazine was added as radical inhibitor. A solution of 32.79 mg acrylic acid (0.45 mmol, 2 eq.) and 69.27 mg DBU (0.45 mmol, 5 eq.) was prepared separately and added to the polymer solution. The reaction was stirred for 5 days at 45°C in argon atmosphere. Afterwards, silica was added to the reaction mixture and stirred for 1 hour. The reaction mixture was then filtered over basic alumina to remove the remaining acrylic acid. The solvent was evaporated, the end-modified polymer was dried *in vacuo* and obtained as a yellowish oil. A polymer with DP 40 was synthesized accordingly.

Model study for the amine-thiol-ene conjugation

100 mg P(nBA-*co*-$TLA_{10\%}$) (6.67 µmol, 1 eq.) was dissolved in 0.5 mL THF, 2.87 mg methyl acrylate (333.5 µmol, 50 eq.) was added. The coupling was started by addition of the amine (333.5 µmol, 50 eq.). Propyl-, allyl- and benzylamine were used for the model study.

Grafting onto to obtain the graft copolymers

50 mg P(nBA-*co*-$TLA_{10\%}$) (3.34 µmol, 1 eq.) and 66.8 mg PEO-acrylate (33.4 mmol, 10 eq.) were dissolved separately in 1 mL THF. PEO-acrylate was added to the copolymer solution. The coupling was started by addition of a solution of 1.97 mg propylamine (33.4 mmol, 10 eq.) in 1 mL THF. Coupling with 5- and 10% TLA-copolymer as with PEO_{480}-acrylate was performed accordingly.

Grafting onto to obtain the toothbrush copolymer

100 mg of P(*t*BA)-*b*-P(nBA-*co*-$TLA_{10\%}$) (0.05 mmol, 1 eq.) was dissolved in 1 mL THF. Solutions of 136.78 mg $P(nBA)_{20}$-acrylate (0.25 mmol, 5 eq.) and 2.96 mg propylamine (0.25 mmol, 5 eq.) were dissolved separately in 0.5 mL THF. The solutions of $P(nBA)_{20}$-acrylate and propylamine were added to the reaction mixture and stirred for 24h. Toothbrush copolymers with 20 mol% TLA and $P(nBA)_{40}$-acrylate were synthesized accordingly.

Deprotection of the toothbrush copolymer

50 mg P(*t*BA)-*b*-[P(nBA-*co*-TLA_{10})-*g*-$P(nBA)_{20}$] (2.17 µmol, 1 eq.) was dissolved in 5 mL dry DCM. 0.10 mL $MeHSO_3$ was added and the reaction mixture was stirred for 0.5 h. The solvent and acid were evaporated and the polymer was isolated by precipitation. Deprotection of toothbrush copolymers with 20 mol% TLA and $PnBA_{40}$-acrylate were synthesized accordingly.

References

1. Matyjaszewski, K.; Tsarevsky, N. V. *Nature Chemistry* **2009,** 1, (4), 276-288.
2. Lutz, J.-F.; Ouchi, M.; Liu, D. R.; Sawamoto, M. *Science* **2013,** 341, (6146).
3. Braunecker, W. A.; Matyjaszewski, K. *Progress in Polymer Science* **2007,** 32, (1), 93-146.
4. Matyjaszewski, K. *Progress in Polymer Science* **2005,** 30, (8-9), 858-875.
5. Hadjichristidis, N.; Pitsikalis, M.; Pispas, S.; Iatrou, H. *Chemical Reviews* **2001,** 101, (12), 3747-3792.
6. Vamvakaki, M.; Papoutsakis, L.; Katsamanis, V.; Afchoudia, T.; Fragouli, P. G.; Iatrou, H.; Hadjichristidis, N.; Armes, S. P.; Sidorov, S.; Zhirov, D.; Zhirov, V.; Kostylev, M.; Bronstein, L. M.; Anastasiadis, S. H. *Faraday Discussions* **2005,** 128, (0), 129-147.
7. Bulychev, N.; Dervaux, B.; Dirnberger, K.; Zubov, V.; Du Prez, F. E.; Eisenbach, C. D. *Macromolecular Chemistry and Physics* **2010,** 211, (9), 971-976.
8. Burguiere, C.; Pascual, S.; Bui, C.; Vairon, J. P.; Charleux, B.; Davis, K. A.; Matyjaszewski, K.; Betremieux, I. *Macromolecules* **2001,** 34, (13), 4439-4450.
9. Rosler, A.; Vandermeulen, G. W. M.; Klok, H. A. *Adv. Drug Delivery Rev.* **2001,** 53, (1), 95-108.
10. De Smet, S.; Lingier, S.; Du Prez, F. E. *Polymer Chemistry* **2014,** 5, (9), 3163-3169.
11. Verdonck, B.; Goethals, E. J.; Du Prez, F. E. *Macromolecular Chemistry and Physics* **2003,** 204, (17), 2090-2098.
12. Verbrugghe, S.; Bernaerts, K.; Du Prez, F. E. *Macromolecular Chemistry and Physics* **2003,** 204, (9), 1217-1225.
13. Sheiko, S. S.; Sumerlin, B. S.; Matyjaszewski, K. *Progress in Polymer Science* **2008,** 33, (7), 759-785.
14. Pyun, J.; Kowalewski, T.; Matyjaszewski, K. *Macromolecular Rapid Communications* **2003,** 24, (18), 1043-1059.
15. Lessard, B.; Marić, M. *Macromolecules* **2008,** 41, (21), 7870-7880.
16. Zhang, W.; Li, Y.; Liu, L.; Sun, Q.; Shuai, X.; Zhu, W.; Chen, Y. *Biomacromolecules* **2010,** 11, (5), 1331-1338.
17. Petton, L.; Mes, E. P. C.; Van Der Wal, H.; Claessens, S.; Van Damme, F.; Verbrugghe, S.; Du Prez, F. E. *Polymer Chemistry* **2013,** 4, (17), 4697-4709.
18. Bulychev, N.; Van Camp, W.; Dervaux, B.; Kirilina, Y.; Dirnberger, K.; Zubov, V.; Du Prez, F. E.; Eisenbach, C. D. *Macromolecular Chemistry and Physics* **2009,** 210, (3-4), 287-298.
19. Neiser, M. W.; Muth, S.; Kolb, U.; Harris, J. R.; Okuda, J.; Schmidt, M. *Angewandte Chemie International Edition* **2004,** 43, (24), 3192-3195.
20. Muehlebach, A.; Rime, F. *Journal of Polymer Science Part A: Polymer Chemistry* **2003,** 41, (21), 3425-3439.
21. Bernaerts, K. V.; Fustin, C.-A.; Bomal-D'Haese, C.; Gohy, J.-F.; Martins, J. C.; Du Prez, F. E. *Macromolecules* **2008,** 41, (7), 2593-2606.
22. Zhang, M.; Xiong, Q.; Wang, Y.; Zhang, Z.; Shen, W.; Liu, L.; Wang, Q.; Zhang, Q. *Polymer Chemistry* **2014,** 5, (16), 4670-4678.
23. Zehm, D.; Laschewsky, A.; Heunemann, P.; Gradzielski, M.; Prevost, S.; Liang, H.; Rabe, J. P.; Lutz, J.-F. *Polymer Chemistry* **2011,** 2, (1), 137-147.

24. Börner, H. G.; Beers, K.; Matyjaszewski, K.; Sheiko, S. S.; Möller, M. *Macromolecules* **2001,** 34, (13), 4375-4383.
25. Dubois, P.; Krishnan, M.; Narayan, R. *Polymer* **1999,** 40, (11), 3091-3100.
26. Sumerlin, B. S.; Neugebauer, D.; Matyjaszewski, K. *Macromolecules* **2005,** 38, (3), 702-708.
27. Parrish, B.; Breitenkamp, R. B.; Emrick, T. *Journal of the American Chemical Society* **2005,** 127, (20), 7404-7410.
28. Van Camp, W.; Germonpré, V.; Mespouille, L.; Dubois, P.; Goethals, E. J.; Du Prez, F. E. *Reactive and Functional Polymers* **2007,** 67, (11), 1168-1180.
29. Ryu, S. W.; Hirao, A. *Macromolecules* **2000,** 33, (13), 4765-4771.
30. Kolb, H. C.; Finn, M. G.; Sharpless, K. B. *Angewandte Chemie International Edition* **2001,** 40, (11), 2004-2021.
31. Espeel, P.; Du Prez, F. E. *Macromolecules* **2015,** 48, (1), 2-14.
32. Golas, P. L.; Matyjaszewski, K. *Chemical Society Reviews* **2010,** 39, (4), 1338-1354.
33. Davis, K. A.; Matyjaszewski, K. *Statistical, Gradient, Block and Graft Copolymers by Controlled/Living Radical Polymerizations* **2002,** 159, 1-169.
34. Engler, A. C.; Lee, H.-i.; Hammond, P. T. *Angewandte Chemie International Edition* **2009,** 48, (49), 9334-9338.
35. Gao, H.; Matyjaszewski, K. *Journal of the American Chemical Society* **2007,** 129, (20), 6633-6639.
36. Campos, L. M.; Killops, K. L.; Sakai, R.; Paulusse, J. M. J.; Damiron, D.; Drockenmuller, E.; Messmore, B. W.; Hawker, C. J. *Macromolecules* **2008,** 41, (19), 7063-7070.
37. Bousquet, A.; Barner-Kowollik, C.; Stenzel, M. H. *Journal of Polymer Science Part A: Polymer Chemistry* **2010,** 48, (8), 1773-1781.
38. Mommer, S.; Keul, H.; Möller, M. *Macromolecular Rapid Communications* **2014,** 35, (23), 1986-1993.
39. Hoyle, C. E.; Lee, T. Y.; Roper, T. *Journal of Polymer Science Part A: Polymer Chemistry* **2004,** 42, (21), 5301-5338.
40. Hoyle, C. E.; Lowe, A. B.; Bowman, C. N. *Chemical Society Reviews* **2010,** 39, (4), 1355-1387.
41. Espeel, P.; Goethals, F.; Du Prez, F. E. *Journal of the American Chemical Society* **2011,** 133, (6), 1678-1681.
42. Espeel, P.; Du Prez, F. E. *European Polymer Journal* **2015,** 62, (0), 247-272.
43. Espeel, P.; Goethals, F.; Driessen, F.; Nguyen, L. T. T.; Du Prez, F. E. *Polymer Chemistry* **2013,** 4, (8), 2449-2456.
44. Petton, L. Design and Evaluation of Novel Types of Polymeric Dispersants. Ghent University, Gent, 2012.
45. Driessen, F.; Du Prez, F. E.; Espeel, P. *ACS Macro Letters* **2015,** 4, (6), 616-619.
46. Espeel, P.; Goethals, F.; Stamenovic, M. M.; Petton, L.; Du Prez, F. E. *Polymer Chemistry* **2012,** 3, (4), 1007-1015.
47. Reinicke, S.; Espeel, P.; Stamenović, M. M.; Du Prez, F. E. *ACS Macro Letters* **2013,** 2, (6), 539-543.
48. Percec, V.; Guliashvili, T.; Ladislaw, J. S.; Wistrand, A.; Stjerndahl, A.; Sienkowska, M. J.; Monteiro, M. J.; Sahoo, S. *Journal of the American Chemical Society* **2006,** 128, (43), 14156-14165.

49. Anastasaki, A.; Nikolaou, V.; Nurumbetov, G.; Wilson, P.; Kempe, K.; Quinn, J. F.; Davis, T. P.; Whittaker, M. R.; Haddleton, D. M. *Chemical Reviews* **2015**.
50. Rodríguez-Hernández, J.; Chécot, F.; Gnanou, Y.; Lecommandoux, S. *Progress in Polymer Science* **2005,** 30, (7), 691-724.
51. Voorhaar, L.; Wallyn, S.; Du Prez, F. E.; Hoogenboom, R. *Polymer Chemistry* **2014,** 5, (14), 4268-4276.
52. Van Renterghem, L. M.; Lammens, M.; Dervaux, B.; Viville, P.; Lazzaroni, R.; Du Prez, F. E. *Journal of the American Chemical Society* **2008,** 130, (32), 10802-10811.
53. Davis, K. A.; Matyjaszewski, K. *Macromolecules* **2000,** 33, (11), 4039-4047.
54. Kanao, M.; Matsuda, Y.; Sato, T. *Macromolecules* **2003,** 36, (6), 2093-2102.
55. Sato, T.; Kanao, M. *Kobunshi Ronbunshu* **2003,** 60, (4), 158-168.
56. Bulychev, N. A.; Arutunov, I. A.; Zubov, V. P.; Verdonck, B.; Zhang, T.; Goethals, E. J.; Du Prez, F. E. *Macromolecular Chemistry and Physics* **2004,** 205, (18), 2457-2463.
57. Ciampolini, M.; Nardi, N. *Inorganic Chemistry* **1966,** 5, (1), 41-44.

Abstract

The last experimental chapter of this PhD thesis describes the implementation of triazolinediones as building blocks for the efficient synthesis of complex copolymer structures by polymer-polymer conjugation. First, this recently developed chemistry was explored in the synthesis of block copolymers by polymer-polymer conjugation. Linear polymers containing reactive TAD and ene end groups were synthesized and coupled. In a next stage, this chemistry was implemented for the synthesis of amphiphilic graft and toothbrush copolymers in a "grafting-onto" approach. Therefore, a series of well-defined, "ene" containing macromolecular backbones were synthesized. Next, TAD end-functionalized polymers were obtained and linked to the polymer backbone. To evidence the amphiphilic behavior of these graft and toothbrush copolymers, micelle formation tests were performed and measured with DLS. Furthermore, the dispersing features of these complex copolymers were evaluated by pigment stabilization tests.

Parts of this chapter were published as:
Billiet S., De Bruycker K., Driessen F., Goossens H., Van Speybroeck V., Winne J.M., Du Prez F.E., *Nature Chemistry*, **2014**, 6 (9), 815-821

Chapter VI.

Triazolinedione chemistry and copper-mediated RDRP for the development of complex copolymer structures

VI.1 Introduction

The previous chapter described the synthesis of amphiphilic graft and toothbrush copolymers by the use of thiolactone chemistry *via* the amine-thiol-ene conjugation strategy. This strategy of implementing efficient chemistries for the synthesis of complex structures was continued by exploring triazolinediones, interesting building blocks for efficient polymer conjugation reactions, which were introduced within our research group a few years ago.[1] Therefore, this last chapter will focus on the synthesis of complex copolymer structures by the use of the triazolinedione conjugation strategy as efficient click-methodology.

Introduced by Sharpless and coworkers, polymer chemists are continuously inspired by this click-philosophy, containing a set of reactions that allow for the efficient covalent coupling in high yields.[2-4] The copper-catalyzed azide-alkyne cycloaddition (CuAAc) reaction was presented as the first denoted click chemistry.[5] During the last years, the toolbox of efficient methodologies gradually expanded as the well-known thiol-X, Diels-Alder cycloaddition and other recently reported efficient methodologies were developed to design complex copolymer structures as block, star, cyclic, hyperbranched and graft copolymers.[6-12]

A few years ago, 1,2,4-triazoline-3,5-diones (TAD) compounds were presented as interesting building blocks for the efficient Diels-Alder reaction with (di)enes, featuring indispensable click characteristics such as equimolarity, additive-free, single reaction trajectory, yielding only one specific adduct and avoiding laborious purification procedures after coupling. The heterocyclic azodicarbonyl derivatives with distinct red color, display an enhanced reactivity towards (di)enes

in Diels-Alder and Alder-ene reactions.[13-15] Furthermore, the red color can provide the user a visual feedback system as a distinct color switch from red to colorless can be observed during the reaction.[16] As a result of the high reactivity of TAD-moieties, the shelf life of these compounds are an important issue related to this methodology as it readily reacts with water, air, amines or can be degraded by light. To circumvent this problem, TAD reagents are typically stored in their reduced form, urazoles, and generated when desired by simple oxidation methods.[1, 17-19]

As mentioned in the previous chapter, efficient click-methodologies are increasingly used for the synthesis of complex copolymer structures *via* the grafting-onto approach.[20, 21] Therefore, polymer backbones and side chains containing the appropriate functionalities are synthesized separately, enabling the use of different polymerization mechanisms well suited to the respective desired polymer structure and providing the possibility to precisely characterize the individual segments.[22, 23] Because of the interesting results presented in the last chapter for the synthesis of graft and toothbrush copolymers *via* thiolactone chemistry, we were interested in the synthesis of complex copolymers by the use of TAD-chemistry. As a model study, TAD-chemistry was first similar used in the synthesis of block copolymers by polymer-polymer conjugation. Therefore, polymers containing reactive urazole- and ene-groups were synthesized by a Cu(0)-mediated polymerization system. Next, the urazole-moiety was oxidized to the corresponding TAD-structure and these polymers were coupled and analyzed *via* LCxSEC analysis to evidence the success of the conjugation reaction. In a next stage, graft and toothbrush copolymers were synthesized using TAD-chemistry in a grafting onto approach. First, linear and block copolymers were synthesized containing ene-functionalities in the polymer backbone. For this purpose, a Cu(0)-mediated RDRP was applied. To introduce the polymer side-chains as grafts, polymers containing a urazole end-group were synthesized *via* RDRP. In a next stage, these structures were connected by oxidation of the urazole moiety to the corresponding TAD-structure to obtain the amphiphilic graft and toothbrush copolymers. A range of different structures were synthesized and their properties were determined as dispersants.

VI.2 Synthesis of block copolymers by polymer-polymer conjugation

VI.2.1 Introduction

The synthesis of block copolymers in this work was performed by polymer-polymer conjugation through the TAD-strategy. Polymers containing TAD- and "ene" end groups were synthesized *via* a Cu(0)-mediated polymerization methodology and post-polymerization modification reactions. Polymers containing "ene" end groups were obtained by synthesis of polystyrene *via* a Cu(0)-mediated polymerization. Next, the bromine was transformed into a cyclopentadiene unit by post-polymerization modification reaction (PS-Cp). For the TAD-containing polymers, a urazole containing initiator was synthesized suitable for Cu(0)-mediated polymerization and the polymerization of butyl acrylate was performed. Next, the TAD end-group was obtained by oxidation of the urazole-moiety with DABCO-bromine. Finally, the PS-PBA block copolymer was obtained by polymer-polymer conjugation reaction and the outcome was analyzed *via* LC-SEC analysis (Figure VI.1).

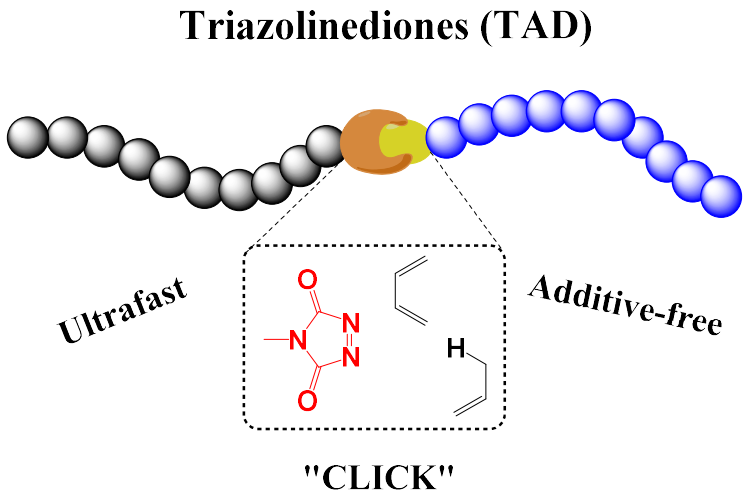

Figure VI.1: General synthetic strategy for the synthesis of block copolymers *via* the TAD-strategy.

VI.2.2 Synthesis of PS-Cp

As mentioned, the initial step in this project was the synthesis of a polymer containing an "ene" end group. Polystyrene was selected due to the ease of which the polymer can be precipitated. Furthermore, a Cu(0)-mediated polymerization system was selected because of the high end group fidelity which can be obtained *via* this method, yielding a polymer with a high degree of bromine end groups that can be transformed into a cyclopentadiene in a following step. The final reaction mixture was precipitated in cold methanol to isolate the PS-Br and the polymer was analyzed *via* SEC, NMR and MALDI-TOF analysis (Figure VI.2). SEC analysis evidenced the synthesis of a polymer with low dispersity and an average molecular weight of 4,4 kDa. From ^{1}H-NMR analysis, the signals of the styrene units can be clearly observed as well as the bromine end group at 4.5 ppm.

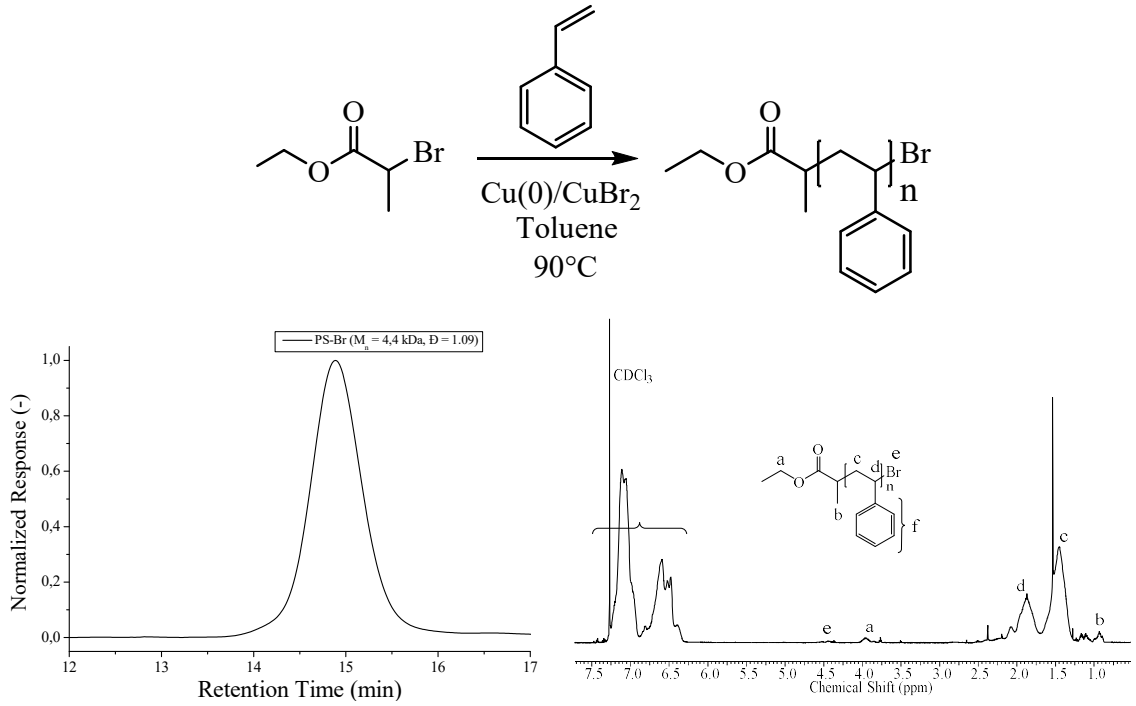

Figure VI.2: Cu(0)-mediated RDRP of styrene and analsys by SEC and ^{1}H-NMR.

MALDI-TOF analysis further confirmed the structure of PS-Br. A mass difference of 104.06 Da was observed between two successive analogous signals, confirming the presence of the styrenic unit. Furthermore, a good agreement between the theoretical and experimental molecular weight numbers provided the final evidence of the PS-Br structure. Also, a second distribution can be

observed between the major series (Ag^+-adduct), which can be attributed to the sodium Na^+-adduct of the polymer (Figure VI.3).

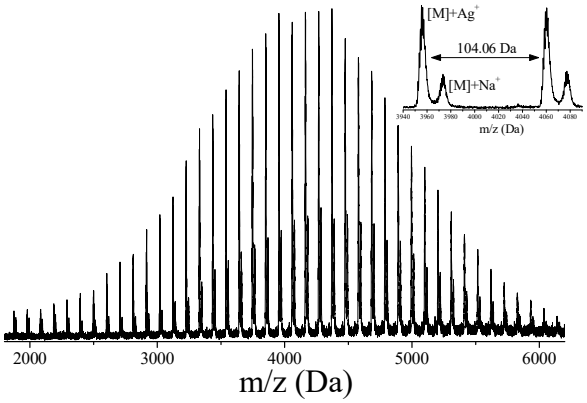

Theoretical Mass (Da)	Experimental Mass (Da)
3851.05	3851.54
3955.11	3955.43
4059.17	4059.22
4163.23	4162.95
4267.29	4265.11

*Second series can be attributed to Na^+-adduct (main series is Ag^+-adduct)

Figure VI.3: MALDI-TOF analysis of PS-Br.

In a next stage, the bromine end group was transformed into a cyclopentadiene unit to obtain the PS-Cp. The polystyrene polymer was reacted overnight with bis(cyclopentadienyl)nickel in the presence of tributylphosphine and sodium iodide at room temperature, and the isolated polymer was analyzed by SEC, ^{1}H-NMR and MALDI-TOF analysis. From SEC analysis, a very small unimodal shift in molecular weight was observed and the dispersity did not increase. ^{1}H-NMR analysis provided further proof for the successful end group modification reaction as the signal of the CH_2 next to the bromine at 4.5 ppm disappeared and the small signals of the cyclopentadiene unit at 6.25 ppm appeared. Final proof of the successful modification reaction was provided by MALDI-TOF analysis as experimental and theoretical mass values were in good agreement and no signal of the remaining PS-Br starting product could be observed (Figure VI.4).

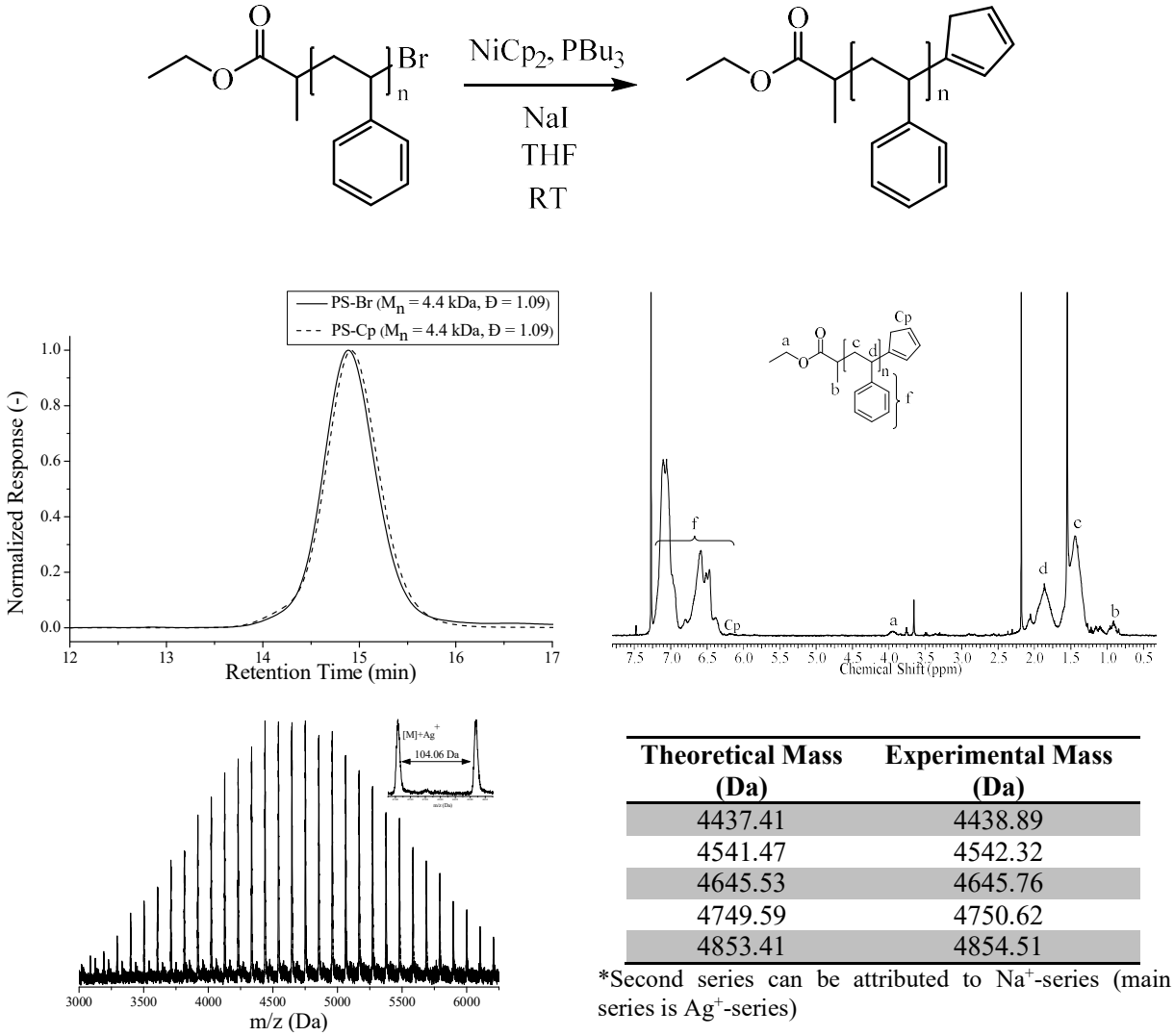

Theoretical Mass (Da)	Experimental Mass (Da)
4437.41	4438.89
4541.47	4542.32
4645.53	4645.76
4749.59	4750.62
4853.41	4854.51

*Second series can be attributed to Na^+-series (main series is Ag^+-series)

Figure VI.4: End group modification of PS-Br to obtain PS-Cp and SEC, ^{1}H-NMR and MALDI-TOF analysis of the resulting polymer structure.

After the synthesis of PS-Cp, this polymer was reacted with butyl-TAD as a model experiment to evidence the high reactivity of TAD-compounds. PS-Cp was dissolved in DCM and 4-butyl-1,2,4-triazoline-3,5-dione (BuTAD) was added in equimolar amounts. During the addition of BuTAD, it was observed that the red color disappeared immediately, indicating a very fast reaction due to the high reactivity of the TAD-compound. After the reaction, the polymer was isolated by precipitation in cold methanol and analyzed by SEC, ^{1}H-NMR and MALDI-TOF analysis. From SEC analysis, a small unimodal increase in molecular weight can be observed as well as a very small decrease in dispersity. ^{1}H-NMR analysis indicated the conversion of the

cyclopentadiene units in the the TAD-Cp adduct, the small signals at 6.25 ppm disappeared and signals from the TAD-Cp adduct at 4.8 ppm appeared. Final proof was provided by MALDI-TOF analysis. Experimental mass values were in good agreement with theoretical mass values and no remaining signals of the PS-Cp starting polymer could be observed (Figure VI.5)

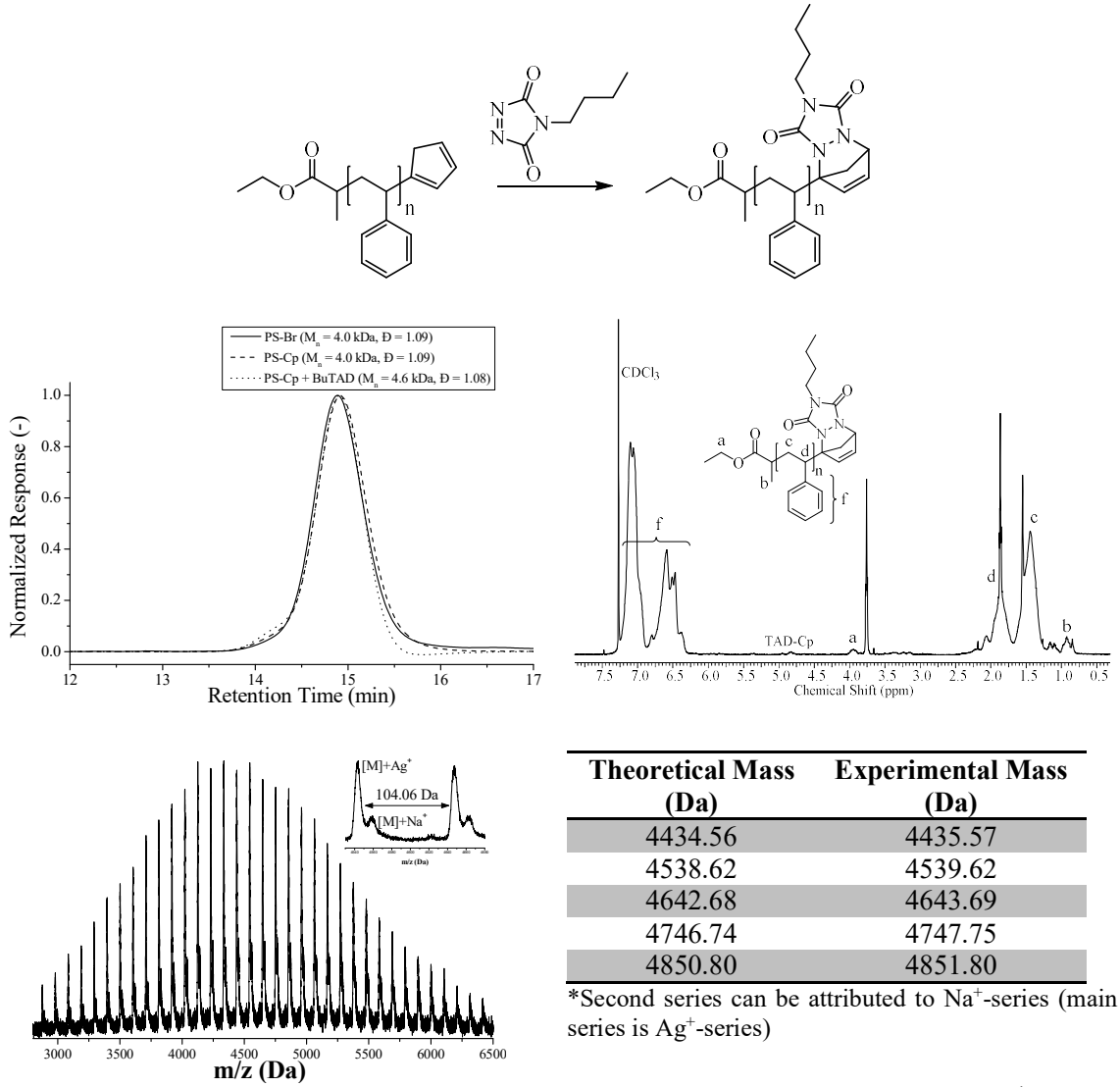

Theoretical Mass (Da)	Experimental Mass (Da)
4434.56	4435.57
4538.62	4539.62
4642.68	4643.69
4746.74	4747.75
4850.80	4851.80

*Second series can be attributed to Na^+-series (main series is Ag^+-series)

Figure VI.5: End group modification of PS-Cp with BuTAD as model experiment and analysis with SEC, ^{1}H-NMR and MALDI-TOF.

VI.2.3 Design of a urazole end-capped polymer

After the synthesis of PS-Cp, a urazole end-capped polymer was designed. A Cu(0)-mediated polymerization was performed *via* an initiator containing a urazole moiety. The polymerization of different monomers was tested in a broad range of different solvents, however with no success as each time no polymer was obtained after the reaction. Finally, it was found that the polymerization of butyl acrylate in DMF was successful (Ur-PBA). However, it should be noted that no successful kinetic analysis of the polymerization could be performed due to variable induction periods of the polymerization and relatively low initiator efficiencies as the measured molecular weights were each time higher in comparison to the expected molecular weight most probably due to side reactions between the acidic protons of the urazole moiety and the copper catalyst (Figure VI.6).

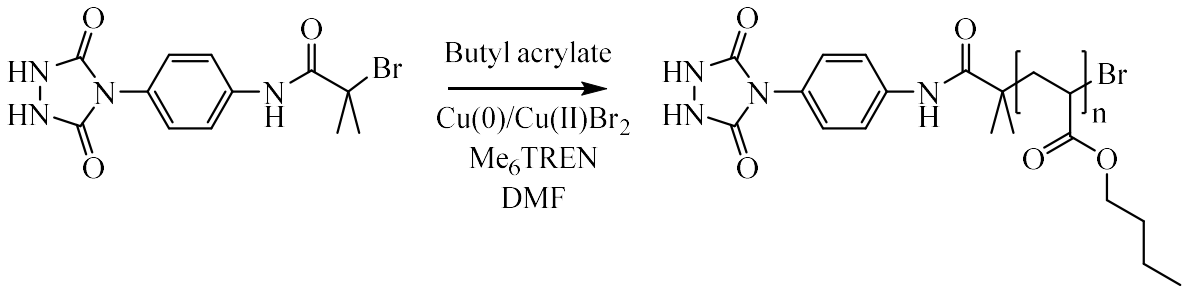

Figure VI.6: Polymerization of butyl acrylate through Cu(0)-mediated polymerization of a urazole-containing initiator.

After the Cu(0)-mediated polymerization, the polymer was analyzed *via* SEC analysis. From SEC analysis, a molecular weight of 9.8 kDa was measured in combination with a relative broad dispersity (Figure VI.7).

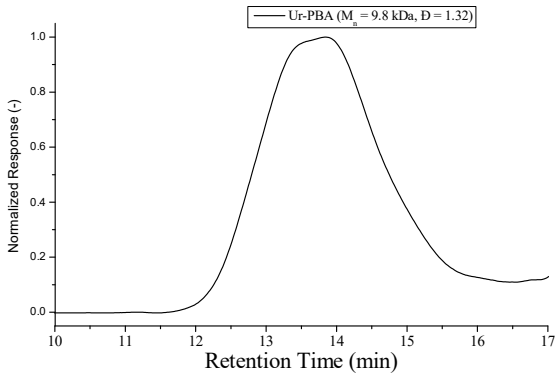

Figure VI.7: SEC analysis of the polybutyl acrylate containing a urazole end group.

VI.2.4 Polymer-polymer conjugation

After the synthesis of PS-Cp as “ene” containing polymer and Ur-PBA as urazole containing structure, these chains were linked together. First the urazole moiety was oxidized to the corresponding TAD by the use of DABCO-bromine. Next, this red-colored polymer was added to a solution of Ps-Cp in DCM. Again, it was observed that the red color disappeared immediately (Figure VI.8).

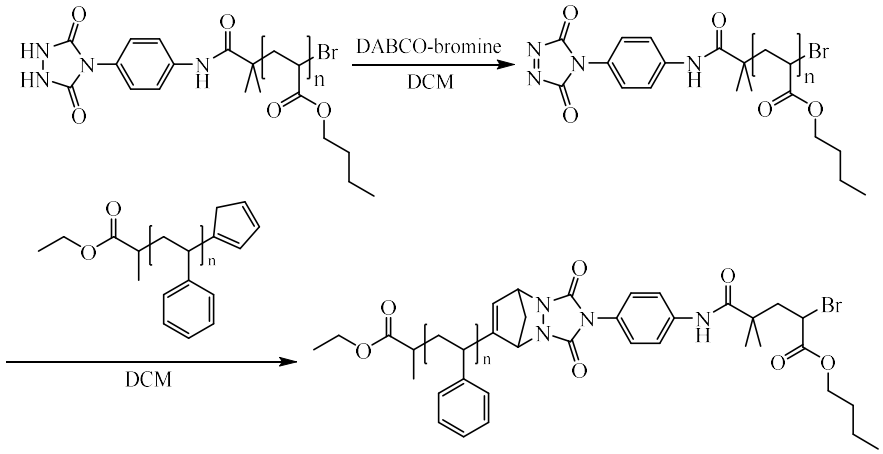

Figure VI.8: Oxidation and coupling of Ur-PBA to PS-Cp.

After the coupling reaction, the resulting polymer mixture was analyzed *via* LCxSEC analysis. From the two chromatograms, the difference in molecular weight (x-axis) and polarity (y-axis) of the two starting products can be monitored. After the reaction, a difference in molecular weight and dispersity can be observed, indicating the successful synthesis of the PBA-PS block copolymer. It should be noted that a small amount of urazole starting polymer was still present due to a small deviation from equimolarity as a result of the dispersity of both polymers (Figure VI.9).

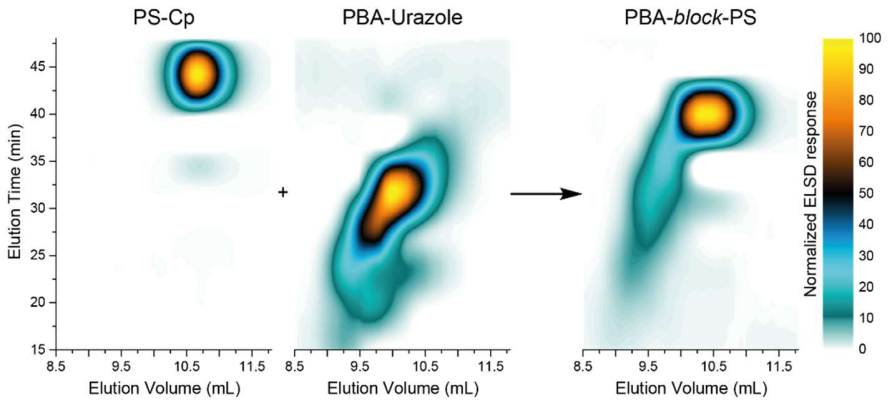

Figure VI.9: LCxSEC analysis of PS-Cp and PBA-urazole and the resulting block copolymer.

VI.3 Synthesis of amphiphilic graft copolymers

VI.3.1 Introduction

The synthesis of the graft copolymers in this chapter was performed *via* the grafting-onto strategy in a similar way as described in the previous chapter, but by the use of triazolinedione chemistry. Again, segment lengths were selected based on the hydrophobic/hydrophilic balance of the backbone and polymer grafts.[24] Regarding the synthesis of the graft copolymers, first a hydrophobic polymer backbone was prepared, containing butyl acrylate (BA) and citronellyl acrylate as "ene"-containing monomer (CA) *via* a Cu(0)-mediated RDRP. Next, the hydrophilic urazole-poly(*N,N*-dimethylacrylamide) was synthesized *via* Reversible Addition Fragmentation Transfer (RAFT) polymerization as a result of the difficulties encountered when applying a Cu(0)-mediated polymerization starting from urazole-containing initiators as explained in section VI.2.3. Finally, the urazole-moiety was oxidized to the corresponding TAD-structure and these side-chains were coupled *via* the triazolinedione conjugation strategy to obtain the amphiphilic graft copolymers (Figure VI.10).

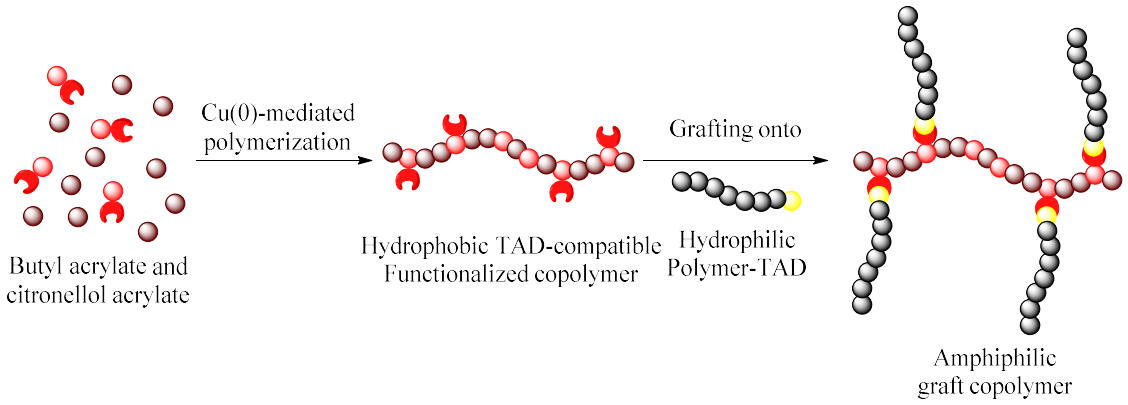

Figure VI.10: General synthetic strategy for the synthesis of amphiphilic graft copolymers *via* the TAD-strategy.

VI.3.2 Preparation of the hydrophobic CA-functionalized copolymer

As described in the introductory part, the first step in this project was the synthesis of a polymeric backbone containing "ene" functionalities. Therefore, an "ene"-containing monomer was synthesized containing a TAD-reactive double bond and an acrylate moiety available for Cu(0)-mediated polymerization. More specifically, citronellyl acrylate (CA) was synthesized as a result of the commercial availability of the corresponding citronellyl alcohol and the ease of which the final monomer can be synthesized and purified. Citronellyl acrylate was obtained by reaction of citronellyl alcohol with acryloyl chloride in the presence of trimethylamine, purified by distillation and analyzed *via* ^{1}H-NMR (Figure VI.11).

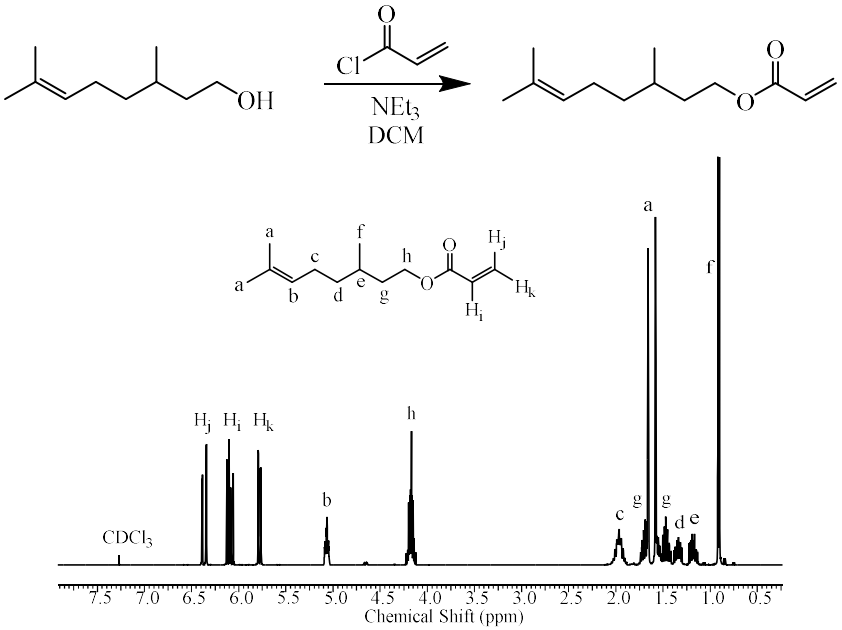

Figure VI.11: Synthesis of a citronellyl acrylate as "ene"-containing monomer and analysis via ^{1}H-NMR.

In a following step, the hydrophobic polymer backbone with "ene"-containing functionalities was obtained by copolymerization of butyl acrylate (BA) with citronellyl acrylate (CA) *via* a Cu(0)-mediated polymerization (Figure VI.12). A kinetic study of the copolymerization was performed to evidence a near-random distribution of the "ene" moieties across the polymer backbone. Samples were taken during the copolymerization at regular time intervals and the molecular weight and dispersity were determined *via* SEC analysis. Furthermore, GC analysis was used to calculate the conversion. From the kinetic results, it can be concluded that the copolymerization proceeded in a controlled manner and that both butyl acrylate and citronellyl acrylate were consumed in an almost equal rate, evidencing a near-random distribution. An induction time was observed which might be explained by the presence of Cu_2O on the surface.[25] It has to be noted that the polymerization had to be stopped at around 90% conversion due to the formation of a small shoulder at high molecular weight (Figure VI.12).

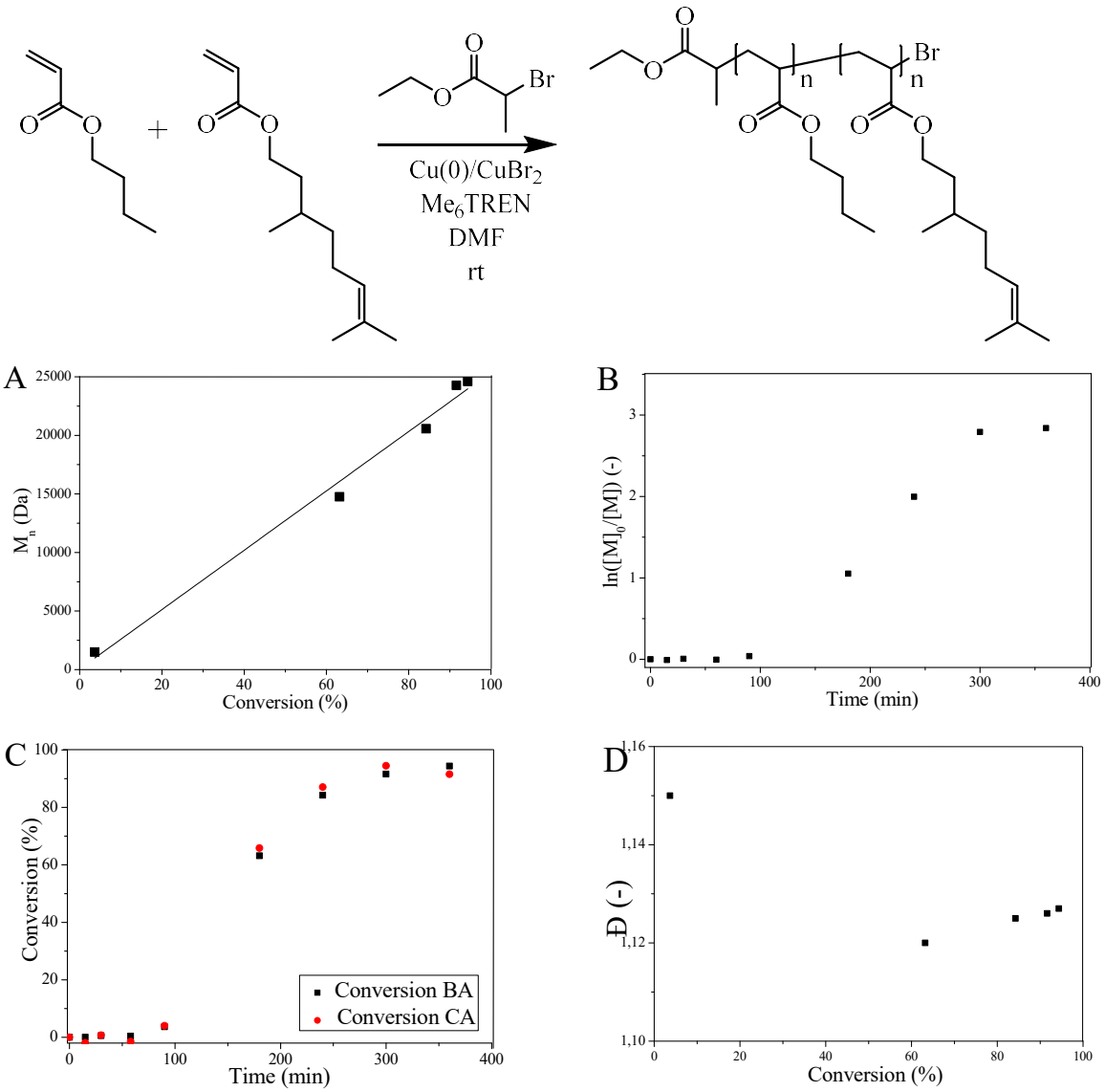

Figure VI.12: Kinetic data for the Cu(0)-mediated copolymerization of butyl acrylate and citronellyl acrylate; molecular weight as a function of conversion (A); first order kinetic plot (B); the conversion of the both nBA and CA as function of time (C) and dispersity as a function of conversion (D).

Next, two different copolymers with a DP of 100 containing 5 and 10 mol% of "ene" units were prepared (Table VI.1). The resulting concentration of "ene"-units in the different copolymers was calculated from NMR by comparing the signal of the "ene"-unit at 5.2 ppm with the signal at 0.9 ppm of both the "ene"-unit and butyl acrylate (Figure VI.13).

Table VI.1: Overview of the different copolymers synthesized *via* Cu(0)-mediated RDRP

Entry	Copolymer	M_n (kDa) (Đ[a])	Experimental % CA[b]
1a	P(nBA-*co*-$CA_{5\%}$)$_{100}$	15.6 (1.11)	4.8
2a	P(nBA-*co*-$CA_{10\%}$)$_{100}$	16.2 (1.12)	9.8

[a]Molecular weights and dispersities determined by SEC in DMA vs. polymethylmethacrylate standards.
[b]Experimental incorporation of citronellyl acrylate in copolymer calculated from NMR-analysis.

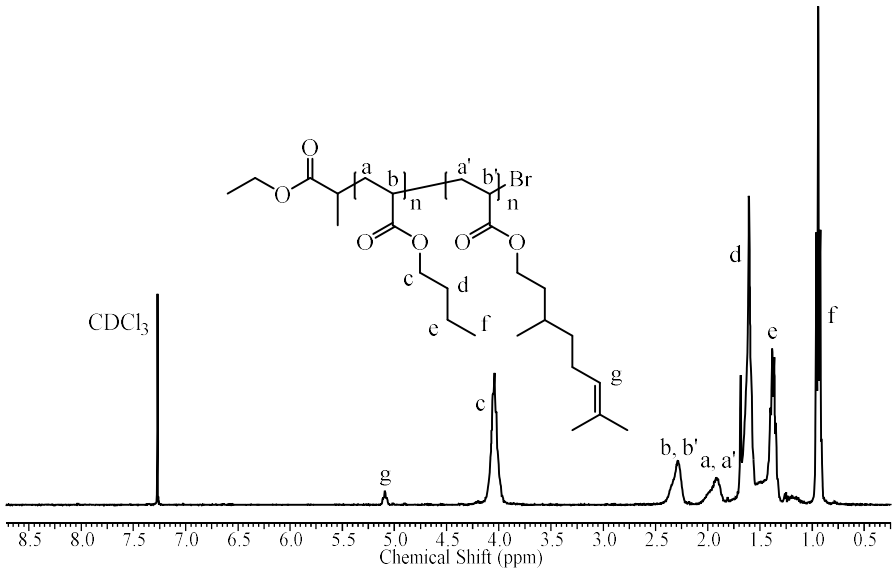

Figure VI.13: ^{1}H-NMR of the P(nBA-co-$CA_{10\%}$)$_{100}$ copolymer.

VI.3.3 Synthesis of PDMA-TAD

In a next stage, the hydrophilic PDMA-TAD was prepared, which will be afterwards linked to the "ene"-containing copolymer as side-chain. First *N,N*-dimethylacrylamide (DMA) was polymerized *via* a urazole-containing RAFT agent. The synthesis of the RAFT agent was developed within the own research group by Stef Vandewalle for the synthesis of urazole endcapped polymer structures.[26] As already mentioned, a Cu(0)-mediated polymerization was not possible due to the difficulties encountered when combining a Cu(0)-mediated polymerization with urazole-containing initiators. The kinetic plot of Figure VI.14 shows a varying induction time, this can be explained by impurities in AIBN (purified AIBN was used in experiment 2 compared to experiment 1).The conversion was measured as a function of reaction time by offline GC measurements to preserve a low conversion and high end group fidelity.

Negative conversions were measured during the induction time due to the experimental error of the GC measurements.

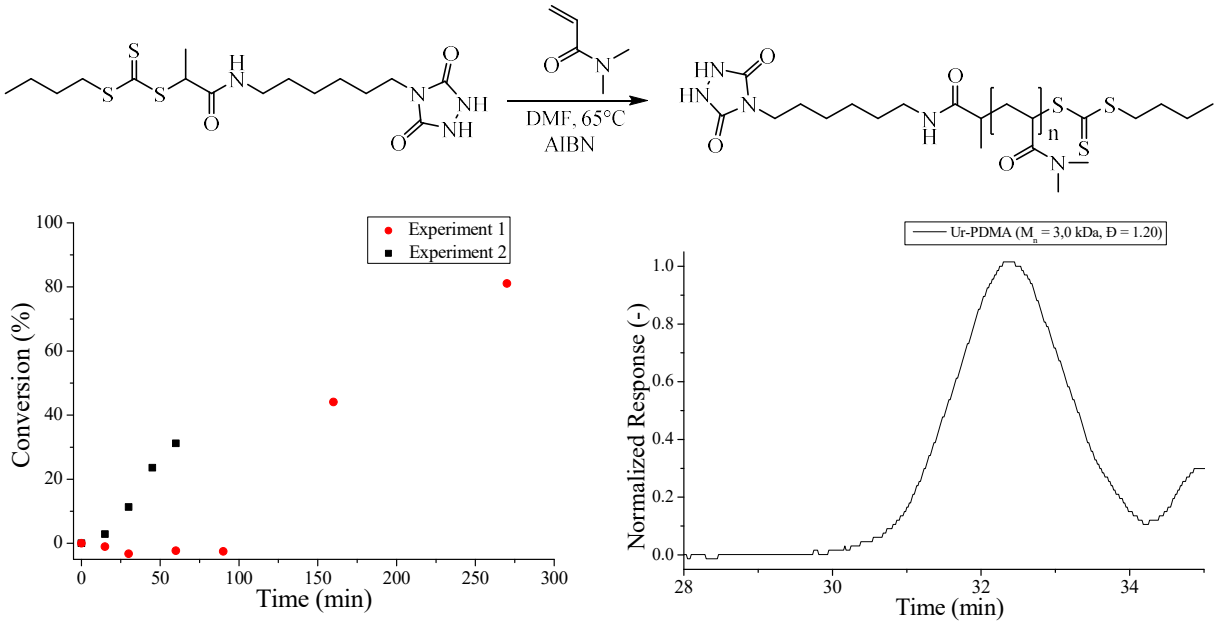

Figure VI.14: Synthesis of Ur-PDMA by polymerization of *N,N*-dimethylacrylamide *via* a urazole-containing RAFT agent and offline GC measurements and SEC analysis.

After the synthesis of Ur-PDMA, the urazole moiety was oxidized to the corresponding TAD-unit. First, the polymer was dried by the use of crushed molecular sieves. Afterwards, the oxidization was performed by the use of DABCO-bromine in DCM for 6 hours. Afterwards, the polymer was filtrated and *trans,trans*-2,4-hexadien-1-ol (HDEO) was added to the red-colored solution to trap the TAD end group. Finally, the conversion of the reaction was analyzed *via* SEC, ^{1}H-NMR and MALDI-TOF analysis (Figure VI.15).

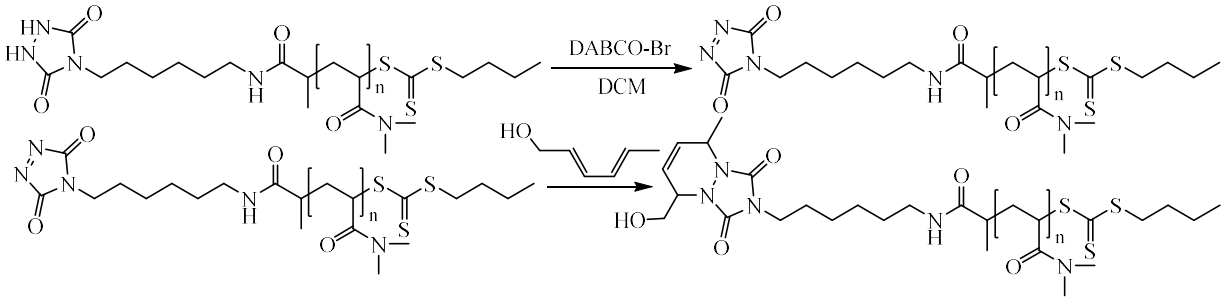

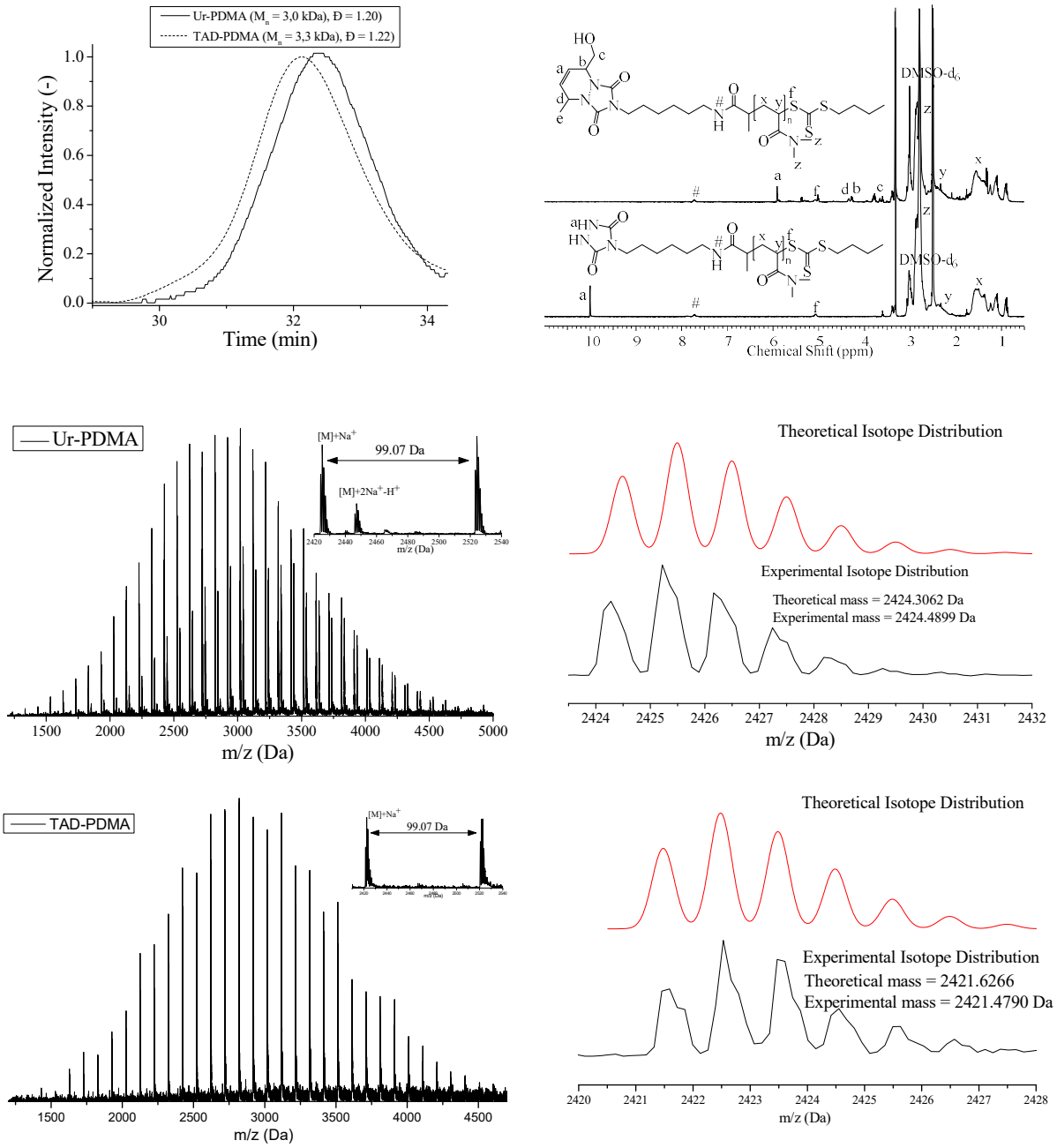

Figure VI.15: Oxidation of Ur-PDMA to TAD-PDMA by the use of DABCO-bromine and analysis *via* SEC ^{1}H-NMR and MALDI-TOF.

From SEC analysis, a unimodal increase in molecular weight was observed after the oxidation reaction and coupling with HDEO. Furthermore, NMR analysis indicated a complete reaction as no signals from the urazole moiety at 10 ppm were present after oxidation. Final proof was provided by MALDI-TOF analysis. The isotopic distributions of the sodium adducts of Ur-

PDMA and the oxidized polymer were in good agreement with the theoretical ones. Furthermore, a second distribution can be observed in the starting polymer, which can be attributed to an extra sodium atom bound to a polymeric unit that lost one proton from the acidic urazole moiety. It has to be noted that no starting product of the Ur-PDMA was present.

VI.3.4 Grafting onto

After the synthesis of the "ene"-containing hydrophobic copolymer and hydrophilic urazole-PDMA side-chains, the corresponding graft copolymers were synthesized *via* the triazolinedione strategy. The urazole-PDMA was oxidized to the corresponding TAD-structure by the use of DABCO-bromine in DCM. Next, the red-colored solution was added to the "ene"-containing hydrophobic copolymer and the color disappeared within minutes. Finally, the graft copolymer was purified by precipitation in methanol or preparative SEC and analyzed *via* SEC and ^{1}H-NMR. From SEC analysis, an increase in molecular weight was observed after coupling of the PDMA side-chains to the copolymer (Figure VI.16).

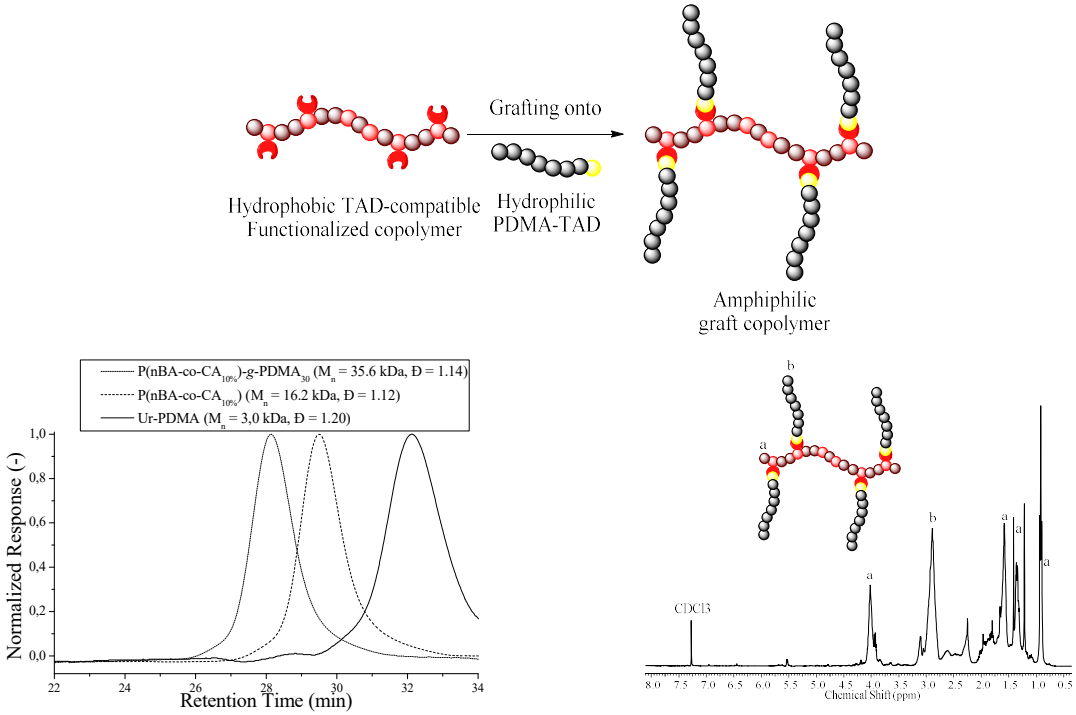

Figure VI.16: Synthetic strategy, SEC and ^{1}H-NMR analysis of the isolated amphiphilic graft copolymer consisting of the hydrophobic "ene"-containing backbone and the hydrophilic PDMA side-chains.

Next, a variety of different graft copolymers with different molecular weight (backbone and PDMA side-arm) and grafting density (CA-content) were synthesized (Table VI.2) and analyzed *via* SEC and ^{1}H-NMR analysis. The average number of grafts was calculated by comparing the signal of PDMA at 2.9 ppm with the signal of the backbone at 0.9 ppm.

Table VI.2: SEC-results of the graft copolymers *via* the TAD-strategy between the hydrophobic P(nBA-co-CA) copolymers and Ur-PDMA.

Entry	Graft copolymer	M_n (kDa)[a] (Đ[a])	Aver. Grafts[b]
1a-g	P(nBA-*co*-$CA_{5\%}$)-*g*-$PDMA_{10}$	26.8 (1.14)	4.6
2a-g	P(nBA-*co*-$CA_{5\%}$)-*g*-$PDMA_{30}$	32.5 (1.17)	4.3
3a-g	P(nBA-*co*-$CA_{10\%}$)-*g*-$PDMA_{10}$	28.3 (1.16)	9.5
4a-g	P(nBA-*co*-$CA_{10\%}$)-*g*-$PDMA_{30}$	35.6 (1.14)	8.9

[a] Molecular weight and dispersities determined by SEC (polymethylmethacrylate standards)
[b] Number of side-arms calculated by NMR after purification

VI.4 Synthesis of amphiphilic toothbrush copolymers

VI.4.1 Introduction

In a following part, the synthesis of amphiphilic toothbrush copolymers was performed, which are known materials to exhibit improved stabilization behavior as dispersing agents as demonstrated in the previous chapter. As with the graft copolymers, the grafting-onto strategy was used *via* the triazolinedione conjugation reaction for the synthesis of the toothbrush copolymers. First, a block copolymer consisting of 1-ethoxyethyl acrylate (EEA) as a protected hydrophilic first segment and a copolymer of nBA and CA as second segment was obtained in a one-pot procedure *via* a Cu(0)-mediated RDRP, evidencing the high end-group fidelity at high monomer conversion. Next, the hydrophobic side-chains, consisting of PnBA were synthesized separately. In order to implement the triazolinedione conjugation strategy, PnBA containing a urazole end-group was synthesized and oxidized, yielding the corresponding TAD-polymer. Next, the toothbrush copolymer was obtained by coupling of the block copolymer and side-

chains *via* the triazolinedione conjugation strategy. Finally, by deprotecting the EEA monomer by the use of heat, yielding the poly(acrylic acid) segment, the amphiphilic character of the complex macromolecular structure was introduced (Figure VI.17).

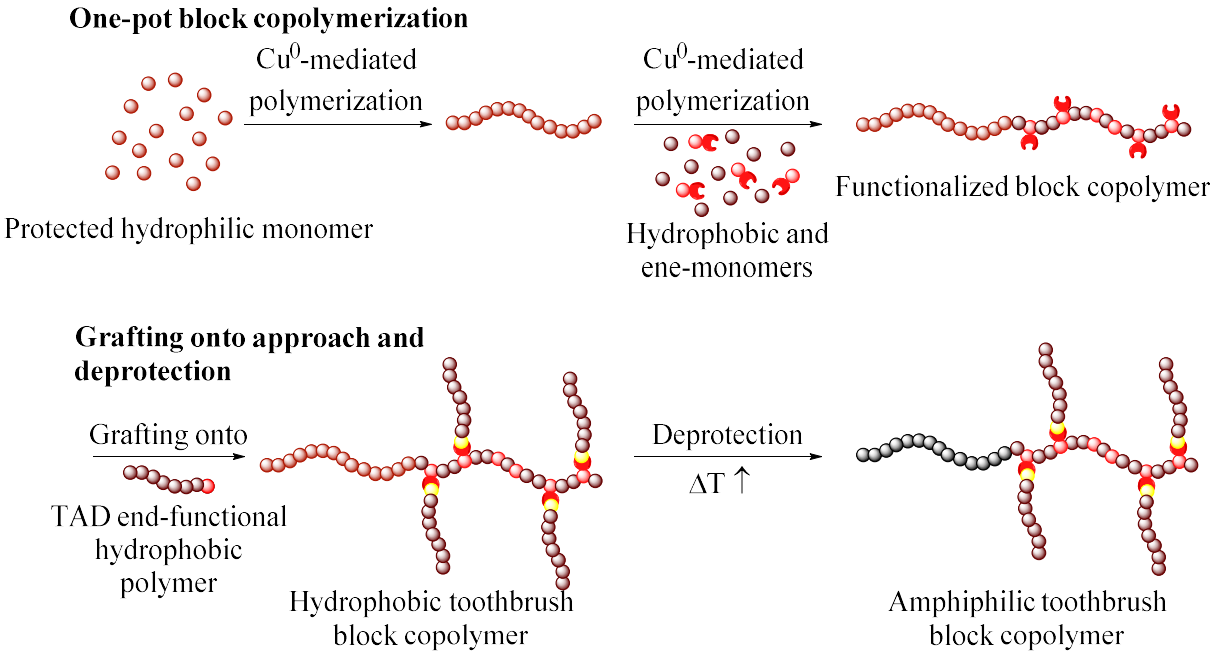

Figure VI.17: General synthetic strategy for the synthesis of amphiphilic toothbrush copolymers *via* the triazolinedione conjugation strategy.

VI.4.2 Synthesis of block copolymer

As described, the first step in the design of the toothbrush copolymer is the synthesis of a block copolymer containing "ene" functionalities in one of the two segments. Therefore, a Cu(0)-mediated polymerization system was again applied due to the high end group fidelities which can be obtained at high conversion, enabling a one-pot procedure of the synthesis of the block copolymer. As hydrophilic block, 1-ethoxyethyl acrylate was selected as a protected hydrophilic monomer, which can be easily hydrolyzed to acrylic acid by the use of heat.

The synthesis started by polymerizing 1-ethoxyethyl acrylate for 8 hours to a near-quantitative conversion *via* a Cu(0)-mediated RDRP. Next, a mixture of butyl acrylate and citronellyl

acrylate was added to the same reaction mixture in a one-pot procedure for the second block and the block copolymer was obtained (Figure VI.18).

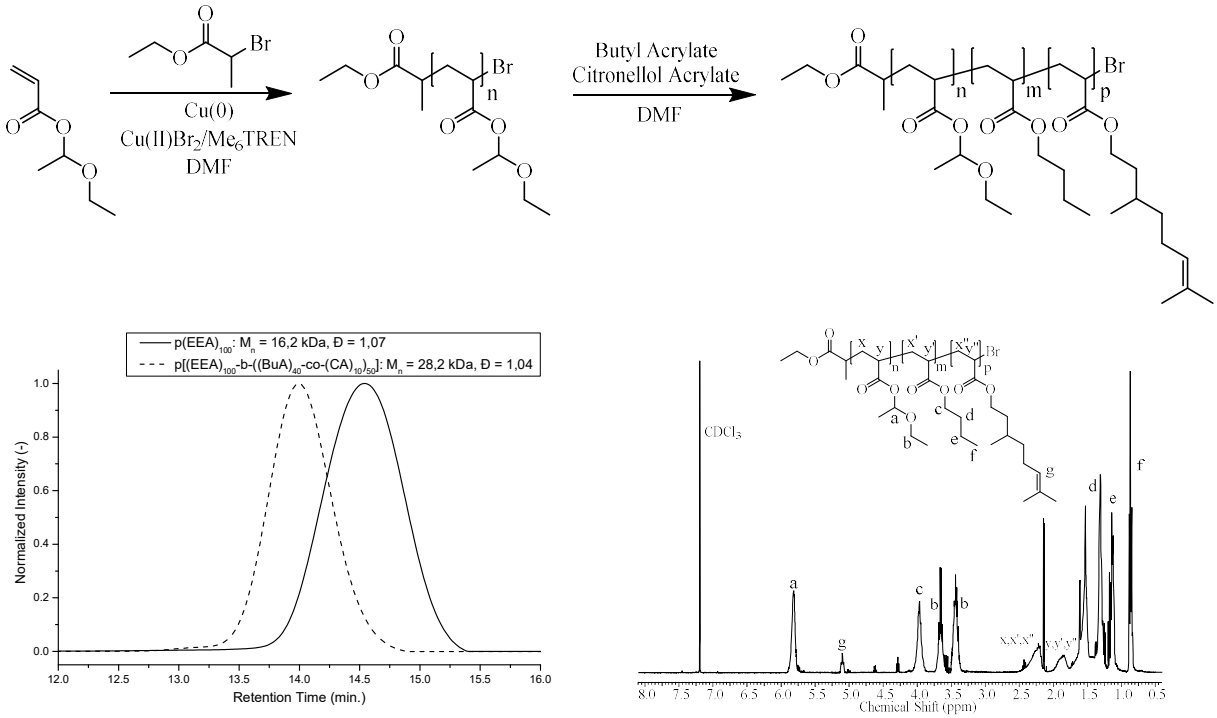

Figure VI.18: Synthesis of the hydrophobic CA-functionalized block copolymer *via* the one-pot block copolymerization and analysis *via* SEC and ^{1}H-NMR.

From SEC analysis, a unimodal increase in molecular weight was observed, demonstrating the successful block copolymerization. As a model example, DP's of 100 and 50 were targeted for P(EEA) and the copolymer respectively. Furthermore, two different block copolymers were synthesized containing 5 and 10 mol% of "ene" units and the resulting concentration of "ene"-units in the different block copolymers was calculated from NMR by comparing the signal of the "ene" unit at 5.2 ppm with the signal at 0.9 ppm of both the "ene"-unit and butyl acrylate (Table VI.3).

Table VI.3: Overview of the different block copolymers synthesized *via* Cu(0)-mediated RDRP.

Entry	Block copolymer	M_n (kDa) (Đ[a])	Experimental % CA[b]
1b	P(EEA)-*b*-P(nBA-*co*-CA$_{5\%}$)	25.3 (1.05)	4.9
2b	P(EEA)-*b*-P(nBA-*co*-CA$_{10\%}$)	28.2 (1.04)	9.6

[a] Molecular weights and dispersities determined by SEC (polystyrene standards)
[b] Experimental incorporation of "ene" in copolymer calculated from NMR-analysis

VI.4.3 Synthesis of PnBA-TAD side-arms

Regarding the synthesis of the hydrophobic side-arms, polybutyl acrylate containing a TAD end-group (TAD-PnBA) was synthesized, which will be linked to the "ene"-containing block copolymer as side-chain. First, butyl acrylate was polymerized *via* a urazole-containing RAFT-agent. As mentioned, a Cu(0)-mediated polymerization was not possible due to problems encountered when combining a Cu(0)-mediated polymerization with urazole-containing initiators. After the synthesis of Ur-PnBA, the urazole moiety was oxidized to the corresponding TAD-unit. The oxidization was performed by the use of DABCO-bromine in DCM for 6 hours (Figure VI.19).

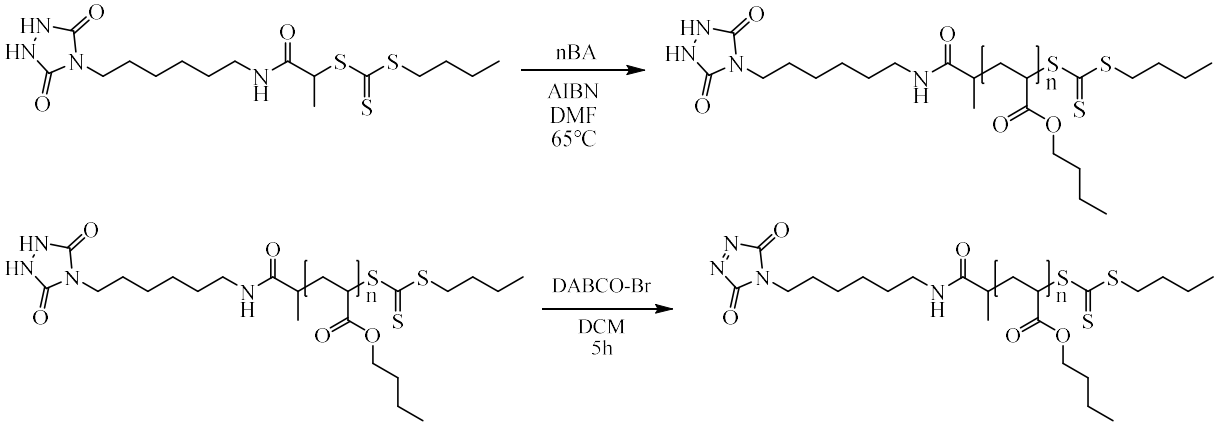

Figure VI.19: Synthetic strategy for the synthesis of TAD-PnBA side-arms.

Afterwards, the polymer was filtrated and *trans,trans*-2,4-hexadien-1-ol (HDEO) was added to the red-colored solution to trap the TAD-structure. Finally, the reaction outcome was analyzed *via* SEC, ^{1}H-NMR and MALDI-TOF analysis (Figure VI.20).

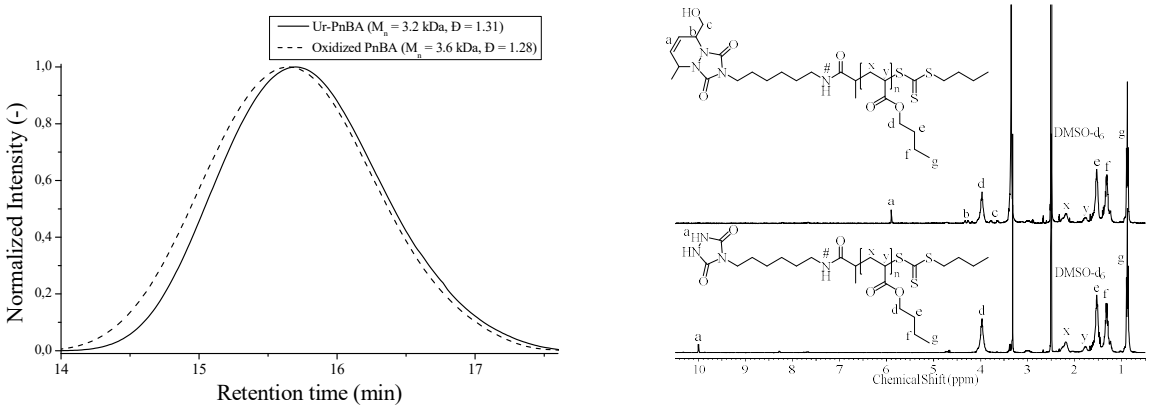

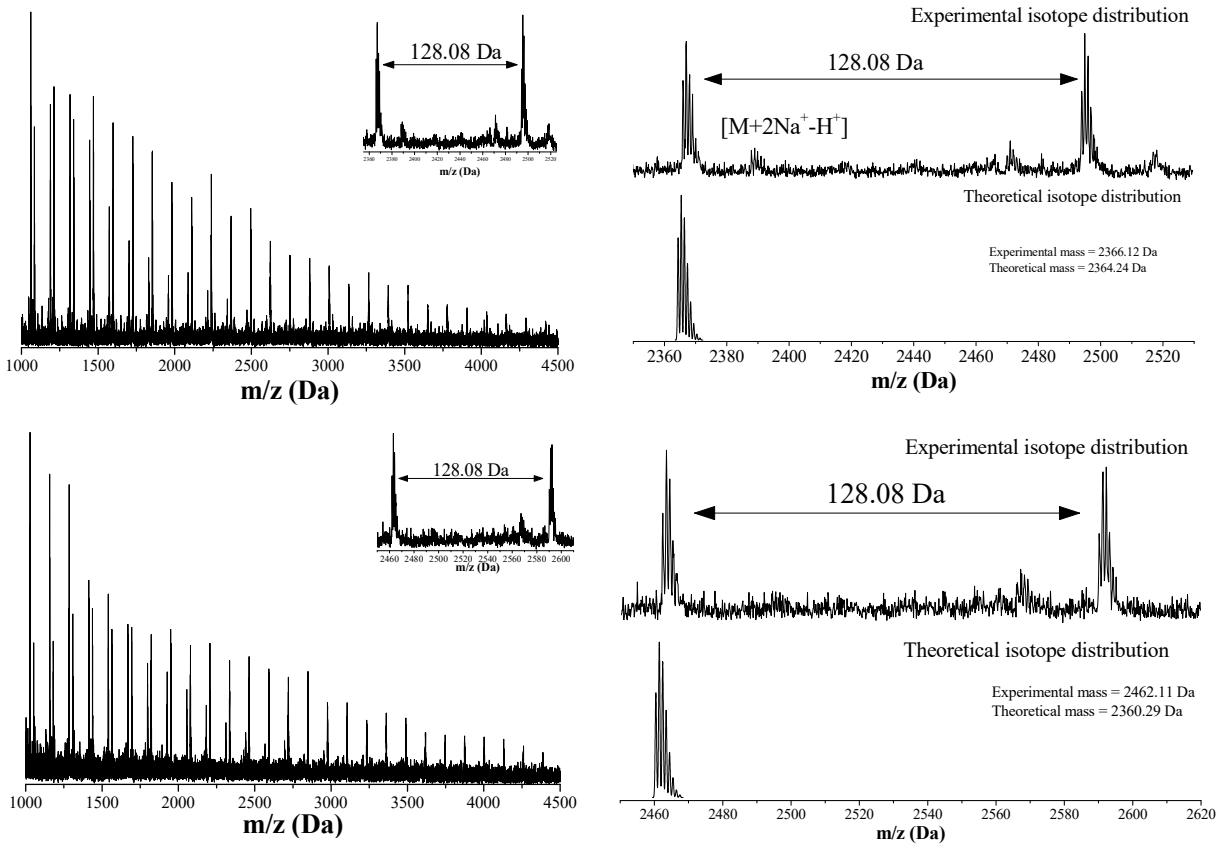

Figure VI. 20: SEC, ^{1}H-NMR and MALDI-TOF analysis of the oxidation of Ur-PnBA.

From SEC analysis, a unimodal increase in molecular weight was observed after the oxidation reaction and coupling with HDEO. Furthermore, NMR analysis indicated a complete reaction as no signals from the urazole moiety at 10 ppm were present after oxidation. Final proof was provided by MALDI-TOF analysis. The isotopic distributions of the sodium adducts of Ur-PDMA and the oxidized polymer were in good agreement with the theoretical ones. Furthermore, a second distribution can be observed in the starting polymer, which can be attributed to an extra sodium atom bound to a polymeric unit which lost one proton from the acidic urazole moiety. A third distribution was assigned to an unknown fragmentation product. It has to be noted that no starting product of the Ur-PnBA was present.

VI.4.4 Grafting onto

For the synthesis of the toothbrush copolymers, the triazolinedione conjugation strategy was applied in the same manner as for the synthesis of the graft copolymers. The urazole-PnBA was oxidized to the corresponding TAD-moiety by the use of DABCO-bromine in DCM. Afterwards, the red-colored solution was added to the "ene"-containing block copolymer and the color again disappeared within minutes. Finally the toothbrush copolymer was purified by precipitation in hexane or preparative SEC and analyzed *via* SEC and ^{1}H-NMR. From SEC analysis, an increase in molecular weight was observed after coupling of the PnBA side-chains to the block copolymer (Figure VI.21).

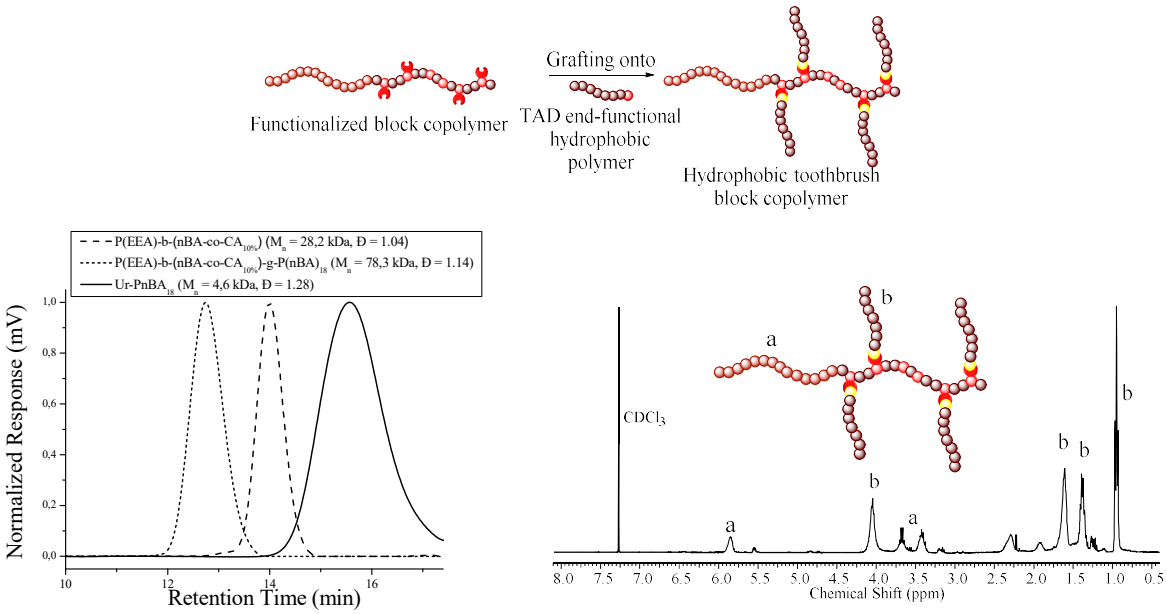

Figure VI.21: Synthetic strategy, SEC and ^{1}H-NMR analysis of the isolated toothbrush copolymer consisting of the hydrophobic "ene"-containing backbone and the PnBA side-chains.

Next, a variety of different toothbrush copolymers with different molecular weight (backbone and PnBA side-arm) and grafting density (CA-content) were synthesized (Table VI.4) and analyzed *via* SEC and ^{1}H-NMR analysis. The average number of grafts was calculated by determining the increase in ratio of the signal of butyl acrylate at 0.9 ppm compared to the signal of 1-ethoxyethyl acrylate at 5.8 ppm.

Table VI.4: SEC-results of the toothbrush copolymers *via* the TAD-strategy between the hydrophobic P(EEA)-*b*-P(nBA-co-CA) copolymers and Ur-PnBA.

Entry	Toothbrush copolymer	M_n (kDa)[a] (Đ[a])	Aver. Grafts[b]
1b-tb	P(EEA)-*b*-(P(nBA-*co*-$CA_{5\%}$)-*g*-$P(nBA)_{18}$)	65.4 (1.15)	2.3
2b-tb	P(EEA)-*b*-(P(nBA-*co*-$CA_{5\%}$)-*g*-$P(nBA)_{32}$)	71.6 (1.16)	2.1
3b-tb	P(EEA)-*b*-(P(nBA-*co*-$CA_{10\%}$)-*g*-$P(nBA)_{18}$)	78.3 (1.14)	4.6
4b-tb	P(EEA)-*b*-(P(nBA-*co*-$CA_{10\%}$)-*g*-$P(nBA)_{32}$)	89.8 (1.13)	4.3

[a] Molecular weight and dispersities determined by SEC (polystyrene standards)
[b] Number of side-arms calculated by NMR after purification

VI.4.5 Deprotection of the EEA

The last step in the synthesis of the toothbrush copolymers is the deprotection of the 1-ethoxyethyl unit in the side chain. Typical procedures for this reaction describe the use of heat, which can be done by dissolving the polymer and heating the solution to 80°C or spreading it as a small film on a glass plate and heating in an oven. After the deprotection reaction, the polymer was analyzed *via* SEC and ^{1}H-NMR to confirm the deprotection reaction (Figure VI.22).

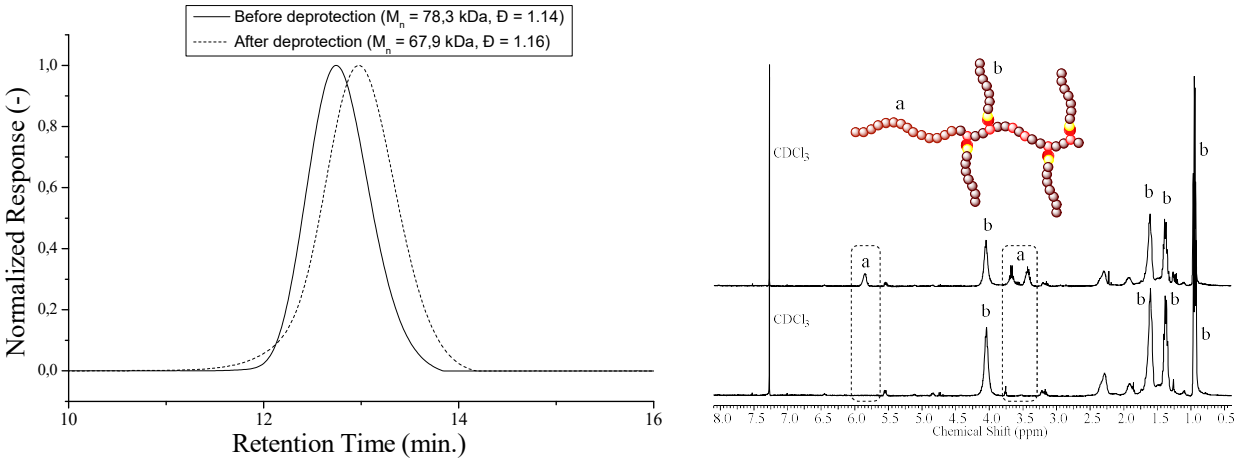

Figure VI.22: Analysis via SEC and ^{1}H-NMR of the deprotection of P(EEA)-*b*-(P(nBA-*co*-$CA_{10\%}$)-*g*-$P(nBA)_{18}$).

VI.5 Characterization of the amphiphilic graft and toothbrush copolymers

VI.5.1 Introduction

As described, amphiphilic polymeric structures are increasingly used as stabilizers in pigment dispersions in industry. By implementing these materials as dispersants, the mixing of hydrophobic particles in water is enabled, creating aqueous dispersions applicable in the painting industry. By implementing these complex architectures, the long-term stabilization of these dispersed materials is enabled. The different graft- and toothbrush copolymers described in this chapter were analyzed by dynamic light scattering (DLS) and pigment stabilization tests to determine and compare their structure-property relationships.

VI.5.2 DLS

In DLS, the hydrodynamic size these polymeric structures in water was determined. It was observed that sample preparation was important for both the graft and toothbrush copolymers. For the graft copolymers, an acidic buffer solution (pH = 4) was required while for the toothbrush copolymers a basic buffer solution (pH = 10) was necessary. For both the graft and toothbrush copolymers, it was observed that the hydrodynamic volume increased when larger side-chains were applied ($PDMA_{10}$ vs. $PDMA_{30}$) and when the grafting density increased (5-10%) (Figure VI.23 – Table VI.5).

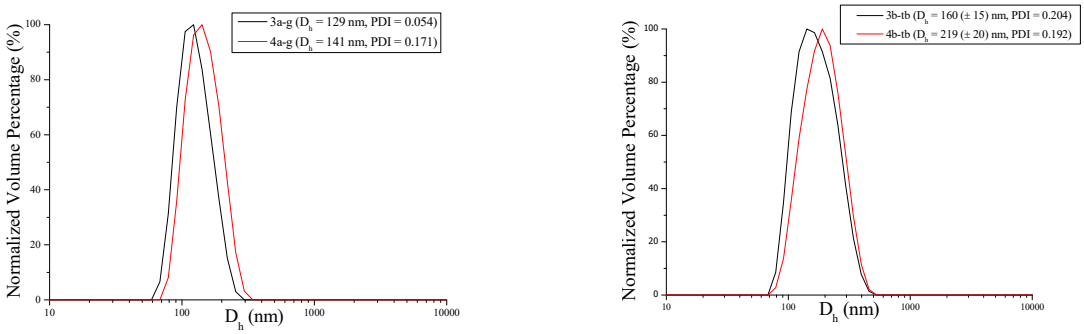

Figure VI.23: Hydrodynamic sizes of the different graft copolymers (left) and toothbrush structures (right) in water.

Table VI.5: DLS-results of the amphiphilic graft and toothbrush copolymers in water.

Entry	Polymer	D_h (nm)	PDI
1a-g	P(nBA-*co*-$CA_{5\%}$)-*g*-$PDMA_{10}$	121 (± 10)	0.098
2a-g	P(nBA-*co*-$CA_{5\%}$)-*g*-$PDMA_{30}$	133 (± 15)	0.153
3a-g	P(nBA-*co*-$CA_{10\%}$)-*g*-$PDMA_{10}$	129 (± 10)	0.054
4a-g	P(nBA-*co*-$CA_{10\%}$)-*g*-$PDMA_{30}$	141 (± 15)	0.171
1b-tb	P(EEA)-*b*-(P(nBA-*co*-$CA_{5\%}$)-*g*-$P(nBA)_{18}$)	144 (± 15)	0.216
2b-tb	P(EEA)-*b*-(P(nBA-*co*-$CA_{5\%}$)-*g*-$P(nBA)_{32}$)	211 (± 15)	0.169
3b-tb	P(EEA)-*b*-(P(nBA-*co*-$CA_{10\%}$)-*g*-$P(nBA)_{18}$)	160 (± 15)	0.204
4b-tb	P(EEA)-*b*-(P(nBA-*co*-$CA_{10\%}$)-*g*-$P(nBA)_{32}$)	219 (± 20)	0.192

VI.5.3 Dispersion tests

The amphiphilic graft and toothbrush copolymers that have been synthesized were implemented for stabilizing dispersions of copper phtalocyanine (CuPc) as well-known hydrophobic pigment in water (Figure VI.24). In each case, the hydrophobic backbone of the copolymer structure will adsorb onto the particle, while the hydrophilic side chains will prevent flocculation of the particles by steric and/or electronic repulsion. As in the previous chapter, a literature procedure was applied for the pigment stabilization tests. A copolymer solution in water (5 wt%) was prepared and added to the hydrophobic pigment (1 wt.-%). Furthermore, the solubilization of the pigment particles was induced by applying an ultrasonic treatment and stirring at high shear rate (700 rpm) in which a dark blue pigment solution was obtained. Next, the stability of the different dispersions was determined by observing the half-time of sedimentation, or the required period of time in which the dispersion boundary between the turbid and transparent zone reaches 50% of its initial height (Table VI.6).

Figure VI. 24: Visual confirmation of the formation of stable pigment dispersions: (a) the pigment floating in water without any copolymer added, (b) a stable pigment dispersion, (c) sedimentation of the pigment dispersion.

The results of the stabilization tests indicated an increased stabilization when toothbrush copolymers were applied (> 30 days) in comparison to the graft copolymers. When comparing the graft copolymers, an increased stabilization was observed when longer side-chains or higher grafting densities were utilized, introducing more sterical stabilization. In the case of the toothbrush copolymers, a small difference was observed when increasing the grafting density in comparison to a small decrease of $\tau/2$ when increasing the length of the side-chains, probably due to sterical hindrance between the brushes.

Table VI. 6: Sedimentation stability ($\tau/2$) of the CuPc aqueous dispersions stabilized by the graft- and toothbrush copolymers.

Entry	Polymer	$\tau/2$ (days)
1a-g	P(nBA-*co*-$CA_{5\%}$)-*g*-$PDMA_{10}$	11
2a-g	P(nBA-*co*-$CA_{5\%}$)-*g*-$PDMA_{30}$	17
3a-g	P(nBA-*co*-$CA_{10\%}$)-*g*-$PDMA_{10}$	14
4a-g	P(nBA-*co*-$CA_{10\%}$)-*g*-$PDMA_{30}$	26
1b-tb	P(AA)-*b*-(P(nBA-*co*-$CA_{5\%}$)-*g*-$P(nBA)_{18}$)	34
2b-tb	P(AA)-*b*-(P(nBA-*co*-$CA_{5\%}$)-*g*-$P(nBA)_{32}$)	30
3b-tb	P(AA)-*b*-(P(nBA-*co*-$CA_{10\%}$)-*g*-$P(nBA)_{18}$)	36
4b-tb	P(AA)-*b*-(P(nBA-*co*-$CA_{10\%}$)-*g*-$P(nBA)_{32}$)	29

VI.6 Conclusions

This last experimental chapter described the synthesis of block, amphiphilic graft and toothbrush copolymers as complex macromolecular structures by the use of triazolinedione chemistry. In the case of the synthesis of the block copolymers, a polymer containing a TAD end group was obtained by polymerization of butyl acrylate *via* a urazole-containing initiator for Cu(0)-mediated polymerization and subsequent oxidation. The ene-containing polymer was isolated by polymerization of styrene and end group modification to introduce a cyclopentadiene moiety. Next, the polymers were linked and the outcome was analyzed *via* LCxSEC analysis. For the synthesis of the grafts, a series of copolymers containing butyl acrylate and a varying amount of citronellyl acrylate were synthesized. Next, PDMA was synthesized containing a TAD end group

by polymerization *via* the corresponding urazole RAFT-agent and oxidation by the use of DABCO-bromine, since problems occurred when using a Cu(0)-mediated polymerization system. The graft copolymer was obtained by coupling of the different polymer segments. For the synthesis of the toothbrush copolymers, a series of different block copolymers were synthesized containing 1-ethoxyethyl acrylate as protected hydrophilic segment, and a copolymer of butyl acrylate and citronellyl acrylate as second segment in a one-pot procedure *via* a Cu(0)-mediated polymerization. Next, poly(butyl acrylate) was synthesized *via* a urazole-containing RAFT-agent and the TAD-moiety was obtained *via* the corresponding oxidation reaction. The final toothbrush copolymer was obtained *via* the triazolinedione-conjugation strategy and the amphiphilic properties were obtained by deprotection of 1-ethoxyethyl acrylate to the corresponding acrylic acid by the use of heat. Finally, the material properties were analyzed by DLS and pigment stabilization tests. DLS indicated an increase in hydrodynamic radius when longer side-chains were used. The pigment stabilization tests evidenced an increased stabilization behavior for toothbrush copolymers compared to the graft copolymers, due to their specific stabilization properties.

In comparison to thiolactone chemistry, it can be noted that triazolinedione chemistry has certain advantages and disadvantages for the synthesis of complex macromolecular architectures. First of all, due to the high reactivity of these TAD compounds, these structures are known to be relatively unstable compared to their thiolactone counterparts, and precautions such as working under dry conditions and keeping the starting compounds at low temperature have to be taken. However, this issue can be circumvented by generating the TAD-moiety by oxidation *on-demand* of the corresponding urazole-moiety. Another issue is the synthesis of these interesting TAD-compounds, which is known to be challenging. This in contrast to the synthesis of functional thiolactone compounds, which are made from commercially available structures on large scale, facilitating the synthesis to their corresponding initiators and monomers. On the other hand, it has to be noted that triazolinedione chemistry has significant advantages surpassing the drawbacks of this method. First of all, an interesting benefit when utilizing TAD chemistry in comparison to thiolactone chemistry is the colour switch from red to colourless during the reaction of triazolinediones with “ene” compounds, providing the possibility for the titration of the reactive TAD compound to the “ene”-solution. Furthermore, TAD compounds are known to

be very reactive moieties enabling higher grafting efficiencies in comparison to thiolactone chemistry. Therefore, it can be concluded that the triazolinedione chemistry is a quite interesting method for the synthesis of complex amphiphilic copolymers for dispersing applications.

VI.7 Experimental part

VI.7.1 Methods

^{1}H NMR

^{1}H- and ^{13}C-NMR (APT, HSQC, COSY) spectra were recorded in $CDCl_3$ on a Bruker AM500 spectrometer (500 MHz or 125 MHz for ^{1}H or ^{13}C respectively) or on a Bruker Avance 300 (300 MHz or 75 MHz for ^{1}H or ^{13}C respectively). Chemical shifts are presented in parts per million (δ) relative to $CDCl_3$ (7.26 ppm in ^{1}H- and 77.23 ppm in ^{13}C-NMR respectively) as internal standard. Coupling constants (*J*) in ^{1}H-NMR are given in Hz. The resonance multiplicities are described as *d* (doublet), *t* (triplet) or *m* (multiplet).

LC-MS

An Agilent technologies 1100 series LC/MSD system equipped with a diode array detector and single quad MS detector (G1946C) with an electrospray source (ESI-MS) was used for classic reversed phase LC-MS. Analytic reversed phase HPLC was performed with a Phenomenex Kinetex C_{18} column (5 µ, 150 x 4.6 mm) using a solvent gradient (0 → 100% acetonitrile in H_2O in 15 min) and the eluting compounds were detected *via* UV-detection (λ = 214 nm). High resolution mass spectra (HRMS) were collected using an Agilent 6220A time-of-flight (TOF) equipped with a multimode ionization (MMI) source.

SEC

Size Exclusion Chromatography (SEC) was performed using two different systems: (i) a Varian PLGPC50plus instrument, using a refractive index detector, equipped with two Plgel 5 µm MIXED-D columns 40 °C. Polystyrene standards were used for calibration and THF as eluent at a flow rate of 1 mL/min. Samples were injected using a PL AS RT autosampler. The preparative

SEC system consists of a Shimadzu LC-2OAT pump, a Shimadzu SIL-IOAF autosampler, a RID-IOA Differential Refractive Index Detector, a FRC-1OA Fraction Collector, CBM-2OA PC Interface/System Controller. Software is LC solutions including LC solutions SEC software. Columns are originating from Shodex: a K-LG guard column and a KF-2004 prep column (elution 2.5 mL/min, THF, rt); (ii) a Waters instrument, with a refractive-index (RI) detector (2414 Waters), equipped with 3 Polymer Standards Services GPC serial columns (1 X GRAM Analytical 30 Å, 10 µm and 2 x GRAM Analytical 1000 Å, 10 µm) at 35 °C. Poly(methyl methacrylate) (PMMA) standards were used for calibration and N,N-dimethylacetamide (DMA), containing LiBr (0.42 g/mL) was used as a solvent at a flow rate of 1 mL/min. Molar mass and dispersity were determined using the Empower software.

LCxSEC

For two-dimensional liquid chromatography, sample fractions from the first dimension were transferred to the second-dimension column via an electronically controlled eight-port valve system (VICI Valco instruments, Houston, TX, USA), equipped with two 100 µL sample loops. The second dimension consisted of an Agilent Infinity 1260 isocratic pump and a PSS SDV LIN M 5 µm column. Detection in the second dimension was accomplished by using an ELSD. Nitrogen was used as carrier gas in the ELSD at a flow rate of 2.5 L/min. Spray Chamber, Drift Tube and Optical Cell temperatures were set at 30 °C, 80 °C and 70 °C, respectively. The flow rates used in the first and second dimensions were 0.02 mL/min and 5 mL/min, respectively. Sample concentrations were between 0.25 and 2.0 mg/mL. An isocratic elution of methanol/hexane (70/30) was used as the solvent for the first dimension, THF was used as the solvent for the second dimension analysis. Data were recorded using PSS WinGPC Unichrom software.

MALDI-TOF

Matrix Assisted Laser Desorption Ionisation – Time of Flight (MALDI-TOF) was performed on an Applied Biosystems Voyager De STR MALDI-TOF spectrometer equipped with 2 m linear and 3 m reflector flight tubes, a nitrogen laser operating at 337 nm, pulsed ion extraction source and reflectron. All mass spectra were obtained with an accelerating potential of 20 kV in positive ion mode and in reflector mode. In case of the analysis of PEO, dithranol (10 mg/mL in THF)

was used as matrix, sodium trifluoroacetate (1 mg/mL) was used as cationizing agent, and polymer samples were dissolved in THF (10 mg/mL). Polymer solutions were prepared by mixing 8 µL of the matrix, 1 µL of the salt and 1 µL of the polymer solution. Subsequently 0.5 µL of this mixture was spotted on the sample plate, and the spots were dried in air at room temperature. Regarding the analysis of poly(butyl acrylate), dithranol (25 mg/mL in THF), sodium iodide (20 mg/mL in THF), and polymer samples were dissolved in THF (5 mg/mL). Polymer solutions were prepared by mixing 10 µL of the matrix, 5 µL of the salt and 5 µL of the polymer solution. Subsequently, 0.5 µL of this mixture was spotted on the sample plate, and the spots were dried in air at room temperature. PEO 2000 was used for calibration. All data were processed using the Data Explorer 4.0.0.0 (Applied Biosystems) software package.

GC

GC was performed on an Agilent 7890A system equipped with a VWR Carrier-160 hydrogen generator and an Agilent HP-5 column of 30 m length and 0.320 mm diameter. An FID detector was used and the inlet was set to 240 °C with a split injection ratio of 25 : 1. Hydrogen was used as the carrier gas at a flow rate of 2 mL/min . The oven temperature was increased at 20 °C/min from 50 °C to 120 °C, followed by a ramp of 50 °C/min to 150 °C.

DLS

Dynamic light scattering (DLS) was performed on a Zetasizer Nano-ZS Malvern apparatus (Malvern Instruments Ltd) using disposable cuvettes. The excitation light source was a He−Ne laser at 633 nm, and the intensity of the scattered light was measured at 173°. This method measures the rate of the intensity fluctuation and the size of the particles is determined through the Stokes−Einstein equation. 1 mg of PEO-NH_2 (800 Da) multi-segmented block copolymer was dissolved in 0.1 mL and precipitated in 1 mL H_2O, subsequently the polymer solution was heated at 40°C for 24h to evaporate THF, filtered through Millipore membranes with pore sized of 0.2 µm prior to measurement.

VI.7.2 Materials

Chloroform D ([865-49-6], ≥ 99.8 %) was purchased from Euro-isotop. Triethylamine ([121-44-8], 99 %) was purchased from Acros Organics and dried in a solvent purification system (J.C. Meyer). Acryloyl chloride ([814-68-6], 96%, stabilized with 400 ppm phenothiazine) was purchased from ABCR, 2,2'-azobis(2-methylpropionitrile) ([78-67-1], 98%), bis(cyclopentadienyl)nickel ([1271-28-9]), citronellol ([106-22-9], > 92%) was purchased from TCI Chemicals Aluminium oxide ([1344-28-1], basic), chloroform ([865-49-6], ≥ 99.8 %), Cu(0)-pellets ([7440-50-8], ≥ 99.9%), Cu(II)Br_2 (([7789-45-9], 99 %), 1,8-diazabicyclo[5.4.0]undec-7-ene ([6674-22-2], 98 %), 1,2-dichlorobenzene ([95-50-1], 99%), dichloromethane ([75-09-2], ≥ 99.8 %) was dried in a solvent purification system (J.C. Meyer), *N,N*-dimethyl acrylamide ([2680-03-7], 99%), *N,N*-dimethylformamide ([68-12-2], ≥ 99 %), ethyl α-bromoisobutyrate ([600-00-0], 98 %), ethyl 2-bromopropionate ([535-11-5, 99 %), 2,4-hexadien-1-ol ([111-28-4], > 98%), phenothiazine ([92-84-2], ≥ 98 %), sodium iodide ([7681-82-5], ≥ 99.5%, styrene ([100-42-5], ≥ 99%), tetrahydrofuran (THF, [109-99-9], ≥ 99 %, stabilized with butylated hydroxytoluene), toluene ([108-88-3], ≥99.9%), tributylphosphine ([998-40-3], 97%) were purchased from Sigma Aldrich and used without purification. Me_6TREN, BuTAD, DABCO-Bromine, 1-ethoxyethyl acrylate, citronellyl acrylate and the urazole-initiators for Cu(0)-RDRP and RAFT were synthesized according to literature procedures.[1, 26-29]

VI.7.3 Synthesis

Synthesis of PS-Br

5 mL styrene (43.5 mmol, 50 eq), 5 mL toluene, Cu(0) (30 pellets), 19.43 mg Cu(II)Br_2 (86.9 µmol, 0.1 eq) and 63.6 µL PMDETA (0.304 mmol, 0.35 eq) were weighed into a flask and degassed for 1 hour with a continuous nitrogen sparge. 112.97 µL ethyl 2-bromopropionate (0.87 mmol, 1 eq) was degassed separately in an ampule by nitrogen sparge for 1 hour. After addition of the initiator to the reaction mixture, the flask was placed in an oil bath at 90°C and the reaction started. After 18 hours, the reaction was stopped (82 % conversion) by cooling in liquid nitrogen under air atmosphere and precipitation in 100 mL cold methanol. The precipitate was

filtered off and dissolved in 100 mL THF. The copper catalyst was removed by passing the reaction mixture over a column of Al_2O_3. After evaporating the excess solvent until a volume of 20 mL, the polymer was precipitated in 200 mL of cold methanol. The polymer was filtered, washed with methanol and again dissolved in 20 mL of THF. Finally the polymer was precipitated in 200 mL of cold methanol and dried overnight in a vacuum oven at 40 °C.

Synthesis of PS-Cp

Bromide terminated PS (0.18 mmol) was mixed with 89 µL tributylphosphine (0.36 mmol) and 0.162 g sodium iodide (1.08 mmol) and dissolved in dry THF (2.0 mL). this solution was placed under nitrogen atmosphere. Separately, a stock solution of $NiCp_2$ in dry THF (0.18 mol/L) was prepared under a nitrogen atmosphere. Then 2.0 mL of the $NiCp_2$ was added to the polymer solution and this mixture was stirred overnight at room temperature. After the reaction went to completion, the solution was filtrated over a short column of basis alumina, to remove the precipitated nickel(II)bromide. Then the polymer was precipitated in the cold methanol, filtrated and washed thoroughly with methanol. The resulting powder was then dissolved in chloroform and washed three times with distilled water. To obtain the PS-Cp, the polymer was again precipitated in the cold methanol, filtrated, washed thoroughly with methanol and dried in a vacuum oven overnight at 40°C.

Synthesis of urazole-PBA

2.1 mL butyl acrylate (14.66 mmol, 50 eq), 4 mL DMF, Cu(0) (20 pellets), 100 mg urazole-initiator (0.29 mmol, 1 eq) were weighed into a flask and degassed for 1 hour with a continuous nitrogen sparge. In a separate vial, 3.27 mg Cu(II)Br_2 (0.29 mmol, 0.05 eq), 8.1 mg Me_6TREN (0.04 mmol, 0.12 eq) and 1.22 mL DMF were degassed separately for 1 hour. The reaction was started by the addition of the Cu(II)Br_2/ligand-solution to the reaction mixture, the flask was placed in an oil bath at 25°C. After 22 hours, the reaction was stopped (83 % conversion) by cooling in liquid nitrogen under air atmosphere and removing the copper catalyst by passing the reaction mixture over a column of Al_2O_3. After evaporating the excess solvent, the polymer was poured in a petri dish and dried overnight in a vacuum oven at 40 °C.

Oxidation of urazole-PBA

1 mmol of polymer with an urazole end group is dissolved in 5 mL of dichloromethane. Hereby 0.3 mmol of DABCO-Br is added at room temperature. The solution was allowed to stir for 3 hours at room temperature. Then the solution was filtrated and concentrated *in vacuo* to obtain the polymer with a TAD end group.

Coupling with BuTAD

100 mg of polymer with an Cp end group is dissolved in 1 mL of dichloromethane. Hereby 1.1 eq of BuTAD is added at room temperature under inert atmosphere. The solution is allowed to stir for one minute. When the red color disappeared, the polymer was precipitated in 5 mL cold methanol, filtrated, washed thoroughly with methanol and dried overnight in a vacuum oven at 40°C.

Polymer-polymer conjugation

50 mg of polymer with an Cp end group is dissolved in 0.5 mL of THF. Hereby 1 eq of TAD-polymer (in 0.5 mL THF) is added at room temperature. The solution was allowed to stir until the red color disappeared. The obtained (block) copolymer was precipitated in the appropriate solvent, filtrated, washed thoroughly and dried overnight in a vacuum oven at 40°C.

Synthesis of the P(nBA-co-CA) copolymer

1 mL butyl acrylate (6.98 mmol, 90 eq.), 163 mg citronellyl acrylate (0.78 mmol, 10 eq.), 1.88 mL DMF, Cu(0) (10 pellets), 14.03 mg ethyl 2-bromopropionate (0.078 mmol, 1 eq.) were weighed into a flask and degassed for 30 minutes with a continuous argon purge. In a separate vial, 0.87 mg Cu(II)Br_2 (3.88 µmol, 0.05 eq.), 2.14 mg Me_6TREN (9.30 µmol, 0.12 eq.) and 1 mL DMF were degassed separately via argon bubbling for 30 minutes. The reaction was started by the addition of the Cu(II)Br_2/ligand-solution to the reaction mixture at room temperature. Samples of the reaction mixture were taken for GC and SEC analysis, samples for GC analysis were dissolved in THF with phenothiazine as radical inhibitor (1,2-dichlorobenzene as internal standard), while samples for SEC analysis were diluted with THF, then passed over a basic alumina column to remove metal salts. After the polymerization, the reaction mixture was diluted with THF and filtered over a column of basic Al_2O_3 to remove the copper catalyst. After

evaporating the excess solvent, the product was poured into a beaker and placed into the vacuum oven overnight to remove traces of monomer and residual solvent. The final polymer was obtained as an oil. A polymer with 5 mol% CA was synthesized accordingly.

Synthesis of the P(EEA)-b-P(nBA-co-CA) copolymer

1 g 1-ethoxyethyl acrylate (6.94 mmol, 100 eq.), 0.81 mL DMF, Cu(0) (10 pellets) and 12.56 mg ethyl 2-bromoisobutyrate (0.069 mmol, 1 eq.) were weighed into a flask and degassed for 30 minutes with a continuous argon purge In a separate vial, 0.77 mg Cu(II)Br_2 (3.47 µmmol, 0.05 eq.), 1.91 mg Me_6TREN (8.32 µmol, 0.12 eq.), and 0.5 mL DMF were degassed separately via argon bubbling for 30 minutes. The reaction was started by the addition of the Cu(II)Br_2/ligand solution to the reaction mixture at room temperature. After overnight reaction at near-quantitative conversion, a mixture of 0.45 mL butyl acrylate (3.12 mmol, 45 eq.) and 72.94 mg CA (0.35 mmol, 5 eq.) in 1.18 mL DMF was prepared, degassed for 30 minutes with a continuous argon purge and added to the reaction mixture and the reaction proceeded for 6 hours. Finally, the reaction mixture was diluted with THF and filtered over a column of basic Al_2O_3 to remove the copper catalyst. After evaporating the excess solvent, the product was poured into a beaker and placed into the vacuum oven overnight to remove traces of monomer and residual solvent. The final polymer was obtained as an oil. A polymer with 5 mol% CA was synthesized accordingly.

Synthesis of urazole-PDMA

N,N-dimethylacrylamide, 2,2'-azobisisobutyronitrile (AIBN) as the thermal initiator and DMF as solvent were used with [monomer]/[CTA]/[AIBN] = 100/1/0.1. All compounds were precisely weighed in a schlenk flask to obtain the desired ratios and the concentration of the monomer was fixed at 3M. The reaction mixture was degassed using three freeze-vacuum-thaw cycles and the schlenk flask was subsequently filled with nitrogen and immersed in an oil bath at 65°C to start the polymerization. The polymerization was stopped at the time required for the desired monomer conversion by immersing the reaction mixture in liquid nitrogen and opening the schlenk tube. After the polymerization, the polymer was isolated by removing the DMF solvent under reduced pressure and precipitating the polymer in diethylether. The resulting polymer was

removed by filtration and dried at 40°C under vacuum. The conversion of the monomer was analyzed by GC with DMF as internal standard and molecular weight by SEC analysis.

Oxidation of urazole-PDMA

The Ur-PDMA polymer is dried by stirring in dry DCM in the presence of crushed molecular sieves overnight prior to use. After drying, 50 mg of Ur-PnBA (0.021 mmol, 1 equivalent) is dissolved in 2 ml of dry dichloromethane in a vial that is dried before use. After degassing the reaction mixture with nitrogen, the oxidant DABCO-bromine (32.78 mg, 1 equivalent) is added. The mixture is stirred under nitrogen atmosphere, in the dark for 6 hours. After oxidation, the mixture is purified by removing the DABCO-bromine complex (yellow powder) by filtering through a syringe filter. The obtained clear, red solution is directly evaporated under reduced pressure. After purification, the oxidized TAD-PDMA is reacted with HDEO or coupled to the copolymer.

Synthesis of Ur-PnBA

Butyl acrylate, 2,2'-azobisisobutyronitrile (AIBN) as the thermal initiator and DMF as solvent were used with [monomer]/[CTA]/[AIBN] = 100/1/0.1. All compounds were precisely weighed in a schlenk flask to obtain the desired ratios and the concentration of the monomer was fixed at 3M. The reaction mixture was degassed using three freeze-vacuum-thaw cycles and the schlenk flask was subsequently filled with nitrogen and immersed in an oil bath at 65°C to start the polymerization. The polymerization was stopped at the time required for the desired monomer conversion by immersing the reaction mixture in liquid nitrogen and opening the schlenk tube. After the polymerization, the polymer was isolated by removing the DMF solvent under reduced pressure and precipitating the polymer in methanol. The resulting polymer was removed by decantation and dried at 40°C under vacuum. The conversion of the monomer was analyzed by GC with DMF as internal standard and molecular weight by SEC analysis.

Oxidation of Ur-PnBA

The Ur-PnBA polymer is dried overnight under vacuum at 40 °C prior to use. After drying, 100 mg of Ur-PnBA (0.031 mmol, 1 eq.) is dissolved in 2 ml of dry dichloromethane in a vial that is dried before use. After degassing the reaction mixture with nitrogen, the oxidant DABCO-

bromine (48.77 mg, 1 equivalent) is added. The mixture is stirred under nitrogen atmosphere, in the dark for 3 hours. After oxidation, the mixture is purified by removing the DABCO-bromine complex (yellow powder) by filtering through a syringe filter. The obtained clear, red solution is directly evaporated under reduced pressure to obtain the polymer as a viscous, red liquid. After purification, the oxidized TAD-PnBA polymer is coupled to HDEO or the block copolymer.

References

1. Billiet, S.; De Bruycker, K.; Driessen, F.; Goossens, H.; Van Speybroeck, V.; Winne, J. M.; Du Prez, F. E. *Nat. Chem.* **2014,** 6, (9), 815-821.
2. Barner-Kowollik, C.; Inglis, A. J. *Macromolecular Chemistry and Physics* **2009,** 210, (12), 987-992.
3. Espeel, P.; Du Prez, F. E. *Macromolecules* **2015,** 48, (1), 2-14.
4. Barner-Kowollik, C.; Du Prez, F. E.; Espeel, P.; Hawker, C. J.; Junkers, T.; Schlaad, H.; Van Camp, W. *Angewandte Chemie International Edition* **2011,** 50, (1), 60-62.
5. Kolb, H. C.; Finn, M. G.; Sharpless, K. B. *Angewandte Chemie International Edition* **2001,** 40, (11), 2004-2021.
6. Rostovtsev, V. V.; Green, L. G.; Fokin, V. V.; Sharpless, K. B. *Angewandte Chemie-International Edition* **2002,** 41, (14), 2596-+.
7. Tornoe, C. W.; Christensen, C.; Meldal, M. *Journal of Organic Chemistry* **2002,** 67, (9), 3057-3064.
8. Hoyle, C. E.; Lowe, A. B.; Bowman, C. N. *Chemical Society Reviews* **2010,** 39, (4), 1355-1387.
9. Hoyle, C. E.; Lee, T. Y.; Roper, T. *Journal of Polymer Science Part A: Polymer Chemistry* **2004,** 42, (21), 5301-5338.
10. Espeel, P.; Du Prez, F. E. *European Polymer Journal* **2015,** 62, (0), 247-272.
11. Tasdelen, M. A. *Polymer Chemistry* **2011,** 2, (10), 2133-2145.
12. Xiao, L.; Chen, Y.; Zhang, K. *Macromolecules* **2016,** 49, (12), 4452-4461.
13. Syrgiannis, Z.; Koutsianopoulos, F.; Muir, K. W.; Elemes, Y. *Tetrahedron Letters* **2009,** 50, (3), 277-280.
14. Leach, A. G.; Houk, K. N. *Chemical Communications* **2002**, (12), 1243-1255.
15. Butler, G. B. *Polymer Science U.S.S.R.* **1981,** 23, (11), 2587-2622.
16. Mallakpour, S. E.; Nasr-Isfahani, H. *Indian Journal of Chemistry Section B-Organic Chemistry Including Medicinal Chemistry* **2002,** 41, (1), 169-174.
17. De Bruycker, K.; Billiet, S.; Houck, H. A.; Chattopadhyay, S.; Winne, J. M.; Du Prez, F. E. *Chemical Reviews* **2016,** 116, (6), 3919-3974.
18. Zolfigol, M. A.; Chehardoli, G.; Ghaemi, E.; Madrakian, E.; Zare, R.; Azadbakht, T.; Niknam, K.; Mallakpour, S. *Monatshefte für Chemie - Chemical Monthly* **2008,** 139, (3), 261-265.
19. Cookson, R. C.; Gilani, S. S. H.; Stevens, I. D. R. *Journal of the Chemical Society C-Organic* **1967**, (19), 1905-&.

20. Pyun, J.; Kowalewski, T.; Matyjaszewski, K. *Macromolecular Rapid Communications* **2003,** 24, (18), 1043-1059.
21. Driessen, F.; Herckens, R.; Espeel, P.; Du Prez, F. E. *Polymer Chemistry* **2016**.
22. Börner, H. G.; Beers, K.; Matyjaszewski, K.; Sheiko, S. S.; Möller, M. *Macromolecules* **2001,** 34, (13), 4375-4383.
23. Sheiko, S. S.; Sumerlin, B. S.; Matyjaszewski, K. *Progress in Polymer Science* **2008,** 33, (7), 759-785.
24. Rodríguez-Hernández, J.; Chécot, F.; Gnanou, Y.; Lecommandoux, S. *Progress in Polymer Science* **2005,** 30, (7), 691-724.
25. Levere, M. E.; Willoughby, I.; O'Donohue, S.; de Cuendias, A.; Grice, A. J.; Fidge, C.; Becer, C. R.; Haddleton, D. M. *Polymer Chemistry* **2010,** 1, (7), 1086-1094.
26. Vandewalle, S.; Billiet, S.; Driessen, F.; Du Prez, F. E. *ACS Macro Letters* **2016,** 5, (6), 766-771.
27. Ciampolini, M.; Nardi, N. *Inorganic Chemistry* **1966,** 5, (1), 41-44.
28. Van Camp, W.; Du Prez, F. E.; Bon, S. A. F. *Macromolecules* **2004,** 37, (18), 6673-6675.
29. Worzakowska, M.; Torres-Garcia, E. *Polymer Degradation and Stability* **2016,** 133, 227-233.

Chapter VII.
Conclusions and perspectives

The aim of this work was the synthesis of complex polymer architectures for their use as dispersants, viscosity modifiers or adhesives. The interest in synthesizing these structures arose from a, earlier PhD-project in collaboration with Dow Chemical and previous PhD-studies, during which better results were obtained with these materials as stabilizer for pigments or compatabilizer for polymer blends compared to their linear counterparts. Furthermore, a combination of a Cu(0)-mediated polymerization system and thiolactone and triazolinedione (TAD) chemistry as two efficient linking methodologies were used. On the other hand, the use of a Cu(0)-mediated polymerization system as controlled radical polymerization (RDRP) technique enabled the synthesis of polymeric structures with precise control over molecular weight, end group functionality, chain architecture and dispersity.[1-9] Furthermore and industrially most relevant, this technique offers the possibility to obtain polymers with a high end group fidelity at high conversion in comparison to classical methods[10-12] such as Nitroxide Mediated Polymerization (NMP), Reversible Addition Fragmentation Transfer (RAFT) polymerization or Atom Transfer Radical Polymerization (ATRP).[13-15] Additional to the use of RDRP-methods, efficient linking methodologies or "click"-reactions enable polymer chemists to facilitate the synthesis of complex polymeric structures by simplifying complicated procedures and tedious work-ups.[16-18] In this context, two *in-house* developed "click" chemistries were depicted for the synthesis of complex polymeric structures; thiolactone and triazolinedione (TAD) chemistry.[19, 20] Thiolactone units can be implemented as protected thiol functionalities, which can be liberated upon reaction with an amine and subsequently reacted in a one-pot approach with the acrylate moiety present in the same reaction medium.[21] Triazolinedione moieties can be obtained by oxidation of the corresponding urazole unit and react rapidly with (di)enes *via* a Diels-Alder or Alder-ene reaction.[22]

In **chapter II**, a theoretical description on controlled polymerization methods is provided, with a major focus on copper mediated polymerization systems. An overview was presented on the evolution of classical ATRP to the recently developed Cu(0)-mediated polymerization. Furthermore, a critical comparison was given between Single Electron Transfer Living Radical Polymerization (SET-LRP) and Supplemental Activator and Reducing Agent Atom Transfer Radical Polymerization (SARA-ATRP), two resembling but mechanistically argued to be different methods. Next, the different aspects of "click"-chemistry were elaborated in more detail and the different criteria to be considered "click" were discussed. Additionally, two different *in-house* developed methods, which were implemented in this thesis were described in more detail, thiolactone and triazolinedione chemistry. The theoretical part of this thesis was finished with the description of different methodologies that can be utilized for the synthesis of complex polymer architectures while their use as dispersants was explained.

In order to moderately increase the level of complexity of the polymer synthesis during this thesis, **chapter III** started with the double modification of polymer end groups *via* thiolactone chemistry. First, the synthesis of four different polymers containing a thiolactone end group was performed. Polystyrene (TL-PS) and polybutyl acrylate (TL-PBA) were synthesized *via* Cu(0)-mediated polymerization of a thiolactone-containing initiator. The thiolactone functionality on polyethylene oxide (PEO-OH) and bifunctional polycaprolacton (HO-PCL-OH) was introduced by end group modification with a thiolactone containing isocyanate. Next, a model study was performed regarding the double modification reaction, benzyl amine and benzyl acrylate were added in a one-pot approach in which the amine opens the thiolactone ring, releasing the thiol which on its turn reacted with the acrylate moiety. The success of the modification reaction was confirmed by SEC, ^{1}H-NMR and MALDI-TOF analysis. Next, a library was created by varying the amine and acrylate structure. In this way, a series of double end-functionalized polymers was generated in which aromatic, furan, tetrahydrofurfuryl, double bond, halogen and hydroxyl-moieties were easily introduced. Finally, amphiphilic block copolymers were obtained by linking of PEO-NH_2 as hydrophilic amine with TL-PBA while the full conversion to the amphiphilic block copolymer was confirmed by Liquid Chromatography x Size Exclusion Chromatography (LCxSEC), a technique that separates polymers both on polarity and molecular weight.

In **chapter IV**, the complexity of the polymer synthesis was further increased by the synthesis of precision multisegmented macromolecular line-ups, which are multisegmented copolymers containing chemical functionalities well-located along the polymer backbone between each segment connection. First, a hetero-telechelic polymer was synthesized containing a thiolactone and acrylate functionality *via* Cu(0)-mediated polymerization of a thiolactone-containing initiator and end group modification reactions to transform the bromine end group into an acrylate unit. The success of these modification reactions was confirmed by SEC, ^{1}H-NMR and MALDI-TOF analysis. In a following step, the multisegmented macromolecular line-up was obtained by nucleophilic ring-opening of the thiolactone unit by a functionalized amine and consecutive thiol-Michael addition. Next, a library of macromolecular structures with chemical functionalities precisely positioned onto the polymer backbone was obtained by selective variation of the amine structure introducing aromatic, PEGylated, double bonds and furan moieties at each segment connection. The library of functionalities was extended by post-polymerization modification reactions *via* thiol-ene or furan-maleimide modification reaction of the respective double bond and furan-containing multisegmented line-up. In this way glycosylated polymers were synthesized by thiol-ene reaction with the corresponding sugar-thiol. Subsequently, amphiphilic precision multisegmented graft copolymers were synthesized by the use PEO-NH_2 and the successful synthesis was confirmed by LCxSEC analysis. Finally, chiral benzene-1,3,5-tricarboxamides (BTAs) were introduced *via* the corresponding amine as hydrogen-bonding units and their self-assembly behavior for the synthesis of single chain polymeric nanoparticles (SCPNs) was investigated.

To increase the level of complexity to a final level, **Chapter V** described the synthesis of two interesting complex architectures *via* a Cu(0)-mediated polymerization system and thiolactone chemistry, namely amphiphilic graft and toothbrush copolymers. Regarding the synthesis of the graft copolymers, a series of copolymers of butyl acrylate and a varying amount of a thiolactone-containing acrylate were synthesized. Next, the graft copolymer was obtained by linking the thiolactone-functionalized backbone with PEO-acrylate. For the synthesis of the toothbrush structures, a series of different block-copolymers of *tert*-butyl acrylate as protected hydrophilic first segment and a copolymer of butyl acrylate and thiolactone acrylate as second segment were prepared in a one-pot procedure. Next, the hydrophobic side-arms, consisting of poly(butyl

acrylate), were synthesized separately, introducing the acrylate as end group *via* a post polymerization modification step. The final toothbrush structure was obtained by linking the block copolymer with the hydrophobic side-arms and deprotection of the hydrophilic segment *via* methyl sulphonic acid. Finally, the material properties were investigated by dynamic light scattering (DLS) and dispersion tests. It was observed that toothbrush structures exhibited increased stabilizing features compared to the corresponding graft copolymers.

The last experimental part, **chapter VI**, described the use of TAD-chemistry for the synthesis of block, graft and toothbrush structures. The synthesis of the block copolymers was started by the synthesis of polymers containing TAD and ene end groups. For the synthesis of the ene end group, polystyrene was synthesized and the bromine was transformed into a cyclopentadiene. Polymers containing TAD end groups were obtained *via* Cu(0)-mediated polymerization of butyl acrylate *via* a urazole-containing initiator. Finally, the urazole was oxidized, the polymers were coupled and the successful outcome was analyzed *via* LCxSEC analysis. For the synthesis of the graft copolymers, a series of hydrophobic copolymers containing a varying amount of citronellyl acrylate and butyl acrylate were synthesized. In parallel, the hydrophilic poly(*N,N*-dimethylacrylamide) (PDMA) was synthesized *via* RAFT polymerization of a urazole-containing RAFT agent, since it was observed that a Cu(0)-mediated polymerization was not able to control the polymerization due to side-reactions of the urazole moiety with the copper catalyst. Finally, the graft copolymer was obtained by oxidizing the urazole moiety and linking the polymers. Regarding the synthesis of the toothbrush structures, a series of different block copolymers were synthesized containing 1-ethoxy ethylacrylate and a copolymer of butyl acrylate and citronellyl acrylate as second block in a one-pot procedure *via* a Cu(0)-mediated polymerization. Furthermore, hydrophobic side-arms were obtained *via* RAFT polymerization of butyl acrylate *via* a urazole-containing RAFT agent. Afterwards, the amphiphilic toothbrush copolymer was obtained by oxidation of the urazole moiety, linking the polybutyl acrylate side-arms to the block copolymer and deprotection of the 1-ethoxyethyl acrylate units by heating. Finally, the material properties were again investigated by DLS and dispersion tests. It was observed confirmed that toothbrush structures exhibit increased stabilizing features compared to the corresponding graft copolymers. In comparison to thiolactone chemistry, it has to be noted that triazolinedione chemistry has very interesting advantages, such as the color switch after reaction and the

increased grafting efficiencies, but also drawback such as the stability and synthetic difficulty to obtain these structures in some cases.

Perspectives

In general, it can be expected that the presented results of this work will have an impact on the implementation of Cu(0)-based polymerization systems in industry for the design of complex polymer architectures. First of all, Cu(0)-mediated polymerization provides the possibility of polymerizing monomers to high conversion retaining high end group fidelities. This enables the synthesis of block copolymers in a one-pot approach and facilitates purification at the end of the polymerization, two important aspects for the synthesis of polymers under industrially relevant conditions. In this PhD thesis, the grafting-onto strategy was applied for the synthesis of complex polymer structures, a technique which is strongly competing with the grafting-through method on an industrial level. However, nowadays the grafting-through method is still preferred due to the straightforward synthesis of the reactive macromonomers and corresponding complex structures. However, the grafting-onto method is attracting more attention, as a result of the increased grafting efficiencies that can be obtained by the use of more efficient chemistries. However, the additional cost by implementing new chemistries and related patent issues will still be a big hurdle for implementing this strategy on an industrial level.

Furthermore, this manuscript focused on the use of complex structures for the dispersion of pigment particles in water. By simple varying monomer structures and resulting complex architectures, these materials can be implemented as compatabilizers, viscosity modificiers or adhesives. Moreover, the research on sequence-controlled polymer *via* thiolactone chemistry described in chapter IV is still ongoing. Different strategies, applying both solid- and liquid-phase starting materials are investigated for the design of these highly interesting structures. On the other hand, the research area on the synthesis of complex copolymer structures *via* TAD-chemistry as efficient linking methodology is still ongoing, and will be explored for the synthesis of cyclic and multisegmented structures. Finally, the implementation of bio-based monomers for the synthesis of thermoplastic elastomers *via* controlled radical polymerization techniques,

derived from terpene-based structures is a research project that was recently started within the own research group.

References

1. Matyjaszewski, K., *Controlled Radical Polymerization*. American Chemical Society: 1998; Vol. 685, p 500.
2. Grishin, D.; Grishin, I. *Russian Journal of Applied Chemistry* **2011,** 84, (12), 2021-2028.
3. Lutz, J. F.; Lehn, J. M.; Meijer, E. W.; Matyjaszewski, K. *Nature Reviews Materials* **2016,** 1, (5).
4. Hadjichristidis, N.; Pitsikalis, M.; Pispas, S.; Iatrou, H. *Chemical Reviews* **2001,** 101, (12), 3747-3792.
5. Fournier, D.; Hoogenboom, R.; Schubert, U. S. *Chemical Society Reviews* **2007,** 36, (8), 1369-1380.
6. Sheiko, S. S.; Sumerlin, B. S.; Matyjaszewski, K. *Progress in Polymer Science* **2008,** 33, (7), 759-785.
7. Percec, V.; Guliashvili, T.; Ladislaw, J. S.; Wistrand, A.; Stjerndahl, A.; Sienkowska, M. J.; Monteiro, M. J.; Sahoo, S. *Journal of the American Chemical Society* **2006,** 128, (43), 14156-14165.
8. Rosen, B. M.; Percec, V. *Chemical Reviews* **2009,** 109, (11), 5069-5119.
9. Konkolewicz, D.; Wang, Y.; Krys, P.; Zhong, M.; Isse, A. A.; Gennaro, A.; Matyjaszewski, K. *Polymer Chemistry* **2014,** 5, (15), 4396-4417.
10. Matyjaszewski, K.; Spanswick, J. *Materials Today* **2005,** 8, (3), 26-33.
11. Braunecker, W. A.; Matyjaszewski, K. *Progress in Polymer Science* **2007,** 32, (1), 93-146.
12. Destarac, M. *Macromolecular Reaction Engineering* **2010,** 4, (3-4), 165-179.
13. Wang, J. S.; Matyjaszewski, K. *Journal of the American Chemical Society* **1995,** 117, (20), 5614-5615.
14. Hawker, C. J.; Bosman, A. W.; Harth, E. *Chemical Reviews* **2001,** 101, (12), 3661-3688.
15. Chiefari, J.; Chong, Y. K.; Ercole, F.; Krstina, J.; Jeffery, J.; Le, T. P. T.; Mayadunne, R. T. A.; Meijs, G. F.; Moad, C. L.; Moad, G.; Rizzardo, E.; Thang, S. H. *Macromolecules* **1998,** 31, (16), 5559-5562.
16. Barner-Kowollik, C.; Du Prez, F. E.; Espeel, P.; Hawker, C. J.; Junkers, T.; Schlaad, H.; Van Camp, W. *Angewandte Chemie International Edition* **2011,** 50, (1), 60-62.
17. Espeel, P.; Du Prez, F. E. *Macromolecules* **2015,** 48, (1), 2-14.
18. Kolb, H. C.; Finn, M. G.; Sharpless, K. B. *Angewandte Chemie International Edition* **2001,** 40, (11), 2004-2021.
19. Espeel, P.; Du Prez, F. E. *European Polymer Journal* **2015,** 62, (0), 247-272.
20. De Bruycker, K.; Billiet, S.; Houck, H. A.; Chattopadhyay, S.; Winne, J. M.; Du Prez, F. E. *Chemical Reviews* **2016,** 116, (6), 3919-3974.
21. Espeel, P.; Goethals, F.; Du Prez, F. E. *Journal of the American Chemical Society* **2011,** 133, (6), 1678-1681.
22. Billiet, S.; De Bruycker, K.; Driessen, F.; Goossens, H.; Van Speybroeck, V.; Winne, J. M.; Du Prez, F. E. *Nature Chemistry* **2014,** 6, (9), 815-821.

Chapter VIII.

Nederlandstalige samenvatting

Het doel van dit werk was de synthese van complexe polymeerstructuren, voor het gebruik van deze materialen als dispergeermiddel, viscositeitsregelaar of adhesief. De interesse in deze materialen is voortgekomen uit een eerder doctoraatsproject in samenwerking met Dow Chemicals en voorgaande doctoraatsstudies, waarbij werd aangetoond dat betere eigenschappen van deze materialen als stabilisator van pigmenten of compatabilizer van polymeermengsels werd verkregen ten opzichte van de overeenkomstige lineaire structuren. Daarnaast werd ook gebruik gemaakt van een Cu(0)-gemedieerde polymerisatie en thiolacton en triazolinedion (TAD) chemie als twee efficiënte koppelingsreacties. Het gebruik van een Cu(0)-gemedieerd polymerisatiesystem als gecontroleerde radicalaire polymerisatietechniek (RDRP) laat de gebruiker toe om polymeerstructuren te bereiden met exacte controle over moleculair gewicht, eindgroep functionaliteit, ketenstructuur en polydispersiteit.[1-9] Daarnaast biedt deze techniek ook de industrieel zeer interessante mogelijkheid om polymeren met een hoog eindgroepbehoud bij hoge conversie te bereiden, in vergelijking met klassieke methoden[10-12] zoals Nitroxide Gemedieerde Polymerisatie (NMP), Reversiebele Additie Fragmentatie Transfer (RAFT) polymerisatie of Atoom Transfer Radicalaire Polymerisatie (ATRP).[13-15] Naast het gebruik van RDRP-methoden kunnen efficiënte koppelingsstrategiën of zogenaamde “click”-reacties toegepast worden om de synthese van complexe polymeerstructuren te vergemakkelijken door complexe handelingen en vervelende opwerkingen te vereenvoudigen.[16-18] Binnen deze context werden twee “click” reacties uitgekozen die ontwikkeld werden binnen de eigen onderzoeksgroep voor de synthese van complexe polymeerstructuren; thiolacton en triazolinedion chemie (TAD).[19, 20] Thiolactonen kunnen als bouwstenen toegepast worden als een latente thiol functionaliteit, waarbij het thiol beschikbaar kan gemaakt worden door reactie met een amine en opeenvolgend kan reageren met een acrylaat, aanwezig in hetzelfde reactiemedium, in een één-pot strategie.[21] Triazolinedion componenten kunnen verkregen worden door oxidatie van het overeenkomstige urazool en reageren zeer snel met (di)enen via een Diels-Alder of Alder-een reactie.[22]

In **hoofdstuk II** werd een theoretische beschrijving gegeven over gecontroleerde polymerisatiemethoden, met een voorname focus op koper gemedieerde polymerisatiesystemen. Een overzicht werd voorzien over de evolutie van de gekende klassieke ATRP naar het recent ontwikkelde Cu(0)-gemedieerde polymerisatiesystem. Daarnaast werd ook een kritische vergelijking gegeven tussen "Single Electron Transfer Living Radical Polymerization" (SET-LRP) en "Supplemental Activator and Reducing Agent Atom Transfer Radical Polymerization" (SARA-ATRP), twee gelijkaardige maar mechanistisch sterk verschillende methoden. Vervolgens werden de verschillende aspecten van "click"-chemie uitgediept in meer detail en werden de verschillende criteria om reacties als "click" te beschouwen bediscussieerd. Daarbij werden twee methoden gedetailleerd besproken die in de eigen onderzoeksgroep op punt werden gesteld en in deze thesis uitvoerig toegepast werden, thiolacton en triazolinedion chemie. Het theoretisch gedeelte van deze thesis werd besloten met de beschrijving van verschillende strategieën die toegepast kunnen worden voor de syntheses van complexe structuren alsook het gebruik van deze materialen als dispergeermiddel.

Om geleidelijk aan de moeilijkheidsgraad van de polymeersynthese tijdens deze thesis te verhogen werd in **hoofdstuk III** gestart met de dubbele modificatie van polymer eindgroepen via thiolactonchemie. Eerst werden vier verschillende polymeren gesynthetiseerd met een thiolacton eindgroep. Polystyreen (TL-PS) en polybutyl acrylaat (TL-PBA) werden verkregen door middel van Cu(0)-gemedieerde polymerisatie van een thiolacton-bevattende initiator. De thiolacton functionaliteit op polyethylene oxide (PEO-OH) en het bifunctionele polycaprolacton (HO-PCL-OH) werd geïntroduceerd door eindgroep modificatie van een thiolacton bevattend isocyanaat. Vervolgens werd een modelstudie uitgevoerd voor de dubbele modificatie reactie, benzylamine en benzylacrylaat werden toegevoegd aan het polymeer in een één-pot strategie waarbij het amine het thiolacton opent en het thiol vrijstelt, dat op zijn beurt zal reageren met het acrylaat. Het succes van deze modificatie reactie werd bevestigd door middel van SEC, ^{1}H-NMR en MALDI-TOF analyse. Vervolgens werd een bibliotheek verkregen van verschillende dubbel eindgemodificeerde structuren door variatie van de structuur van het amine en acrylaat. Op deze manier werden verschillende eindgemodificeerde structuren gesynthetiseerd met aromatische, furan, tetrahydrofurfuryl, dubbele bindingen, halogenen en hydroxyl-functionaliteiten. Ten slotte werden amfifiele blokcopolymeren bereid door koppeling van PEO-amine als hydrofiel amine

met TL-PBA en werd de volledige omzetten naar het amfifiel blokcopolymeer bevestigd door middel van "Liquid Chromatography x Size Exclusion Chromatography" (LCxSEC), een techniek waarmee polymeren gescheiden worden op basis van zowel polariteit als moleculair gewicht.

In **hoofdstuk IV** werd de complexiteit van de uitgevoerde polymeersynthese verder opgedreven door de synthese van precisie multigesegmenteerde macromoleculaire line-ups, multigesegmenteerde blokcopolymeren met chemische functionaliteiten exact gelokaliseerd op de polymeerketen tussen elke segmentverbinding. Eerst werd een hetero-telechelisch polymeer gesynthetiseerd met een thiolacton en een acrylaat eindgroep door middel van Cu(0)-gemedieerde polymerisatie van een thiolacton-bevattende initiator en eindgroep modificatiereacties om de bromide eindgroep om te zetten naar een acrylaat. Het succes van deze modificatiereacties werd bevestigd door middel van SEC, ^{1}H-NMR en MALDI-TOF analyse. Vervolgens werd de multigesegmenteerde macromoleculaire line-up verkregen door nucleofiele ring-opening van het thiolacton door een functioneel amine en opeenvolgende thiol-Michael additie. Daarna werd een bibliotheek van macromoleculaire structuren verkregen met chemische functionaliteiten exact gelokaliseerd op de polymeerketen door variatie van de structuur van het amine. Op deze manier werden aromatische, PEG-structuren, dubbele bindingen en furan-eenheden ingevoerd tussen elke segment interconnectie. De bibliotheek van structuren met verschillende functionaliteiten werd uitgebreid door gebruik te maken van post-polymerisatie modificatie reacties door middel van de thiol-een en furan-maleïmide modificatie reactie van de respectievelijke dubbele binding en furan-bevattende multigesegmenteerde line-up, op deze manier werden glycopolymeren bereid door thiol-een reactie met het overeenkomstig suiker-thiol. Vervolgens werden amfifiele precisie multigesegmenteerde graft copolymeren bereid door gebruik te maken van PEO-amine. Daarbij werd het succes van de koppeling bevestigd door LCxSEC analyse. Ten slotte werden chirale benzene-1,3,5-tricarboxamides (BTAs) geïntroduceerd via het overeenkomstig amine als waterstofbrug vormende componenten en werd de vorming van supramoleculaire structuren bestudeerd voor de bereiding van "single chain polymeric nanoparticles (SCPNs).

De complexiteit van de polymeersynthese werd finaal opgedreven in **hoofdstuk V** waarbij de synthese van twee interessante polymeerstructuren, amfifiele graft en 'toothbrush' copolymeren, via een Cu(0)-gemedieerde polymerisatie en thiolacton chemie werd beschreven. Aangaande de synthese van de graft copolymeren werd eerst een reeks van copolymeren van butyl acrylaat en een variërende hoeveelheid van een thiolacton-bevattend acrylaat gesynthetiseerd. Vervolgens werd het graft copolymeer verkregen door koppeling van de thiolacton-bevattende hoofdketen met PEO-acrylaat. Voor de synthese van de 'toothbrush' structuren werd eerst een reeks van blokcopolymeren gesynthetiseerd bestaande uit *tert*-butyl acrylaat als beschermd hydrofiel eerste blok en een copolymeer van butyl acrylaat en het thiolacton acrylaat als tweede segment bereid in een één-pot procedure. Vervolgens werden de hydrofobe zijketens apart bereid, bestaande uit polybutyl acrylaat, waarbij een acrylaat als eindgroep werd geïntroduceerd door middel van een post-polymerisatie modificatie reactie. Uiteindelijk werd de 'toothbrush'-structuur verkregen door koppeling van het blokcopolymeer met de hydrofobe zijketens en de ontscherming van het hydrofiele segment door middel van methyl sulfonzuur. Ten slotte werden de materiaaleigenschappen onderzocht door middel van dynamische licht verstrooiing (DLS) en dispersietesten waarbij werd ondervonden dat 'toothbrush' structuren betere stabiliserende eigenschappen vertonen ten opzichte van de overeenkomstige graft copolymeren.

Hoofdstuk VI als laatste experimenteel gedeelte beschrijft het gebruik van TAD-chemie voor de synthese van blok, graft en 'toothbrush' structuren. De synthese van de blokcopolymeren werd gestart met de synthese van polymeren met TAD of "één" eindgroepen. Voor de synthese van de polymeren met "één" eindgroepen werd eerst polystyreen gesynthetiseerd via Cu(0)-gemedieerde polymerisatie en werd vervolgens het bromide omgezet in een cyclopentadieen. Daarnaast werden polymeren met TAD eindgroepen verkregen door Cu(0)-gemedieerde polymerisatie van butyl acrylaat via een urazool-bevattende initiator. Uiteindelijk werd het urazool geoxideerd, werden de polymeren gekoppeld tot het overeenkomstig blokcopolymeer en werd het resultaat geanalyseerd door middel van LCxSEC analyse. Voor de synthese van de graft copolymeren werd eerst een reeks van hydrofobe copolymeren bereid die een variabele hoeveelheid citronellyl acrylaat en butyl acrylaat bevatten. Daarnaast werd het hydrofiele poly(*N,N*-dimethylacrylamide) (PDMA) gesynthetiseerd door middel van RAFT polymerisatie via een urazool-bevattend RAFT reagens, omdat werd vastgesteld dat de overeenkomstige

polymerisaties door middel van een Cu(0)-gemedieerd systeem niet gecontroleerd verliepen als gevolg van nevenreacties tussen de katalysator en de urazool-eenheid. Ten slotte werd het graft copolymeer verkregen door oxidatie van het urazool en koppeling van de polymeren. In het kader van de synthese van de 'toothbrush' structuren werd eerst een reeks verschillende blokcopolymeren gesynthetiseerd dewelke 1-ethoxy ethyl acrylaat als eerste segment bevatten en een copolymeer bestaande uit butyl acrylaat en citronellyl acrylaat als tweede blok in een één-pot procedure *via* een Cu(0)-gemedieerde polymerisatie. Vervolgens werden hydrofobe zijketens verkregen door middel van RAFT polymerisatie van butyl acrylaat en een urazool-bevattend RAFT reagens. Daarna werden amfifiele 'toothbrush' structuren verkregen door oxidatie van de urazool-eenheid en koppeling van de hydrofobe zijketens met het blockcopolymeer en ontscherming van het 1-ethoxyethyl acrylaat door gebruik van warmte. Ten slotte werden de materiaaleigenschappen onderzocht door DLS analyse en dispersietesten en werd opnieuw geobserveerd dat 'toothbrush' structuren verbeterde stabiliserende eigenschappen vertonen ten opzichte van de overeenkomstige graft copolymeren.

Algemeen kan verwacht worden dat deze resultaten een impact zullen hebben op het gebruik van Cu(0)-gemedieerde polymerisaties in de industrie voor de ontwikkeling van complexe polymeerstructuren. Allereerst biedt Cu(0)-gemedieerde polymerisatie de mogelijkheid om monomeren te polymeriseren tot hoge conversie met behoud van eindgroup functionaliteit. Op deze manier kunnen blokcopolymeren in een één-pot strategie gesynthetiseerd worden en verloopt de opzuivering op het einde van de polymerisatie eenvoudiger, twee belangrijke aspecten voor de synthese van polymeren onder industrieel relevante condities. In deze doctoraatsscriptie werd de "grafting-onto" strategie toegepast voor de synthese van complexe polymeerstructuren, een techniek dat in sterke competitie staat met de "grafting-through" methode op industrieel niveau. Echter, hedendaags verkiest men nog steeds de "grafting-through" methode als gevolg van de eenvoudige synthese van de reactieve macromonomeren en overeenkomstige complexe structuren. Desalniettemin bemoeilijkt de extra kost van het gebruik van een nieuwe chemie en bijkomende patent-kwesties de implementatie van deze strategie op industrieel niveau.

Daarnaast focuste deze scriptie op het gebruik van complexe structuren voor de dispersie van pigment partikels in water. Door eenvoudige variatie van de monomeer structuur en overeenkomstige complexe structuren, kunnen deze materialen toegepast worden als compatabilizerds, viscositeitsregelaars of adhesieven. Bijkomend is het onderzoek rond sequentie gecontroleerde polymeren dat in hoofdstuk IV aan bod kwam lopende in de groep waarbij zowel vaste- als vloeibare fase startmaterialen gebruikt worden voor de synthese van deze interessante structuren. Anderzijds is het onderzoek rond het gebruik van TAD-chemie voor de synthese van complexe structuren nog steeds gaande en zal deze strategie onderzocht worden voor de synthese van cyclische en multigesegmenteerde structuren. Ten slotte, werd recent ook het onderzoek opgestart rond het gebruik van biogebaseerde monomeren zoals terpeen-gebaseerde structuren voor de synthese van thermoplastische elastomeren via gecontroleerde radicalaire polymerisatie methoden.

References

1. Matyjaszewski, K., *Controlled Radical Polymerization*. American Chemical Society: 1998; Vol. 685, p 500.
2. Grishin, D.; Grishin, I. *Russian Journal of Applied Chemistry* **2011,** 84, (12), 2021-2028.
3. Lutz, J. F.; Lehn, J. M.; Meijer, E. W.; Matyjaszewski, K. *Nature Reviews Materials* **2016,** 1, (5).
4. Hadjichristidis, N.; Pitsikalis, M.; Pispas, S.; Iatrou, H. *Chemical Reviews* **2001,** 101, (12), 3747-3792.
5. Fournier, D.; Hoogenboom, R.; Schubert, U. S. *Chemical Society Reviews* **2007,** 36, (8), 1369-1380.
6. Sheiko, S. S.; Sumerlin, B. S.; Matyjaszewski, K. *Progress in Polymer Science* **2008,** 33, (7), 759-785.
7. Percec, V.; Guliashvili, T.; Ladislaw, J. S.; Wistrand, A.; Stjerndahl, A.; Sienkowska, M. J.; Monteiro, M. J.; Sahoo, S. *Journal of the American Chemical Society* **2006,** 128, (43), 14156-14165.
8. Rosen, B. M.; Percec, V. *Chemical Reviews* **2009,** 109, (11), 5069-5119.
9. Konkolewicz, D.; Wang, Y.; Krys, P.; Zhong, M.; Isse, A. A.; Gennaro, A.; Matyjaszewski, K. *Polymer Chemistry* **2014,** 5, (15), 4396-4417.
10. Matyjaszewski, K.; Spanswick, J. *Materials Today* **2005,** 8, (3), 26-33.
11. Braunecker, W. A.; Matyjaszewski, K. *Progress in Polymer Science* **2007,** 32, (1), 93-146.
12. Destarac, M. *Macromolecular Reaction Engineering* **2010,** 4, (3-4), 165-179.
13. Wang, J. S.; Matyjaszewski, K. *Journal of the American Chemical Society* **1995,** 117, (20), 5614-5615.
14. Hawker, C. J.; Bosman, A. W.; Harth, E. *Chemical Reviews* **2001,** 101, (12), 3661-3688.

15. Chiefari, J.; Chong, Y. K.; Ercole, F.; Krstina, J.; Jeffery, J.; Le, T. P. T.; Mayadunne, R. T. A.; Meijs, G. F.; Moad, C. L.; Moad, G.; Rizzardo, E.; Thang, S. H. *Macromolecules* **1998,** 31, (16), 5559-5562.
16. Barner-Kowollik, C.; Du Prez, F. E.; Espeel, P.; Hawker, C. J.; Junkers, T.; Schlaad, H.; Van Camp, W. *Angewandte Chemie International Edition* **2011,** 50, (1), 60-62.
17. Espeel, P.; Du Prez, F. E. *Macromolecules* **2015,** 48, (1), 2-14.
18. Kolb, H. C.; Finn, M. G.; Sharpless, K. B. *Angewandte Chemie International Edition* **2001,** 40, (11), 2004-2021.
19. Espeel, P.; Du Prez, F. E. *European Polymer Journal* **2015,** 62, (0), 247-272.
20. De Bruycker, K.; Billiet, S.; Houck, H. A.; Chattopadhyay, S.; Winne, J. M.; Du Prez, F. E. *Chemical Reviews* **2016,** 116, (6), 3919-3974.
21. Espeel, P.; Goethals, F.; Du Prez, F. E. *Journal of the American Chemical Society* **2011,** 133, (6), 1678-1681.
22. Billiet, S.; De Bruycker, K.; Driessen, F.; Goossens, H.; Van Speybroeck, V.; Winne, J. M.; Du Prez, F. E. *Nature Chemistry* **2014,** 6, (9), 815-821.

Publications included in this thesis

1. F. Driessen, S. Martens, B. De Meyer, F.E. Du Prez, P. Espeel, Double Modification of Polymer End Groups Through Thiolactone Chemistry, *Macromolecular Rapid Communications*, **2016**, 37 (12), 947-951
2. F. Driessen, R. Herckens, P. Espeel, F.E. Du Prez, Thiolactone chemistry and copper-mediated CRP for the development of well-defined amphiphilic dispersing agents, *Polymer Chemistry*, **2016**, 7 (8), 1632-1641
3. F. Driessen, F.E. Du Prez, P. Espeel, Precision Multisegmented Macromolecular Lineups: A Display of Unique Control over Backbone Structure and Functionality, *ACS Macro Letters*, **2015**, 4 (6), 616-619
4. S. Billiet, K. De Bruycker, F. Driessen, H. Goossens, V. Van Speybroeck, J.M. Winne, F.E. Du Prez, Triazolinediones enable ultrafast and reversible click chemistry for the design of dynamic polymer systems, *Nature Chemistry*, **2014**, 6 (9), 815-821

Publications apart from the thesis

5. X. Pan, F. Driessen, X. Zhu, F.E. Du Prez, Selenolactone as a Building Block toward Dynamic Diselenide-Containing Polymer Architectures with Controllable Topology, *ACS Macro Letters*, **2017**, 6, 89-92
6. S. Martens, F. Driessen, S. Wallyn, O. Türünç, F.E. Du Prez, P. Espeel, One-Pot Modular Synthesis of Functionalized RAFT Agents Derived from a Single Thiolactone Precursor, *ACS Macro Letters*, **2016**, 5 (8), 942-945
7. S. Vandewalle, S. Billiet, F. Driessen, F.E. Du Prez, Macromolecular Coupling in Seconds of Triazolinedione End-Functionalized Polymers Prepared by RAFT Polymerization, *ACS Macro Letters*, **2016**, 5 (6), 766-771
8. S. Wallyn, Z. Zhang, F. Driessen, J. Pietrasik, B.G. De Geest, R. Hoogenboom, F.E. Du Prez, Straightforward RAFT Procedure for the Synthesis of Heterotelechelic Poly(acrylamide)s, *Macromolecular Rapid Communications*, **2014**, 35 (4), 405-411
9. P. Espeel, F. Goethals, F. Driessen, L-T. T. Nguyen, F.E. Du Prez, One-pot, addive-free preparation of functionalized polyurethanes via amine-thiol-ene conjugation, *Polymer Chemistry*, **2013**, 4 (8), 2449-2456